The function of E. coli YidC for the membrane insertion of the M13 procoat protein

Dissertation zur Erlangung des Doktorgrades

der Naturwissenschaften (Dr. rer. nat.)

Fakultät Naturwissenschaften

Universität Hohenheim

Institut für Mikrobiologie

vorgelegt von

Dirk Spann

aus Stuttgart

2018

Parts of this thesis have been published

Spann D., Pross E., Chen Y., Dalbey R. and Kuhn A., 2018. Each protomer of a dimeric YidC functions as an independent membrane insertase. *Scientific Reports* 8, Article number: 589

Parts of this thesis have been presented at an international conference

Gordon Conference, Galveston USA 2014: Protein transport across cell membranes.

Poster presentation "*A tandem YidC is functionally active for membrane insertion*"

TABLE OF CONTENT

1 INTRODUCTION

1.1 Protein targeting and translocation in bacteria

All living cells have the need to uphold their metabolism by keeping their proteome in a balanced state to assure viability (proteostasis). This requires the constant creation, localization and correct folding of proteins in a controlled manner. Newly generated proteins emerging from ribosomes tend to fold without being completely translated without control mechanisms. Chaperones bind to these nascent chains and keep the premature protein in a partially- or unfolded state that allows transportation to the target region in the cell and proper folding (Powers et al. 2009, Hartl et al. 2011).
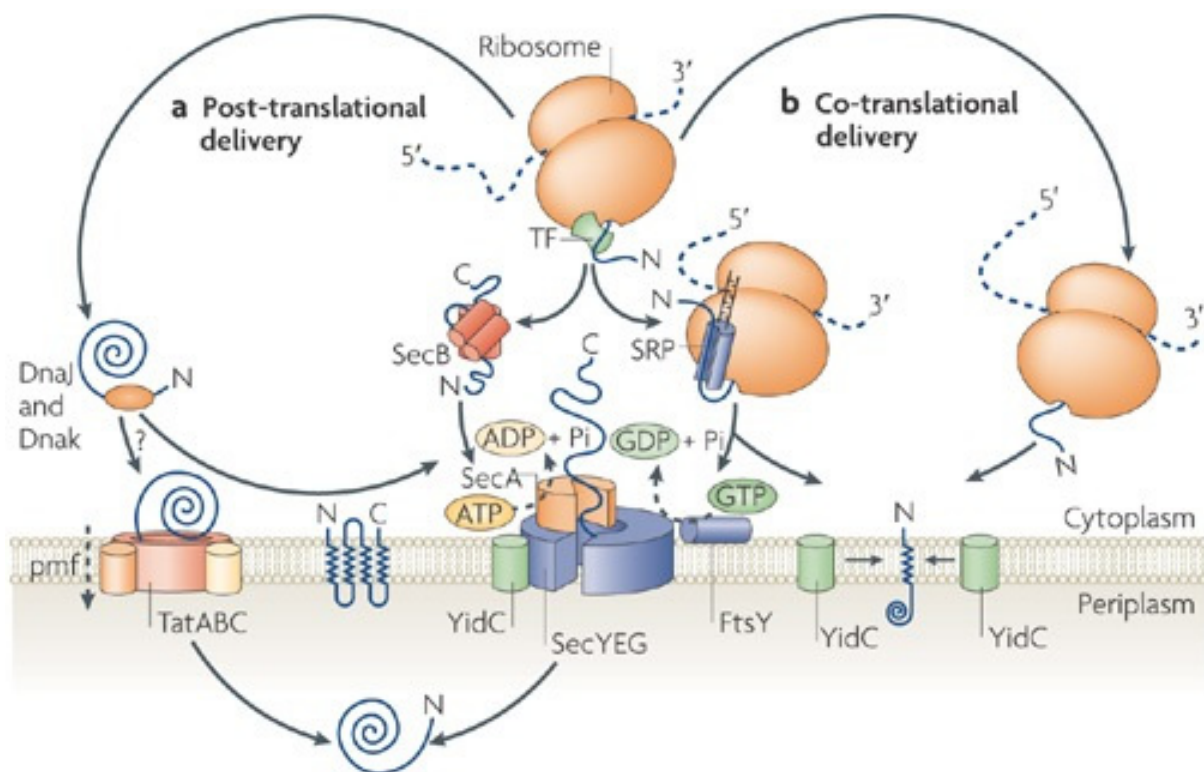
Fig. 1: Overview of the translocation/insertion pathways in prokaryotes. Two major routes exist, the post-translational and the co-translational way. **(a)** Secretory proteins are either kept in an unfolded state via SecA/SecB and are translocated via the Sec or Sec/YidC pathway under ATP hydrolysis or fold to their final conformation and translocated with the twin arginine translocase TatABC. **(b)** Co-translational translocation/insertion is facilitated via the SRP-mediated pathway. SRP binds to the nascent chain and directs the ribosome to the Sec/YidC translocon where it binds to its receptor FtsY and releases the substrate for insertion under GTP hydrolysis. Some smaller proteins are inserted by YidC alone via SRP or by direct binding of the ribosome (Cross et al. 2009).

Membrane proteins play a vital role in all known forms of life and fulfill a vast number of tasks in prokaryotic and eukaryotic cells. Some of them include signal transduction, ion transport, ATP generation or transporters for various molecules including other proteins. Approximately 20 to 30% of all ORFs encode for integrated membrane proteins (Wallin and von Heijne 1998).

In bacteria, there are three major ways how integral membrane proteins are inserted/translocated to their target region (see Fig. 1). The first is the Sec translocon, which translocates or inserts the majority of the membrane proteins in bacteria. The second is YidC, an insertase that inserts smaller membrane proteins by itself but also cooperates with the Sec translocon (Scotti et al. 2000, Samuelson et al. 2000, Dalbey et al. 2014). The third is the twin arginine translocation (TAT) pathway (Berks 1996, Berks et al. 2000).

1.2 Translocation pathways

1.2.1 Sec translocon

The Sec translocon in bacteria is formed by up to seven subunits, SecA, SecY, SecE, SecG, SecD, SecF and YajC. SecYE forms the core complex, which is already able to perform protein translocation with SecA. SecG and the SecDFyajC complex can also associate with SecYE to support the efficiency of the translocation process (Brundage et al. 1990, Duong and Wickner 1997).

The structure of the SecA/SecY complex has been solved with proteins from different organisms. SecA from *Bacillus subtilis* was crystallized with either SecYE from *Thermotoga maritima* or with SecYEG from *Aquifex aeolicus*. Another crystallization, that gave the best resolution, was performed with SecA and SecYEG from *T. maritima* (see Fig. 2) where SecYEG was derivatized with seleno-methionine. All the solved structures showed architectural similarities despite being from different organisms. One SecA monomer is bound to one copy of the SecY channel. It was also shown that SecA binds its substrate in a clamp-like structure. This clamp holds its substrate when ADP is bound to SecA and releases it with ATP (Zimmer et al. 2008).

The two-helix finger domain of SecA (Zimmer et al. 2008) contacts its substrates with a tyrosine, or another bulky hydrophobic amino acid, at its tip. After binding to SecY, it might

push the substrate chain into the channel using energy from ATP hydrolysis (Erlandson et al. 2008). Allen et al. (2016) recently published data that suggests a different way how SecA interacts with SecY. By using molecular dynamics (MD) simulations and FRET analysis it was discovered that the opening state of the lateral gate and the pore of SecY depends on the bound nucleotide in SecA. It is indicated that this communication between the two proteins goes both ways and that alterations in the lateral gate modify the affinity of SecA to ATP. Additionally the two-helix finger domain is believed to function as a sensor for polypeptide chains instead of pushing the substrate into the channel. The insertion model postulates a ratchet mechanism where the polypeptide chain can diffuse freely inside the pore until blocks at either end occur. A block on the cytoplasmic side leads to a nucleotide exchange in SecA and an opening of the lateral gate that widens the channel. The channel again becomes more narrow after ATP hydrolysis and ADP release and the block is either still on the cytoplasmic side and the process is repeated or on the periplasmic site and further diffusion can occur. This generates a one-way mechanism for polypeptide chain transport (Allen et al. 2016).

In the cytosol, SecA occurs mainly in its dimeric form, however, the dimers exchange their monomers constantly between each other and a small pool of monomeric SecA also exists. By contacting acidic phospholipids in the membrane or the SecYEG complex or binding a signal sequence, SecA dissociates into its monomeric form (Or et al. 2002). A recent study discovered, that SecA targeting and translocation with the Sec-complex might not work only posttranslationally but also cotranslationally. It was indicated, that SecA is able to bind to the ribosome and to the ribosomal nascent chains (RNCs) in an early stage of translation. SecB binds to the RNC after SecA and the complex is directed to the Sec translocase. The ATPase functionality is activated, which allows the RNC to be translocated through the inner membrane cotranslationally while the ribosome is not directly associated with the Sec complex. This new postulated variant is called the "uncoupled co-translational secretion" (Huber et al. 2017).

The lateral gate of SecYEG is crucial for protein translocation. Closing the gate by the formation of a disulfide crosslink between TM2b and TM7 of SecY led to a total stop of proOmpA translocation. The ATPase activity of SecA was also halted by forcing the gate shut. This suggests a connection between the opening of the lateral gate and the ATPase activity of SecA (du Plessis et al. 2009).

Translocation is facilitated either via the posttranslational SecA/SecB pathway or via the cotranslational signal recognition particle-pathway (SRP). The targeting is dependent on the signal sequence that is exiting the ribosome during translation (Lee and Bernstein 2001). Signal sequences for the Sec translocase are on average 20-24 amino acids long and are comprised of three distinct parts: first, a positively charged amino-terminal region (n-region) followed by a hydrophobic core (h-region) and finally a polar region (c-region). The n- and h-region are both very important for binding either to SRP or to SecA (von Heijne 1985 and 2005, Natale et al. 2008).
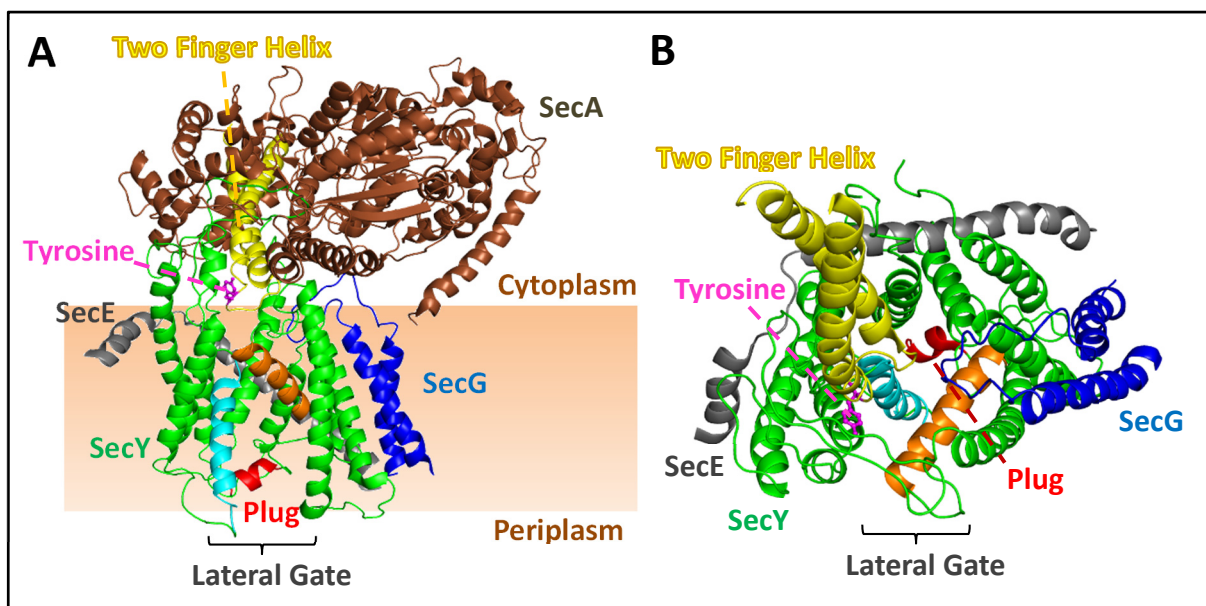
Fig. 2: Structure of the SecYEG complex of *Thermotoga maritima* with bound SecA. (A) Side view on the SecYEG complex with bound SecA. The Two Finger Helix (yellow) of SecA (brown) is reaching into the SecY (green) channel with the substrate-contacting tyrosine (magenta) at the tip of the domain. SecE (grey) is wrapped around the channel. SecG (blue), which is believed to stimulate the translocation process, is directly associated to SecY. Red: the plug that closes the channel when no translocation is taking place. Orange: TM 2a of SecY forming one half of the lateral gate to the membrane. Cyan: TM7 of SecY forming the other half of the lateral gate. **(B)** Top view into the SecYEG complex. SecA has been removed excluding the Two Helix domain for better visibility. Images created with PyMOL v. 1.3 and PDB entry 3DIN (Zimmer et al. 2008, Lycklama a Nijeholt and Driessen 2012).

SRP

The SRP in *E. coli* is consisting of the fifty-four-homologue (Ffh), a homologue to the SRP54 protein, and a 4.5S RNA (Herskovits et al. 2000). Both parts of the SRP are essential for cell viability and protein translocation (Brown and Fournier 1984, Phillips and Silhavy 1992). The SRP has an intrinsic GTPase activity that is dependent on the presence of Mg^{2+} ions (Samuelsson et al. 1995). The role of the 4.5S RNA lies in the acceleration of the interaction and binding of SRP to its receptor FtsY. It also stimulates GTP hydrolysis in the complex (Peluso et al. 2001, Siu et al. 2007).

FtsY is the receptor to which SRP binds during the targeting step. It is also capable of binding and hydrolyzing GTP. Similar to SRP, Mg^{2+} ions are required for enzyme activity (Miller et al. 1994, Kusters et al. 1995). FtsY contains N- and G- domains similar to SRP in structure and function (see Fig. 3) (Montoya et al. 1997, Ataide et al. 2011). Membrane association of the receptor is facilitated via an amphipathic helix in the N-Domain of the protein (Parlitz et al. 2007).
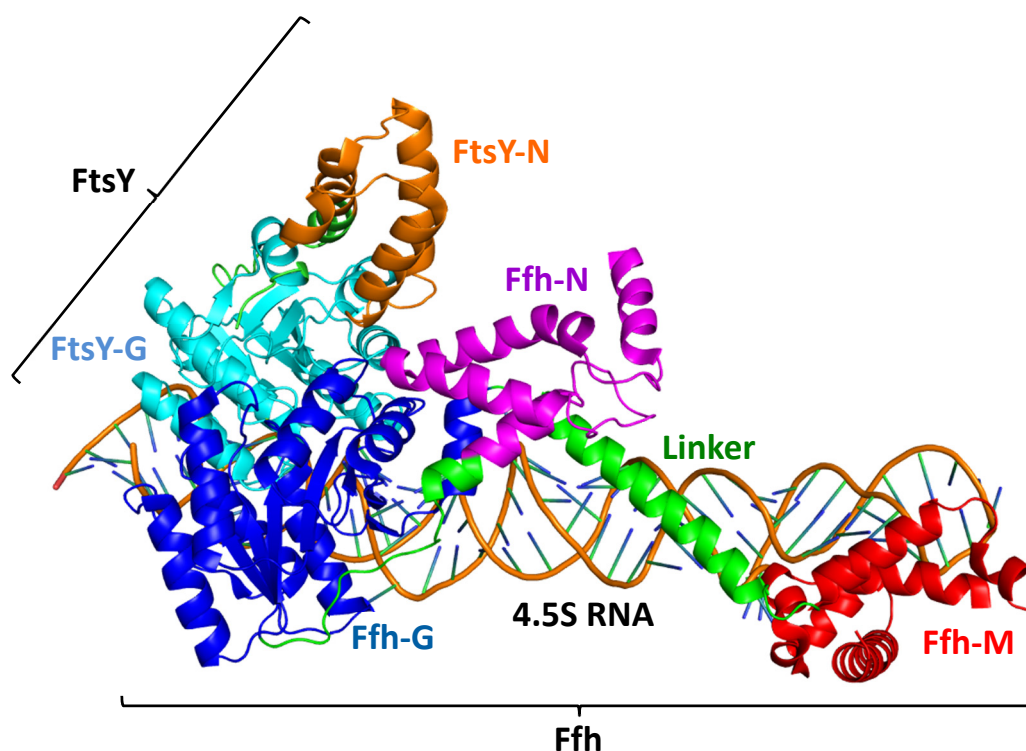
Fig. 3: Structure of the SRP-FtsY Complex. FtsY and Ffh form a heteromeric dimer with their N and G domains. The RNA-binding M-domain of Ffh is connected via a helical linker to the rest of the protein. Orange: N-domain of FtsY, cyan: G-domain of FtsY, blue: G-domain of Ffh, magenta: N-domain of Ffh, red: M-domain of Ffh. Image created with PyMOL 1.3 and PDB entry 2XXA (Ataide et al. 2011).

1.2.2 Twin arginine translocation (TAT)

The TAT system in *E. coli* translocates proteins across membranes in their folded state. Many substrates also incorporate redox cofactors before translocation (Jack et al. 2001, Müller et al. 2005). It is a homologous system to the ΔpH pathway that has been discovered in maize thylakoid membranes encoded by the Hcf106 gene (Settles and Martienssen 1998). The substrates of the TAT system are recognized via a signal peptide at the N-terminus of the protein. This peptide has some similarities to the signal sequence of the Sec pathway, it can also be divided into three distinct regions: the n-region containing a twin arginine (RR), h-region and c-region and is cleaved off after translocation (von Heijne 1985, Berks 1996, Berks et al. 2000). The core unit for a functioning TAT system in *E. coli* consists of TatA/TatE, TatB and TatC. (Bogsch et al. 1998, Sargent et al. 1999, Berks et al. 2000).

1.2.3 The YidC/Oxa1/Alb3 insertase family

The YidC/Oxa1/Alb3 family is comprised of insertase homologues that facilitate the insertion and folding of membrane proteins. Oxa1 resides in the inner membrane of mitochondria, Albino3 (Alb3) is located in the thylakoid membranes in chloroplasts and YidC is found in the inner membrane of bacteria (Wang and Dalbey 2011, Hennon et al. 2015). All members of this family share structural and functional features: The transmembrane core structure that contains a hydrophilic groove which is open to the membrane through a hydrophobic slide and the long amphipathic C1 loop (Hennon et al. 2015).

A recently found homologue in *Methanocaldococcus jannaschii* represents the first discovered member of the YidC/Oxa1/Alb3 family in archaea. All domains of life therefore contain members of this insertase family, which shows how highly conserved this insertion pathway is (Borowska et al. 2015, Dalbey and Kuhn 2015).

1.2.3.1 YidC

The YidC insertase has been studied in many aspects. The latest important discovery was the crystal structure of the insertase (Kumazaki et al. 2014b). YidC is essential for cell viability and inserts small membrane proteins with one, like the Pf3 coat protein, or two TMs like the M13 procoat protein, on its own. This requires the membrane potential to function (Samuelson et al. 2000).

Endogenous substrates

The mechanosensitive channel with large conductance (MscL) and the subunit c of the F_1F_o-ATPase are both endogenous proteins that require only YidC for proper insertion (van der Laan et al. 2004, Yi et al. 2004, Facey et al. 2007, Neugebauer et al. 2012).

MscL

MscL spans the inner membrane twice (see Fig. 4) and has an N-in/C-in topology with a loop in the periplasm that connects both TMs and an additional helix in the cytoplasm towards the C-terminus (Steinbacher et al. 2007). For MscL, YidC also functions as a chaperone for assembling the pentameric channel (Facey et al. 2007, Neugebauer et al. 2012).
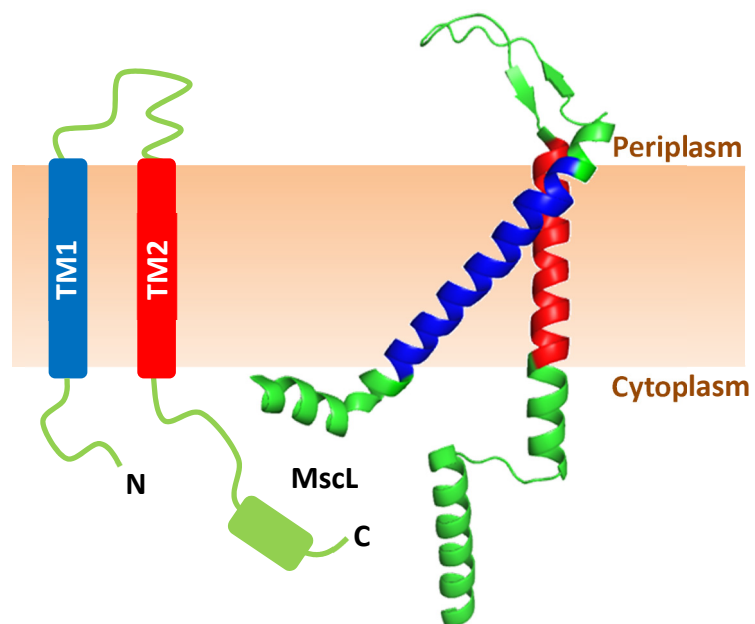
Fig. 4: Diagram and structure of MscL from *Mycobacterium tuberculosis*. MscL spans the membrane twice with two TMs that are connected via a loop in the periplasm. An additional helix is found near the c-terminus of the protein. Blue: first TM of MscL. Red: Second TM of MscL. Structure figure created with PyMOL 1.3 and PDB entry 2OAR (Steinbacher et al. 2007).

Results were published, that indicated a YidC independent insertion in the inner membrane and that YidC is only important for its chaperone function in the membrane (Pop et al. 2009). However, these results could not be reproduced, but were disproved by showing that

insertion with the same mutants did not occur when YidC was depleted (Neugebauer et al. 2012).

Subunit c of the F_1F_o ATPase

The Subunit c of the F_1F_o ATPase is an integral membrane protein with two TMs (see Fig. 5). Both termini are oriented to the periplasm and the short loop that connects the TMs is located in the cytoplasm (Hensel et al. 1990, Girvin et al. 1998). The peptide is inserted independently from the Sec machinery. It also does not need the proton motive force (PMF) for insertion, which has been shown with in vitro and in vivo experiments (van der Laan et al. 2004, Yi et al. 2004). It does however require the bacterial SRP and YidC for

Fig. 5: Diagram and structure of subunit c of the F_1F_o ATPase from *E. coli*. The subunit c spans the membrane two times with two TMs that are connected via a loop in the cytoplasm. Blue: first TM. Red: Second TM. Structure figure created with PyMOL 1.3 and PDB entry 1C0V (Girvin et al. 1998).

insertion. Depleting one of the components abolishes insertion into the inner membrane (van Bloois et al. 2004). After integration, the F_1F_o ATPase subunit c assembles into decamers forming the rotor of the F_1F_o-ATPase in the membrane (Jiang et al. 2001).

Phage coat proteins

M13 procoat and Pf3 coat are the major capsid proteins of the bacteriophages M13 and Pf3. Both proteins are inserted into the inner membrane via the YidC-only pathway (Samuelson et al. 2000, Chen et al. 2002 and 2003).

Pf3 coat

Pf3 coat is the major capsid protein of the filamentous bacteriophage Pf3 (see Fig. 6). It requires the proton motive force and YidC for proper insertion into the inner membrane and is independent from the Sec translocase (Kiefer et al. 1997, Kiefer and Kuhn 1999, Chen et al.

2002). It has an N-out/C-in orientation after its insertion into the inner membrane (Welsh et al. 1998, Kiefer and Kuhn 1999). Its orientation in the membrane is dependent on the charged residues in the N- and C-terminal regions. Removing the negatively charged residues at the N-terminus does not inhibit the insertion into the inner membrane via the *E. coli* YidC. However, adding positive charges led to a stop of insertion (Kiefer et al. 1997). A completely charge-free Pf3 coat mutant shows no insertion but a single negative charged amino-acid on either terminus suffices and orients the negatively charged end to the periplasm of the cell (Kiefer and Kuhn 1999).

Fig. 6: Diagram and structure of the hull protein of the filamentous bacteriophage Pf3. The protein spans the membrane once with one TM Blue: TM. Structure figure created with PyMOL 1.3 and PDB entry 1IFP (Welsh et al. 1998).

Klenner and Kuhn (2012) showed that Pf3 coat contacts YidC in TM1, TM3, TM4 and TM5 during insertion. In addition, binding studies with arginine mutants that add a positive charge to the N-terminus revealed, that the substrate was capable to bind to the parts of YidC near the cytoplasmic leaflet. Further towards the membrane core or the periplasmic leaflet no binding could be observed showing that a positive charge cannot be transferred through the membrane via YidC (Klenner and Kuhn 2012).

M13 procoat

M13 procoat is the precursor of the major capsid protein of the M13 phage. It spans the membrane twice and has both termini in the cytoplasm (Kuhn et al. 1986). A detailed view on the M13 phage and its proteins, including M13 procoat, is provided in 1.3 since it plays a central role in this study.

YidC and the Sec translocase

YidC cooperates with the Sec translocon to insert large membrane proteins into the inner bacterial membrane and is associated with the lateral gate of SecY (Scotti et al. 2000, Sachelaru et al. 2013). Crosslinking experiments have shown that YidC binds to the lateral gate of the Sec translocon, where it contacts both sites of the lateral gate through which integral membrane proteins enter the membrane (Sachelaru et al. 2013). A recent study proposes a more invasive interaction of YidC with the Sec channel. Here YidC forms a heterotetrameric complex with SecYEG by entering the pore of SecY and decreasing its diameter. Upon binding of a nascent chain, however, YidC is moved from the pore to the rim of the complex allowing insertion to commence and to interact with the TMs that go through SecY for membrane insertion (Sachelaru et al. 2017). A substrate that requires SecYEG but also contacts YidC during insertion is the cell division protein FtsQ (Scotti et al. 2000, van der Laan et al. 2001).

FtsQ

FtsQ is a single spanning membrane protein with a small cytoplasmic oriented N-terminal domain and a large periplasmic domain (Carson et al. 1991). It is localized in the cell division site of dividing *E. coli* cells and supports the septum formation. Localization to the cell division site is mediated by the periplasmic domain of FtsQ (Chen et al. 1999). Results from Scheffers et al. (2007) indicate that the transmembrane domain also plays a role in the localization of the protein.

Mutants of M13 procoat

An M13 procoat mutant with an elongated periplasmic loop with additional 174 amino acids was found to be YidC and Sec dependent for insertion (Samuelson et al. 2001). Another Sec dependent mutant is the H5EE M13 procoat mutant, where two additional glutamates were mutated into the loop to increase the negative charge. Efficient in vitro insertion into either YidC or SecYEG proteoliposomes still required the membrane potential (Stiegler et al. 2011). Another approach was performed with an M13 procoat-leaderpeptidase (PClep) construct *in vivo*, where residues 220 to 323 of the leader peptidase were fused to the C-terminus of M13

procoat. Increasing the charge of the loop from -3 (wild type) to up to +3 by substituting arginines lead to a gradual decrease of YidC and an increase in Sec dependency. However, adding one additional negative charge into the loop of PC-lep kept the insertion YidC dependent. Mutating a second negative charge into the loop shifted the dependency from YidC towards the Sec translocon in combination with YidC (Soman et al. 2014).

Structure of YidC and its homologues in bacteria and archaea

The *E. coli* YidC is a membrane protein with six TMs and a large hydrophilic domain (P1 loop) between TM1 and TM2 and an N-in/C-in topology (see Fig 9). This large domain is located in the periplasm of the bacterial cell (Sääf et al. 1998). However, known homologues in gram-positive bacteria lack the *E. coli* TM1 and the P1 loop (Hennon et al. 2015). YidC insertion into the inner membrane requires SecYEG, SecA and the bacterial SRP and its receptor FtsY (Koch et al. 2002). In 2014, two YidC structures, from *Bacillus halodurans* and *E. coli,* were solved (Kumazaki 2014a and 2014b).

Structure of YidC2 of *Bacillus halodurans*

One solved structure was the second YidC (YidC2) of *B. halodurans*, showing that the five predicted TMs of the insertase form a hydrophilic groove (see Fig. 7) that is open to the membrane via a hydrophobic slide formed by TM2 and TM4 of the protein. Molecular dynamics simulations predicted that this cavity contains approx. 20 water molecules. An arginine at position 72 (73 in SpoIIIJ, YidC1 of *B. halodurans*) inside the groove is essential for the insertion activity. Mutation analysis showed that only the R73K mutant of SpoIIIJ is capable of complementing in the YidC depleted cells. All other substitutions lead to a loss of function (Kumazaki et al. 2014a, Shimokawa-Chiba et al. 2015). The surface of the cavity contains hydrophilic amino acids that provide the hydrophilic environment. By substituting selected positions with hydrophobic amino acids like alanine or leucine, the function of YidC is reduced (Shimokawa-Chiba et al. 2015).

Gram-negative bacteria generally only possess one YidC gene whereas many gram-positive bacteria encode for two (Chiba et al. 2009). In *Bacillus subtilis,* it was discovered that the level

of expression of YidC2 is regulated over the activity of SpoIIIJ as a way to upregulate the insertion capability of the cell if necessary. If sufficient SpoIIIJ is present in the cell the expression of YidC2 is downregulated via the insertion of the "membrane protein insertion and folding monitor" (MifM) protein, which is encoded upstream of the YidC2 gene. As long as MifM is correctly inserted, a hairpin structure in the mRNA blocks the access to the Shine-Dalgarno sequence of YidC2. If not enough active SpoIIIJ is present the hairpin is unfolded by the ribosome and the translation of MifM is stalled. This allows recognition and translation of YidC2 and therefore upregulation of the membrane insertion capacity of the cell (Chiba et al. 2009).

Structure of the *E. coli* YidC

Shortly after the structure of the *B. halodurans* YidC2 has been published, the structure of the *E. coli* YidC has been solved. The similarity of both structures is very high (see Fig. 9). The *E. coli* YidC also forms a hydrophilic cavity with TM2 to TM6 (homologous to TM1 to TM5 in *B. halodurans* YidC) with the conserved arginine at position 366 in its center (see Fig. 7). However, unlike the arginine in the *B. halodurans* YidC, its presence in the hydrophilic groove of the *E. coli* YidC is not essential for functionality and can be replaced by several other amino acids like alanine, cysteine, lysine and leucine. The negatively charged glutamic and aspartic acid are not capable of restoring functionality (Kumazaki et al. 2014b, Chen et al. 2014). The C1-loop of YidC plays an essential role for cell viability. It was shown, that deletion of the second half of the C1 loop, residues 399 to 415, impairs the functionality of YidC. However, alanine substitutions showed that the precise sequence of the loop is not important as long as the hairpin is intact (Chen et al. 2014). Before the structure of the *E. coli* YidC was known a model of YidC was proposed. Molecular dynamics (MD) simulations showed that this model is stable and consistent with the structure of the *B. halodurans* YidC. On basis of this model several discovered stabilizing residues were mutated to alanines and two positions, 362 and 517, led to an inactivation of YidC. Another feature of the molecular model in simulation was an observed thinning of the membrane during simulation with the strongest effect near TM3 and TM5 (Wickles et al. 2014).
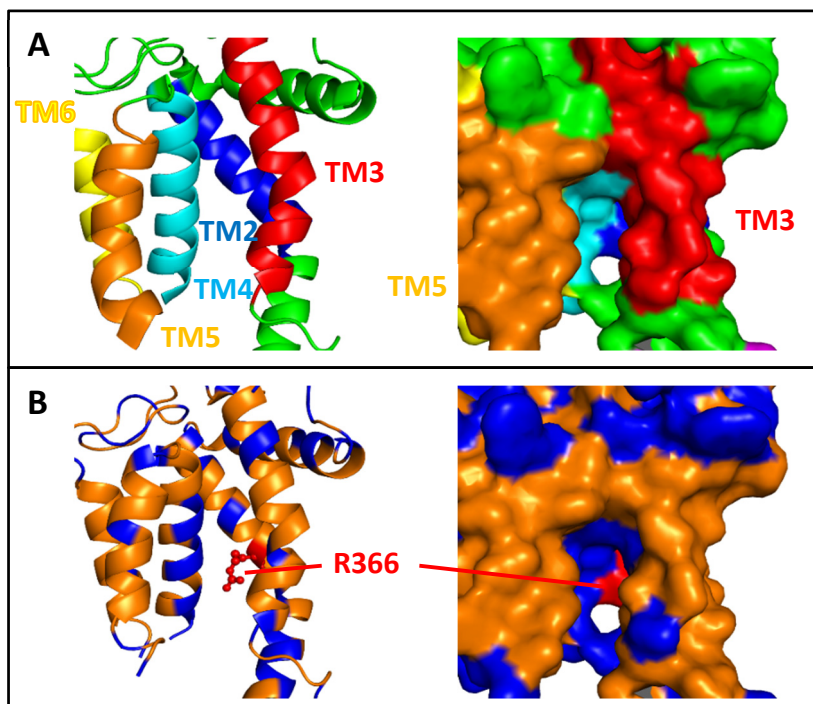
Fig. 7: Hydrophilic groove of YidC. (A) Cartoon and surface rendering of the TM region of YidC. Red/blue/yellow/orange/cyan: TMs of YidC **(B)** Rendering of the same perspective with the hydrophobic (orange) and hydrophilic (blue) amino acids colorized. The hydrophilic groove inside of the YidC structure can be observed, with the arginine at position 366 (red) in its center. Figures created with PyMOL 1.3 and PDB entry 3WVF (Kumazaki et al. 2014b).

During the insertion conformational changes take place in YidC. Imhof et al. (2011) showed that residues 332, 334, 354, 454 and 508 undergo environmental changes when Pf3 coat was bound to YidC, indicating structural changes for these positions. For the cotranslational insertion Kedrov et al. (2016) discovered that binding of a ribosomal nascent chain of the subunit c of the F_1F_o ATPase led to conformational changes in TM2, TM3 and the amphipathic helix EH1 of YidC that result in a widening of the hydrophilic groove. The RNC of subunit c was found between TM3 and TM5. EH1 moves towards the membrane core and it was proposed, that this further amplifies the membrane thinning effect that was predicted before by Wickles et al. (2014), which in return would make it easier for substrates to leave the groove and be inserted into the membrane (Kedrov et al. 2016).

YidC homologue in archaea

In 2015, the first homologue in archaea was discovered. The protein Mj0480, a member of the DUF proteins, has a low overall sequence identity of approx. 14% but shows common features

in the secondary structure despite being a lot smaller. The crystal structure reveals a small transmembrane protein with three TMs. Here the TMs form, like in YidC, a hydrophilic groove that is open toward the membrane core (see Fig. 9). The C1 loop could not be crystallized but is predicted to form a coiled coil structure similar to the bacterial homologues. It was shown, that Mj0480 is capable of binding ribosomal nascent chains (RNCs) in *E. coli*. With its much smaller size and fewer structural features, this newly discovered small insertase is considered the necessary minimal core for a functional YidC homologue (Borowska et al. 2015, Dalbey and Kuhn 2015).

Current insertion model for the YidC-only pathway

Along with the structure Kumazaki et al. (2014a) published an insertion model for single spanning substrates based on the structural features and functionality studies performed with SpoIIIJ was proposed. Due to the positive charge in the groove being essential for the YidC functionality in *B. halodurans* an attraction between the negative charged terminus of the substrate and the arginine at position 72/73 was indicated that could support the interaction with the hydrophilic groove. The insertion model is shown in Fig. 8 (Kumazaki et al. 2014a).
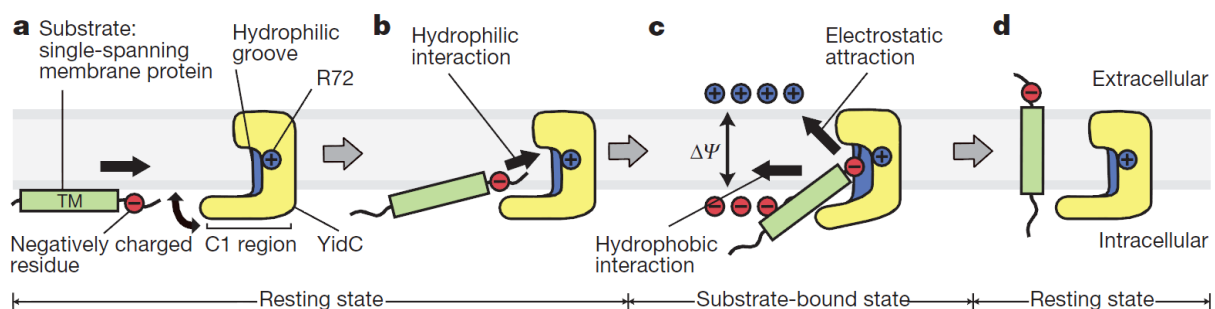
Fig. 8: Insertion model for single spanning substrates. (a) The substrate is a single spanning membrane protein with a negative charge at one of its termini. **(b)** The substrate interacts with the C1 loop of YidC and is moved towards the hydrophilic groove. **(c)** The charged terminus enters the hydrophilic groove. **(d)** Release of the substrate into the membrane via electrostatic attraction to the positively charged periplasmic membrane surface. Model and figure by Kumazaki et al. (2014a)
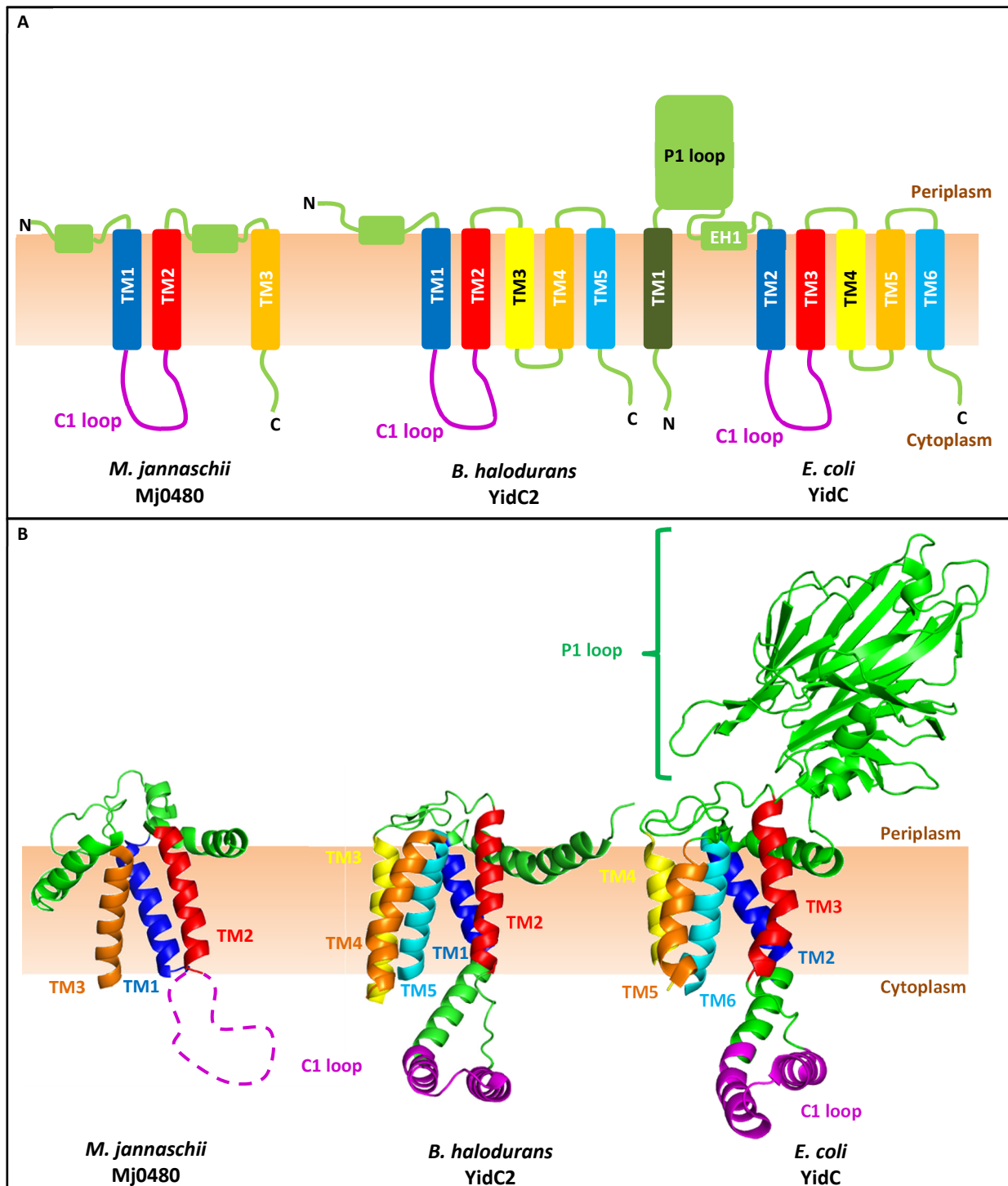
Fig. 9: Topology and structures of the YidC homologues in archaea and bacteria. (A) Topology of the YidC homologues Mj0480 (*M. jannaschii*), YidC2 (*B. halodurans*) and YidC (*E. coli*). The archaeal Mj0480 has three TMs while the bacterial homologues have five to six TMs. All homologues share the C1 loop that is located in the cytoplasm near the membrane surface. The first TM of the *E. coli* YidC is connected via a big P1 loop in the periplasm. **(B)** Structures of the homologues. The TMs form a hydrophilic groove that is open to the membrane core. Orange and red: TMs that form the entrance to the hydrophilic region inside the protein. The C1 loop from *E. coli* is, compared to *B. halodurans* YidC2, more tilted. Red/blue/yellow/orange/cyan/dark green: TMs of the homologues, EH1: amphipathic helix of YidC, magenta: C1 loop. Figures created with PyMOL 1.3 and PDB entries 5C8J (modified, Borowska et al. 2015), 3WO6 (Kumazaki et al. 2014a) and 3WVF (Kumazaki et al. 2014b).

1.2.3.2 Oxa1

oxa1 is a nuclear gene that encodes for Oxa1p, an integral membrane protein and insertase in the inner membrane of mitochondria. In *Saccharomyces cerevisiae*, the precursor pOxa1p is 402 amino acids in length (42 kDa) and is imported into the mitochondrial matrix in an mt-HSP70 dependent manner, which requires an existing membrane potential (Bonnefoy et al. 1994, Herrmann et al. 1997). The N-terminus contains a cleavable mitochondrial matrix-targeting signal with the cleavage site between residues 42 and 43 that is cleaved in the matrix by the mitochondrial processing peptidase (MPP) prior to insertion into the inner membrane (Herrmann et al. 1997). The mature protein, with a length of 360 residues (36 kDa) is then inserted into the inner mitochondrial membrane via already present mature Oxa1p (mOxa1p) (Hell et al. 1998).

S. cerevisiae **mOxa1p**
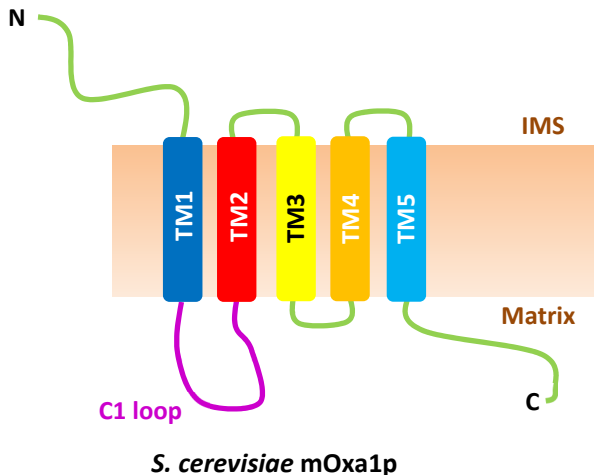
Fig. 10: Topology of mOxa1p of *S. cerevisiae*. The core of the insertase is formed by five TMs. The N- and C-termini are relatively long and contain the majority of the charged amino acids. (Bonnefoy et al. 1994, Wang et al. 2011).

The inserted protein spans the membrane five times with a N_{out}-C_{in} topology (see Fig. 10) sharing the homologous five core TMs of this insertase family. Following the "positive inside rule" the loops in the matrix and the C-terminus are positively charged while the loops in the inter membrane space (IMS) and the N-terminus are negatively charged (Herrmann et al. 1997, Wang and Dalbey 2011).

mOxa1p is essential for cell viability in *S. cerevisiae*. It is responsible for the co-translational insertion of subunit II of the cytochrome oxidase (pCoxII) and exports the N- and C-termini into the IMS (Hell et al. 1997). Truncating the long C-terminus of mOxa1p leads to an accumulation of pCoxII in the matrix indicating its important role for protein insertion of mitochondrial encoded membrane proteins. Additionally Cox3 and cytochrome b, two other substrates of mOxa1p, also are not inserted with the truncated variant, indicating a general role of the C-terminus for substrate integration. However, posttranslational integration of nuclear encoded proteins, like mOxa1p itself or Cox18, is not impaired by the truncation.

Fractioning in sucrose gradients of wild type and truncated mOxa1p showed that only the intact insertase associates with ribosomes, indicating that the C-terminus plays an important role in ribosome binding and co-translational insertion. It was also shown, that a ribosomal nascent chain (RNC) is not required for this interaction (Szyrach et al. 2003).

1.2.3.3 Alb3

Alb3 was discovered in *Arabidopsis thaliana* with the maize transposon Ac/Ds as a tool for insertional mutagenesis. During the experiments, several plants showed an albino phenotype and one was determined Alb3. Further investigation showed that this mutation is recessive and that therefore only homozygous plants are showing albinism (Long et al. 1993). Alb3 is nuclear-encoded and further research revealed, that the Alb3 locus encodes for a protein that has similarities to Oxa1p in

Fig. 11: Predicted topology of Alb3. Similar to Oxa1 five TMs are predicted for the general topology of Alb3. The N- and C-termini are relatively long and contain the majority of the charged amino acids. L1 and L2: Loops in the Lumen of the chloroplast. S1 and S2: Loops in the Stroma. (Falk et al. 2010).

yeast and YidC/SpoIIIJ in *E. coli* and *B. subtilis* respectively. It was also shown, that, despite the similarities, it does not share the same functionality in the cell as mOxa1p since it is not involved in the biogenesis of cytochrome oxidase in chloroplasts. Via immunogold labeling with an anti-Alb3 antibody it could be shown that Alb3 is localized in chloroplasts, mainly in the thylakoid membranes (Sundberg et al. 1997). The protein spans the membrane five times with a N_{out}-C_{in} topology (see Fig. 11) sharing the homologous five core TMs of this insertase family (Falk et al. 2010).

Alb3 can work together with the chloroplast SRP (cpSRP) to integrate proteins into the thylakoid membrane. This was shown for the post-translational integration of the light harvesting chlorophyll-binding protein (LHCP) in pea chloroplasts. Here, integration of the LHCP was only facilitated when Alb3 was not blocked by bound Alb3-antibodies. The targeting to Alb3 is performed by cpSRP and chloroplast FtsY (cpFtsY) in a posttranslational manner and

requires GTP (Kogata et al. 1999, Tu et al. 1999, Moore et al. 2000). Unlike the bacterial SRP the cpSRP is a trimer that consists of two subunits of cpSRP43 and one subunit of cpSRP54 and does not contain RNA (Schuenemann et al. 1998, Tu et al. 1999). Alb3 recruits the cpSRP-LHCP complex with bound cpFtsY by interacting with cpSRP43 with its C-terminus. The C-terminus goes from an unfolded to a folded state during this interaction and cpSRP-LHCP binds to Alb3 followed by integration of LHCP and dissociation of the complex. This insertion is independent from the chloroplast Sec-system (Falk et al. 2010, Hennon et al. 2015). However, it has also been shown that Alb3 can be associated with chloroplast SecY (cpSecY) which suggests a possible cooperation between these proteins (Klostermann et al. 2002, Pasch et al. 2005). Interestingly, Alb3 is capable to complement in YidC deficient *E. coli* cells restoring cell growth (Jiang et al. 2002).

1.3 The M13 bacteriophage

The M13 bacteriophage is a member of the genus *Inovirus*. Members of this genus are filamentous bacteriophages that show high similarities in their structure. The differences between the M13 bacteriophage and several other members of the genus, namely fd and f1, are extremely low. Therefore, these phages are considered identical for most purposes. While fd was mostly researched for its structural properties, the bacteriophages M13 and f1 were used for physiological and genetic studies (Marvin et al. 2014).

The M13 bacteriophage was first isolated in Munich in 1963 from purified sewage water. It was also discovered that the phage was only able to infect male *E. coli* cells harboring the genes for the F-pilus for horizontal gene transfer. Electron microscopy showed flexible filamentous phages (Hofschneider 1963).

1.3.1 Phage genome

The genome consists of circular positive single stranded DNA (ssDNA (+)) (Hofschneider 1963, Rasched and Oberer 1986, Rakonjac 2012) with a length of 6407 bases that have been completely sequenced. Compared to the closely related filamentous bacteriophage fd the genome shows only a difference of 3% in the DNA sequence and 1 base in size, the M13 genome being the shorter one. Only 12 of these substitutions lead to changes in
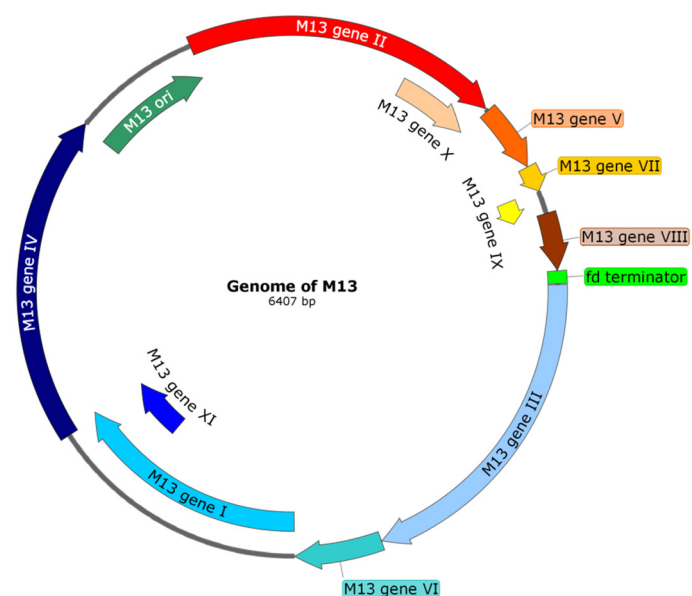
Fig. 12: Map of the genome of the M13 bacteriophage. The genome is organized in 2 operons. Genes II, X, V, VII, IX and VIII are transcribed on one (red colors) while the genes III, VI, I, XI and IV are transcribed on the other (blue colors). Sequence from NCBI (Ref. Seq. NC_003287.2). Map created with SnapGene Viewer.

the amino acid sequence of viral proteins. Most of the differences however were found in the last base of a codon resulting in no difference in the primary structure of the protein (van Wezenbeek et al. 1980). The circular ssDNA (+) forms 2 loops at its ends. One of them creates

a hairpin structure that contains the packaging signal that initiates the phage assembly in the inner membrane (Day et al. 1988, Rakonjac 2012). In the assembled phage only approx. 25% of the DNA forms nucleotide pairs due to the lack of complementarity in the ss-DNA (Rakonjac 2012).
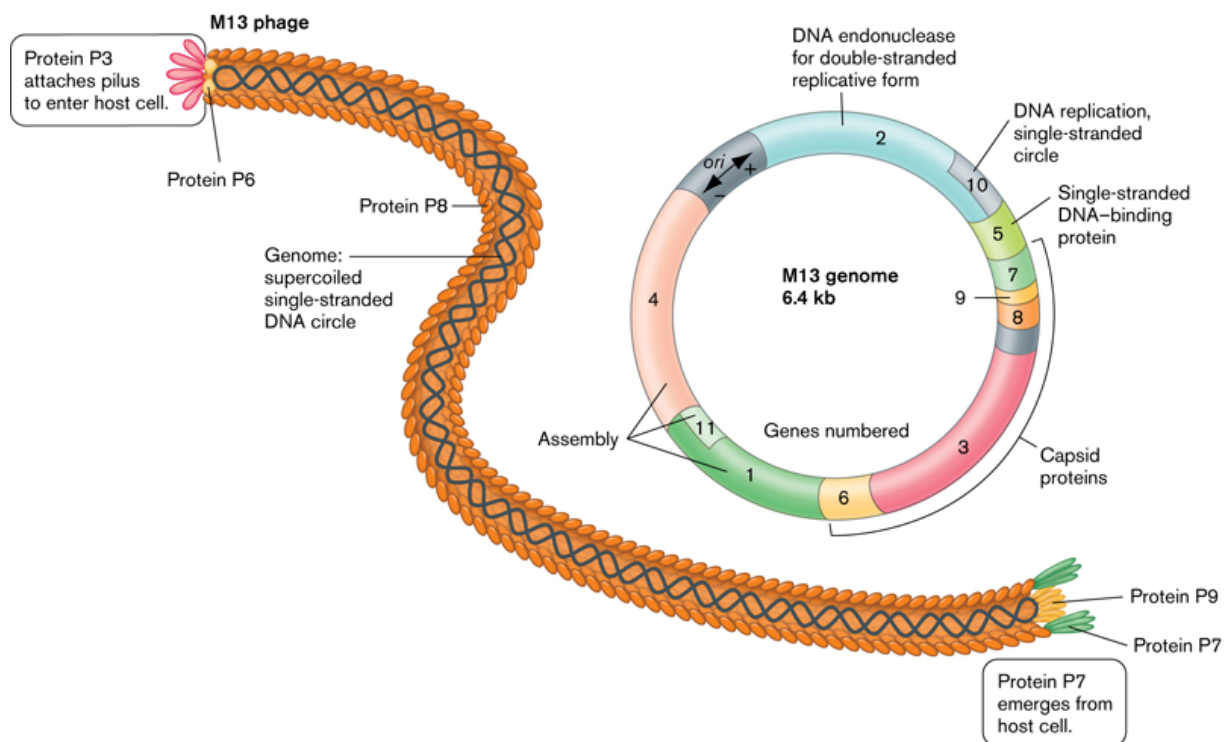
Fig. 13: The M13 phage structure and genome. The circular ss-DNA is coiled and encapsulated in the mature major capsid protein pVII (p8). p3 (pIII) and p6 (pVI) form the tip responsible for pilus attachment. p9 (pXI) and p7 (pVII) form the other tip that starts phage assembly and leaves the cell first during extrusion of the particle. Numbers on the plasmid represent the genes I to XI on the viral genome (Slonczewski and Foster 2010)

The DNA contains 11 genes (I to XI) that encode proteins for different purposes (see Fig 12 and 13). The genome is organized in two operons, one containing the genes II, V, VII, IX and VIII and the other III, VI, I and IV. Protein X (pX) is a truncated translation product of gene II and protein XI (pXI) of gene I respectively (Russel and Model 2006, Raconjak 2012). The start of Gene XI overlaps by one base with the end of gene VII and also by one base with the start of gene VIII. Furthermore, 20 bases of the starting region of gene IV overlap with the end of genes I and XI without being in frame though (van Wezenbeek et al. 1980).

1.3.2 Phage structure

The bacteriophage M13 has a size of approx. 900 nm in length and a diameter of 6-7 nm in the shape of a long flexible rod (see Fig 13) (Rakonjac and Model 1998, Russel and Model 2006). Structural proteins are the products of genes III (pIII), VI (pVI), VII (pVII), VIII (pVIII) and IX (pIX) with pVIII being the major coat protein of the M13 phage while the rest are minor coat proteins (Endemann and Model 1995, Marvin et al. 2014). Mature pVIII encapsulates the viral circular ssDNA (+) with approx. 2700 copies. The minor capsid proteins pIII and pVI, 5 copies each per phage particle, are mediating the absorption to the F-pilus and are located at the base of the phage that is formed at the end of the assembly (Simons et al 1981, Gray et al. 1981). pIII and pVIII are both synthesized as precursors and are processed into their mature form after membrane insertion with the C-terminus reaching into the cytoplasm (Russel and Model 2006). pVII and pIX form the tip of the phage with 3 copies per particle. It also contains the DNA with the packaging signal and is the starting point of the phage assembly in the inner bacterial membrane (Simons et al 1981, Russel et al. 1989).

The proteins of genes II (pII), V (pV) and X (pX) are responsible for phage replication. Protein II (pII) is a endonuclease that plays a role in the "rolling circle" DNA replication (Rakonjac 2012). pX is important for accumulating ssDNA (+) for the phage assembly and functions as an inhibitor for pII (Fulford and Model 1988). Protein V (pV) binds to viral ssDNA (+) in large numbers, forming a pV-ssDNA (+) complex that initiates the phage assembly. The concentration of pV in the bacterial cells also functions as an indicator for the start of the assembly (Rakonjac 2012).

Protein I (pI), IV (pIV) and XI (pXI) play an important role in the phage assembly and secretion. pI and pXI form a complex in the inner cell membrane that mediates the assembly of the phage. Both proteins are indispensable for this function (Rapoza and Webster 1995, Haigh and Webster 1999). pIV is located in the outer membrane and forms a secretin with 14 monomers, that has an inner diameter of 80 angstroms. This secretin allows the extruding phage particle to pass through the outer membrane (Linderoth et al. 1997). The assembly of phage particles requires the proton motive force and ATP (Feng et al. 1997).

1.3.3 Infection of *E. coli*

The M13 phage needs the F-pilus for infection of the host cell (Hofschneider 1963, Russel et al. 1997). This property is also shared with the closely related bacteriophages fd and f1 (Russel et al. 1997, Marvin et al. 2014). Binding of the phage particle to the tip of the F-pilus of the host cell occurs via pIII that is located at the base of the phage (Armstrong et al. 1981). This binding protein is associated with the minor coat protein

Fig. 14: Binding of M13 phage to an *E. coli* cell. The pIII protein contains multiple domains (D1 and D2) that play different roles during the infection. D2 binds to the F-pilus of the cell causing the F-pilus to retract. Then D1 binds to TolA, an important anchor of the *E. coli* cell envelope, and facilitates the insertion of the phage ssDNA (+) via an unknown mechanism (modified from Slonczewski and Foster 2010, Deng et al. 1999)

pVI that is found between pIII and the capsid forming pVIII (see Fig. 14) (Simons et al 1981). Two N-terminal domains of pIII, D1 and D2, play an important role in phage binding and infection. D1 is comprised of the residues 1 – 66 of pIII while D2 is from residue 86 - 216, separated by a glycine-rich linker. D2 binds to the F-pilus which consequently retracts causing the phage to get closer to the cell. This allows the D1 domain to bind to TolA, an important anchor of the *E. coli* cell envelope, to initiate the infection. The DNA is then inserted into the host cell by a yet unknown mechanism (Deng et al. 1999, Russel and Model 2006). Interestingly, unlike other bacteriophages like T4 the M13 phage does not stay intact outside the host cell after infection. Its capsid proteins are partitioned into the inner membrane of the *E. coli* cell and are reused for the newly formed phage during assembly (Armstrong et al. 1983). It has also been shown, that no insertion of pVIII and a massively reduced efficiency in infection occurs when parts of the Tol complex are deleted. It was therefore suggested that

the Tol complex plays a role in DNA insertion into the cell and that pVIII might also be involved (Click and Webster 1998).

1.3.4 Phage replication and assembly

Phage DNA is replicated by a rolling circle mechanism. After the ssDNA (+) has entered the *E. coli* cell, the *E. coli* RNA polymerase binds to a hairpin in the DNA and synthesizes a RNA primer. This primer allows the DNA polymerase III to bind and synthesize the second strand of the DNA forming the replicative form of the DNA (RF). pII binds to the double stranded viral DNA and nicks it in the + strand origin region, the 3' end serves as a primer for the DNA polymerase III and a copy of the + strand is synthesized. At the end of the synthesis pII closes the new DNA strand and releases the old ssDNA (+) resulting in an intact RF DNA and one free + strand (Russel et al. 1989, Rakonjac 2012). The RF DNA serves as template for the expression of the viral proteins. In early stages of the infection more RF DNA is synthesized while later on, when larger amounts of pV are available, more of the DNA is bound as pV-ssDNA (+) complex for phage assembly (Rakonjac 2012).
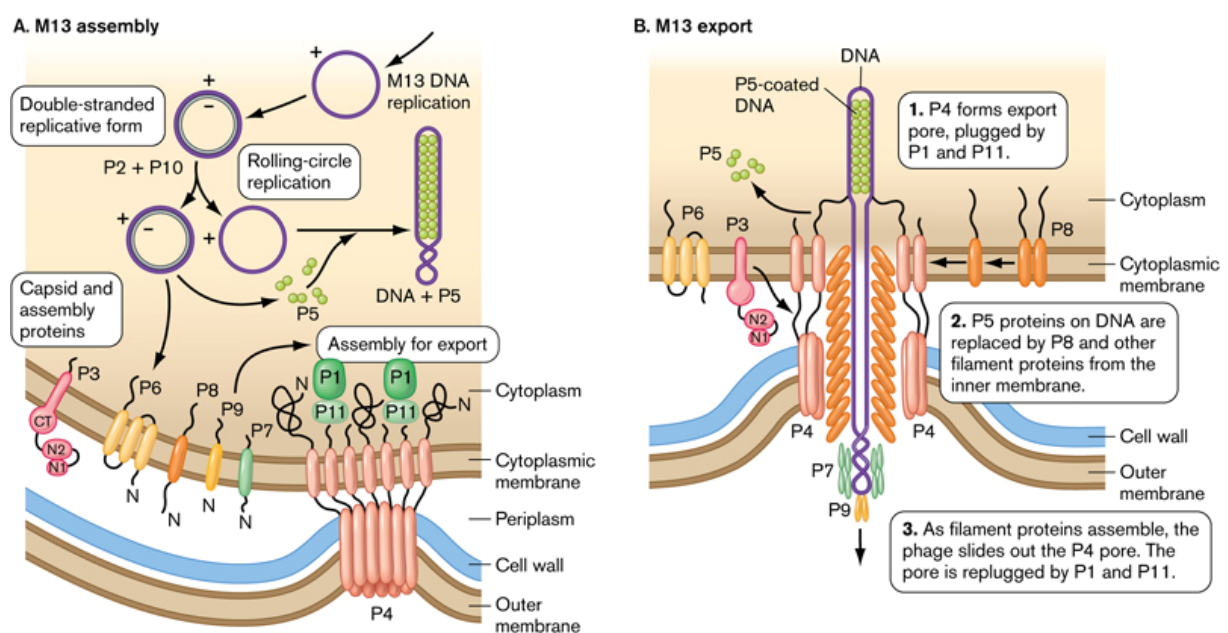
Fig. 15: Assembly and export of M13 phages from *E. coli* cells. (A) Assembly of phages. ssDNA (+) is either used to generate the RF form of the DNA for protein expression or to replicate additional ssDNA (+) strands for the phage assembly. The pV bound ssDNA (+) is brought to the pI/pXI complex at the inner membrane and the assembly is initiated. **(B)** pVII and pIX form the first tip that includes the packaging signal. pVIII is added from the inner membrane to the phage DNA replacing pV in the process. (Slonczewski and Foster 2010)

Prior to assembly, all structural proteins are inserted and located in the inner bacterial membrane (Endemann and Model 1995). The phage assembly is initiated by the interaction of pVII and pIX with the packaging signal on the ssDNA (+) (Russel et al 1989, Rakonjac 2012). From this point on, while being extruded through the pI/pXI complex in the inner membrane and the pVI secretin in the outer membrane, mature pVIII is replacing pV on the viral DNA and completely covering the viral DNA, forming the capsid of the virion (see Fig. 15) (Linderoth et al. 1997, Rakonjac 2012). At the base of the phage pVI and pIII are attached which leads to the termination of the assembly and the release of the completed particle (Rakonjac et al. 1999, Rakonjac 2012).

In molecular biology, many applications have been found for M13 phages. Its genome was used as cloning vector and could be multiplied either by normal double stranded replication or by repackaging of single stranded phage vectors in particles. The latter is achieved with the origin of replication being present on the vector, including the packaging signal. This allows, with a helper phage to complement missing genes, to form phages that contain the normal genome and phages with the desired plasmid encapsulated inside of them. Another application is the phage display, where a coat protein is fused with parts of a protein of interest to check for interaction partners inside of a culture (Rakonjac et al. 2012).

1.3.5 The major capsid protein pVIII

The gene for M13 procoat is positioned from base 1301 to 1525 in the viral genome (Wezenbeek et al. 1980). It encodes a 73 amino acid long peptide that is comprised of a leader peptide of 23 amino acids and the mature coat protein of 50 amino acids in length (Banner et al. 1981, Hunter et al. 1987). It requires YidC and the membrane potential for proper insertion (Samuelson et al. 2001, Stiegler et al. 2011)

Membrane targeting is mediated via positive charged residues at the N- and C-terminus of pVIII, most likely interacting with the negatively charged phospholipid heads of the membrane (see Fig. 16). Removing these charges leads to a loss of insertion of the protein *in vitro* (Gallusser and Kuhn 1990). The negative charge of the loop is not mandatory to facilitate insertion in *E. coli*. Interestingly, the stronger the negative charge is in the loop, the more important is the role that the membrane potential plays in the insertion of M13 procoat. It
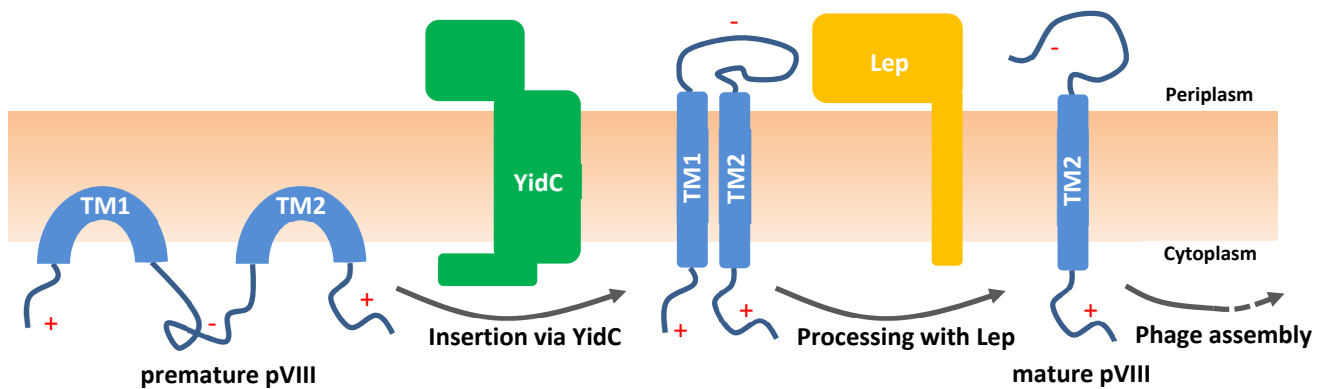
Fig. 16: pVIII insertion and processing in the inner membrane. pVIII procoat binds to the membrane and is then inserted via the YidC pathway. After insertion pVIII is processed into its mature form by the leaderpeptidase (Lep), cleaving off TM1. The mature protein can then be used for phage assembly. +/- charge of the respective part of the protein (Mandel and Wickner 1979, Gallusser and Kuhn 1990, Nagler et al. 2007, Rakonjac et al. 2012).

was also shown that YidC is important for the insertion, but not for the targeting of pVIII to the membrane (Samuelson et al. 2001). After binding to the membrane, pVIII is inserted via the YidC insertase pathway (Samuelson et al. 2000). M13 procoat does not require the bacterial SRP for insertion and only interacts with the membrane after release from the ribosome (de Gier et al. 1998). The leader peptide is cut off by the leader peptidase after insertion into the inner membrane.

Approximately 2700 copies of processed pVIII form the capsid of the M13 bacteriophage (Mandel and Wickner 1979, Hunter et al. 1987, Banner et al. 1981). Insertion studies with temperature sensitive *E. coli* strains for the proteins SecA and SecY showed that M13 procoat inserts independently from the Sec translocase system (Wolfe et al. 1985).

Mature pVIII forms a hydrophobic α-helix from residues 6-48 that interacts with the helices from neighboring pVIII. The capsid itself is formed by pentamers of pVIII. These pentamers are stacked on top of each other rising the height of the capsid by 16.6-16.7Å per level. The right-handed tilt that occurs has an angle of 36.1-36.6°. The structure is stabilized by strong hydrophobic interactions between the α-helices in-between the monomers and the pentamers respectively (see Fig.17 and 18) (Morag et al. 2015).
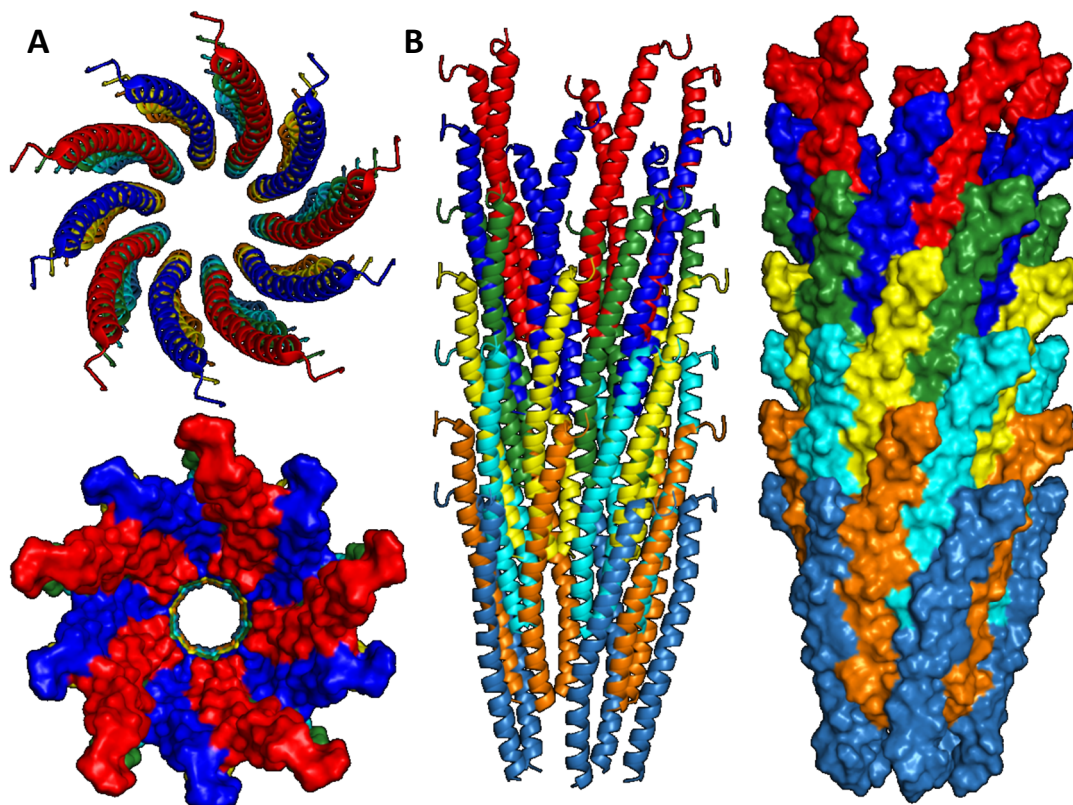
Fig. 17: Structure of the M13 phage capsid. Each color represents one pentamer aligned in one plane. **(A)** Top view in the capsid, showing the pentameric symmetry of the capsid and the cavity that holds the DNA in the assembled phage. The right handed tilt of the monomers along to the viral axis is also visible. **(B)** Side view of the capsid. The stacking of the pentamers is visible. Figures created in PyMOL v. 1.3 with PDB entry 2MJZ (Morag et al. 2015)

Complementation studies were performed with mutated M13 procoat protein. Different classes (I to V) of mutants were obtained, that had different influence on phage assembly. The class III mutants (see Tab. 1) showed that the positions -1, -3 and -6 play an important role for the processing of pVIII to its mature form. Mutations in these positions lead to insertable but not cleavable protein. The H10 mutant of M13 procoat has an amino acid change from Ala to Thr at position -1, H5 from Ser to Phe at position -3 and H9 from Pro to Ser at -6 (Kuhn and Wickner 1985b). The H5 mutant, with its property of being uncleavable by the leader peptidase, will be of importance in this work later on.
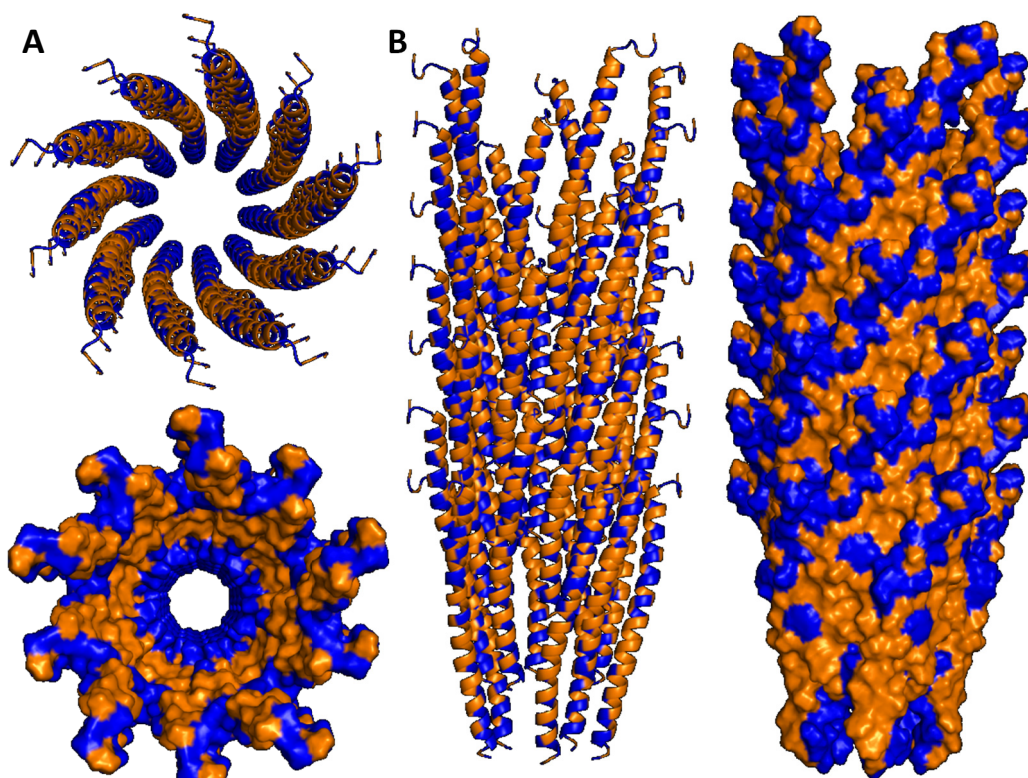
Fig. 18: Hydrophobicity and hydrophilicity in the M13 capsid. (A) Top view in the capsid. The inner layer of the capsid is coated with hydrophilic residues creating a suitable environment for the viral DNA. The core between inner and outer layer is hydrophobic, stabilizing the capsid via hydrophobic interactions of the mature pVIII monomers. **(B)** Side view on the capsid. The outside is also partly layered with hydrophilic amino acid residiues. Blue: Hydrophilic amino acids. Orange: hydrophobic amino acids. Figures created in PyMOL v. 1.3 with PDB entry 2MJZ (Morag et al. 2015)

A different approach was tried later by single substitutions of amino acids with cysteines in the two transmembrane regions of M13 procoat. Most of the tested mutants showed no

Tab. 1: Different pVIII mutants and their behavior. Different mutants of pVIII have been generated and tested for their functionality (Kuhn and Wickner 1985a and 1985b).

Class	Mutant	Behaviour
I	H3	No expression
II	H4	Fast degradation in the cells
III	H10, H5, H9	No processing to the mature pVIII due to mutations at postion -1, -3 and -6 in the leader peptide
IV	H1	No plaque formation
V	H7	No plaque formation

difference in cell growth or procoat insertion into the inner membrane. However, some mutants in the leader peptide, at the position -6, -10 and -12, influenced the growth of the cells. -10C and -12C stalled the growth of the culture while the -6C mutant even lead to cell lysis 2 hours after of induction. -6C also impeded the processing with the leader peptidase to M13 coat (Nagler et al. 2007).

Chen et al. (2003) created temperature sensitive mutants of YidC that treated M13 procoat and Pf3 coat differently during insertion, which indicates differences in the structural or functional requirements for the proper insertion of these proteins.

1.4 Disulfide crosslinking of proteins

Transient interactions that do not involve the formation of covalent bonds can be observed by artificially binding the interacting partners to each other. Various methods exist that promote the formation of protein-protein complexes, even at specific positions in both interaction partners. This generates structural data that give further insight into the interaction itself (Trakselis et al. 2005).

Natural formation of disulfides in proteins is one way cells protect and stabilize proteins that must function in the extracellular environment. These bonds restrain the protein backbone and increase its resistance against denaturation or degradation (Bulaj 2005). Artificially introducing a disulfide bond into a protein in a specific position can increase its stability, which has been shown for a thermolysin-like protease from *Bacillus stearothermophilus*. Here one additional disulfide bond increased the stability of the protein significantly (Mansfeld et al. 1997). Another important field is the mapping of protein-protein interactions. This is done by substituting amino acids with cysteines in specific positions of the interaction parters followed by oxidation with a crosslinking agent (Greene et al. 2007, Klenner and Kuhn 2012, Neugebauer et al. 2012).

Disulfide crosslinking requires two thiol groups in close proximity and an oxidative environment to promote the formation of a covalent bond between the two sulfur atoms (see Fig. 19). This also depends on the accessibility of said thiol groups, which is influenced by the folding state and general structure of the involved proteins (Creighton et al. 1995).

$$2\ \text{R-S-H} + \tfrac{1}{2}\ O_2 \xrightarrow{\text{Cu-P}} \text{R-S-S-R} + H_2O$$

Thiol   Oxygen   Disulfide   Water

Fig. 19: Disulfide formation with copper phenanthroline as example. Copper phenanthroline functions as a catalyst that promotes the formation of the disulfide bond. Oxygen is required to catalyze the reaction constantly. Cu-P: copper phenanthroline (Kobashi 1968).

Copper phenanthroline is one of several crosslinking agents for disulfide formation between macromolecules. Falke and Koshland (1987) used disulfide crosslinking to investigate the flexibility and functionality of the *E. coli* aspartate receptor. Klenner and Kuhn (2012) successfully mapped contact sites between YidC and the Pf3 coat protein and Neugebauer et al. (2012) successfully crosslinked MscL to YidC. Greene et al. (2007) mapped the oligomeric state and importance of single residues of *E. coli* TatA. The reaction is catalyzed over several minutes by copper phenanthroline (Kobashi et al. 1968).

Iodine is also used for crosslink formation between proteins *in vitro* (Hughson et al. 1997) and *in vivo* (Lee et al. 1995, Hughson et al. 1997). Since iodine does not work as a catalyst but as a reagent, the formation of the disulfide occurs in a very short period of time and the amount of crosslinking product is limited to the amount of iodine that is used (Hughson et al. 1997).

DTNB (Bis(3-carboxy-4-nitrophenyl) disulfide), also known as Ellman's reagent, is a reagent that is originally used to quantify thiol groups (Ellman et al. 1959). Wickles et al. (2014) used DTNB to successfully crosslink RNCs of the subunit c of the F_1F_o ATPase of *E. coli* to YidC *in vitro* and Park and Rapoport (2012) crosslinked SecY to OmpA-GFP *in vivo*.

Other crosslinking methods

Aside from the disulfide crosslinking, other methods exist that allow the formation of stable complexes between proteins. Two are mentioned here.

Amine reactive crosslinkers use amine groups to form bridges between primary amines and/or lysines with a certain length that depends on the used reagent. A commonly used reagent is disuccinimidyl suberate (DSS) (Haniu et al. 1993, Zybailov et al. 2013). Another reagent, glutaraldehyde, was used by Szegedi and Garrow (2004) to analyze the oligomeric state of a Betaine-homocysteine methyltransferase (BHMT) by crosslinking lysine residues on the surface of the adjacent proteins with each other.

Photo reactive crosslinking agents form a covalent bond upon activation via UV radiation. This adds an extra layer of control to the experiment since the reaction won't start without the UV activation. (Trakselis et al. 2005). p-benzoyl-L-phenylalanine (pBpa) is a non-natural photo reactive amino acid, that can be incorporated at specific positions into proteins via an amber codon and the corresponding amber suppressor tRNA and aminoacyl-tRNA synthetase (Hino et al. 2007). Upon activation with UV radiation pBpa binds to the next polypeptide chain in an unspecific position (Hino et al. 2005). Another approach is the synthesis of a photoactive ATP analogue that can be used to crosslink two protein tyrosine kinases to each other. Here, the crosslinking agent is not built in one of the crosslinking partners but added to the purified interacting proteins (Parang et al. 2002). Cysteines can also be used to bind a photo crosslinking agent to specific positions prior to activation and crosslinking. 4-maleimidobenzophenone (8.6–11.4 Å span) was used to crosslink two proteins of the DNA repair system of *E. coli* by modifying a single cysteine mutant with the reagent and afterwards crosslinking it to a wildtype/cysteine free mutant of the interaction partner under UV light exposition (Giron-Monzon et al. 2004).

1.5 Aim of the study

YidC as an essential membrane protein in bacteria has been a target for extensive research over the past decades. Its role as an insertase and chaperone for other small proteins has been well studied by now. However, the mechanism itself is still unknown, only models based on structural and crosslinking data have been published so far. This work wants to expand the available data for the YidC-substrate interaction in different ways.

The first part is the interaction of M13 procoat with YidC, mapped via *in vivo* disulfide crosslinking. Data of already available contact sites of other substrates like Pf3 coat (Klenner and Kuhn 2012) and few in MscL (Neugebauer et al. 2012) influenced the choice of mutants that were picked for these experiments. However, M13 procoat has distinctive features compared to the other tested substrates, which might also change the way YidC interacts with it during insertion. Chen et al. (2003) showed that YidC treats Pf3 coat and M13 procoat differently during the insertion process. Compared to Pf3, M13 procoat has two TMs and a loop region that have to pass through the membrane core. The signal peptide of M13 procoat is cleaved off by the leader peptidase after insertion, a feature not shared by Pf3 coat or MscL. During this study, Kumazaki et al. (2014b) published the crystal structure of the *E. coli* YidC, which had a significant impact on the investigation of the insertion of M13 procoat with YidC. The hydrophilic groove and the structure of the C1 loop of YidC are intriguing features of the insertase that need to be analyzed for possible interactions with M13 procoat. A proposed insertion model (Kumazaki et al. 2014a) and the structure itself suggest an important role for these regions of YidC for the interaction with its substrates. Therefore, using the disulfide crosslinking approach in these regions with M13 procoat became an important part of this study.

The second part focuses on the active YidC configuration in the membrane with the aim to gain further data on the stoichiometric structure. Data for an active mono- or dimer have been published over the years, though recent data, including the structure of YidC, point towards an active monomer. A tandem/double YidC (dYidC), consisting of two YidC monomers connected by a cleavable linker, was designed. Complementation studies with various defective YidC mutants were performed with monomeric and the double YidC. Additionally, their capability to insert M13 procoat *in vivo* was tested and one distinct defective mutant was analyzed for its ability to bind its substrate. In the last part of this work the purification of YidC

and dYidC with and without crosslinked M13 procoat was initiated for future *in vitro* structural analysis.

2 MATERIAL AND METHODS

2.1 Culture media and additives

LB medium (Miller)

tryptone (Sigma-Aldrich)	10g/l
yeast extract (Sigma-Aldrich)	5g/l
NaCl (Sigma-Aldrich)	10g/l

The pH was adjusted to 7.4 with the addition of NaOH. For agar-plates 15g/l agar were added before autoclaving. Sugars and antibiotics were added after autoclaving and cooling down to approximately 50°C.

TB medium (Terrific Broth)

tryptone	12g/l
yeast extract	24g/l
glycerol (Sigma-Aldrich)	4ml /l

In 900ml ddH$_2$0

Potassium phosphate buffer

K$_2$HPO$_4$ (Sigma-Aldrich)	9,4g/100ml
KH$_2$PO$_4$ (Roth)	2,2g/100ml

The pH was adjusted to 7.4 with the addition of NaOH. The potassiumphosphate buffer was added to the medium after autoclaving and cooling down.

SOB medium (Super optimal broth)

tryptone	20 g/l
yeast extract	5 g/l
NaCl	0,5 g/l
KCl (Sigma-Aldrich)	0,186 g/l

The pH was adjusted to 7.0 with the addition of NaOH (Sigma-Aldrich). After autoclaving 10mM MgCl (Sigma-Aldrich) was added before usage.

M9 minimal medium

10x M9 salt mix

$Na_2HPO_4 * 2H_2O$ (Applichem)	390mM
KH_2PO_4	220mM
NaCl	80mM
NH_4Cl (Riedel-de Haën)	180mM

Amino acid mix (19aa –Met, Sigma-Aldrich)

200µg/ml of each proteogenic amino acid except methionine

M9 minimal medium

M9 salt mix	1x
Amino acid mix	20µg/ml
$MgSO_4$ (Merck)	1mM
$CaCl_2$ (Fluka)	0.1mM
Thiamine	0.005mg/ml

Ferric citrate (Applichem)   0.0005%

glucose or arabinose (Sigma)   0.2%

2.2.1 Antibiotics

antibiotic	stock solution	working concentration
ampicillin (Sigma-Aldrich)	200mg/ml	200µg/ml
chloramphenicol (Sigma-Aldrich)	25mg/ml	25µl/ml

2.2.2 Sugars

arabinose	20%	0,2%
glucose	20 – 40%	0,2 - 0,4%

2.3 Bacterial strains

Tab. 2: Plasmids used in the crosslinking studies

E. coli strain	Origin	Properties	Additional Info
MK6S (Klenner et al. 2008)	MC1061 derivate (Casadaban et al. 1980)	F$^-$ araD139 Δ(ara-leu) 7696 galE15 galK16 Δ(lac) X74 rpsL (Str^r) hsdR2 (rk$^-$ mk$^-$) mcrA mcrB1 para YidC	YidC depletion strain with the YidC gene under control of the araBAD promotor. Expression of YidC can be induced with arabinose and depleted with glucose in the medium.
XL1-Blue	Stratagene	recA1 endA1 gyrA96 thi-1 hsdR17 supE44 relA1 lac [F′ proAB lacI^{q}ZΔM15 Tn*10* (Tet^r)]	This strain is endo-nuclease (endA) and recombination (recA) deficient, which makes it ideal for cloning and miniprepping plasmid DNA.

2.4 Plasmids

2.4.1 Crosslinking studies

Tab. 3: Plasmids used in the crosslinking studies

Nr.	Vector	Gene	Modificaton	Cloning
1	pGZ119 EH	*E. coli* YidC	C-terminal His$_{10}$-tag Single cysteines in different positions Some mutants were from lab collection and others were made via site-directed muta-genesis.	Lab collection Expression under control of the tac promoter
2	pGZ119 EH	*E. coli* YidC dimer	C-terminal His$_{10}$ Tag Single cysteines in different positions for some experiments Prescission site linker between protomers YidC defective mutants in the protomers for some of the experiments	Modified pGZ119EH *E. coli* YidC EcoRI and MunI shine dalgarno sequence and first protomer MunI and HindIII linker and second protomer Expression under control of the tac promoter
3	pACYC184	*E. coli* YidC	Single cysteines in various positions yidC gene including the upstream promotor and ribosome binding site for constant expression	Lab collection Expression under control of the YidC promoter
4	pMS119 EH	M13 H5 Procoat (gp8)	Serine to phenylalanine in position -4 Single cysteines in different positions Some mutants were from lab collection and others were newly made via site-directed mutagenesis	Lab collection Expression under control of the tac promoter
5	pT7-7 Pf3	dYidC protomer 1 or 2	Prescission protease linker at the start and a His$_{10}$-tag at the end of protomer 2;	pT7-7 plasmid with the gene encoding for Pf3 coat (provided by Dr. Kiefer). Plasmid was picked because a MunI site was already present. EcoRI and MunI shine dalgarno sequence and first protomer MunI and HindIII linker and second protomer

2.4.1.1 List of used mutants in the crosslinking studies

YidC cysteine mutants

Tab. 4: List of pGZ119 EH YidC cysteine mutants

Nr.	Vector	Name	Gene	Cysteine position
1	pGZ119 EH	pGZ YidC M18C	*E. coli* YidC	18
2	pGZ119 EH	pGZ YidC R366C	*E. coli* YidC	366
3	pGZ119 EH	pGZ YidC M369C	*E. coli* YidC	369
4	pGZ119 EH	pGZ YidC T373C	*E. coli* YidC	373
5	pGZ119 EH	pGZ YidC Y377C	*E. coli* YidC	377
6	pGZ119 EH	pGZ YidC Q387C	*E. coli* YidC	387
7	pGZ119 EH	pGZ YidC R394C	*E. coli* YidC	394
8	pGZ119 EH	pGZ YidC E395C	*E. coli* YidC	395
9	pGZ119 EH	pGZ YidC G398C	*E. coli* YidC	398
10	pGZ119 EH	pGZ YidC K401C	*E. coli* YidC	401
11	pGZ119 EH	pGZ YidC S405C	*E. coli* YidC	405
12	pGZ119 EH	pGZ YidC M408C	*E. coli* YidC	408
13	pGZ119 EH	pGZ YidC M409C	*E. coli* YidC	409
14	pGZ119 EH	pGZ YidC 423C	*E. coli* YidC	423
15	pGZ119 EH	pGZ YidC F424C	*E. coli* YidC	424
16	pGZ119 EH	pGZ YidC P425C	*E. coli* YidC	425
17	pGZ119 EH	pGZ YidC L427C	*E. coli* YidC	427
18	pGZ119 EH	pGZ YidC I428C	*E. coli* YidC	428
19	pGZ119 EH	pGZ YidC Q429C	*E. coli* YidC	429
20	pGZ119 EH	pGZ YidC M430C	*E. coli* YidC	430
21	pGZ119 EH	pGZ YidC T474C	*E. coli* YidC	474
22	pGZ119 EH	pGZ YidC M475C	*E. coli* YidC	475
23	pGZ119 EH	pGZ YidC I501C	*E. coli* YidC	501
24	pGZ119 EH	pGZ YidC F502C	*E. coli* YidC	502
25	pGZ119 EH	pGZ YidC T503C	*E. coli* YidC	503
26	pGZ119 EH	pGZ YidC V504C	*E. coli* YidC	504
27	pGZ119 EH	pGZ YidC F505C	*E. coli* YidC	505
28	pGZ119 EH	pGZ YidC F506C	*E. coli* YidC	506
29	pGZ119 EH	pGZ YidC L507C	*E. coli* YidC	507
30	pGZ119 EH	pGZ YidC W508C	*E. coli* YidC	508
31	pGZ119 EH	pGZ YidC F509C	*E. coli* YidC	509
32	pGZ119 EH	pGZ YidC Y517C	*E. coli* YidC	517
33	pGZ119 EH	pGZ YidC S520C	*E. coli* YidC	520
34	pGZ119 EH	pGZ YidC C0	*E. coli* YidC	no cysteine

Tab. 5: List of pACYC184 YidC cysteine mutants

Nr.	Vector	Name	Gene	Cysteine position
1	pACYC184	pACYC YidC M18C	*E. coli* YidC	18
2	pACYC184	pACYC YidC F424C	*E. coli* YidC	424
3	pACYC184	pACYC YidC P425C	*E. coli* YidC	425
4	pACYC184	pACYC YidC L427C	*E. coli* YidC	427
5	pACYC184	pACYC YidC I428C	*E. coli* YidC	428
6	pACYC184	pACYC YidC Q429C	*E. coli* YidC	429
7	pACYC184	pACYC YidC M430C	*E. coli* YidC	430
8	pACYC184	pACYC YidC F502C	*E. coli* YidC	502
9	pACYC184	pACYC YidC T503C	*E. coli* YidC	503
10	pACYC184	pACYC YidC V504C	*E. coli* YidC	504
11	pACYC184	pACYC YidC F505C	*E. coli* YidC	505
12	pACYC184	pACYC YidC F506C	*E. coli* YidC	506
13	pACYC184	pACYC YidC L507C	*E. coli* YidC	507
14	pACYC184	pACYC YidC C0	*E. coli* YidC	no cysteine

YidC dimer cysteine mutants

Tab. 6: List of YidC dimer cysteine mutants

Nr.	Vector	Name	Gene	Cysteine position
1	pGZ119 EH	pGZ dYidC 427c/427c	*E. coli* YidC dimer	Protomer1: 427 Protomer2: 427
2	pGZ119 EH	pGZ dYidC 427c/C0	*E. coli* YidC dimer	Protomer1: 427 Protomer2: no cysteine
3	pGZ119 EH	pGZ dYidC C0/427c	*E. coli* YidC dimer	Protomer1: no cysteine Protomer2: 427
4	pGZ119 EH	pGZ dYidC C0/C0	*E. coli* YidC dimer	no cysteine
5	pGZ119 EH	pGZ dYidC 430c/430c	*E. coli* YidC dimer	Protomer1: 430 Protomer2: 430
6	pGZ119 EH	pGZ dYidC 430c/C0	*E. coli* YidC dimer	Protomer1: 430 Protomer2: no cysteine
7	pGZ119 EH	pGZ dYidC C0/430c	*E. coli* YidC dimer	Protomer1: no cysteine Protomer2: 430

All YidC mutants were mutated to substitute the natural occurring cysteine at position 423 with a serine, except for the pGZ YidC wild type plasmid.

M13 Procoat (gp8) cysteine mutants

Tab. 7: List of M13 H5 procoat cysteine mutants

Nr.	Vector	Name	Gene	Cysteine position
1	pMS119 EH	pMS H5 A-12C	M13 H5 Procoat (gp8)	-12
2	pMS119 EH	pMS H5 A-10C	M13 H5 Procoat (gp8)	-10
3	pMS119 EH	pMS H5 T-9C	M13 H5 Procoat (gp8)	-9
5	pMS119 EH	pMS H5 Y24C	M13 H5 Procoat (gp8)	13
6	pMS119 EH	pMS H5 V29C	M13 H5 Procoat (gp8)	29
7	pMS119 EH	pMS H5 V30C	M13 H5 Procoat (gp8)	30
8	pMS119 EH	pMS H5 V31C	M13 H5 Procoat (gp8)	31
9	pMS119 EH	pMS H5 I32C	M13 H5 Procoat (gp8)	32
10	pMS119 EH	pMS H5 V33C	M13 H5 Procoat (gp8)	33
11	pMS119 EH	pMS H5 G34C	M13 H5 Procoat (gp8)	34
12	pMS119 EH	pMS H5 A35C	M13 H5 Procoat (gp8)	35
13	pMS119 EH	pMS H5 wild type	M13 H5 Procoat (gp8)	no cysteine

Complementation and translocation assays

Tab. 8: Plasmids used in the complementation and translocation assays

Nr.	Vector	Gene	Modificaton	Cloning
1	pGZ119 EH	*E. coli* YidC	C-terminal His_{10} Functional and nonfunctional mutants	Lab collection Expression under control of the tac promoter
2	pGZ119 EH	*E. coli* YidC dimer	C-terminal His_{10} Tag Functional and nonfunctional mutants Prescission site linker between protomers	Modified pGZ119EH E.coli YidC EcoRI and MunI shine dalgarno sequence and first protomer MunI and HindIII linker and second protomer
4	pMS119 EH	M13 Procoat (gp8)	Serine to phenylalanine in position -4 Single cysteines in different positions Some mutants were from lab collection and others were newly made via site-directed mutagenesis	Lab collection Expression under control of the tac promoter

2.4.1.2 List of used mutants in the complementation and translocation assays

YidC alanine mutants

Tab. 9: List of YidC alanine mutants

Nr.	Vector	Name	Gene	Alanine position
1	pGZ119 EH	pGZ YidC T362A	*E. coli* YidC	362

YidC dimer alanine mutants

Tab. 10: List of YidC dimer alanine mutants

Nr.	Vector	Name	Gene	Alanine position
1	pGZ119 EH	pGZ dYidC T362A/T362A	*E. coli* YidC dimer	Protomer1: 362 Protomer2: 362
2	pGZ119 EH	pGZ dYidC T362A/C0	*E. coli* YidC dimer	Protomer1: 362 Protomer2: C0
3	pGZ119 EH	pGZ dYidC C0/T362A	*E. coli* YidC dimer	Protomer1: C0 Protomer2: 362

YidC serine mutants

Tab. 11: List of YidC serine mutants

Nr.	Vector	Name	Gene	Serine position
1	pGZ119 EH	pGZ YidC 5S	*E. coli* YidC	430, 435, 468, 505, 509

YidC dimer serine mutants

Tab. 12: List of YidC dimer serine mutants

Nr.	Vector	Name	Gene	Serine position
1	pGZ119 EH	pGZ dYidC 5S/5S	*E. coli* YidC dimer	Protomer1: 430, 435, 468, 505, 509 Protomer2: 430, 435, 468, 502, 509
2	pGZ119 EH	pGZ dYidC 5S/C0	*E. coli* YidC dimer	Protomer1: 430, 435, 468, 505, 509 Protomer2: C0
3	pGZ119 EH	pGZ YidC C0/5S	*E. coli* YidC dimer	Protomer1: C0 Protomer2: 430, 435, 468, 505, 509

YidC deletion mutants

Tab. 13: List of YidC deletion mutants

Nr.	Vector	Name	Gene	Deleted aminoacids
1	pGZ119 EH	pGZ YidC ΔC1	*E. coli* YidC	399-415

YidC dimer deletion mutants

Tab. 14: List of YidC dimer deletion mutants

Nr.	Vector	Name	Gene	Deletion position
1	pGZ119 EH	pGZ dYidC ΔC1/ΔC1	*E. coli* YidC dimer	Protomer1: 399-415 Protomer2: 399-415
2	pGZ119 EH	pGZ dYidC ΔC1/C0	*E. coli* YidC dimer	Protomer1: 399-415 Protomer2: --
3	pGZ119 EH	pGZ dYidC C0/ΔC1	*E. coli* YidC dimer	Protomer1: -- Protomer2: 399-415

YidC dimer mixed defective mutants

Tab. 15: List of YidC dimer mixed defective mutants

Nr.	Vector	Name	Gene	Mutation position
1	pGZ119 EH	pGZ dYidC ΔC1/5S	*E. coli* YidC dimer	Protomer1: Δ399-415 Protomer2: 430S, 435S, 468S, 502S, 509S
2	pGZ119 EH	pGZ dYidC 5S/ΔC1	*E. coli* YidC dimer	Protomer1: 430S, 435S, 468S, 502S, 509S Protomer2: Δ399-415
3	pGZ119 EH	pGZ dYidC ΔC1/362A	*E. coli* YidC dimer	Protomer1: Δ399-415 Protomer2: T362A
3	pGZ119 EH	pGZ dYidC 362A/ΔC1	*E. coli* YidC dimer	Protomer1: T362A Protomer2: Δ399-415

2.5 PCR primer

2.5.1 Mutagenesis primer

The following lists contain the primer pairs used to construct additional mutants for this study in addition to the present lab collection. The changed triplets are marked with bold letters.

Cysteine mutants

M13 Procoat cysteine mutation primer:

H5 M13 Procoat Y24C

H5 24c FW: [5`- 3`]: TATCGGT **TGT** GCGTGG

H5 24c RV: [5`- 3`]: CCACGC **ACA** ACCGATA

H5 M13 Procoat V29C

Procoat+29c_A: [5`- 3`]: GTGGGCGATG **TGT** GTTGTCATTG

Procoat+29c_B: [5`- 3`]: CAATGACAAC **ACA** CATCGCCCAC

H5 M13 Procoat G34C

Procoat+34c_A: [5`- 3`]: GTCATTGTC **TGC** GCAACTATCGG

Procoat+34c_B: [5`- 3`]: CCGATAGTTGC **GCA** GACAATGAC

H5 M13 Procoat A35C

PC_35c_FW: [5`- 3`]: GTCATTGTCGGC **TGC** ACTATCGGTATC

PC_35c_RV: [5`- 3`]: GATACCGATAGT **GCA** GCCGACAATGAC

Template DNA: pMS119 EH H5 M13 Procoat wild type

Primers were ordered from Sigma-Aldrich.

YidC cysteine mutation primer:

YidC T373C

YidC_T373C_FW: [5`- 3`]: GTACCCGCTG **TGC** AAAGCGCAG

YidC_T373C_RV: [5`- 3`]: CTGCGCTTT **GCA** CAGCGGGTAC

YidC Y377C

YidC_Y377C_FW: [5`- 3`]: GCGCAG **TGC** ACCTCC

YidC_Y377C_RV: [5`- 3`]: GGAGGT **GCA** CTGCGC

YidC Q387C

YidC 387c fw: [5`- 3`]: GTATGTTG **TGC** CCGAAGATTC

YidC 387c rv: [5`- 3`]: GAATCTTCGG **GCA** CAACATAC

YidC R394C

YidC 394c fw: [5`- 3`]: GGCAATG **TGC** GAGCGTC

YidC 394c rv: [5`- 3`]: GACGCTC **GCA** CATTGCC

YidC E395C

YidC 395c fw: [5`- 3`]: CAATGCGT **TGC** CGTCTGGG

YidC 395c rv: [5`- 3`]: CCCAGACG **GCA** ACGCATTG

YidC G398C

YidC 398c fw: [5`- 3`]: CGTCTG **TGC** GATGAC

YidC 398c rv: [5`- 3`]: GTCATC **GCA** CAGACG

YidC K401C

YidC 401c fw: [5`- 3`]: GCGATGAC **TGC** CAGCGTATC

YidC 401c rv: [5`- 3`]: GATACGCTG **GCA** GTCATCGC

YidC S405C

 YidC 405c fw: [5`- 3`]: CGTATC **TGC** CAGGAAATG

YidC 405c rv: [5`- 3`]: CATTTCCTG **GCA** GATACG

YidC M408C

YidC 408c fw: [5`- 3`]: GCCAGGAA **TGC** ATGGCGCTG

YidC 408c rv: [5`- 3`]: CAGCGCCAT **GCA** TTCCTGGC

YidC M409C

YidC 409c fw: [5`- 3`]: GGAAATG **TGC** GCGCTG

YidC 409c rv: [5`- 3`]: CAGCGC **GCA** CATTTCC

YidC I501C

YidC_501c_Fw_kurz: [5`- 3`]: GCCGGTC **TGC** TTCACCGTG

YidC_501c_Rv_kurz: [5`- 3`]: CACGGTGAA **GCA** GACCGGC

YidC F509C

YidC F509C Fw: [5`- 3`]: CCTGTGG **TGC** CCGTCAG

YidC F509C Rv: [5`- 3`]: CTGACGG **GCA** CCACAGG

YidC S520C

YidC_520c_MutF: [5`- 3`]: CTATATCATC **TGC** AACCTGGTAAC

YidC_520c_MutR: [5`- 3`]: GTTACCAGGTT **GCA** GATGATATAG

Template DNA: pGZ119 EH *E. coli* YidC C0

Primers were ordered from Sigma.

Serine mutants

YidC serine mutation primer

YidC F509S

YidC F509S Fw: [5`- 3`]: CCTGTGG **TCC** CCGTCAG

YidC F509S Rv: [5`- 3`]: CTGACGG **GGA** CCACAGG

Template DNA: pGZ119 EH *E. coli* YidC 4S, serines at positions 430, 435, 468 and 502 were already present

Primers were ordered from Sigma-Aldrich.

Alanine mutants

YidC alanine mutant primer

YidC T362A

YidC_T362A_FW: [5`- 3`]: CATCATC **GCC** TTTATCG

YidC_T362A_RV: [5`- 3`]: CGATAAA **GGC** GATGATG

Template DNA: pGZ119 EH *E. coli* YidC C0

Primers were ordered from Sigma-Aldrich.

Deletions

Deletion in YidC

C1_Del_399-415_fw:

[5`- 3`]: GCAATGCGTGAGCGTCTGGGC**|**AAGGTTAACCCGCTGGGCGGC

C1_Del_399-415_rv:

[5`- 3`]: GCCGCCCAGCGGGTTAACCTT**|**GCCCAGACGCTCACGCATTGC

Partly deletion of the C1 loop in YidC, **|** indicates the position of the deletion

Template DNA: pGZ119 EH *E. coli* YidC C0

Primers were ordered from Sigma-Aldrich.

2.5.2 Amplification

Primer for cloning the dYidC construct

YidCI_XbaI(Shine)SphI:

[5`- 3`]: TCTAGAAGGAGATCATCATGCATGCAGTCGCAACGCAATC

YidCI_MunI:

[5`- 3`]: CATATGCAATTGGGATTTTTTCTTCTCGCGGC

Template DNA: pGZ119 EH *E.coli* YidC C0

DYidCMetLeuF:

[5`- 3`]: CCCAATTGCAT C TGGATTCGCAACGCAATC

DYidCMetLeuR:

[5`- 3`]: GATTGCGTTGCGAATCCA G ATGCAATTGGG

Template DNA: pGZ119 EH *E.coli* dYidC C0/C0

Primers were ordered from Sigma-Aldrich.

2.5.3 Linker

Prescission Site dYidC

PrecSiteDYidC_Fw: [5`- 3`]: AATTGCTGGAAGTGCTGTTTCAGGGCCCGG

PrecSiteDYidC_Rv: [5`- 3`]: AATTCCGGGCCCTGAAACAGCACTTCCAGC

Template DNA for cloning the linker: pGZ119 EH *E. coli* dYidC C0/C0

Primers were ordered from Sigma-Aldrich.

2.5.4 Sequencing

Licor

Primer Name	Sequence	Label	Wavelength
Tac Forward	[5`- 3`]: GTTGACAATTAATCATCGGCTCG	DY-681	700nm
Tac-Back	[5`- 3`]: GGCTGAAAATCTTCTCTCATCCG	DY-781	800nm
IMID	[5`- 3`]: GCAACAGTATTTCGCGACGG	IRD-800	800nm
IMID2	[5`- 3`]: CGCTTATGTGCTGGCTGAAGGTC	IRD-800	800nm
IMID3	[5`- 3`]: CAGGCAATGCGTGAGCGTCGT	DY-681	700nm
T7 Forward	[5`- 3`]: TAATACGACTCACTATAGGG	DY-682	700nm
T7 rev	[5`- 3`]: CGCTGAGATAGGTGCCTCAC	IRD-800	800nm

Primer Name	Sequence	Label	Wavelength
T7 Terminator	[5`- 3`]: GCTAGTTATTGCTCAGCGG	DY-781	800nm
Universal FW	[5`- 3`]: GTTTTCCCAGTCACGACGTTGTA	DY-781	800nm
Universal Reverse	[5`- 3`]: CACACAGGAAACAGCTATGACC	DY-681	700nm

Primers were ordered from Biomers or MWG Operon.

Macrogen EZ-seq sequencing service

Tac Forward	[5`- 3`]: GTTGACAATTAATCATCGGCTCG
Tac-Back Long	[5`- 3`]: GTAGCAGGCTGAAAATCTTCTCTCATCCG
T7 Forward	[5`- 3`]: TAATACGACTCACTATAGGG
T7 rev	[5`- 3`]: CGCTGAGATAGGTGCCTCAC
DYidC_LinkerSeq_FW	[5`- 3`]: CCAATTGCATCTGGATTC
DYidC_LinkerSeq_RW	[5`- 3`]: GAATCCAGATGCAATTGG
PrecSiteDYidC_Fw	[5`- 3`]: AATTGCTGGAAGTGCTGTTTCAGGGCCCGG
PrecSiteDYidC_Rv	[5`- 3`]: AATTCCGGGCCCTGAAACAGCACTTCCAGC
pMSYidC9SS367GF	[5`- 3`]: CGTTCGTGGCATCATGTAC

Primers were ordered from Sigma-Aldrich

2.6 Methods in molecular biology

2.6.1 Site directed mutagenesis

The site directed mutagenesis was used to delete, add or substitute bases in the plasmid, resulting in respective changes in the translated protein. The used primer pairs were complementary to each other.

Reaction table	Final volume	Final concentration
10x Pfu Ultra II buffer (Agilent)	5µl	1x
Primer A (10 µM)	1µl	0.2µM
Primer B (10 µM)	1µl	0.2µM
Template DNA	Xµl	50-100µg/50µl
dNTP-Mix (10mM each, Sigma-Aldrich)	1µl	0.2µM
Pfu Ultra II Polymerase (Agilent)	1µl	
ddH$_2$O	ad to 50µl total Volume	

Thermocycler program

95°C	2 minutes
95°C	30 seconds
50°C	30 seconds
72°C	x seconds

18 cycles

72°C	7 minutes
8°C	∞

The elongation time depended on the size of the plasmid (30sec per 1000bp). 1µl of DpnI (Thermo Fisher Scientific) was added after the reaction and incubated at 37°C for at least 3 hours or overnight to digest the methylated parental DNA. After that the DNA was precipitated.

Precipitation

51µl sample

5µl 3M Sodium acetate (Merck) pH 5.2

140µl Ethanol pure (Sigma-Aldrich)

The sample was carefully mixed and stored for 1h at -20°C to let the DNA precipitate followed by a centrifugation at 14000 rpm for 15 minutes at 4°C. The supernatant was discarded and the pellet was dried in a vacuum concentrator. 10µl of ddH$_2$O was added to the precipitate before the transformation (see 2.6.7)

2.6.2 Restriction digestion of DNA

The restriction reactions were performed with one or two enzymes simultaneously and incubated at 37°C. If the fast digest system from Thermo Fisher Scientific (former Fermentas) was used, the FastDigest Green buffer was added and the samples were incubated for 1 hour. In case of normal enzymes the respective buffer for each enzyme was used or the best suited one in case of two enzymes. The reactions were then incubated for 3 hours.

Reaction table	Final volume	Final concentration
10x Restriction buffer (Thermo Fisher Scientific /NEB)	2µl	1x
Template DNA	Xµl	
Restriction enzyme (Thermo Fisher Scientific /NEB)	1µl	
ddH$_2$O	ad to 20µl total volume	

The completed reactions were loaded on an agarose gel electrophoresis for further analysis and gel extraction.

2.6.3 Agarose gel electrophoresis

Agarose gel electrophoresis was performed in gel chambers from Owl Separation Systems, model B1A.

Reaction table	Final volume
Agarose (Sigma-Aldrich)	0.4g
1x TBE buffer (Sigma-Aldrich)	ad to 40ml total volume
Ethidium bromide (Sigma-Aldrich)	2µl

The agarose was mixed with the TBE buffer and heated until it was completely dissolved. After cooling down for a brief period ethidium bromide was added and the gel was cast into the chamber and the comb was inserted. The samples were mixed 6:1 with DNA loading dye (10 mM Tris pH 8.0, 25% Ficoll 400 (Sigma-Aldrich), 0.05% bromophenol blue). After the samples and the marker were loaded, a voltage of 90V was applied to the chamber for 60 - 90 minutes.

2.6.4 Agarosegel extraction

Gel slices of interest, containing digested plasmid and fragment DNA for ligation purposes, were cut out on a UV-Table using a scalpel. The extraction was performed with the Fermentas Gene Jet Gel Extraction Kit (Thermo Fisher Scientific) according to protocol.

2.6.5 Ligation of DNA fragments

DNA fragments and cut open plasmids from restriction digestion reactions or PCRs were used for ligation reactions.

Reaction table	Final volume	Final concentration
Vector DNA	varies	20-100ng/20µl
Insert DNA	1x to 5x mole of Vector DNA	varies
10x T4 DNA Ligase buffer (Promega)	2µl	1x
T4 DNA Ligase (5 Weiss U/µl) (Promega)	0.5µl	0.125 Weiss U/µl
ddH$_2$O	ad to 20µl	

Ligation reactions were performed at 4°C overnight and then transformed (see 2.5.7.2) in *E.coli* XL1 cells.

2.6.6 Preparation of chemical competent *E.coli* cells

Competent E.coli cells were prepared with the rubidium-chloride method (Hanahan 1983, Green and Rogers 2013). These cells were then directly used for transformation with different plasmids or stored at -80°C for later usage.

100ml of LB medium was inoculated 1:100 with an overnight culture of the respective cells. The cells were grown to an OD$_{600}$ = 0.5 and checked with a Thoma counting chamber before centrifugation at 5000g for 5 minutes in a JA20 centrifugation rotor. The cell-pellet was resuspended in 10ml TFB1 buffer (100 mM RbCl (Serva), 50 mM MnCl2 (Sigma-Aldrich), 30 mM KAc (Sigma-Aldrich), 10 mM CaCl2 (Fluka), 15 % glycerol; pH 5.8) and incubated on ice for 60 minutes. After another centrifugation step at 5000g for 5 minutes the pellet was resuspended in 2.5ml ice cold TFB2 buffer (10 mM MOPS (Sigma-Aldrich), 10 mM RbCl, 75 mM CaCl2, 15 % glycerol; pH 7). The cells were then directly used for transformation or frozen at -80°C in 100µl aliquots.

2.6.7 Transformation of chemical competent *E.coli* cells

Transformation of plasmid DNA

Chemical competent cells were used for transformation (see 2.6.6). 2µl of plasmid DNA were added to 30µl of competent cells and incubated on ice for 20 minutes. A heat shock was applied at 40°C for 90 seconds followed by 2 more minutes on ice. 80µl of SOB medium were added and the cells were incubated at 37°C for an hour. 80µl were plated out on agar plates containing the respective antibiotics and sugars.

Transformation of ligated plasmid DNA

See above but instead of 30µl cells 100µl are used with 10µl of the ligation and 200µl of SOB medium are added after the heat shock. All cells were plated out.

Transformation of mutated plasmid DNA

See above but instead of 30µl cells 100µl are used with 10µl of the mutated plasmid DNA and 200µl of SOB medium are added after the heat shock. All cells were plated out.

2.6.8 Isolation of plasmid DNA from bacterial cultures

The Zippy plasmid miniprep kit (Zymo Research) was used for plasmid isolation. A few steps in the manufacturer's protocol were modified for higher DNA yields.

2ml overnight culture of XL1 cells containing the respective plasmid were used for DNA isolation. The cells were grown in LB medium with antibiotics. The culture was centrifuged (13000rpm, 1min) and resuspended in 600µl of 1x TE buffer followed by the lysis, neutralization and binding steps according to protocol. After the two washing steps an additional centrifugation (13000rpm, 2min) was performed to remove residues of washing buffer. The DNA was eluted in 50µl of ddH$_2$O.

2.6.9 DNA sequencing (Sanger *et al.* 1977)

DNA sequencing with the LI-COR Long Reader 4200 system

Most of the sequencing was performed this way. The LI-COR Long Reader system uses the Sanger chain termination method. The samples were labeled using fluorescently labelled primers.

The reaction mix for each sample:

Reaction table	Final volume
Plasmid DNA	13µl
Thermo RX buffer (Affymetrix)	2µl
Sequencing primer (2pmol/µl)	1µl
Thermo Sequenase (4U/µl) (Affymetrix)	1.5µl
Total volume	17.5µl

4µl of this mix were added to 4µl of each di-deoxynucleosidetriphosphate (ddNTP) separately in an extra tube. These ddNTPs (ddATP, ddCTP, ddGTP and ddTTP, Affymetrix) caused the termination of the elongation of the DNA, resulting in fragments of different sizes that end on the ddNTP of the respective mix. The annealing temperature varied depending on the primer that was used in the reaction.

Thermocycler program

95°C	2 minutes	
95°C	30 seconds	
X°C	1 minute	40 cycles
72°C	1 minute	
72°C	3 minutes	
8°C storage		

The reaction was stopped by adding 3.5µl of stopping buffer (95% formamide (Merck), 10mM EDTA (Promega), 0.1% basic fuchsine (Serva), 0.01% bromophenol blue (Serva), pH9) and heated for 2 minutes at 72°C before being loaded on the SDS Urea gel for separation.

The DNA fragments were then separated by SDS-Urea gel electrophoresis (6% acrylamide (Long Ranger, Lonza), 7M urea (Sigma-Aldrich), 1.2x TBE (107mM Tris (Sigma-Aldich), 107mM boric acid (Affymetrix), 2.4mM EDTA), 0.05% TEMED (Sigma-Aldrich), 0,05% APS (Serva)). Detection was performed at 700nm or 800nm depending on the fluorescence marker that was used to label the primer.

DNA sequencing using the Macrogen Ez-Seq service

DNA samples were prepared according to recommendations from Macrogen. 5µl of sample DNA (>100µg/µl) were mixed with 5µl of the sequencing primer (5pmol/µl) and sent to Macrogen for sequencing.

2.7 *In vivo* complementation assay

To analyze the functionality of different YidC and dYidC constructs/mutants a series of *in vivo* complementation assays were performed using the pGZ119EH plasmid as vector. The constructs were expressed in the YidC depletion strain MK6S. Overnight cultures in LB medium, containing 25µg/ml chloramphenicol, 0.2% arabinose and 0.4% glucose were washed with LB and inoculated 1:100 in fresh LB medium with 25µg/ml chloramphenicol and 0.4% glucose to deplete the chromosomal YidC. After growth to an OD_{600} = 0.5 a serial dilution in LB medium (no additives) was prepared from 10^{-1} to 10^{-5}. The dilutions were spotted on LB agarplates (3µl) containing 0.2% arabinose (positive control), 0.2% arabinose + 1mM IPTG, 0.2% glucose (negative control) or 0.2% glucose + 1mM IPTG (Sigma-Aldrich). The IPTG induced the plasmid encoded YidC constructs and allowed cell growth on the glucose plates if the tested mutant was viable.

Parallel to the complementation assay after the serial dilution was prepared, 1 mM IPTG was added to the remaining culture for a three hour induction. 20% TCA was added to the cells.

The precipitated cells were centrifuged (14000rpm for 5 minutes at 4°C), the supernatant was discarded and 500µl acetone was added to wash the pellet. After another centrifugation (14000rpm for 5 minutes at 4°C) the supernatant was discarded again and the pellets were dried at 95°C for 5 minutes. 50µl loading buffer was added (5 parts Solution I: 200 mM Tris, 20 mM EDTA pH 7.0; 4 parts Solution II: 8.3% SDS, 83,3 mM Tris/HCl pH 6.8, 29.2 % glycerol, 0.146% bromophenol blue; 1 part 1 M DTT or ddH$_2$O) and the pellets were resuspended and heated at 95°C for 5 minutes. A SDS-gel was loaded with the samples followed by Western blotting analysis with an anti His$_{10}$-tag antibody.

2.8 Protein purification

2.8.1 Purification of *E. coli* YidC

Different amounts of cell culture were used for purification purposes, depending on the amount of protein that was necessary for the subsequent procedures. Between 200ml and 6l culture volume was used for protein purification.

Protein expression (LB)

MK6S cells were transformed (2.6.7) with pGZ119 EH YidC C0 and inoculated in LB medium (25µg/ml chloramphenicol, 0.4% glucose). The cultures were grown at 37°C to an OD$_{600}$ = 0.5 and then induced with 0.5 mM IPTG for 4 hours.

Protein expression (TB)

MK6S cells were transformed (2.6.7) with pGZ119 EH YidC C0 and inoculated in TB medium (25µg/ml chloramphenicol, 0.4% glucose). The cultures were grown at 37°C to an OD$_{600}$ = 0.7 and were then induced with 0.5 mM IPTG for 4.5 hours.

Membrane preparation

The cells were pelleted (8000g for 10 minutes at 4°C) and resuspended in Buffer A (10% sucrose (Sigma-Aldrich), 50mM Tris, 500mM NaCl, 1mM EDTA, pH8) with the addition of DNAseI and 0.1mM PMSF. Cell-lysis was performed using a One Shot cell disruption instrument (Constant Systems LTD) at 1.3 kbar. The fragmented cells were centrifuged (8000g for 10 minutes at 4°C) to precipitate cell debris and unbroken cells. The supernatant was transferred in an ultracentrifuge tube and spun down at 140000g for 2 hours at 4°C to precipitate the membrane vesicles. Depending on how the purification was continued the membrane pellet was resuspended in Buffer A for a subsequent sucrose gradient or in Buffer B (10% glycerol, 50mM Tris, 500mM NaCl, pH8) if the pellet has been directly solubilized after this step.

Optional step: sucrose gradient

A sucrose gradient was used to separate the inner (IMV) and outer membrane vesicles (OMV). The gradient consists of three different phases with three different sucrose concentrations (see Fig. 20).

Phase 1: 770mM sucrose, 50mM Tris, 1mM EDTA

Phase 2: 1440mM sucrose, 50mM Tris, 1mM EDTA

Phase 3: 2020mM sucrose, 50mM Tris, 1mM EDTA

The phases were carefully laid under each other with a syringe, starting with the lowest concentration on top. The gradients were stored at 4°C for 1 hour for the phases to stabilize. Afterwards, the resuspended membrane vesicles were carefully pipetted on the gradient and were centrifuged at 110000g for 16 hours. The IMVs concentrate at the separation layer between phase 1 and phase 2 while the OMVs concentrate between phase 2 and phase 3. The IMVs were carefully collected with a syringe and mixed 1:4 with sucrose free Tris buffer (50mM Tris, pH8). The IMVs
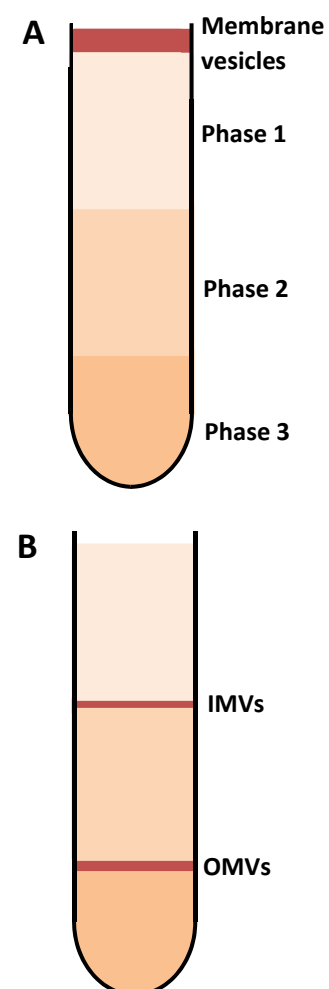

Fig. 20: Composition of a sucrose gradient before (A) and after (B) centrifugation. IMV: inner membrane vesicles, OMV: outer membrane vesicles

were then centrifuged at 140000g for 2 hours at 4°C to precipitate. The supernatant was discarded and Buffer B was used to resuspend the IMVs.

Solubilization

2% n-Dodecyl β-D-maltoside (DDM) was added to the membrane vesicles and incubated for 2 hours on a rotary wheel. After another ultracentrifugation step at 100000g for 1 hour at 4°C the supernatant was transferred to be used in the immobilized metal ion chromatography.

Immobilized metal ion chromatography (IMAC)

Nickel-Sepharose beads (GE-Healthcare) were prepared by washing twice with 10 times of the column volume (CV) with buffer C (10% glycerol, 50mM Tris, 500mM NaCl, 20mM imidazole, 0.03% DDM, pH8). 20mM of imidazole (Sigma-Aldrich) was also added to the solubilized membranes before adding the Ni-Sepharose. After 2 hours of incubation on a rotary wheel at 4°C, the sample was loaded on an empty 10 ml Column with a filter and flew through by gravity flow, allowing the beads to settle on the filter (see Fig. 21). The column was then washed with at least 10 up to 40 column volumes (CV,
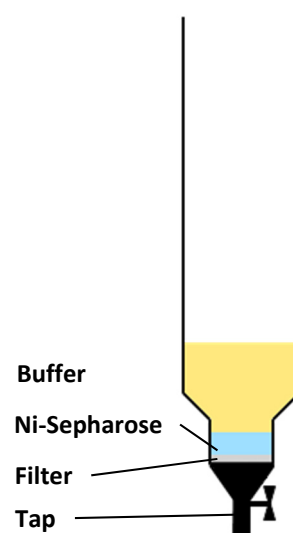

Fig. 21: Structure of a flow column for an IMAC

amount of Ni-Sepharose that settles in the column) of Buffer D (10% glycerol, 50mM Tris, 500mM NaCl, 40mM imidazole, 0.03% DDM, pH8) to remove undesired weak bound contaminations on the Ni-Sepharose. The Protein was then eluted with Buffer E (10% glycerol, 25mM Mes (Sigma-Aldrich), 300mM NaCl, 600mM imidazole, 0.02% DDM, 0.01% Cymal6 (6-Cyclohexyl-1-Hexyl-β-D-Maltoside, Affymetrix), pH6.5) by incubating the Ni-Sepharose for 10 minutes and then collecting the eluate by gravity flow. The flow through, wash buffer and the elution fractions were analyzed on a 10% or 12% SDS acrylamide gel and visualized by Coomassie staining (25% Isopropanol (Sigma-Aldrich), 10% acetic acid (Sigma-Aldrich), 0.05% Coomassie R250 (Serva)).

Size exclusion chromatography (SEC)

The eluted protein was further purified on a Superdex 200 10/300 increase column. Depending on the total volume of the elution fractions the protein had to be concentrated to a volume of 500µl with Amicon® Ultra 4 ml Filters (Merck Millipore). Before loading, the protein was centrifuged at 140000rpm for 15 minutes at 4°C to remove potential aggregates. The size exclusion chromatography was performed at room temperature in Buffer G (10% glycerol, 10mM Ada (Fluka), 300mM NaCl, 0.02%DDM, 0.01% Cymal6, pH6). The collected fractions were analyzed on a 10% or 12% SDS acrylamide gel and visualized by Coomassie staining. The purified protein was stored at 4°C.

2.8.2 Purification of *E. coli* dYidC

The purification protocol was the same as for the monomeric YidC C0.

2.8.3 Purification of crosslinked *E.coli* YidC with M13 procoat gp8 wildtype

Protein expression in LB medium

MK6S cells were transformed (see 2.6.7) with different dYidC cysteine mutants cloned in the pGZ119 EH plasmid combined with the cysteine mutant H5 V33C procoat in the pMS119 EH plasmid.

The double transformed cells were inoculated in 200ml LB medium (200µg/ml ampicillin, 25µg/ml chloramphenicol, 0.4% glucose). The cultures were grown at 37°C to an $OD_{600} = 0.5$ and were then induced with 0.5mM IPTG for 10 minutes before the addition of 200µM DTNB. After three more hours, the cells were harvested.

Membrane preparation

The cells were pelleted (8000g for 10 minutes at 4°C) and resuspended in Buffer A (10% sucrose, 50mM Tris, 500mM NaCl, 1mM EDTA, pH8) with the addition of DNAseI and 0.1mM PMSF. Cell-lysis was performed using a One Shot cell disruption instrument (Constant Systems

LTD) at 1.3 kbar. The fragmented cells were centrifuged (8000g for 10 minutes at 4°C) to precipitate cell debris and unbroken cells. The supernatant was transferred in an ultracentrifuge-column and spun down at 140000g for 2 hours at 4°C to pellet the membrane vesicles. The membrane pellet was resuspended in Buffer B (10% glycerol, 50mM Tris, 500mM NaCl, pH8) and again centrifuged at 140000g for 2 hours at 4°C and resuspended in Buffer B. This additional step was necessary to remove remaining DTNB from the membranes.

Solubilization

2% DDM was added to the membrane vesicles and incubated for 2 hours on a rotary wheel. After another ultracentrifugation step at 100000g for 1 hour at 4°C the supernatant was used for the immobilized metal ion chromatography.

Immobilized metal ion chromatography (IMAC)

Nickle-Sepharose beads were prepared by washing 2 times with 10 CV of buffer C (10% glycerol, 50mM Tris, 500mM NaCl, 20mM imidazole, pH8). 20mM of imidazole was also added to the solubilized membranes before adding the Ni-Sepharose. Due to the low volume of the sample the further IMAC was done in 2ml eppendorf tubes and not on a column. After 2 hours of incubation on a rotary wheel at 4°C, the sample was carefully spun down at 3000g for 3 minutes, allowing the beads to settle down at the bottom of the tube and the supernatant to be removed by pipetting. The beads were then washed with 10 CV of Buffer D and centrifuged at 3000g for 3 minutes with the supernatant again being carefully removed. The protein was then eluted with 300 µl buffer E (10% glycerol, 50mM Tris, 500mM NaCl, 600mM imidazole, 0.05% DDM, pH8) by incubating the Ni-Sepharose for 10 minutes in it and then collecting the eluate by spinning down at 3000g for 3 minutes and carefully pipetting it off the Ni-Sepharose beads. The purified protein was then dialyzed in 500 ml buffer E_2 (10% glycerol, 50mM Tris, 500mM NaCl, 0.05% DDM, pH8) using the Micro Float-A-Lyzer system (Spectrumlabs) according to protocol for 1.5 hours. The dialyzed protein was used in the prescission protease assays (see 2.11).

2.9 *In vivo* crosslinking

2.9.1 Radioactive labeling

Pulse

Overnight cultures in LB (200µg/ml ampicillin, 25µg/ml chloramphenicol, 0.2% arabinose, 0.4% glucose) of MK6S cells, harboring plasmids encoding cysteine mutants of YidC (pGZ119EH) and H5 M13 procoat (pMS119EH) were inoculated 1:100 in fresh LB medium (200µg/ml ampicillin, 25µg/ml chloramphenicol, 0.4% glucose) and grown under depletion conditions to an OD_{600} = 0.5 at 37°C. 200µl of the cells were then washed two times with 200µl 1x M9 salt mix and resuspended in 200µl M9 medium (-met). After 45 minutes at 37°C in the incubator 1mM IPTG was added to induce the plasmid encoded genes for 10 minutes. 2µl of radioactive methionine (10 mCi/ml (Perkin Elmer, American Radiolabeled Chemicals)) was added for 1 minute for labeling followed by the crosslinking agent (see Tab. 16).

Tab. 16: List of crosslinking agents their solvents and incubation times

Crosslinking agent	Final vol.	Dissolved in	Final conc.	Inc. time
Copper phenanthroline (Sigma-Aldrich)	4µl	H_2O + EtOH (1:2)	1mM	10 minutes
DTNB (Sigma-Aldrich)	5µl	100mM in KPhos. pH 7.4	200µM	10 minutes
Iodine (Sigma-Aldrich)	5µl	EtOH	250µM	30 seconds
o-PDM (Sigma-Aldrich)	4µl	DMSO	500µM	10 minutes

After the incubation a final concentration of 20% TCA (Th. Geyer) was added to the culture and the cells were stored over night at 4°C.

Immunoprecipitation

The precipitated cells were centrifuged (14000rpm for 5 minutes at 4°C), the supernatant was discarded and 500µl acetone was added to wash the pellet. After another centrifugation (14000rpm for 5 minutes at 4°C) the supernatant was discarded again and the pellets were dried at 95°C for 5 minutes. 50µl of resuspension buffer (2% SDS, 10mM Tris, pH8) was added and the pellet was resolved and incubated at 95°C for 5 minutes. 1ml of TENT-X buffer (150mM

NaCl, 10mM Tris, 1mM EDTA, 2% TritonX-100 (Sigma-Aldrich), pH8) and 20µl of Zysorbin (fixed and killed S*taphylococcus aureus* Protein A pos. strain, Invitrogen) were added and incubated at 4°C on a rotating wheel for 30 minutes. The samples were then centrifuged (14000rpm for 5 minutes at 4°C) to precipitate the Zysorbin. The supernatant was transferred in a new tube containing the antibody for the immunoprecipitation.

Tab. 17: Antibodies used for immunoprecipitation

Antibody	Final Volume
YidC100	1µl
M13 AII/AIII	4µl

The samples were incubated on the rotary wheel for at least 3h or overnight at 4°C before adding 20µl of Zysorbin and incubating for another hour. Zysorbin was pelleted by centrifugation (9000rpm for 1 minute at 4°C) and washed 2 times with TENT-X buffer followed by a washing step with TEN-buffer (150mM NaCl, 10mM Tris, 1mM EDTA, pH8) . The pellets were resuspended in 50µl loading buffer with or without DTT and heated at 95°C for 5 minutes. Afterwards the samples were centrifuged (14000rpm for 2 minutes at 4°C) and loaded on a 10-12% SDS-gel (YidC antibody, lab-stock) or a 22% SDS Urea-gel (M13 antibody, lab-stock) without disturbing the Zysorbin pellet.

The gel was dried in a gel drier and put in a cassette with a phosphoimager plate (IP VM, Dürr Medical) to detect the radioactive signals. The plate was analyzed after an incubation time of one to three days using a phosphoimaging system (BAS Reader-1500 Fujifilm, Raytest GMBH and CR35 Bio, Dürr Medical).

2.9.2 Western Blot detection

Overnight cultures in LB (200µg/ml ampicillin, 25µg/ml chloramphenicol, 0.2% arabinose, 0.4% glucose) of MK6S cells, harboring plasmids encoding cysteine mutants of YidC (pGZ119EH) and H5 M13 procoat (pMS119EH) were inoculated 1:100 in fresh LB medium (200µg/ml ampicillin, 25µg/ml chloramphenicol, 0.4% glucose) and grown under depletion conditions to an OD_{600} = 0.5 at 37°C. The cells were then induced with 1mM IPTG and grown

for additional 10 minutes before adding 200µM of DTNB. After 3 hours of induction/oxidation, 1ml of the culture was precipitated with 20% TCA for further analysis.

The precipitated cells were centrifuged (14000rpm for 5 minutes at 4°C), the supernatant was discarded and 500µl acetone was added to wash the pellet. After another centrifugation (14000rpm for 5 minutes at 4°C) the supernatant was discarded again and the pellets were dried at 95°C for 5 minutes. 50µl SDS loading buffer was added with or without DTT and the pellets were resuspended and heated at 95°C for 5 minutes. A SDS-gel was loaded with the samples followed by Western blotting.

Blotting

The blotting chamber was assembled according to protocol and performed in a Trans-Blot® Electrophoretic Transfer Cell (BIO-RAD) with transfer buffer (187 mM glycine (Sigma-Aldrich), 25 mM Tris-base, 0.01% SDS, 20% methanol (Sigma-Aldrich)) in an ice box and an inserted cooling coil attached to a RM20 recirculating cooling bath (LAUDA). Nitrocellulose membranes (Whatman Protran, 0.2 µm pore size) were used for blotting proteins. 1.5A were applied for 2 hours and the buffer was stirred with a stir bar for the duration to balance out the ion concentration during the electrophoresis.

The membrane was then reversibly stained with Ponceau S (0.1% Ponceau S (Sigma-Aldrich) in 5% acetic acid, Sigma-Aldrich) for protein fixation and observation of blotting efficiency. Afterwards most of the remaining Ponceau S was removed by carefully washing the membrane with distilled water followed by adding 50 ml of a 5% solution of blotting grade blocker (BIO-RAD) in 1x phosphate buffered saline with Tween 20 (140 mM NaCl, 2.7 mM KCl, 10.1 mM Na_2HPO_4, 1.8 mM KH_2PO_4, 0.1% Tween 20 (Sigma-Aldrich) pH 7.3, PBS-T). To block the membrane it was carefully shaken overnight at 4°C.

Immunodetection

The membrane was washed 3 times with PBS-T for 10 minutes followed by the addition of the anti His$_{10}$tag (Sigma-Aldrich) antibody, diluted 1:7500 in PBS-T. After the incubation for 1.5 hours the primary antibody solution was removed and the membrane was again washed 3 times with PBS-T for 10 minutes. Then the anti-mouse antibody (Sigma-Aldrich), diluted 1:10000 in PBS-T, was added. After an additional hour, the secondary antibody was discarded and the membrane was again washed 3 times with PBS-T for 10 minutes. After the last washing step the remaining PBS-T was carefully removed and 5 ml of the ECL mix was added (2.5 ml HRP Substrate Peroxide Solution, 2.5 ml HRP Substrate Luminol Reagent, Millipore) and incubated for 5 minutes. Detection of protein bands was done with the ImageQuant LAS 4000 imaging system (GE Healthcare Lifesciences).

2.10 Translocation assay

Pulse

Overnight cultures in LB (200µg/ml ampicillin, 25µg/ml chloramphenicol, 0.2% arabinose, 0.4% glucose) of MK6S cells, harboring plasmids encoding defective mutants and controls of YidC (pGZ119EH) and the M13 procoat 805 wild type (pMS119EH) were washed 2 times with LB medium and then inoculated 1:100 in fresh LB medium (200µg/ml ampicillin, 25µg/ml chloramphenicol, 0.4% glucose). The cells were grown under depletion conditions to an OD$_{600}$ = 0.5 at 37°C. 200µl were taken and washed two times with 200µl 1x M9 salt mix and resuspended in 200µl M9 medium (-met). After 45 minutes at 37°C in the incubator 1 mM IPTG was added to induce the plasmid encoded genes for 10 minutes. 2µl of radioactive methionine (10 mCi/ml) were added for 1 minute prior to adding 20% TCA.

Immunoprecipitation

The immunoprecipitation was done similar to the protocol for the radioactive labeling (see 2.9.1) with a few exceptions. Only the M13AII antibody was used for these experiments and the samples were analyzed on 22% SDS Urea-gels.

2.11 Protein processing assay with the prescission protease

A prescission protease site was cloned between the dYidC protomers. This allows the digestion of the dYidC into its two protomers after the dimer was purified (see 2.8.2).

Reaction table	Final volume
Purified dYidC protein	100µl
Prescission buffer	100µl
Prescission protease/water (Lab stock)	5µl
Total volume	205µl

Prescission buffer (500 mM NaCl, 50 mM Tris, 1 mM EDTA, pH8) was added to the protein. The samples were incubated at 4°C for 3h then a final concentration of 75% methanol was added overnight. After centrifugation at 14000rpm for 10 minutes at 4°C the supernatant was discarded and the pellet was dried at 95°C for 5 minutes. Sample buffer (DTT free) was added and the pellet was vortexed and heated at 95°C for 5 minutes. The samples were then analyzed via SDS gel electrophoresis on a 10% gel followed by western blotting on a nitrocellulose membrane.

Blotting

The blotting chamber was assembled according to protocol and performed in a Trans-Blot® Electrophoretic Transfer Cell with transfer buffer in an ice box and an inserted cooling coil attached to a RM20 recirculating cooling bath. 1.5A were applied for 2 hours and the buffer was stirred with a stir bar for the duration to balance out the ion concentration during the electrophoresis.

The membrane was then reversibly stained with Ponceau S for protein fixation and observation of blotting efficiency. Afterwards most of the remaining Ponceau S was removed by carefully washing the membrane with distilled water followed by adding 50 ml of a 5% solution of blotting grade blocker in 1x phosphate buffered saline with Tween 20 (PBS-T). To block the membrane it was carefully shaken overnight at 4°C.

Immunodetection

The membrane was washed 3 times with PBS-T for 10 minutes followed by the addition of the YidC100 antibody, diluted 1:7500 in PBS-T. After the incubation for 1.5 hours the primary antibody solution was removed and the membrane was again washed 3 times with PBS-T for 10 minutes. Then the anti-mouse antibody, diluted 1:10000 in PBS-T, was added. After an additional hour the secondary antibody was discarded and the membrane was again washed 3 times with PBS-T for 10 minutes. After the last washing step the remaining PBS-T was carefully removed and 5 ml of the ECL mix was added and incubated for 5 minutes. Detection of protein bands was done with the ImageQuant LAS 4000 imaging system.

3 RESULTS

3.1 Crosslinking studies to determine contact sites between *E. coli* YidC and M13 Procoat

Crosslinking studies are one way to get insight into protein-protein interactions in living cells. Mapping contact sites between an enzyme and its substrate can give necessary information to help decipher the mechanism that occur during the interaction. In case of the insertase YidC and one of its substrates, M13 procoat, molecular contact data can help to understand how small proteins are inserted into the inner bacterial membrane.

YidC and the dimeric YidC (dYidC)

The monomeric YidC and the dYidC play an important role during the experiments presented here (see Fig. 22). The latter is an artificial dimer of YidC connected by a short linker and is central part of the second half of this work (see 3.2). Both proteins are shown here from a purification, which is later displayed in more detail (see 3.2.5).
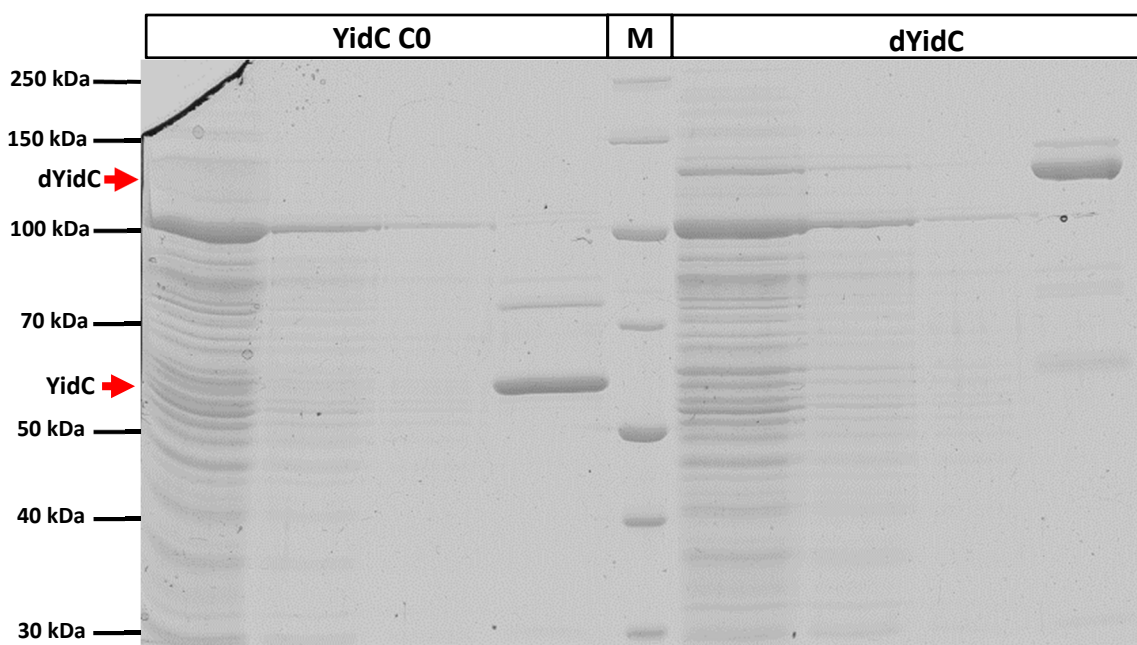
Fig. 22: The YidC mono and dimer on a Coomassie gel. The monomer runs at approx. 60 kDa and the dimer at approx. 125 kDa according to the marker. M: Marker PageRuler Broad Range #26630 (Thermo Fisher Scientific). Samples were separated on a 10% SDS acrylamide gel and Coomassie stained afterwards. A more detailed description of this purification can be found in 3.2.5.

Disulfide crosslinking utilizing different crosslinking agents

Disulfide crosslinking is a way to determine if two proteins get into contact with each other at specific positions. To screen for contacts between the *E. coli* YidC and the M13 procoat protein, cysteines were substituted in different positions to create a collection of single cysteine mutants that could easily be tested in different combinations. Many of these positions were already screened with other substrates like the mechanosensitive channel with large conductance (MscL) (Neugebauer et al. 2012), the subunit c of the F_1F_o ATP-Synthase (Yu et al. 2008) and the coat protein of the bacteriophage Pf3 (Klenner et al. 2008). The determination of differences and similarities among the different substrates can help to understand the basics of the insertion process. M13 procoat and MscL also have two TMs (Blount et al. 1996) whereas Pf3 spans the inner membrane once (Kiefer and Kuhn 1999). Comparing the known contact sites of the other substrates with those found in this work for M13 procoat might benefit to understand the way YidC functions.

Crosslinking studies were performed here with different parts of YidC and its substrate M13 procoat. In YidC, the TM3, TM5, parts of the C1- loop and residues in the hydrophilic groove were tested. For M13 procoat, cysteine mutants in both TMs and one in the loop were used for the experiments. A variety of crosslinking agents were utilized for the oxidation reactions to obtain disulfides.

3.1.1 DTNB as disulfide promoting agent

DTNB (Bis(3-carboxy-4-nitrophenyl) disulfide), also known as Ellman's reagent, was originally developed as a reagent to quantify thiol groups in unknown aqueous solutions (Ellman et al. 1959). Its capability as a disulfide promoting agent was discovered at a later point in time.

Other proteins have already been successfully crosslinked with DTNB *in vitro* (Tomishige and Vale 2000, Wickles et al. 2014) and *in vivo* (Park and Rapoport 2012). However, in this work an attempt to successfully crosslink two proteins *in vivo* with each other was performed with the goal to detect and even purify protein complexes in amounts fitting for biochemical analysis. To achieve this, the crosslinking agent had to have specific properties to be usable for this task. The first was to not interfere with cell growth too much or even kill the cells during oxidation. The second was the capability to oxidize the target proteins over a longer

time during their expression in the cells. And finally, a sufficient high efficiency in forming the desired crosslinking products is important. To test for these properties several known crosslinking agents have been tested (see Tab. 18).

Tab. 18: List of crosslinking agents and their solvents

Crosslinking agent/Reagent	Dissolved in	Final conc.
Copper phenanthroline	H_2O + EtOH (1:2)	1 mM
DTNB	100 mM in KPhos. pH 7.4	200 µM
Iodine	EtOH	250 µM
N,N'-(o-Phenylene)dimaleimide (o-PDM)	DMSO	500 µM
IPTG	$_{dd}H_2O$	1 mM

First, MK6S cells were grown with the addition of the different crosslinking agents to test their toxicity. To achieve this, MK6S cells were grown to an OD_{600} of approx. 0.2 before the addition of the respective reagent. Cell viability was observed regularly by measuring the optical density at 600 nm (see Fig. 23).
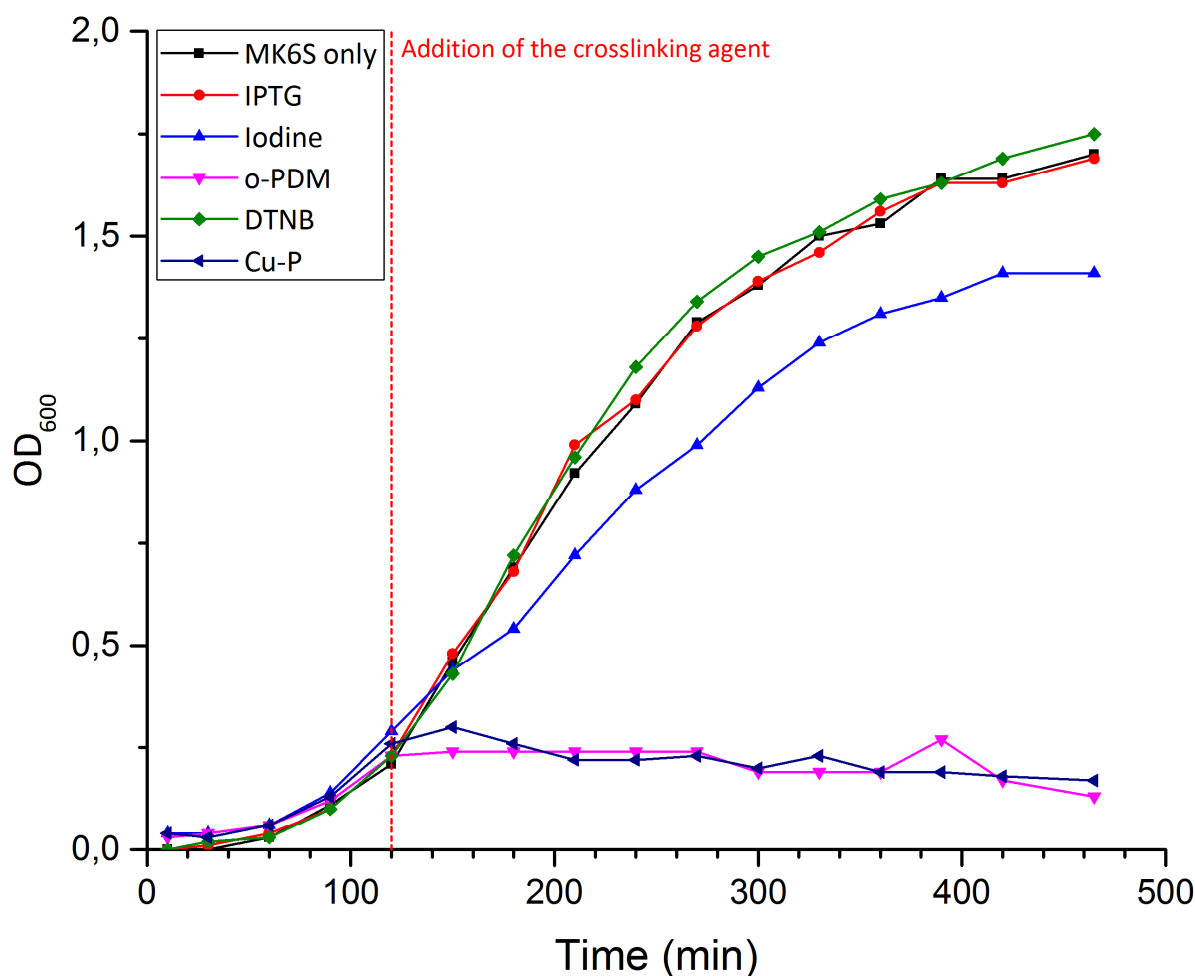
Fig. 23: Growth curves of *E. coli* MK6S cells after the addition of different crosslinking agents. o-PDM and copper-phenanthroline (Cu-P) arrested cell growth shortly after their addition. Iodine slowed bacterial growth down but did not stop it. Only DTNB, and IPTG as a control, did not influence the cell growth compared to the untreated cells.

From the tested crosslinking agents, only DTNB and iodine allowed the cells to grow, even though iodine impaired the cell growth to some extent. o-PDM and copperphenanthroline were lethal for the cells after a short period of time, which wouldn't allow the expression and crosslinking of protein over a longer period of time. DTNB and iodine were then used for crosslinking attempts *in vivo* in their tested concentrations (see Tab. 18).

The constructs pMS119EH H5 M13 procoat V33C, which encodes for a M13 procoat mutant with a cysteine at position 33, in combination with pGZ119EH YidC F424C or L427C, which encode for two YidC mutants with cysteines at position 424 or 427 respectively, were used for testing the crosslinking efficiency over a longer period of time. These positions were known to get into contact with each other from other pulse experiments (see 3.1.2). Two plasmids were transformed into MK6S cells. Overnight cultures were prepared in LB medium with the

respective antibiotics, 0.4% glucose and 0.2% arabinose. After incubation, the cultures were washed twice with additive free LB medium. The washed cells were inoculated 1:100 in fresh LB containing the same antibiotics and 0.4% glucose for depleting the chromosomal YidC. After at least 3 hours of incubation at 37°C and at an OD_{600} of 0.5, the cultures were induced with 1mM IPTG. 30 minutes after induction either a final concentration of 250 μM iodine or 200 μM DTNB was added to the cells. A control without DTNB or iodine was tested as well. 30, 90 and 180 minutes and overnight (o.n.) after the addition of the crosslinking agents, samples were taken from the cultures and mixed with a final concentration of 20% TCA for protein precipitation and Western blot analysis.

The results show, that iodine did not lead to crosslinks between H5 procoat V33C and YidC F424C for acquiring larger amounts of crosslinked protein over time (see Fig. 24A). DTNB on the other side is efficient to allow crosslinking the two proteins in living cells for at least 3 hours. This allows crosslinking experiments *in vivo* without radioactive labeling and the attempt to purify a YidC-substrate complex for further analysis later on. The crosslinking kinetic experiment (see Fig. 24B) also showed that over time more and more YidC was crosslinked with more than half of the YidC being complexed after 4.5 hours.
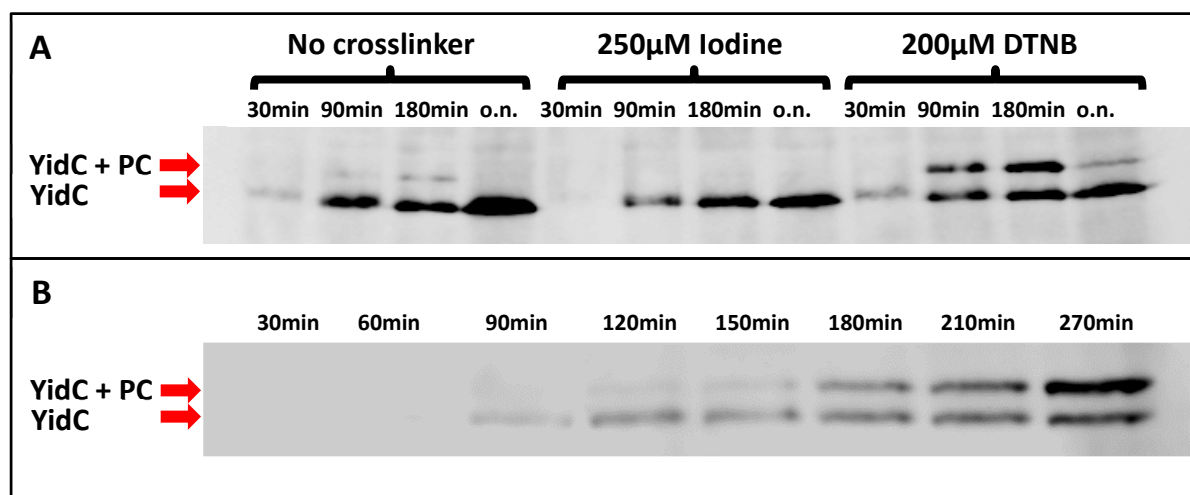
Fig. 24: Iodine and DTNB in a crosslinking attempt and accumulation over time of YidC and the YidC substrate complex. (A) Iodine treatment shows no crosslinking between H5 M13 procoat V33C and YidC F424C. DTNB treatment shows a clear crosslinking band in the 90, 180 min and overnight sample. The signal in the last sample however became weaker again. The 30 min sample showed no crosslinking. Surprisingly in absence of crosslinking agents, a weak crosslinking signal at the 180 minute mark could be observed. (B) Crosslinking over 4.5 hours with the L427C YidC mutant. DTNB was used as disulfide promoting agent added 20 minutes after induction. The accumulation of YidC and the substrate complex was observed. Numbers are the time in minutes after the addition of the crosslinking agent, PC = H5 M13 procoat. Western Blot with anti His_{10}tag antibody (Sigma-Aldrich). O.n.: over night.

The results show, that DTNB is suitable to attempt further crosslinking experiments *in vivo*. With more than half of YidC crosslinked with its substrate over time this crosslinking agent shows high efficiency in generating a protein-protein complex.

3.1.2 Crosslinking between YidC and M13 procoat gp8

To screen for contacts between the M13 procoat protein and YidC, cysteine substitutions in various positions were constructed. These mutants were then co-expressed in YidC-depleted MK6S cells for either pulse labeling experiments (see 2.9.1) or in Western blot crosslinking studies (see 2.9.2). Different crosslinking agents (see Tab. 18) were used during the screening for contact sites in the pulse experiments. However, for the Western blot, only DTNB was used since it was found to be the only reagent that could be added during the expression without harming the cells for a longer period of time (see 3.1.1). It was also the only reagent that kept its oxidizing property over the course of several hours.

3.1.2.1 Crosslinking with TM3 and TM5 of YidC

The transmembrane domain three (TM3) and five (TM5) of YidC have been tested for contacts with other substrates in the past. Several sites have been found for the Pf3 coat protein (Klenner et al. 2012) and the MscL (Neugebauer et al. 2012). Therefore, these regions in YidC were also tested with the M13 procoat protein. The solved structure of YidC also showed that TM3 and TM5 form a "gate" to a hydrophilic groove inside of the protein, which is believed to play an important role in the insertion process (Kumazaki et al. 2014b). This groove should only be accessible by the cytoplasm and laterally by passing between TM3 and TM5. Here, a variety of cysteine mutants of H5 M13 procoat was crosslinked with YidC. These M13 mutants are harboring cysteines in their transmembrane domains (TMs), either in the leader peptide or the mature protein (see Tab. 19). The expression of the tested YidC mutants in the crosslinking experiments was tested and documented on the respective gels. Immunoprecipitation was performed with anti YidC100 (Lab-stock) antibody if not stated otherwise. For the radioactive crosslinking experiments, the YidC mutant M18C was coexpressed with H5 M13 procoat V30C as a positive controls. For the non-radioactive experiments with DTNB as crosslinking agent, the YidC mutants F424C, L427C or M430C were

combined with H5 M13 procoat V33C. As negative controls either cysteine-less YidC (YidC C0) or the cysteine-less H5 M13 procoat wildtype were expressed. In the beginning of this study, YidC was expressed from the pACYC184 low copy plasmid instead of pGZ119EH. These exceptions are indicated with an asterisk and described.

Tab. 19: Cysteine mutants used for crosslinking experiments with YidC. The substitutions were in either the TM1 (leader sequence) or TM2 (mature sequence) of the M13 procoat protein.

H5 M13 procoat mutant	Cysteine position
H5 M13 procoat A-12C	Alanine substitution at position -12 in the leader sequence
H5 M13 procoat A-10C	Alanine substitution at position -10 in the leader sequence
H5 M13 procoat T-9C	Threonine substitution at position -9 in the leader sequence
H5 M13 procoat Y24C	Tyrosine substitution at position 24 in the mature sequence
H5 M13 procoat V29C	Valine substitution at position 29 in the mature sequence
H5 M13 procoat V30C	Valine substitution at position 30 in the mature sequence
H5 M13 procoat V31C	Valine substitution at position 31 in the mature sequence
H5 M13 procoat I32C	Isoleucine substitution at position 32 in the mature sequence
H5 M13 procoat V33C	Valine substitution at position 33 in the mature sequence
H5 M13 procoat G34C	Glycine substitution at position 34 in the mature sequence
H5 M13 procoat A35C	Alanine substitution at position 35 in the mature sequence

Expression of the different H5 M13 procoat cysteine mutants

To assure that all H5 M13 procoat mutants are expressed, pulse experiments were conducted. The samples were pulse labeled and immunoprecipitated as described without crosslinking agents (see 2.9.1). The different plasmids showed good levels of expression, some mutants formed dimers even without any oxidizing agents added to the culture (see Fig. 25 and 26).

The next part covers the results with the detected contact sites between YidC TM3/TM5 and M13 procoat. Cysteine substitutions in both TMs of M13 procoat were crosslinked with YidC, which enables to see where YidC contacts its substrate during the insertion process.
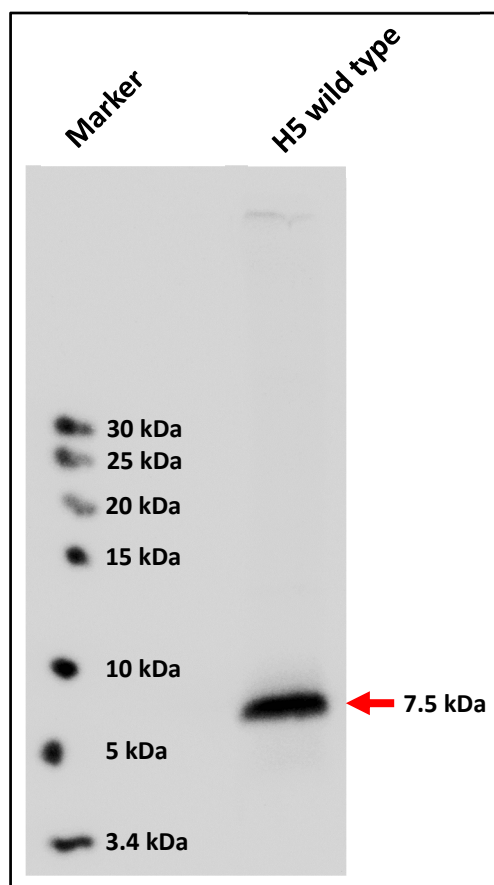
Fig. 25: Expression of the H5 procoat wild type with the Marker #26632 (Thermo Fisher Scientific). A cleat band is shown at approx. 7.5 kDa. Detection via phosphorimaging after pulse-labeling for 1 minute. Immunoprecipitation with anti M13 antibody (Lab-stock).
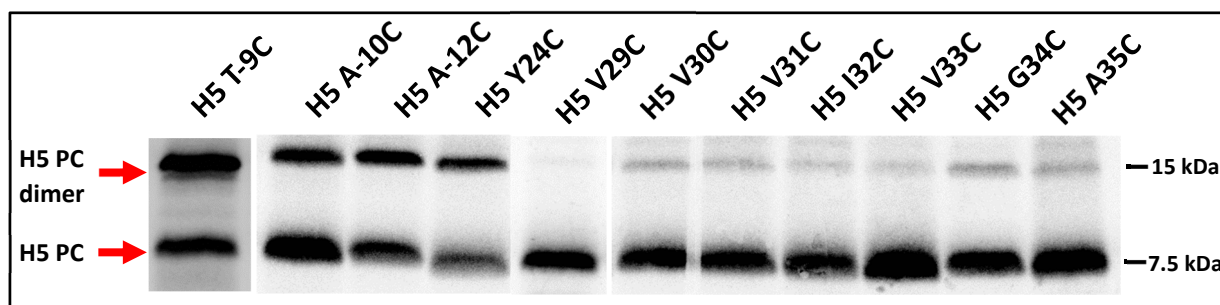
Fig. 26: Expression of the different H5 M13 procoat cysteine mutants. Expression was clearly detectable for all used mutants. Some mutants form dimers even without adding a crosslinking agent. Detection via phosphorimaging after pulse-labeling for 1 minute. Immunoprecipitation with anti M13 antibody.

H5 M13 Procoat A-12C mutant

The A-12C mutant is the first tested cysteine mutant of TM1. In this mutant, an alanine in the leader peptide has been replaced by cysteine. It is located in the first TM of M13 procoat near the cytosolic membrane surface (see Fig. 27). In the pulse experiments, crosslinking was induced by the addition of copper phenanthroline (see 2.9.1) and the found contacts are shown in Fig. 28.
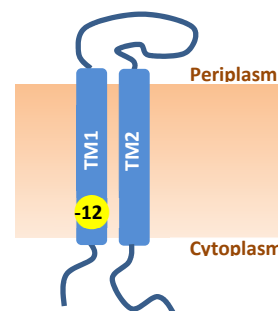

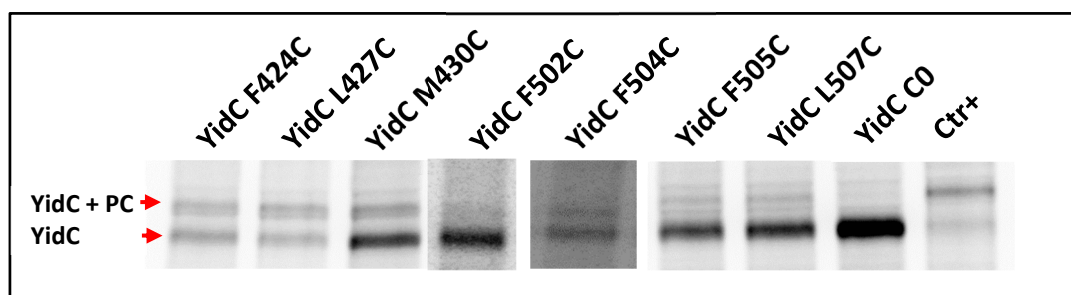**Fig. 27: Position of the substituted alanine in the H5 M13 A-12C procoat protein.**

Fig. 28: Contacts found with pulse experiments with the M13 H5 procoat A -12C mutant. Oxidation was performed with copper phenanthroline. Strong contacts are located within the TM3 of YidC at position 424 and 427 and weak signals could be observed for position 430 and 504. Samples were immunoprecipitated with the YidC antibody. YidC C0 was used as negative control. Detection was performed via phosphorimaging. Crt+: positive control with YidC M18C and H5 M13 Procoat V30C as crosslinking partners.

With DTNB as crosslinking agent and Western blotting as detection method (see 2.9.2) the contacts in TM3 found by pulse labeling could be confirmed and some neighboring positions also showed crosslinking signals. However, the tested sites in TM5 did not show crosslinking products. (See Fig. 29).
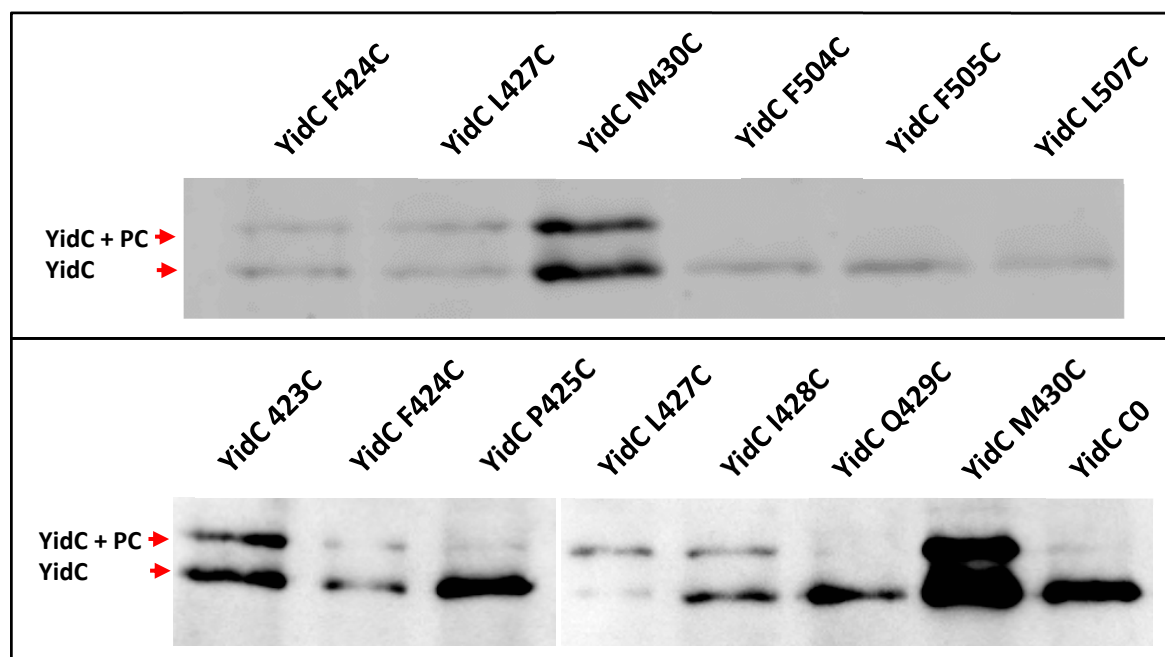
Fig. 29: Non-radioactive crosslinks found by oxidation by DTNB with the M13 procoat A-12C mutant. MK6S cells were treated with DTNB and analyzed on a Western blot with anti-His$_{10}$tag antibody. The contacts in the TM3 have been detected with this method. YidC C0 was used as negative control.

Altogether, the results show contact sites in the lower and middle part of TM3 and the middle and higher part of TM5 (see Fig. 30). The positions of the contacts are listed in Tab. 20. Interestingly, this H5 procoat mutant is contacting both TMs even though only at one position in TM5 with a weaker signal. However, the interaction with TM5 could not be confirmed with the non-radioactive protocol.

Tab. 20: Detected contact positions in the respective TMs of YidC with the H5 M13 procoat A-12C mutant. Strong contact sites are indicated with bold numbers.

YidC TM3	YidC TM5
423, 424, 427, 428, **430**	504
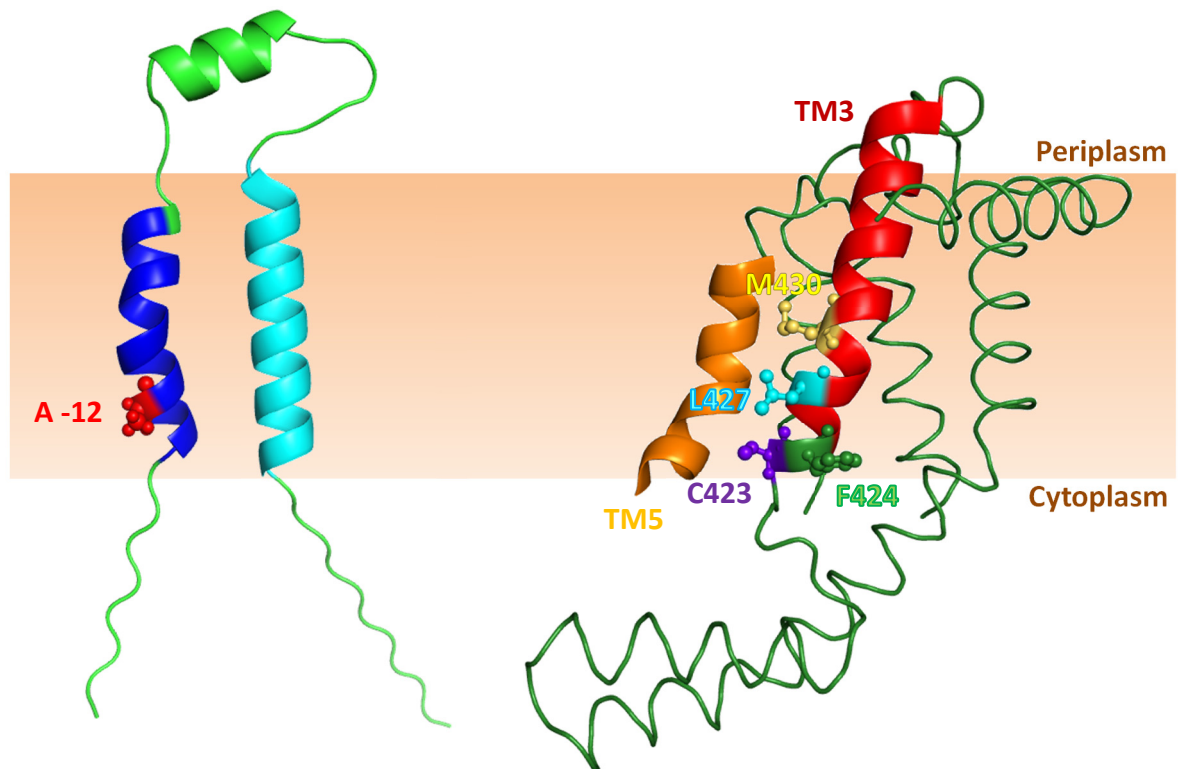
Fig. 30: Strong contact sites between H5 M13 procoat A -12C and YidC in the TM3 and TM5. The strong contacts found are located in the cytoplasmic and central oriented part of TM3 of YidC at position 423, 424, 427 and 430. The cysteine mutant of H5 M13 procoat is positioned towards the cytoplasmic leaflet of the transmembrane domain of the leader peptide. Blue helix: TM1 of M13 procoat, cyan helix: TM2 of M13 procoat, red helix: TM3 of YidC, orange helix: TM5 of YidC, variously colored and labeled amino acid residues: contact sites between M13 procoat and YidC. Model of M13 procoat visualized with PyMol 1.3. Figure of YidC created with PDB entry 3WVF in PyMol 1.3, the P1 domain has been removed for a better overview (Kumazaki et al. 2014b).

H5 M13 Procoat A-10C mutant

An alanine in the leader peptide at position -10 has been replaced by a cysteine. It is located slightly below the middle of the first TM towards the cytoplasm (see Fig. 31). In the pulse experiments crosslinking was induced by the addition of copper phenanthroline (see 2.9.1) and the detected contacts are shown in Fig. 32. The contacts at position 424 and 427 are weak but detectable indicating a protein-protein interaction at this position while the contacts at positions 430 (TM3) and 504 (TM5) are strong.
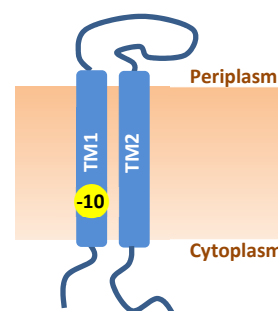
Fig. 31: Position of the substituted alanine in the H5 M13 procoat A-10C protein.
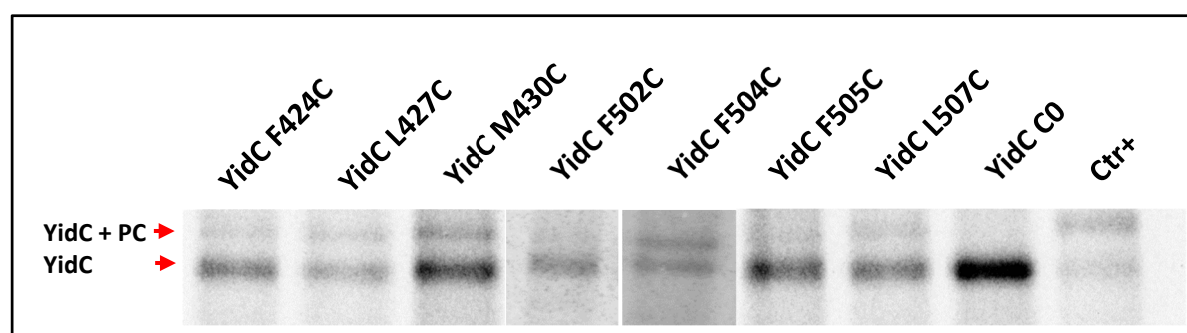
Fig. 32: Contacts found with pulse experiments with the M13 H5 procoat A-10C mutant. The contacts are located within the TM3 and TM5 of YidC. Copper phenanthroline was used as crosslinking agent. Samples were immunoprecipitated with the YidC antibody. YidC C0 was used as negative control. Detection was performed via phosphorimaging.

With DTNB as crosslinking agent and Western blot as detection method (see 2.9.2) some of the contacts found in TM3 by pulse labeling could be confirmed. However, for some sites no crosslinking products could be detected. In TM5, no contacts were detected (See Fig. 33).
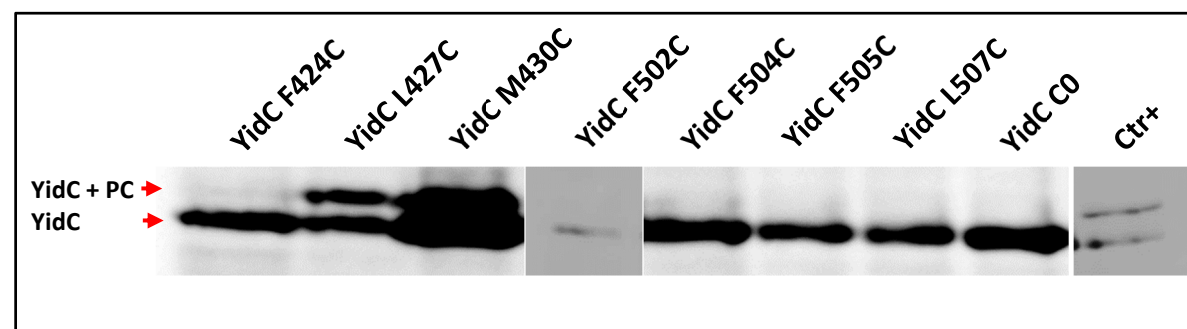

Fig. 33: Non-radioactive crosslinks found by oxidation with DTNB with the M13 procoat A-10C mutant. In vivo crosslinking with DTNB via western blot detection with anti-His$_{10}$tag antibody. With this method only some of the contacts could be confirmed. YidC C0 was used as negative control.

Tab. 21: Detected contact positions in the respective TMs of YidC with the H5 M13 procoat A-10C mutant. Strong contact sites are indicated with bold numbers.

YidC TM3	YidC TM5
424, 427, **430**	**504**

The results show contacts in the lower and middle part of TM3 and the central and periplasmic part of TM5 (see Fig. 34). The positions of the contacts are listed in Tab. 21. This H5 procoat mutant also contacts TM3 and TM5 of YidC.
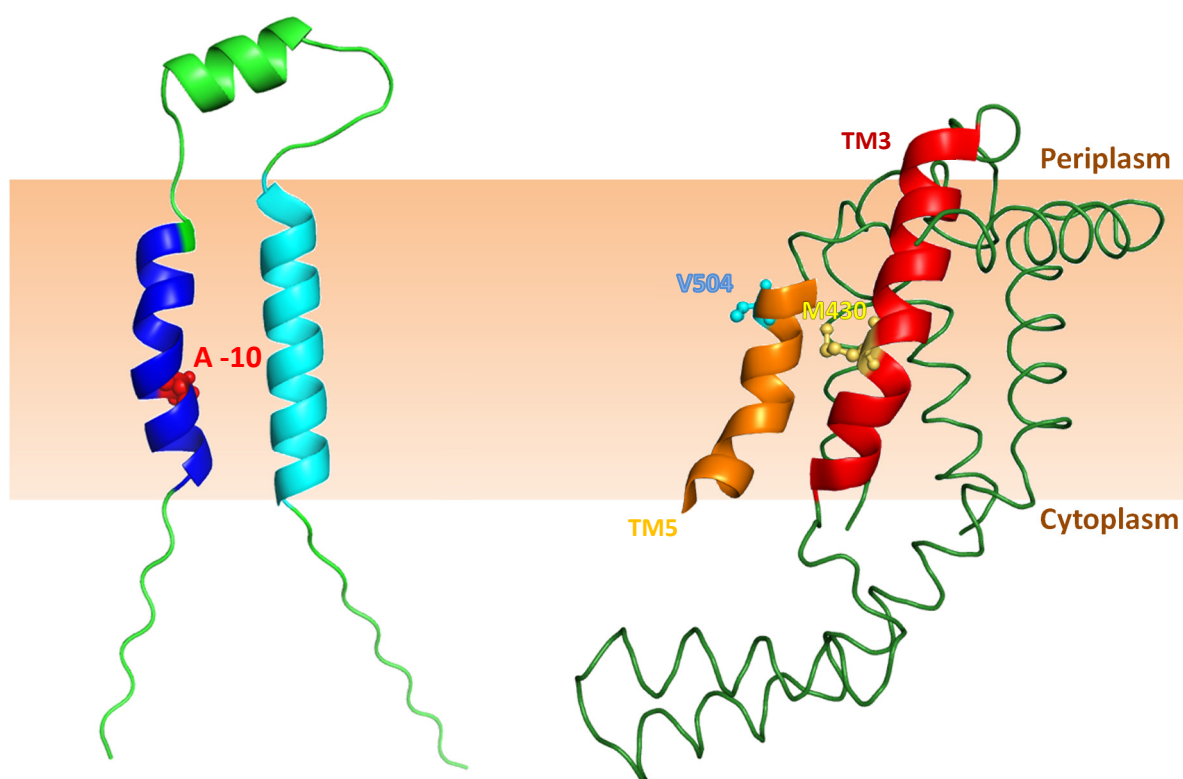

Fig. 34: Strong contact sites between H5 M13 procoat A-10C and YidC in the TM3 and TM5. The contacts found are located in the parts in the center and towards the cytoplasm of TM3 of YidC at position 424, 427 and 430. The cysteine mutant of H5 M13 procoat is positioned near the center of the transmembrane domain of the leader peptide. Blue helix: TM1 of M13 procoat, cyan helix: TM2 of M13 procoat, red helix: TM3 of YidC, orange helix: TM5 of YidC, variously colored and labeled amino acid residues: contact sites between M13 procoat and YidC. Model of M13 procoat visualized with PyMol 1.3. Figure of YidC created with PDB entry 3WVF in PyMol 1.3, the P1 domain has been removed for a better overview (Kumazaki et al. 2014b).

H5 M13 Procoat T-9C mutant

A threonine in the leader peptide at position -9 has been replaced by a cysteine. It is located in the middle of the first TM of M13 procoat (see Fig. 35). In the pulse experiments crosslinking was induced by the addition of copperphenanthroline (see 2.9.1) and the found contacts are shown in Fig. 36.
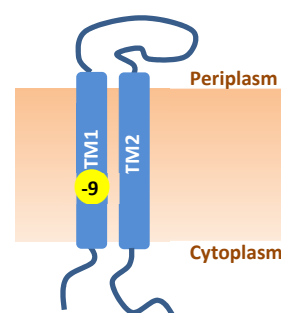

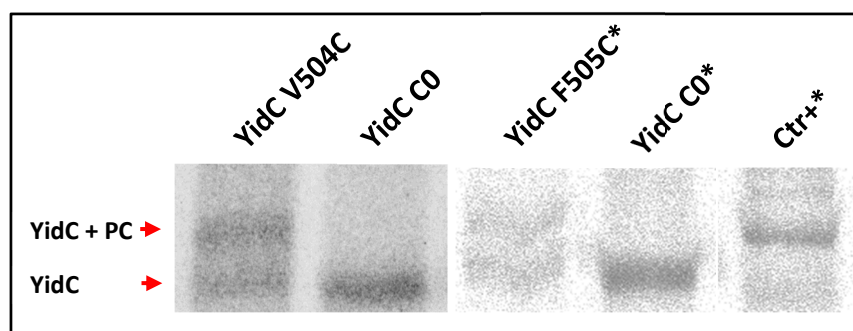**Fig. 35: Position of the substituted threonine in the H5 M13 procoat T-9C protein.**

Fig. 36: Contact found with pulse experiments with the M13 H5 procoat T-9C mutant. The contacts are located within the TM5 of YidC. Samples were immunoprecipitated with the YidC antibody. YidC C0 was used as negative control. Detection was performed via phosphoimaging. *YidC expressed from the pACYC184 plasmid instead of pGZ119EH

The results show contacts in the periplasmic oriented parts of TM5 (see Fig. 37). The positions of the contacts are listed in Tab. 22.

Tab. 22: Detected contact positions in the respective TMs of YidC with the H5 M13 procoat T-9C mutant. Strong contact sites are indicated with bold numbers.

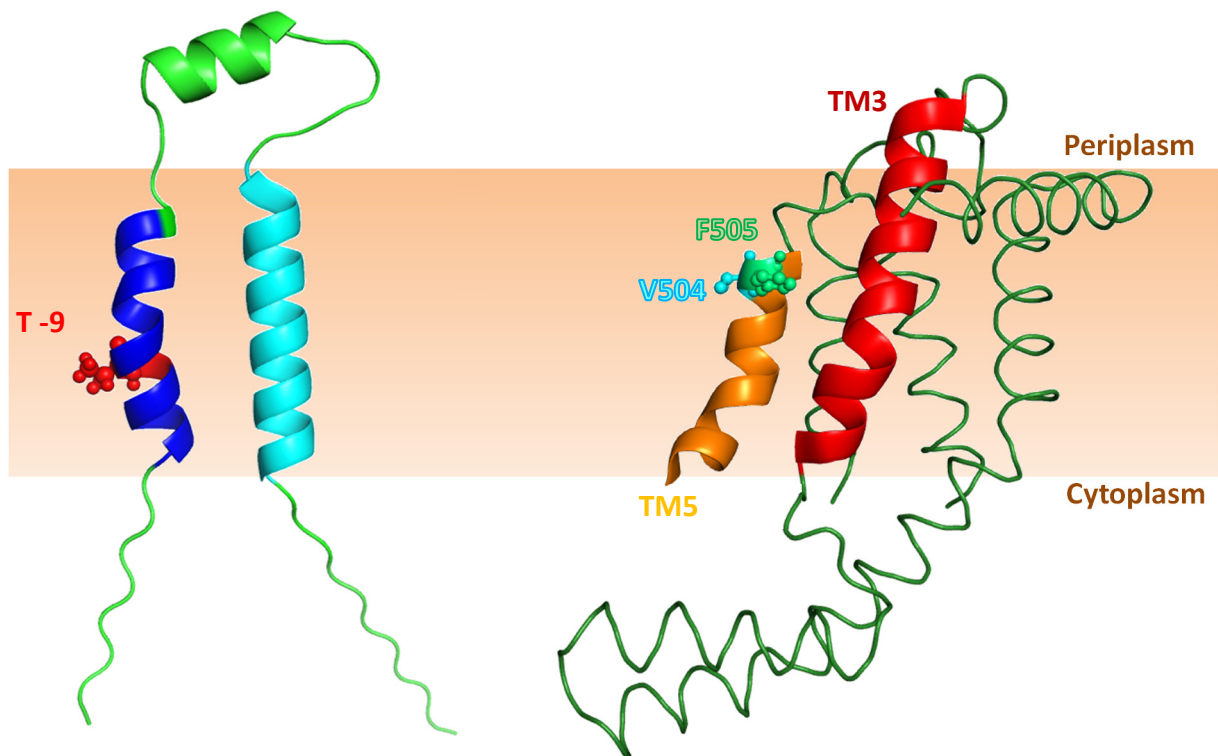| YidC TM5 |
| --- |
| **504, 505** |

Fig. 37: Strong contact sites between H5 M13 procoat T-9C and YidC in the TM5. The contacts that were detected are positioned in the periplasmic oriented parts of TM5 of YidC at position 504 and 505. The cysteine mutant of H5 M13 procoat is positioned in the center of the transmembrane domain of the leader peptide. Blue helix: TM1 of M13 procoat, cyan helix: TM2 of M13 procoat, red helix: TM3 of YidC, orange helix: TM5 of YidC, variously colored and labeled amino acid residues: contact sites between M13 procoat and YidC. Model of M13 procoat visualized with PyMol 1.3. Figure of YidC created with PDB entry 3WVF in PyMol 1.3, the P1 domain has been removed for a better overview (Kumazaki et al. 2014b).

H5 M13 Procoat Y24C mutant

In this mutant a tyrosine in the mature part of the peptide has been replaced by cysteine. It is located in the second TM of M13 procoat near the membrane surface towards the periplasm (see Fig. 38). In the pulse experiments crosslinking was induced by three different crosslinking agents: iodine, copperphenanthroline and DTNB (see 2.9.1). The contact sites found are shown in Fig. 39.
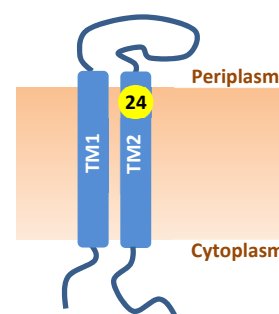

Fig. 38: Position of the substituted tyrosine in the H5 M13 procoat Y24C protein.
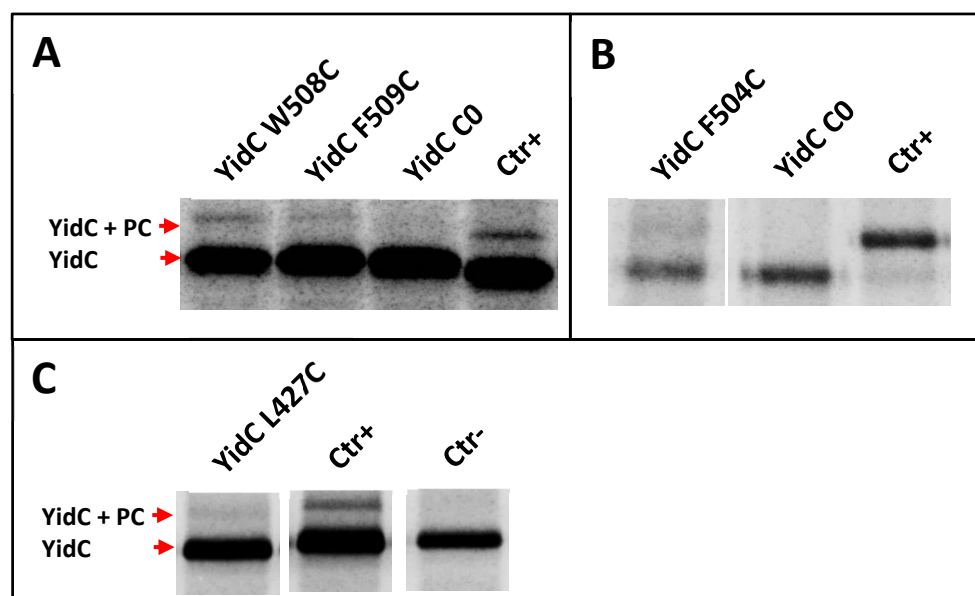

Fig. 39: Contacts found with pulse experiments with the M13 H5 procoat Y24C mutant. The contacts are located within the TM3 and TM5. (A) Weak contacts found with iodine as crosslinking agent. (B) Contacts found with copperphenanthroline as crosslinking agent. (C) Contacts found with DTNB as crosslinking agent. Samples were immunoprecipitated with the YidC antibody. YidC C0 was used as negative control in most cases. Detection was performed via phosphoimaging. Crt- is a negative control with the cysteine-free H5 procoat.

The results showed weak contacts in the middle part of TM3 and the upper part of TM5 (see Fig. 40). The positions of the contacts are listed in Tab. 23.

Tab. 23: Weak contact positions in the respective TMs of YidC with the H5 M13 procoat Y24C mutant.

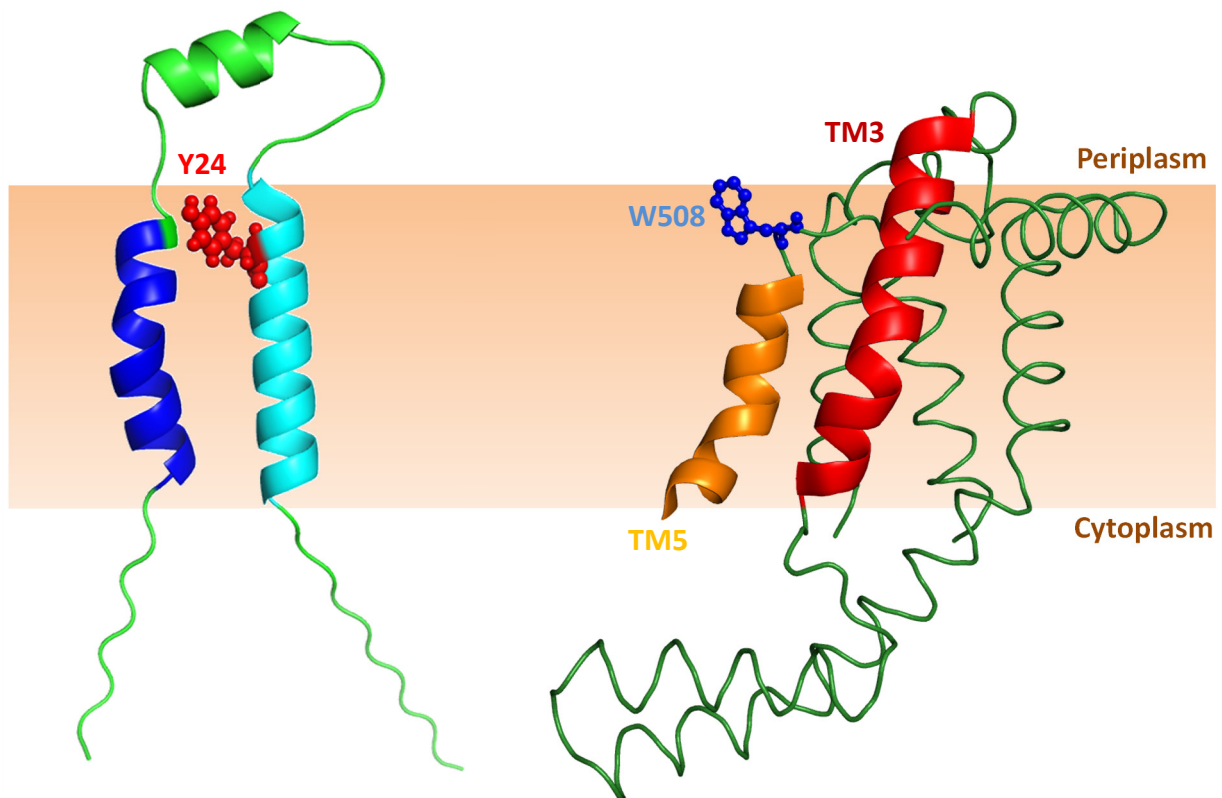| YidC TM3	YidC TM5
427	504, 508, 509

Fig. 40: Contact site between H5 M13 procoat Y24C and YidC in the TM5. The contact found is located in the periplasmic oriented parts of TM5 of YidC at position 508. The cysteine mutant of H5 M13 procoat is positioned near the periplasm in the transmembrane domain of the mature peptide. Blue helix: TM1 of M13 procoat, cyan helix: TM2 of M13 procoat, red helix: TM3 of YidC, orange helix: TM5 of YidC, variously colored and labeled amino acid residues: contact sites between M13 procoat and YidC. Model of M13 procoat visualized with PyMol 1.3. Figure of YidC visualized with PDB entry 3WVF in PyMol 1.3, the P1 domain has been removed for a better overview (Kumazaki et al. 2014b).

H5 M13 Procoat V29C mutant

In this mutant, a valine in the mature part of the peptide has been replaced by cysteine. It is located above the center of the second TM towards the periplasm (see Fig. 41). In the pulse experiments crosslinking was induced by copper phenanthroline. (see 2.9.1). The contact sites found are shown in Fig. 42.
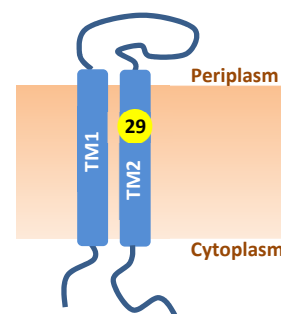

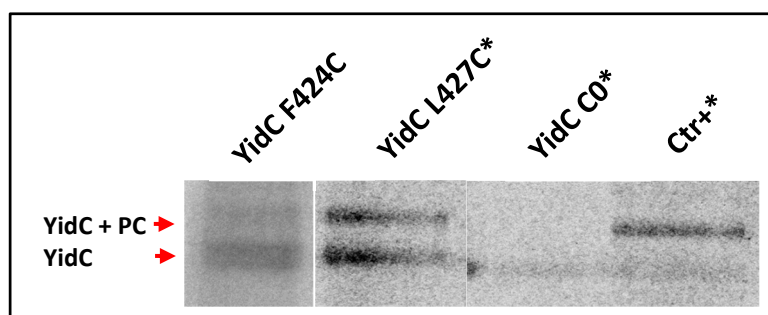**Fig. 41: Position of the substituted valine in the H5 M13 procoat V29C protein.**

Fig. 42: Contacts found with pulse experiments with the M13 H5 procoat V29C mutant. The contacts are located within the TM3. TM5 hasn't been tested with this procoat mutant. Contacts found with copper phenanthroline as crosslinking agent. Samples were immuno-precipitated with the YidC antibody. YidC C0 was used as negative control. Detection was performed via phosphoimaging. *YidC expressed from the pACYC184 plasmid instead of pGZ119EH

The results show contacts in the cytoplasmic oriented part of TM3 (see Fig. 43). The positions of the contacts are listed in Tab. 24.

Tab. 24: Detected contact positions in the respective TMs of YidC with the H5 M13 procoat V29C mutant. Strong contacts are indicated with bold numbers.

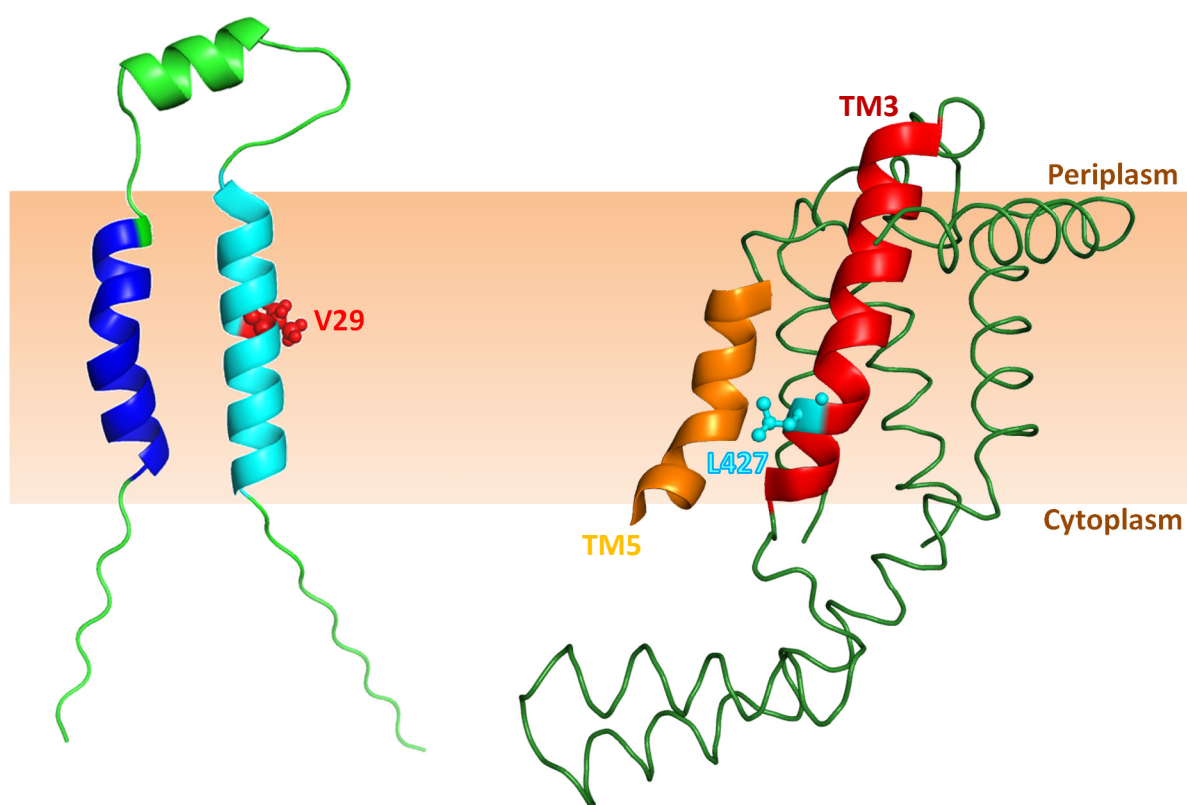| YidC TM3 |
| --- |
| 424, **427** |

Fig. 43: Strong contact site between H5 M13 procoat V29C and YidC in the TM3. The contact found is located in the cytoplasmic parts of TM3 of YidC at position 427. The V29C cysteine mutant of H5 M13 procoat is positioned in the middle of the transmembrane domain of the mature peptide. Blue helix: TM1 of M13 procoat, cyan helix: TM2 of M13 procoat, red helix: TM3 of YidC, orange helix: TM5 of YidC, variously colored and labeled amino acid residues: contact sites between M13 procoat and YidC. Model of M13 procoat visualized with PyMol 1.3. Figure of YidC visualized with PDB entry 3WVF in PyMol 1.3, the P1 domain has been removed for a better overview (Kumazaki et al. 2014b).

H5 M13 Procoat V30C mutant

In this mutant, a valine at position 30 in the mature part of the procoat protein has been replaced by cysteine. It is located in the center of the second TM of M13 procoat (see Fig. 44). In the pulse experiments crosslinking was induced by copper phenanthroline (see 2.9.1). The contacts for the positions 424 and 425 in YidC are relatively weak but a signal can be seen. Also a contact has been found after the DTNB-treatment on a Western blot. Interestingly, in comparison with the pulse experiments with copperphenanthroline,

Fig. 44: Position of the substituted valine in the H5 M13 procoat V30C protein.

YidC M18C and H5 M13 procoat V30C, were not crosslinked with DTNB (see 2.9.2). The contact
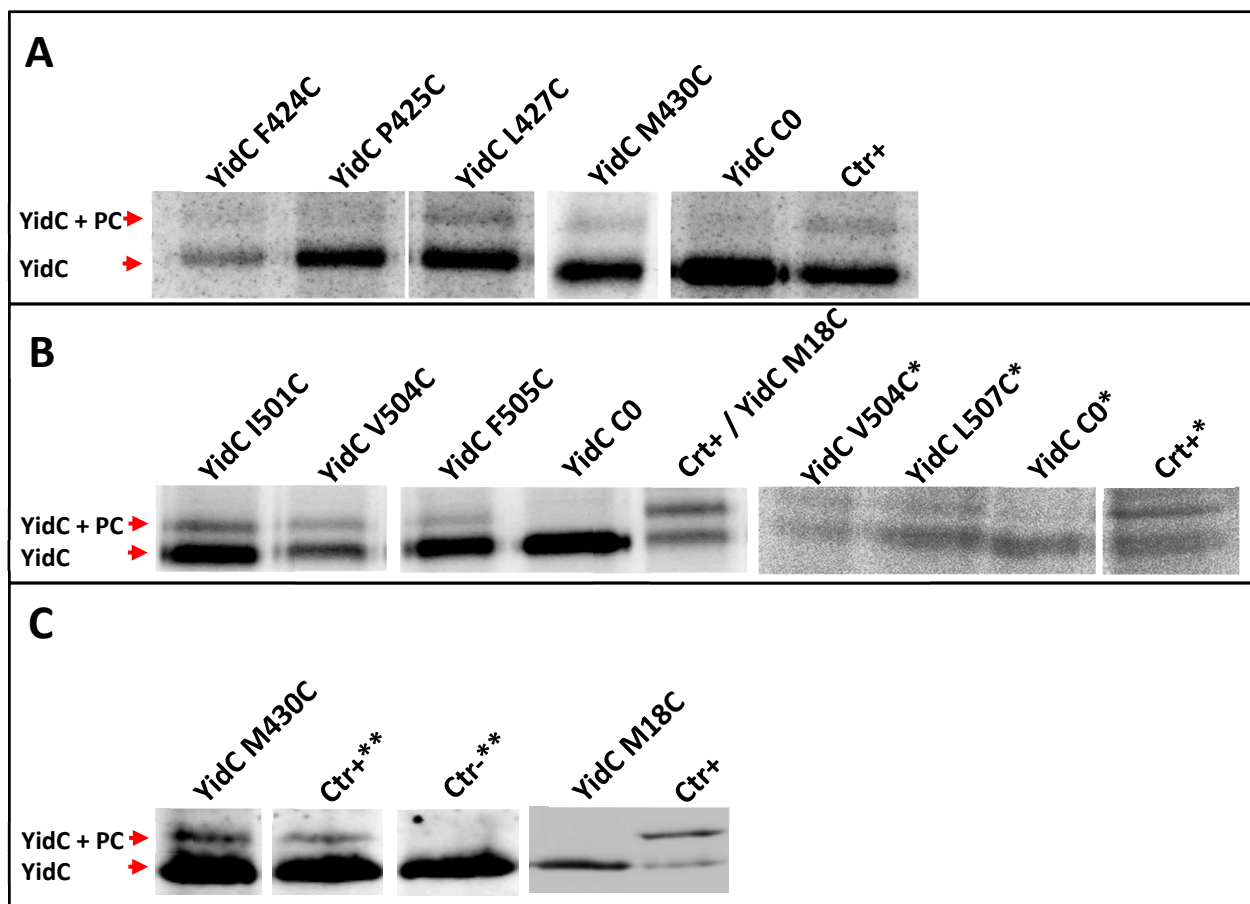

Fig. 45: Contacts found with pulse experiments with the M13 H5 procoat V30C mutant. The contacts are located within the TM3 and TM5. Contacts found with copper phenanthroline as crosslinking agent. (A) Contact sites with TM3 of YidC with a strong signal at position 427. (B) Strong contact sites with TM5 of YidC at positions 501, 504 and 507 and a strong contact in TM1 (M18C). Samples were immunoprecipitated with the YidC antibody. YidC C0 was used as negative control. Detection was performed via phosphorimaging. *YidC expressed from the pACYC184 plasmid instead of pGZ119EH. (C) Contact with the M430C YidC mutant crosslinked via DTNB oxidation and detection by Western blot with an anti-His$_{10}$tag antibody. The used positive control for copper phenanthroline crosslinking with YidC M18C does not show a signal with DTNB. Ctr- is a negative control with the cysteine-free H5 procoat and the M430C YidC mutant. ** These controls were used in a crosslinking attempt for the M430C mutant with the H5 M13 procoat mutants V30C, V31C, I32C, V33C, G34C and A35C that are displayed in the next experiments.

sites found are shown in Fig. 45. The results show contacts in the cytoplasmic and central oriented parts of TM3 and the central and periplasmic oriented parts of TM5 (see Fig. 46). The positions are listed in Tab. 25.

Tab. 25: Detected contact positions in the respective TMs of YidC with the H5 M13 procoat V30C mutant. Strong contacts are indicated with bold numbers.

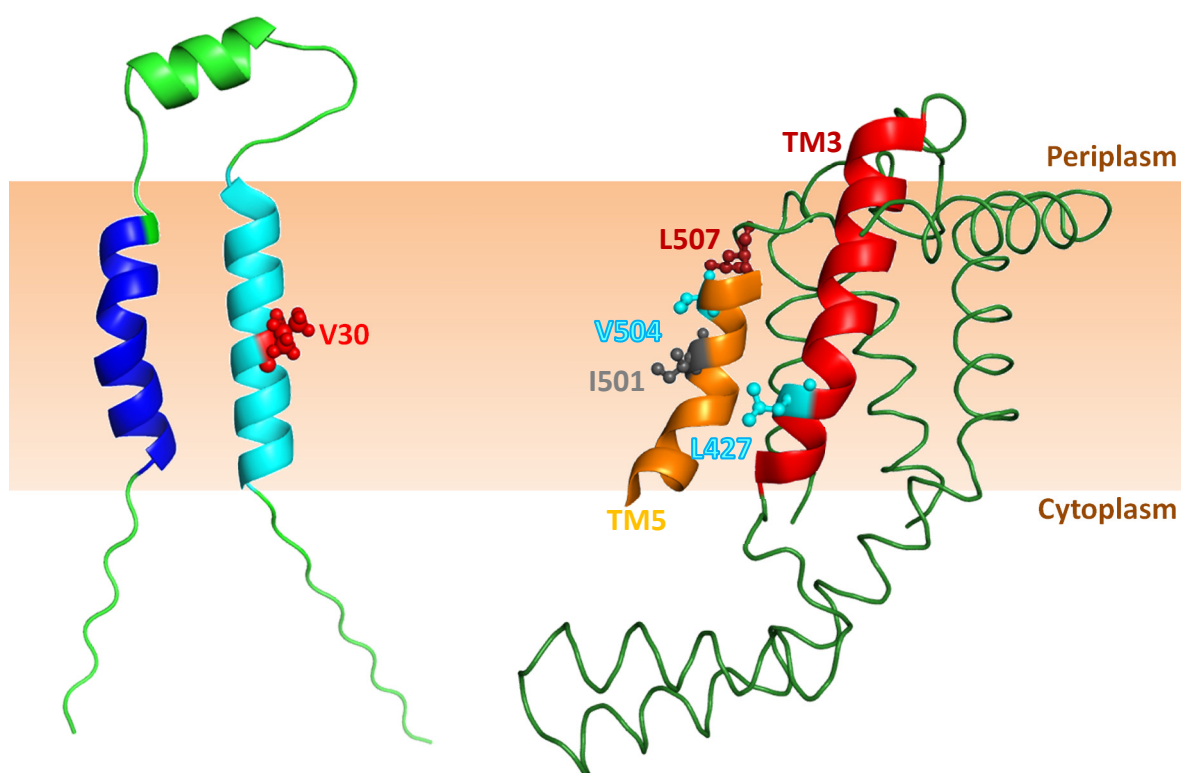| YidC TM1	YidC TM3	YidC TM5
18	**427**, 430	**501, 504**, 505, **507**

Fig. 46: Contact sites between H5 M13 procoat V30C and YidC in the TM3 and TM5. The contacts found are located in the cytoplasmic part of TM3 at position 427 and in the central to periplasmic parts of TM5 of YidC at position 501, 504 and 507. The contact detected in TM1 of YidC can't be shown in the structure, it is positioned in the center of the first TM of YidC. The cysteine mutant of H5 M13 procoat is positioned near the center of the transmembrane domain of the mature peptide. Blue helix: TM1 of M13 procoat, cyan helix: TM2 of M13 procoat, red helix: TM3 of YidC, orange helix: TM5 of YidC, variously colored and labeled amino acid residues: contact sites between M13 procoat and YidC. Model of M13 procoat visualized with PyMol 1.3. Figure of YidC visualized with PDB entry 3WVF in PyMol 1.3, the P1 domain has been removed for a better overview (Kumazaki et al. 2014b).

H5 M13 Procoat V31C mutant

The valine at position 31 in the mature part of the peptide has been replaced by cysteine. It is located in the second TM in the center of the lipid bilayer (see Fig. 47). In the pulse experiments crosslinking was induced by copper phenanthroline. (see 2.9.1). In the Western blot detection experiments DTNB was used for oxidation (see 2.9.2). For position 430 in YidC, oxidation with copper phenanthroline did not yield a crosslinking product. However, crosslinking with DTNB followed by Western blotting and immunodetection showed a clear crosslinking signal. The
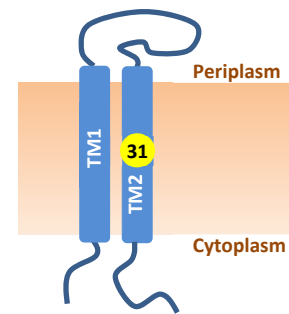
Fig. 47: Position of the substituted valine in the H5 M13 procoat V31C protein.
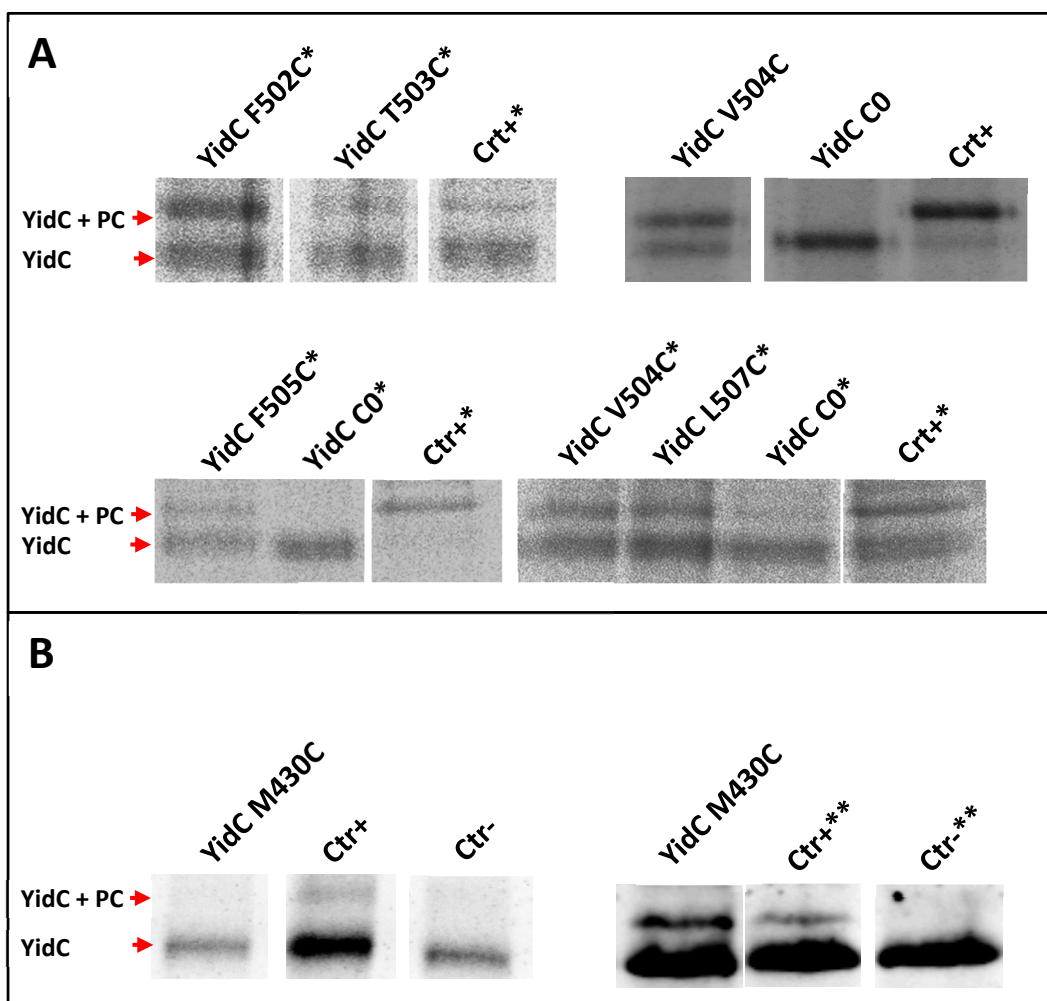
Fig. 48: Contacts found with pulse experiments with the M13 H5 procoat V31C mutant. The contacts are located within the TM3 and TM5. (A) Contact sites with TM5 of YidC. Contacts found with copper phenanthroline as crosslinking agent. (B) Contact site with TM3 of YidC. Left: Oxidation with copper phenanthroline didn't yield a crosslinking product. Right: Crosslinking with DTNB followed by Western blotting and immunodetection with a His$_{10}$tag antibody showed a clear crosslinking signal. Pulse samples were immunoprecipitated with the YidC antibody. YidC C0 was used as negative control. Detection was performed via phosphorimaging. *YidC expressed from the pACYC184 plasmid instead of pGZ119EH. Ctr- is a negative control with the cysteine-free H5 procoat and the M430C YidC mutant. ** Same controls as in Fig. 23

contact sites found are documented in Fig. 48. The results show contacts in the central part of TM3 and the central and periplasmic oriented parts of TM5 (see Fig. 49). The positions of the contacts are listed in Tab. 26.

Tab. 26: Found contact positions in the respective TMs of YidC with the H5 M13 procoat V30C mutant. Strong contacts are indicated with bold numbers.

YidC TM3	YidC TM5
430	**502,** 503, **504**, 505, **507**
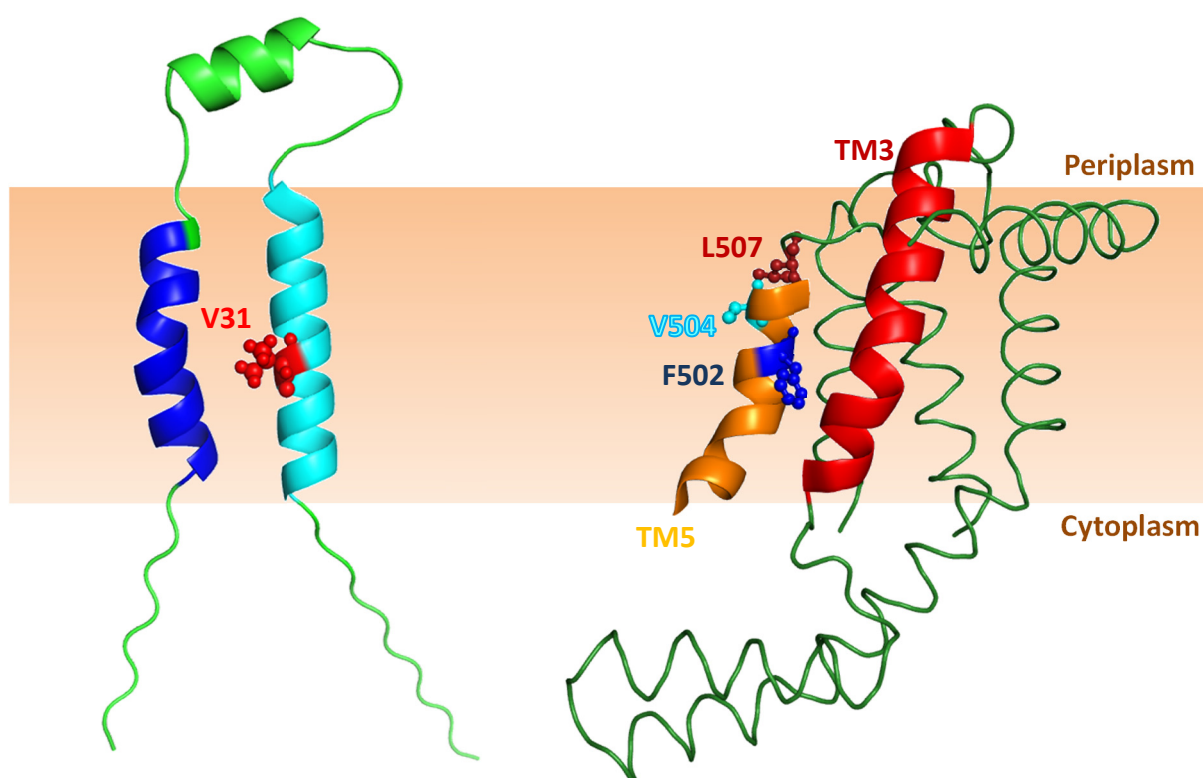
Fig. 49: Strong contact sites between H5 M13 procoat V31C and YidC in the TM5. The contacts found are located in the central to periplasmic parts of TM5 of YidC at position 502, 504 and 507. The cysteine mutant of H5 M13 procoat is positioned in the center of the transmembrane domain of the mature peptide. Blue helix: TM1 of M13 procoat, cyan helix: TM2 of M13 procoat, red helix: TM3 of YidC, orange helix: TM5 of YidC, variously colored and labeled amino acid residues: contact sites between M13 procoat and YidC. Model of M13 procoat visualized with PyMol 1.3. Figure of YidC visualized with PDB entry 3WVF in PyMol 1.3, the P1 domain has been removed for a better overview (Kumazaki et al. 2014b).

H5 M13 Procoat V33C mutant

A valine at position 33 in the mature part of the peptide has been replaced by cysteine. It is located in the middle part of the second TM of M13 procoat towards the cytoplasmic side (see Fig. 50). In the pulse experiments, crosslinking was promoted by iodine, DTNB or copperphenanthroline. (see 2.9.1). In the Western blot detection experiments DTNB was used to induce oxidation (see 2.9.2). The crosslink-signals were very clear for this procoat mutant with all three methods used. The contact sites found are shown in Fig. 51 and Fig. 52.
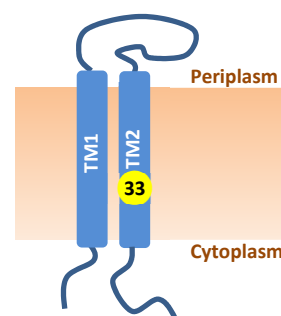
Fig. 50: Position of the substituted valine in the H5 M13 procoat V33C protein.
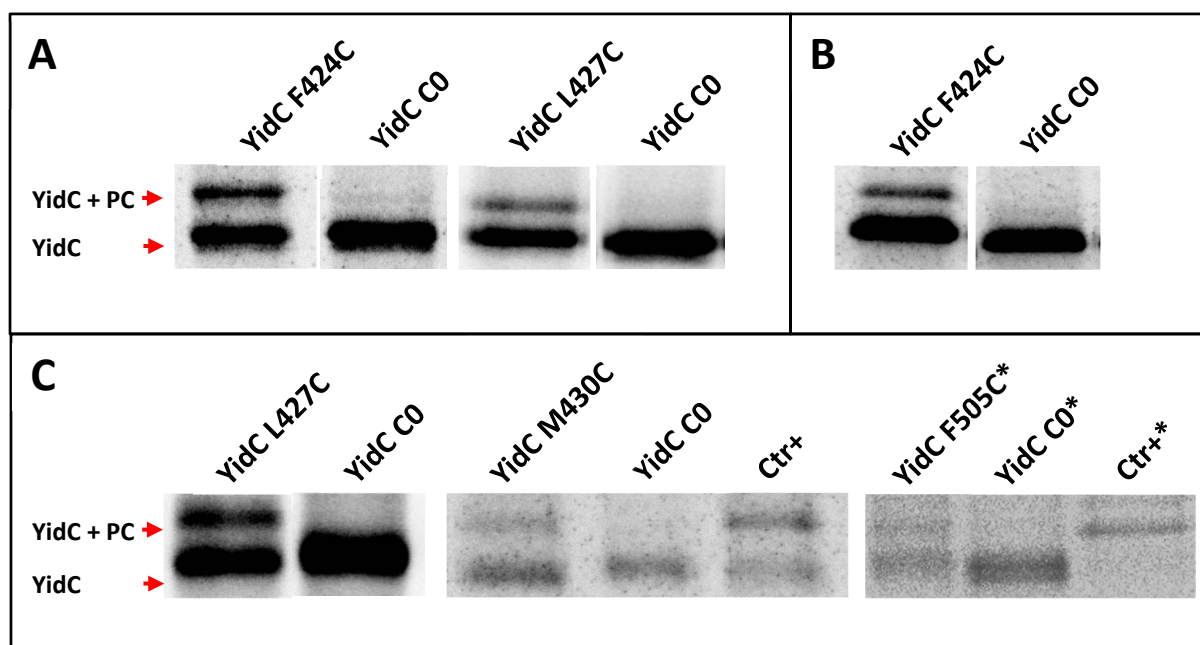
Fig. 51: Contacts found with pulse experiments with the M13 H5 procoat V33C mutant. The contacts are located within the TM3 and TM5. (A) Contact found by oxidation with iodine. (B) Contacts found by pulse labeling and crosslinking with DTNB (C) Crosslinking products detected via oxidation with copper phenanthroline. Pulse samples were immunoprecipitated with the YidC antibody. YidC C0 was used as negative control. Detection was performed via phosphoimaging. *YidC expressed from the pACYC184 plasmid instead of pGZ119EH.

The results show contacts in the lower and middle part of TM3 and the higher part of TM5 (see Fig. 53). The positions of the contacts are listed in Tab. 27.

Fig. 52: YidC contacts with the M13 H5 procoat V33C mutant found via DTNB crosslinking and analyzed by Western blot. Detected contacts are located in the TM3 of YidC. Detection via immunoblotting with an anti His$_{10}$tag antibody. Ctr- is a negative control with the cysteine-free H5 procoat and the F424C (left), L427C (middle) or M430C (right) YidC mutant. ** Same controls as in Fig. 23

Tab. 27: Detected contact positions in the respective TMs of YidC with the H5 M13 procoat V33C mutant.

Strong contacts are indicated with bold numbers.

YidC TM3	YidC TM5
424, 427, 430	505

Fig. 53: Strong contact sites between H5 M13 procoat V33C and YidC in the TM3. The contacts found are located in the cytoplasmic oriented part of TM3 at position 424 and of YidC. The cysteine mutant of H5 M13 procoat is positioned in the center towards the cytoplasm of the transmembrane domain of the mature peptide. Blue helix: TM1 of M13 procoat, cyan helix: TM2 of M13 procoat, red helix: TM3 of YidC, orange helix: TM5 of YidC, variously colored and labeled amino acid residues: contact sites between M13 procoat and YidC. Model of M13 procoat visualized with PyMol 1.3. Figure of YidC created with PDB entry 3WVF in PyMol 1.3, the P1 domain has been removed for a better overview (Kumazaki et al. 2014b).

H5 M13 Procoat G34C mutant

The glycine at position 34 in the mature part of the peptide has been replaced by cysteine. It is located in the middle of the second TM of M13 procoat towards the cytoplasm (see Fig. 54). In the pulse experiments, crosslinking was induced by DTNB or copperphenanthroline. (see 2.9.1). In the Western blot detection experiments DTNB was used for oxidation (see 2.9.2).). For position 430 in YidC, oxidation with copper phenanthroline showed a very weak signal. However, crosslinking with DTNB showed a clear shift indicating the formation of a crosslinking product. The contact sites found are shown in Fig. 55.
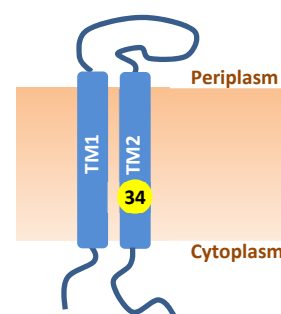
Fig. 54: Position of the substituted glycine in the H5 M13 procoat G34C protein.
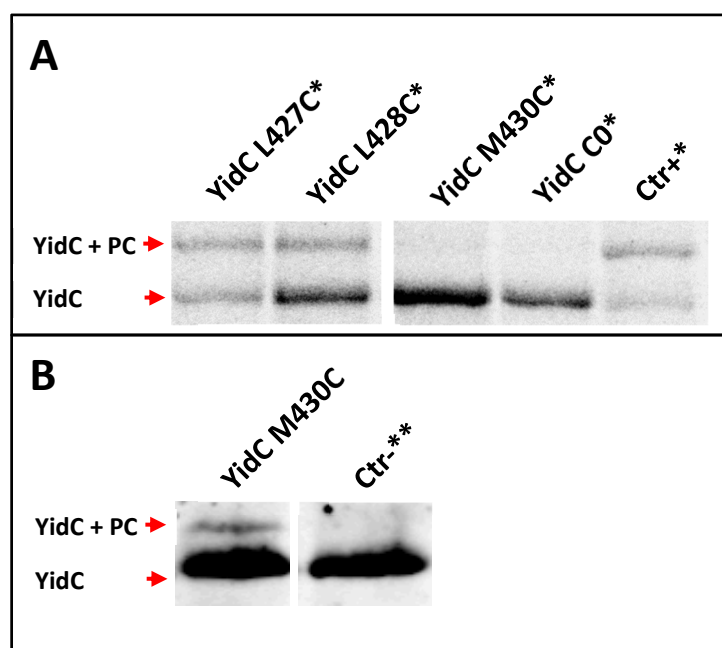
Fig. 55: Contacts found with pulse experiments or western blotting with the M13 H5 procoat G34C mutant. The contacts are located within the TM3 of YidC. (A) Contact found via crosslinking with copperphenanthroline and pulse labeling. *YidC expressed from the pACYC184 plasmid instead of pGZ119EH (B) Contact found with the DTNB crosslinking method. Detection via immunoblotting with an anti His$_{10}$tag antibody. **Same control as in Fig. 23

The results show contacts in the lower and middle part of TM3 (see Fig. 56). The positions of the contacts are listed in Tab. 28.

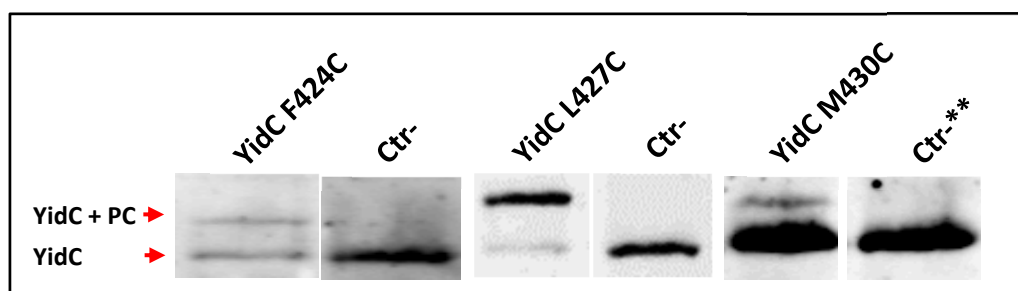**Tab. 28: Found contact positions in the respective TMs of YidC with the H5 M13 procoat V30C mutant.** Strong contacts are indicated with bold numbers.
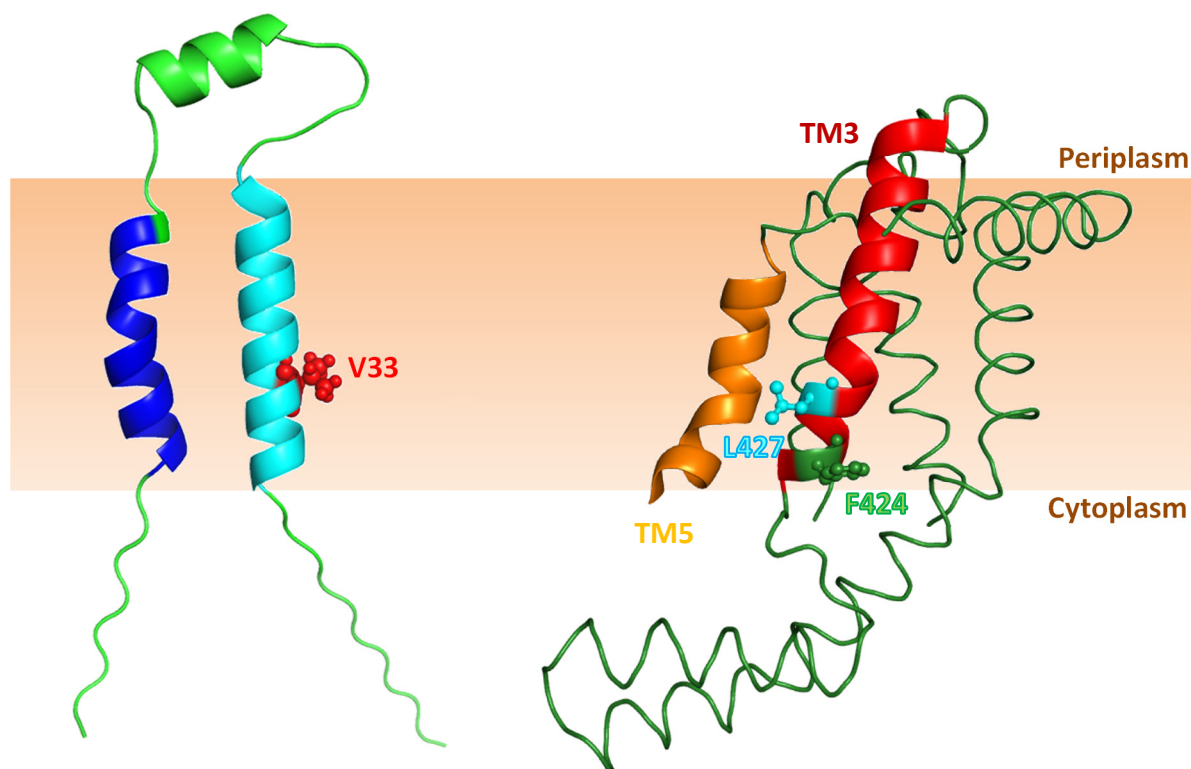
YidC TM3
427, 428, 430
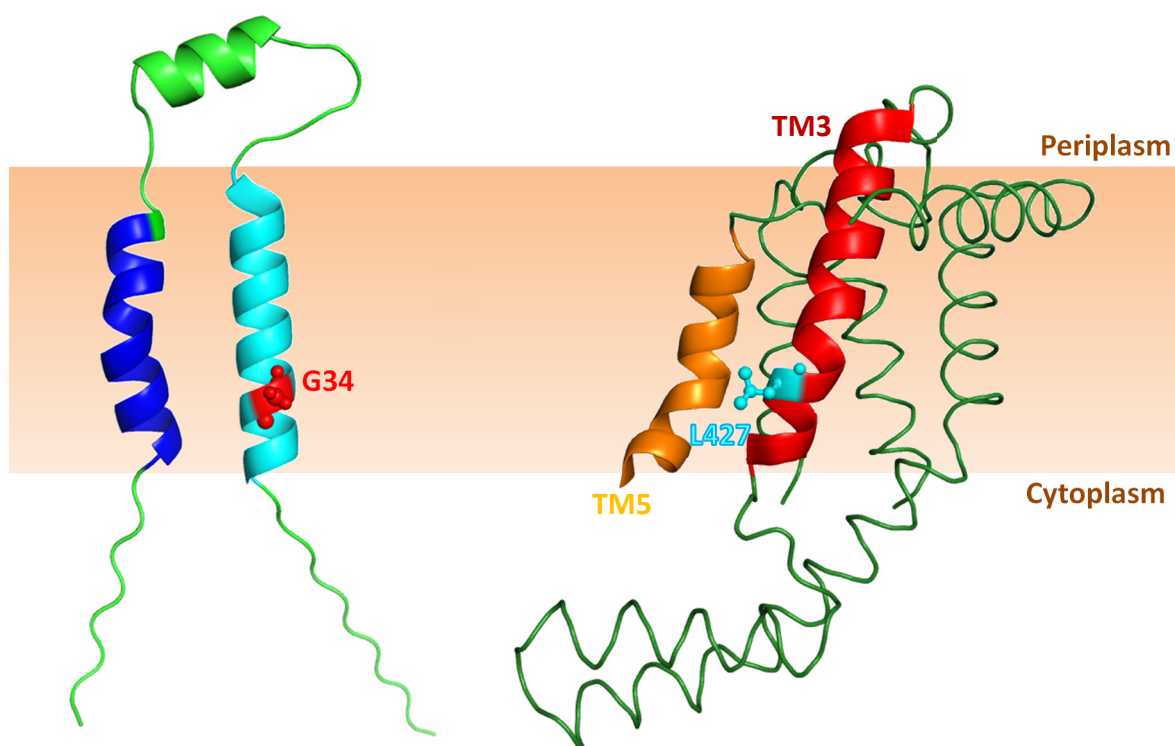
Fig. 56: Strong contact site between H5 M13 procoat G34C and YidC in the TM3. The contact found is located in the cytoplasmic oriented part of TM3 of YidC at position 427. The cysteine mutant of H5 M13 procoat is positioned in the cytoplasmic oriented part of the transmembrane domain of the mature peptide. Blue helix: TM1 of M13 procoat, cyan helix: TM2 of M13 procoat, red helix: TM3 of YidC, orange helix: TM5 of YidC, variously colored and labeled amino acid residues: contact sites between M13 procoat and YidC. Model of M13 procoat visualized with PyMol 1.3. Figure of YidC visualized with PDB entry 3WVF in PyMol 1.3, the P1 domain has been removed for a better overview (Kumazaki et al. 2014b).

3.1.2.2 Crosslinking with the C1-loop of YidC and M13 procoat

Another interesting part to investigate for substrate interaction is the C1 loop that resides near the membrane surface and is believed to play an important role in the protein insertion process of YidC (Kumazaki et al. 2014b). The discovered contact sites with TM3 and TM5 already indicate the interaction between YidC and M13 procoat. This raises the question, how the substrate gets to the TM3 and TM5 of YidC. It was postulated that the substrate "slides" on the C1 loop of YidC towards the hydrophobic slide (Kumazaki et al. 2014a), so contacts between this part of YidC and its substrate might occur. Finding contacts would also support the postulated step-wise insertion-model and might give some insight into the mechanism that drives the insertion. Three H5 M13 procoat mutants were selected for the experiments: S13C, Y24C and V30C (see Fig. 57).
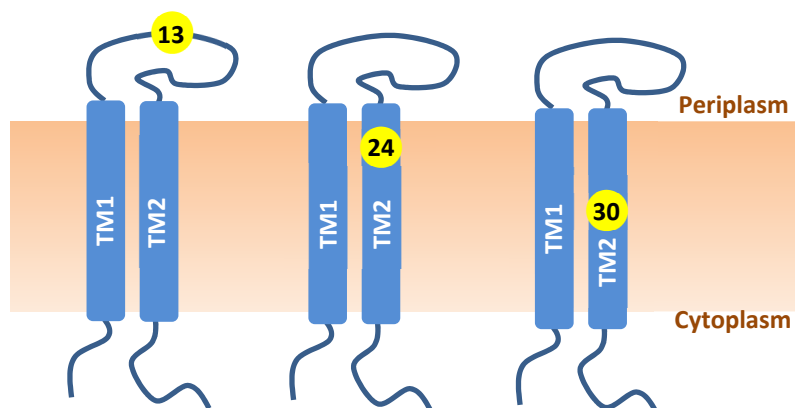
Fig. 57: Positions of the three tested H5 M13 procoat mutants in the C1 loop crosslinking experiments. H5 M13 procoat mutants S13C, Y24C and V30C. Yellow: Amino acid position, that was substituted with a cysteine.

A cysteine in the loop at position 13 or in the periplasmic oriented parts of the second TM at position 24 would most likely have more time to "slide" on the C1 loop towards the hydrophobic slide and the groove than mutants with a cysteine further down the helix. The V30C mutant was additionally selected for the case that possible contacts occur in later parts of the insertion process when the TMs of M13 procoat are already near the hydrophobic slide formed by TM3 and TM5 of YidC. For YidC, the amino acid residues of the chosen mutants would face towards the membrane surface, according to the structure. This would make the discovery of new contacts more likely (see Tab. 29 and Fig. 58).

Tab. 29: Tested residues in YidC for crosslinking with M13 procoat Y24C

YidC positions tested in the C1 loop
387, 394, 395, 398, 405, 408, 409

Copper phenanthroline was used with all tested H5 M13 procoat mutants. An additional attempt with o-PDM was performed with the Y24C mutant of procoat. The experiments with
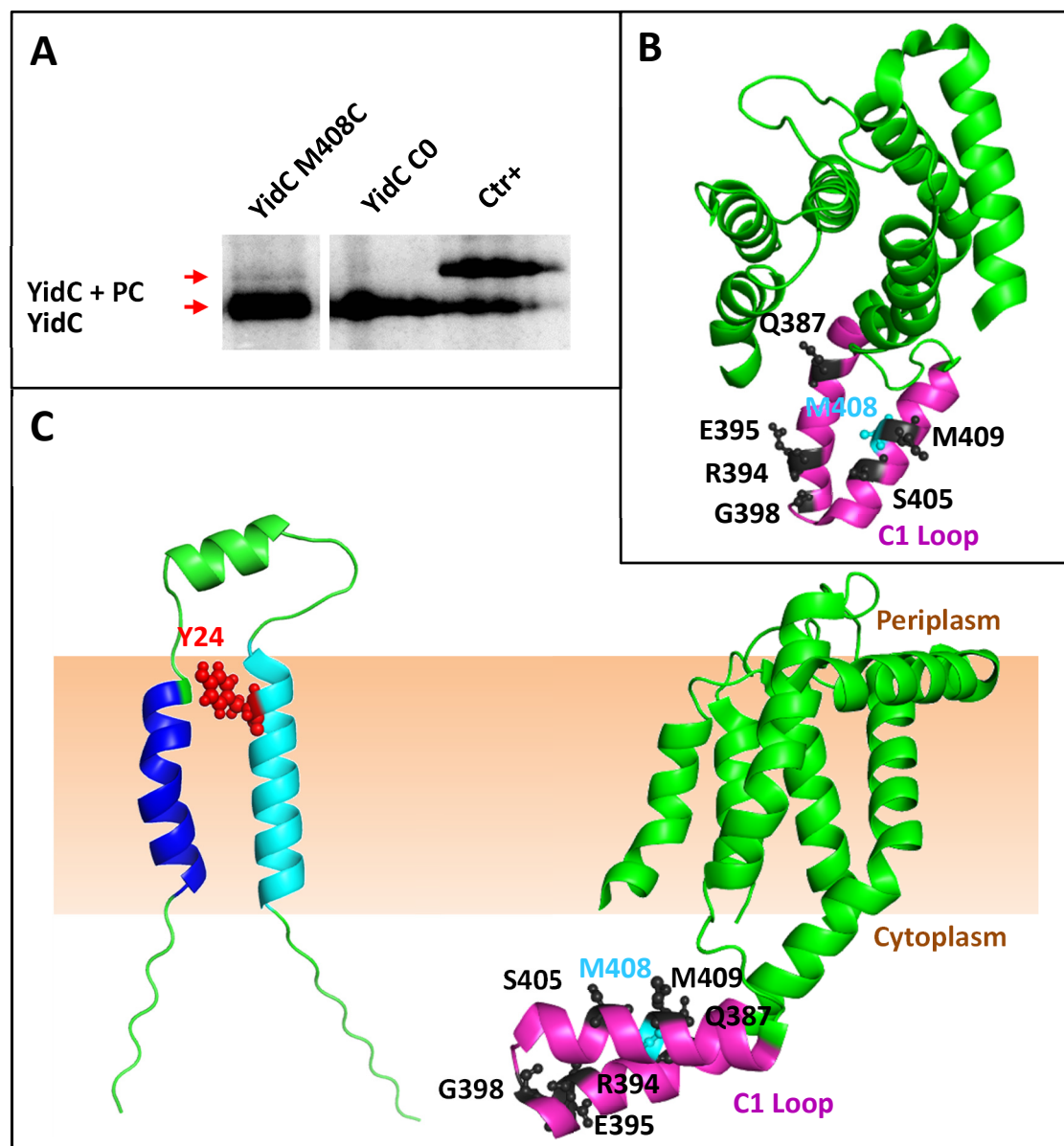
Fig. 58: Contact site between H5 M13 procoat Y24C and YidC in the C1 loop. *The contact found is positioned in the second half of the C1 loop of YidC. (A) Contact found with o-PDM as crosslinking agent. (B) Top view on YidC showing the C1 loop and the positions that were tested with the three procoat mutants. (C) Left: The cysteine mutant of H5 M13 procoat is positioned near the periplasmic leaflet of the membrane. Right: Side view of YidC with the tested positions highlighted. Blue helix: TM1 of M13 procoat, cyan helix: TM2 of M13 procoat, magenta helix: C1 loop of YidC, cyan: The position of the contact site 408 in the C1 loop. Dark grey: the other tested but negative sites, red: contact site in M13 procoat. Model of M13 procoat created with PyMol 1.3. Figure of YidC visualized with PDB entry 3WVF in PyMol 1.3, the P1 domain has been removed for a better overview (Kumazaki et al. 2014b).*

copper phenanthroline showed no crosslinking with any of the described combinations. Only the o-PDM attempt lead to the only weak contact that could be observed so far (see Fig. 58).

3.1.2.3 Crosslinking in the hydrophilic groove of YidC with M13 procoat

With the discovery of the hydrophilic groove and its putative important role in protein insertion (Kumazaki et al. 2014a) it became relevant to test for possible contact sites for a substrate. Two cysteine mutants, S13C and E20C (see Fig. 59), of H5 M13 procoat were selected that have their cysteines positioned in the loop between the two TMs. This is, due to its charged nature, the part of the substrate that is most likely to enter the groove during the insertion process.
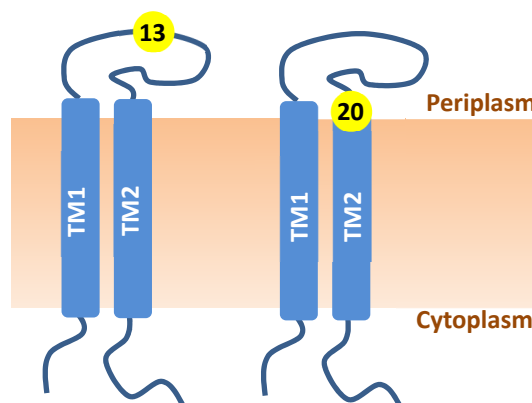
Fig. 59: Positions of the two tested H5 M13 procoat mutants in the hydrophilic groove crosslinking experiments. H5 M13 procoat mutants S13C and E20C. Yellow: Amino acid, that was substituted with cysteine

A number of YidC cysteine mutants were constructed. The residues that were substituted are, according to the structure of Kumazaki et al. (2014b), facing inside the hydrophilic groove or are at least positioned near it (see Fig. 60 and Tab. 30).

DTNB and o-PDM were used for the radioactive crosslinking experiments (see 2.9.1). Copper phenanthroline, due to its hydrophobic nature, was not used for this hydrophilic environment. The pulse time was 60 seconds followed by 10 minutes of oxidation with the respective crosslinking agent before the reaction was stopped with a final concentration of 20% TCA. For the H5 M13 procoat E20C mutant, DTNB was used for crosslinking with residues 373 and 377. The focus lied on the S13C mutant where both crosslinking agents were used for most residues tested (see Fig. 61).
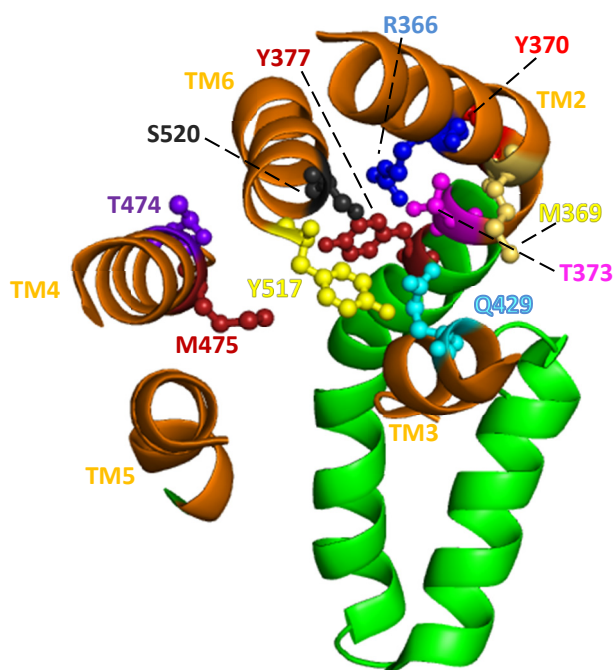
Fig. 60: Top view in the hydrophilic groove of YidC. The mutations are present in different TMs of YidC, facing into the groove. The different positions for the cysteine substitutions are labeled and marked with various colors. Orange: TMs of YidC. Figure of YidC visualized with PDB entry 3WVF in PyMol 1.3, the P1 domain and parts of the TMs including the loops between them have been removed for a better overview (Kumazaki et al. 2014b).

No crosslinks were observed in these crosslinking experiments, indicating that the tested mutants either do not enter the hydrophilic groove deep enough for a crosslinking reaction to occur, or that the crosslinking agent might not be able to enter the groove to start the reaction. Another possibility is that the insertion occurs too fast for the disulfide formation to occur.
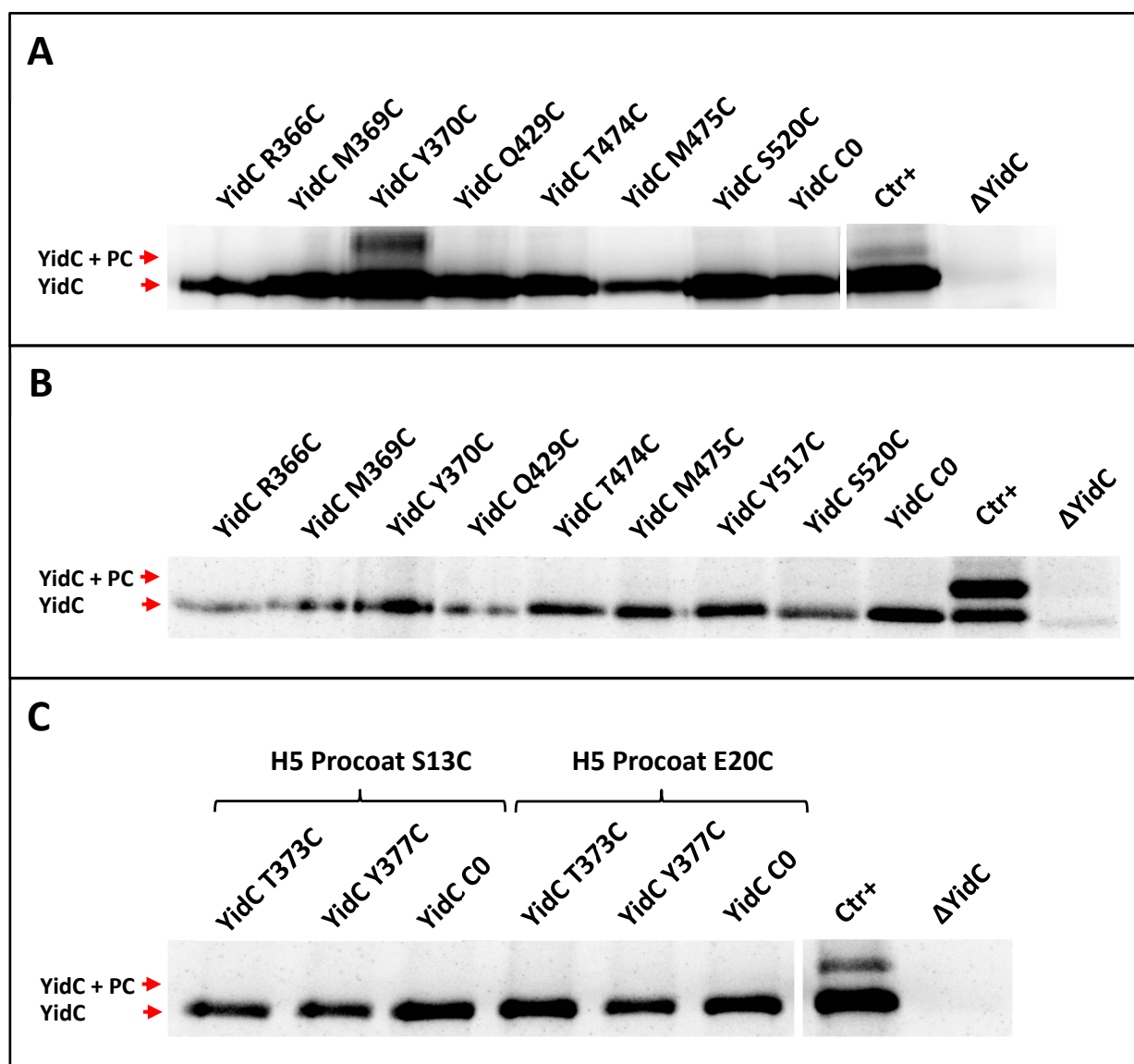
Fig. 61: Crosslinking attempts inside the hydrophilic groove of YidC. (A) Pulse experiment with the H5 S13C mutant and DTNB as crosslinking agent. No contacts were found, the upper band for the Y370C mutant is an unkown band that runs too high in the gel to be the desired crosslinked complex. It could not be reproduced in the o-PDM experiment and is unlikely to be the desired crosslinking product. (B) Similar experiment with the H5 S13C mutant. o-PDM was used for crosslinking and the Y517C mutant was tested. No crosslinks were observed. (C) Pulse experiment with both H5 mutants and DTNB as crosslinking agent. No contacts were found. Immunoprecipitation for all gels was performed with the YidC antibody, detection via phosphorimaging.

Tab. 30: Tested residues in the YidC hydrophilic groove.

YidC	H5 S13C		H5 E20C
	DTNB	o-PDM	DTNB
R366C	negative	negative	
M369C	negative	negative	
Y370C	negative	negative	
T373C	negative		negative
Y377C	negative		negative
Q429C	negative	negative	
T474C	negative	negative	
M475C	negative	negative	
Y517C		negative	
S520C	negative	negative	

Summary of the crosslinking experiments

An overview is presented Fig. 62, which summarizes the strong contact sites in YidC in TM3 and TM5. In the published structure (Kumazaki et al. 2014b) the positions in TM3 (423, 427 and 430) are mostly facing towards the hydrophobic slide. Only the phenylalanine at position 424 points outward. The weak contact site in TM3 at position 428 points into the hydrophilic groove of YidC. Interestingly, the detected strong interactions of YidC with M13 procoat are spread in a wider angle around the helix. The phenylalanines at position 502 and 505 are facing
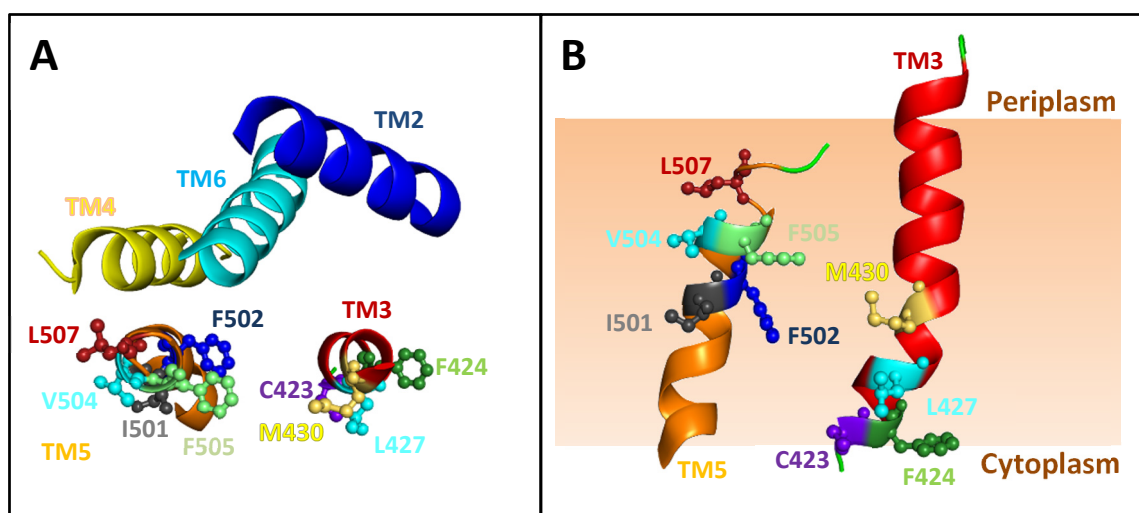
Fig. 62: Summary of the detected strong contact sites so far in the TM3 and TM5 with H5 M13 procoat as substrate. These are the positions where the tested M13 procoat mutants showed strong interactions with YidC in the displayed crosslink experiments. (A) Top view on the TMs of YidC with the contact sides marked in TM3 and TM5. Part of TM3 has been removed for a better overview. (B) Front view of the putative hydrophobic slide that TM3 and TM5 form, the other parts of YidC have been removed for better visibility. Red: TM3, orange: TM5, yellow: TM4, cyan: TM6, blue: TM2 of YidC, variously colored amino acids: strong contact sites of M13 procoat in YidC in TM3 and TM5. Figures of YidC visualized with PDB entry 3WVF in PyMol 1.3. (Kumazaki et al. 2014b)

towards the slide while the other sites are facing outwards into the membrane (501 and 504) or towards TM4 (507). The weak contacts in TM5 (503, 508 and 509) are oriented in various directions. For position 503 it is similar to the strong contact at position 507, both point towards TM4 of YidC, though 503 is located closer to the membrane core while 507 is near the periplasmic leaflet. The residue at position 508 points upward towards the periplasmic membrane surface and the phenylalanine at position 509 points into the top of the hydrophobic slide.

The M13 H5 procoat cysteine mutants that contact YidC in various locations were not restricted to specific regions inside the insertase. Many mutants, for example the V30C mutant of M13 procoat contact YidC in positions that are located in the cytoplasmic or periplasmic leaflet or the membrane core.

For the crosslinking experiments in the C1 loop only one faint contact could be discovered at position 408. The other tested sites did not show crosslinking products.

The crosslinking attempts with residues in the hydrophilic groove did not lead to any contacts with the charged loop of M13 procoat. An unrelated band that appeared with DTNB as oxidation inducing agent could not be confirmed with o-PDM and was regarded as negative.

3.2 Functionality studies with the *E. coli* YidC and an artificial *E. coli* YidC dimer (dYidC)

Complementation and binding studies with different defective YidC mutants were performed as a preparation for further experiments with an artificial dimeric construct (dYidC). It was constructed to analyze different aspects of the activity and functionality of YidC. Further data regarding the stoichiometry of the active insertase were obtained, a topic that has been discussed without a clear result (Lotz et al. 2008, Kohler et al. 2009, Boy and Koch 2009, Kumazaki et al. 2014a/2014b, Shimokawa-Chiba et al. 2015). Additionally, complementation assays and binding studies give further insight into the functionality of YidC and of dYidC and its interaction with its substrate M13 procoat.

3.2.1 Cloning of the dYidC

For the construction of the YidC dimer the plasmid pGZ119 YidC C0 was used as a base for cloning. The primers YidCI_XbaI(Shine)SphI and YidCI_MunI were used to amplify the YidC gene from the plasmid, which allowed the addition of a Shine-Dalgarno sequence in front of the gene and the implementation of additional restriction sites (see Fig. 63).
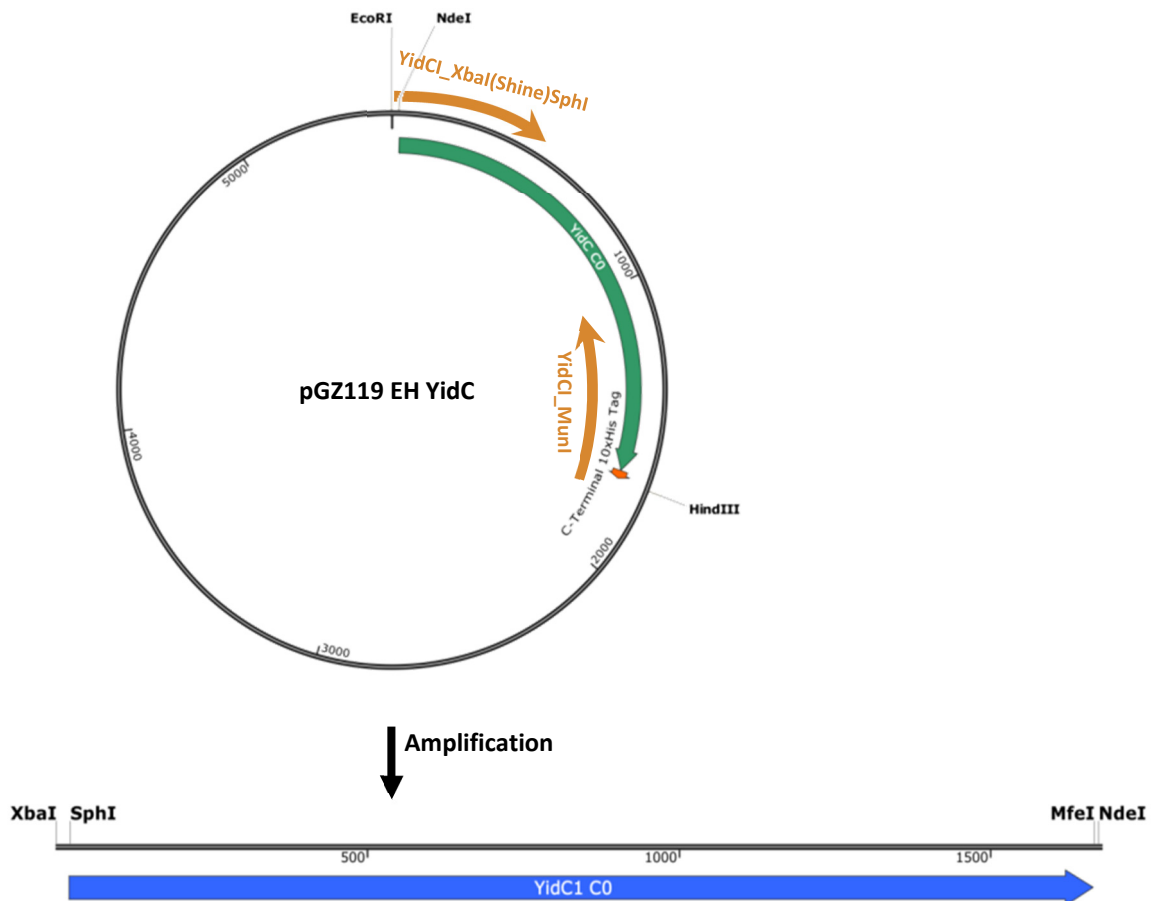
Fig. 63: Amplification of YidC from the plasmid pGZ119 EH YidC C0. The amplification added a Shine-Dalgarno sequence in front of the YidC gene and applied an XbaI site in the front and a MfeI site at the start of the linker. Additionally the NdeI site at the starting codon was changed to a SphI site to avoid problems later on with the new NdeI site at the end of the amplified DNA. Plasmid map was generated with SnapGene Viewer v3.2.1.

The resulting PCR product was cloned in the pGEMT-easy vector via the T overhangs in the plasmid and the A overhang that was created during the PCR (see Fig 64).
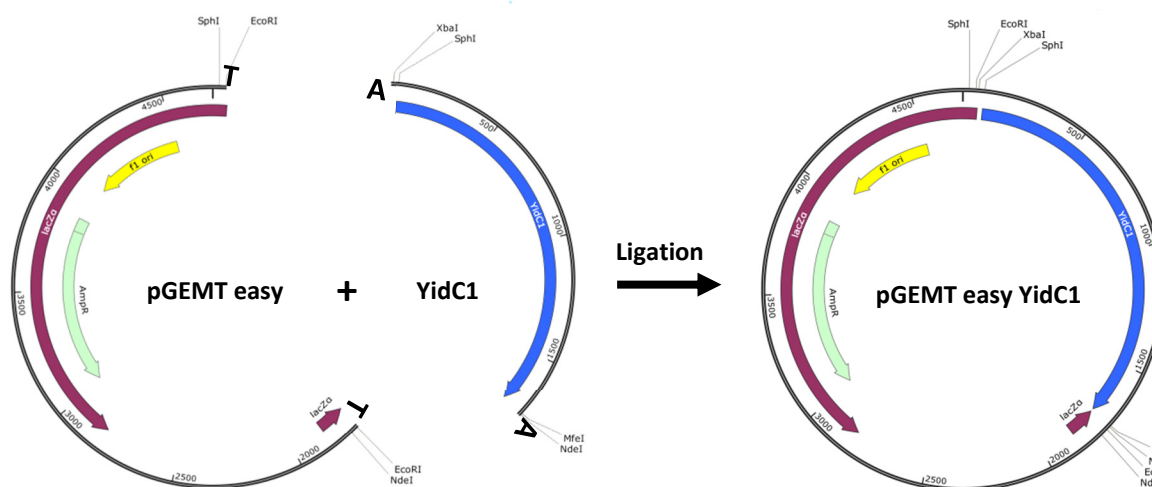
Fig. 64: Ligation of the YidC1 C0 fragment in the pGEMT-easy plasmid. The A overhangs created by the DNA polymerase were used for cloning the fragment into the plasmid with T overhangs. Plasmid maps were generated with SnapGene Viewer v3.2.1.

This construct was digested with EcoRI and NdeI. The fragment was then cloned in front of the YidC in the pGZ119 YidC C0 plasmid, leading to the dYidC construct pGZ119 dYidC C0/C0 encoding the protomers YidC1 and YidC2 (see Fig. 65).
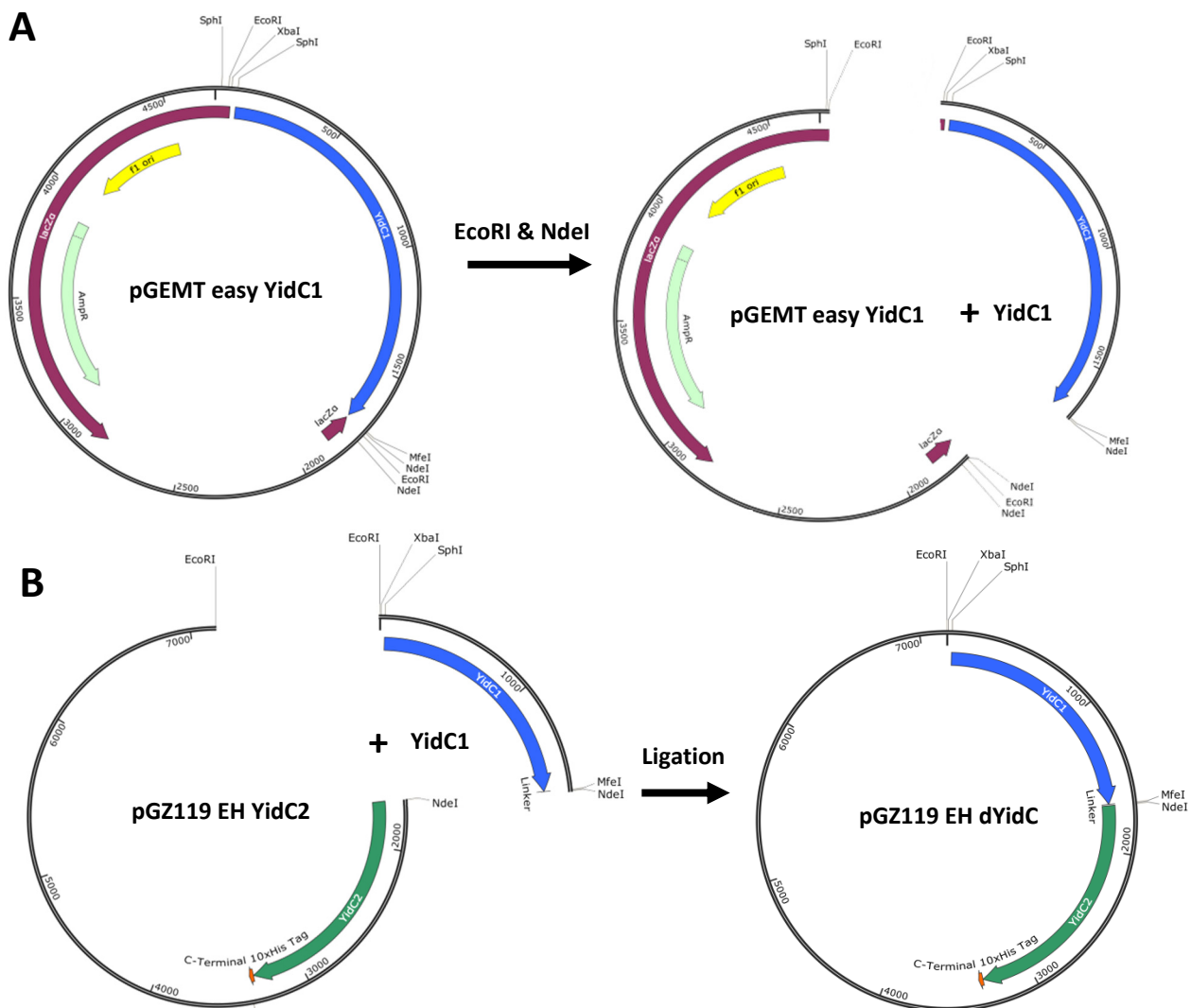
Fig. 65: Cloning of the dYidC in pGZ119 EH YidC C0. (A) The pGEMT plasmid containing the modified YidC protomer is digested with EcoR1 and NdeI. (B) This results in a YidC fragment that is cloned in the with EcoR1 and NdeI opened pGZ119EH YidC C0 plasmid leading to the dYidC plasmid pGZ119EH dYIdC C0/C0. Plasmid maps were generated with SnapGene Viewer v3.2.1.

Further modifications were necessary in the construct. The first was the removal of the starting codon of the second protomer, that was causing problems with unwanted ribosomal binding in the center of the dYidC mRNA (data not shown). This was achieved by site directed mutagenesis using the primers DYidCMetLeuF and DYidCMetLeuR changing the methionine to a leucine. The NdeI site was lost due to this mutation.

Another change was the insertion of a longer linker containing the recognition site for the prescission protease. The primer pair PrecSiteDYidC_Fw and PrecSiteDYidC_Rv was annealed forming the new linker for the dYidC. The plasmid was cut with MfeI and the linker was cloned

in the linearized plasmid. This was done by Sandra Fischer during her bachelor thesis (see Fig. 66).
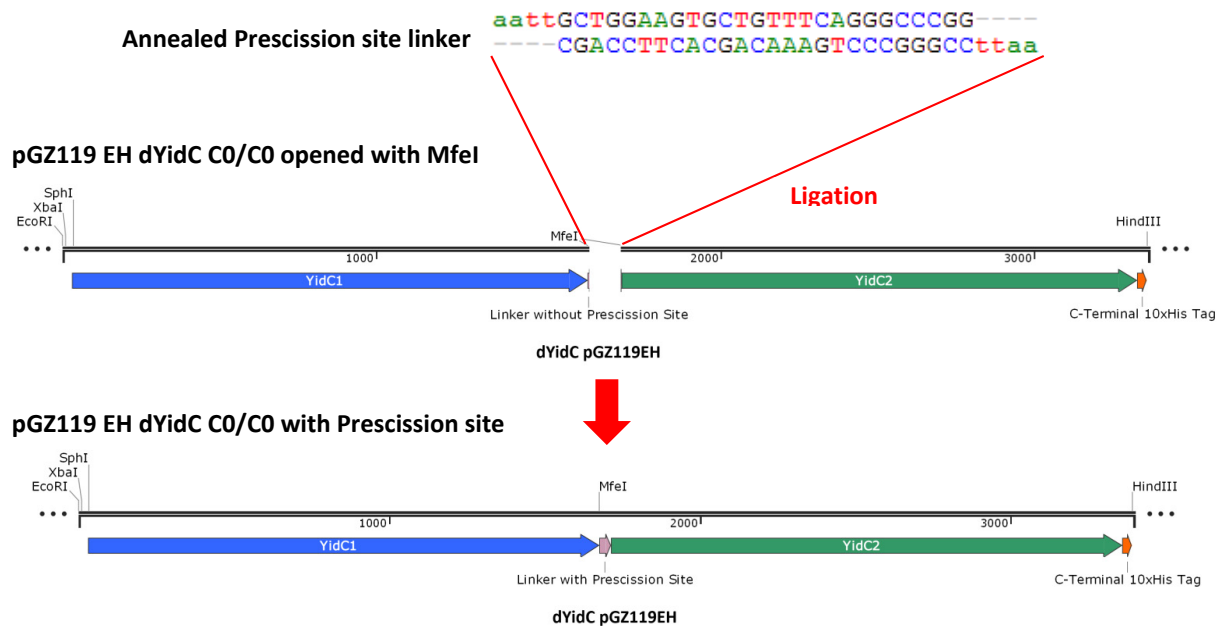
Fig. 66: Ligation of the Prescission site linker in the dYidC. The plasmid was cut open using MfeI and the annealed linker was ligated. This resulted in a longer linker containing the Prescission Site, which can be used for cleaving the dYidC after expression. Plasmid maps were generated with SnapGene Viewer v3.2.1.

To enable the exchange of mutants in the dYidC protomers two more plasmid constructs were prepared to aid in the cloning of different variants of YidC. The plasmid pT7-7 Pf3 (provided by Dr. Kiefer) was used as template.

The restriction sites SmaI, XbaI and PstI needed to be removed first by cutting with SmaI and PstI followed by using T4 polymerase to obtain blunt ends. The removal of those restriction sites was necessary to avoid complications when cloning inside the YidC gene. The plasmid was then religated. Both protomers in the pGZ119 EH dYidC C0/C0 plasmid were separately cut out to be independently cloned in the modified pT7-7 Pf3.

The first protomer was cloned via XbaI and MfeI, the second via MfeI and HindIII. This allowed the exchange of mutants with the internal restriction sites PstI and CsiI in YidC from already available other constructs. This allows to clone them back in the dYidC by exchanging the respective protomer.

3.2.2 Construction of defective YidC mutants for functionality studies

Different defective mutants of YidC were constructed by site directed mutagenesis (see 2.5.1). The changes were alanine or serine substitutions or deletion of parts of the protein that lead to a compromised YidC that cannot complement in *E. coli* MK6S cells. The complementation assays were performed as described (see 2.7).

YidC ΔC1 deletion mutant

In this mutant the amino acids 399 to 415, which form the C-terminal half of the C1 loop in YidC, were deleted from the protein. Chen et al. (2014) reported that deletion of this region impairs YidC in complementing in living cells and inserting some of the YidC only substrates. The complementation assay shows the inability of the YidC ΔC1 mutant to complement in glucose depleted MK6S cells (see Fig. 67).
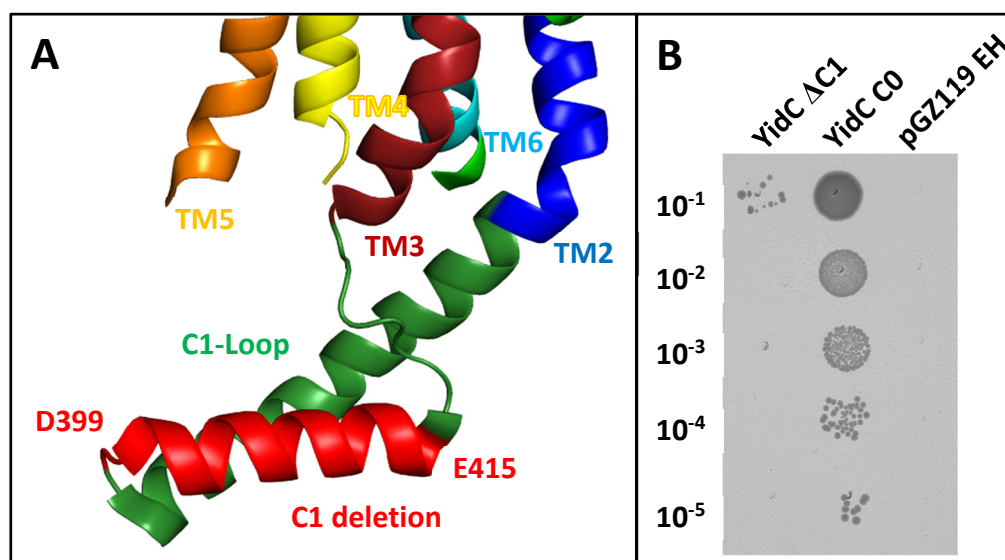
Fig. 67: Partial deletion of the C1-loop of YidC. (A) Area of YidC with the deletion of the C1-Loop. (B) Complementation Assay in MK6S cells with the YidC ΔC1 mutant. Comparison of YidC ΔC1 (lane 1) to a cysteine free mutant (lane 2) that complements on wildtype level and the empty pGZ119 EH vector (lane 3). OD_{600}=0.5 for serial dilution, LB agar plate with 0.2% glucose and 1mM IPTG. Dark green: C1-loop. Red helix: Deleted part of the C1-loop. Deep red: TM3 of YidC. Orange: TM5 Yellow: TM4 Blue: TM2. Figure of YidC visualized with PDB entry 3WVF in PyMol 1.3, the P1 domain has been removed for a better overview (Kumazaki et al. 2014b).

YidC 362A alanine mutant

The YidC T362A mutant has a single amino acid change at position 362 from threonine to alanine. This single substitution has been reported to impair the growth of *E. coli* cells due to the inability of YidC to complement for its depleted chromosomal counterpart (Wickles et al. 2014). The complementation assay shows the inability of the YidC 362A mutant to complement in YidC-depleted MK6S cells (see Fig. 68).
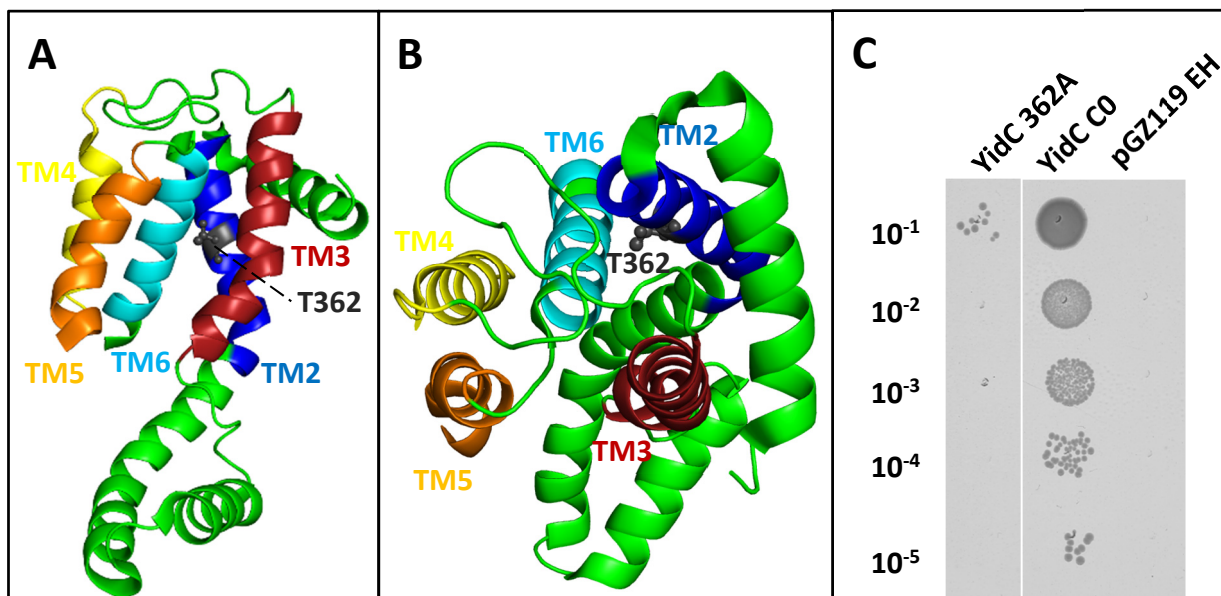
Fig. 68: Alanine substitution in YidC at position 362. (A) Overview of the *E. coli* YidC structure without the P1-loop. Black: Position of the alanine substitution. Red: TM3 of YidC. Orange: TM5 Yellow: TM4 Blue: TM2. (B) Top view inside YidC: The mutation inside the hydrophilic groove (C) Complementation assay in MK6S cells with the YidC T362A mutant. Comparison of YidC 362A to a cysteine free mutant that complements on wildtype level and the empty pGZ119 EH vector. OD_{600}=0.5 for serial dilution, LB agar plate with 0.2% glucose and 1mM IPTG. Figure of YidC visualized with PDB entry 3WVF in PyMol 1.3, the P1 domain has been removed for a better overview (Kumazaki et al. 2014b)

YidC 5S serine mutant

The YidC 5S mutant has five serine substitutions in YidC at position 430, 435 in TM3, 468 in TM4 and 505 and 509 in TM5. These substitutions lead to a loss of function of YidC and the inability to complement for the depleted chromosomal counterpart. The complementation assay shows the inability of the YidC 5S mutant to complement in YidC-depleted MK6S cells (see Fig. 69).
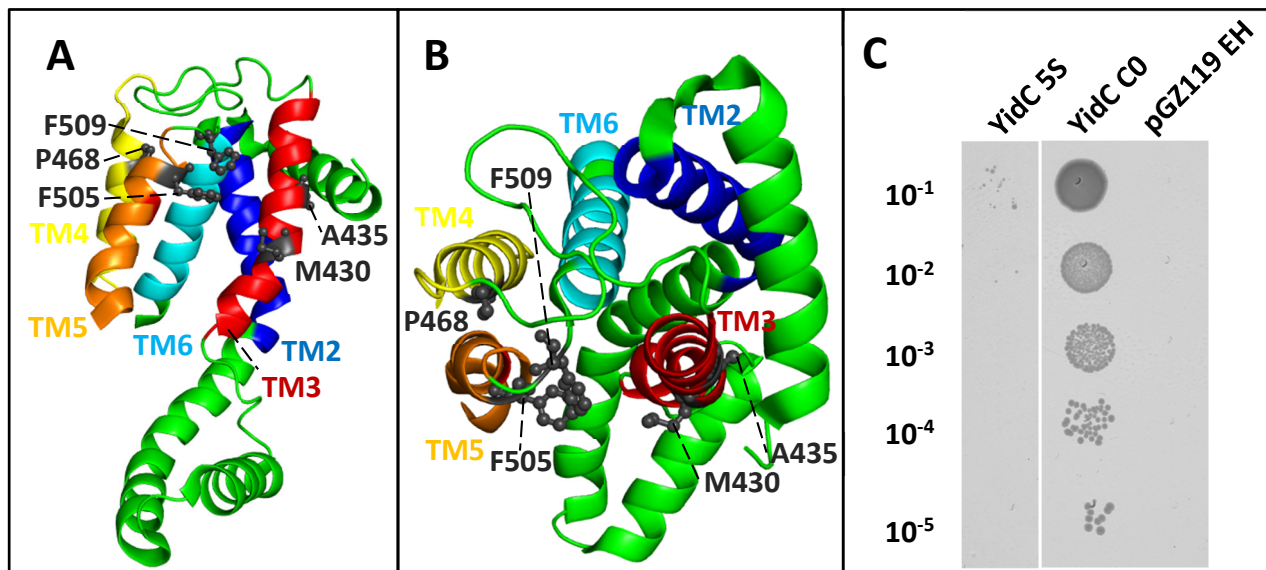
**Fig. 69: Serine substitutions in YidC at positions 430, 435, 468, 505, 509.** (A) Overview of the *E. coli* YidC structure without the P1-loop. Black: Positions of the serine substitutions. Deep red: TM3 of YidC. Orange: TM5 Yellow: TM4 Blue: TM2. (B) Top view inside YidC: The mutation inside the hydrophilic groove (C) Complementation assay in MK6 cells with the YidC 5S mutant. Comparison of YidC 5S to a cysteine free mutant that complements on wildtype level and the empty pGZ119 EH vector. OD_{600}=0.5 for serial dilution, LB agar plate with 0.2% glucose and 1mM IPTG. Figure of YidC visualized with PDB entry 3WVF in PyMol 1.3, the P1 domain has been removed for a better overview (Kumazaki et al. 2014b).

3.2.3 Complementation studies with the monomeric and dimeric YidC

Complementation and expression experiments were conducted to analyze the different YidC and dYidC defective mutants and to compare them for different behavior in MK6S cells. Combinations of different defective mutants in the dYidC were then tested for their complementation capabilities.

Summary of the complementation of monomeric defective YidC mutants

As seen before (see 3.2.2) the monomeric mutants were tested together for better comparison of the complementation capabilities of each YidC variant. This was done as preparation for testing the mutants in the dYidC constructs later on.

E. coli MK6S cells were transformed with the pGZ119 EH plasmid harboring the different defective YidC mutants (see 3.2.2). Complementation and expression studies were performed as described (see 2.7). The defective mutants show no capability to complement in the YidC depleted *E. coli* cells. The only sample that showed complementation was the positive control YidC C0. The Western blot of the expression test shows YidC protein indicating that the cells
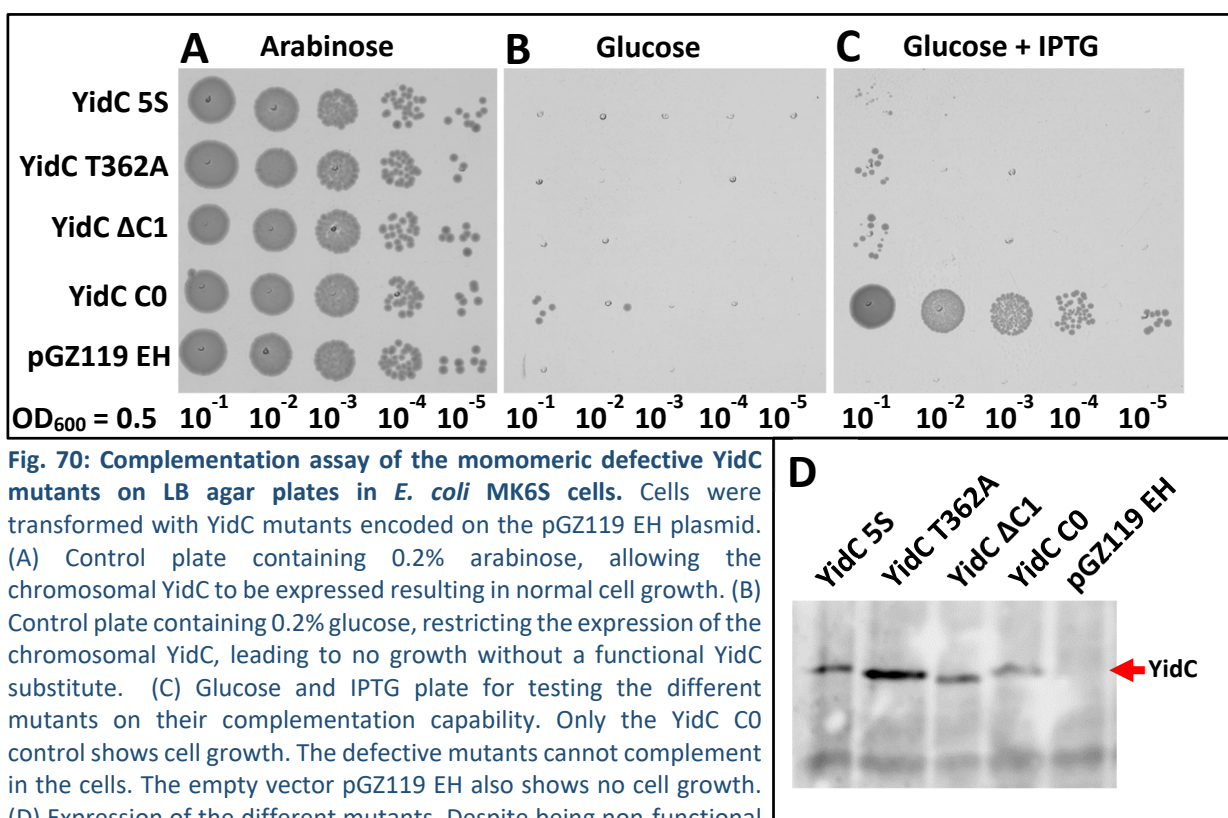
Fig. 70: Complementation assay of the momomeric defective YidC mutants on LB agar plates in *E. coli* MK6S cells. Cells were transformed with YidC mutants encoded on the pGZ119 EH plasmid. (A) Control plate containing 0.2% arabinose, allowing the chromosomal YidC to be expressed resulting in normal cell growth. (B) Control plate containing 0.2% glucose, restricting the expression of the chromosomal YidC, leading to no growth without a functional YidC substitute. (C) Glucose and IPTG plate for testing the different mutants on their complementation capability. Only the YidC C0 control shows cell growth. The defective mutants cannot complement in the cells. The empty vector pGZ119 EH also shows no cell growth. (D) Expression of the different mutants. Despite being non-functional the mutants were expressed and detectable. Western blot with anti His$_{10}$tag antibody.

were able to express the protein but were not able to complement the lack of chromosomal YidC with it (see Fig. 70).

dYidC single defective mutants

It has been discussed previously whether YidC is active as a monomer or dimer. Recent data, including the structure, support the idea of YidC acting as a monomer only (Kedrov et al. 2013, Herrmann 2013, Kumazaki et al. 2014a/2014b, Shimokawa-Chiba et al. 2015). We asked the question here whether the dYidC is capable to complement with only one functional protomer or not. The dYidC construct was constructed and the different defective mutants were substituted as described (see 3.2.1). By substituting one of the protomers with a defective mutant it was tested if only one active YidC is sufficient for complementation. This also shows the importance of the position of the functional YidC in the dimer and it will allow to determine if the artificial dimer needs one or both protomers to function properly.

Fig. 71: Complementation assay of the single defective dYidC mutants on LB agar plates in *E. coli* MK6S cells. Cells were transformed with dYidC mutants encoded on the pGZ119 EH plasmid. (A) Control plate containing 0.2% arabinose, allowing the chromosomal YidC to be expressed resulting in normal cell growth. (B) Control plate containing 0.2% glucose, restricting the expression of the chromosomal YidC, leading to no growth without a functional dYidC substitute. (C) Glucose and IPTG plate for testing the different dYidC mutants on their functionality.The dYidC mutants with a single defective protomer show normal cell growth except for the 5S/C0 mutant. The empty vector pGZ119 EH shows no cell growth.

E. coli MK6S cells were transformed with the pGZ119 EH plasmid harboring the different single defective dYidC mutants (see 3.2.2). Complementation and expression studies were performed as described (see 2.7).

The single defective mutants in the dYidC were able to complement in the *E. coli* cells. The only exception was the dYidC 5S/C0 mutant that showed strongly reduced growth on the agar plate. Only few colonies proliferated in this case (see Fig. 71).

Detection via Western blot showed that all the tested mutants were expressed in YidC-depleted *E. coli* MK6S cells. The lack of functionality of the 5S/C0 mutant, despite being expressed, is peculiar (see Fig. 72).
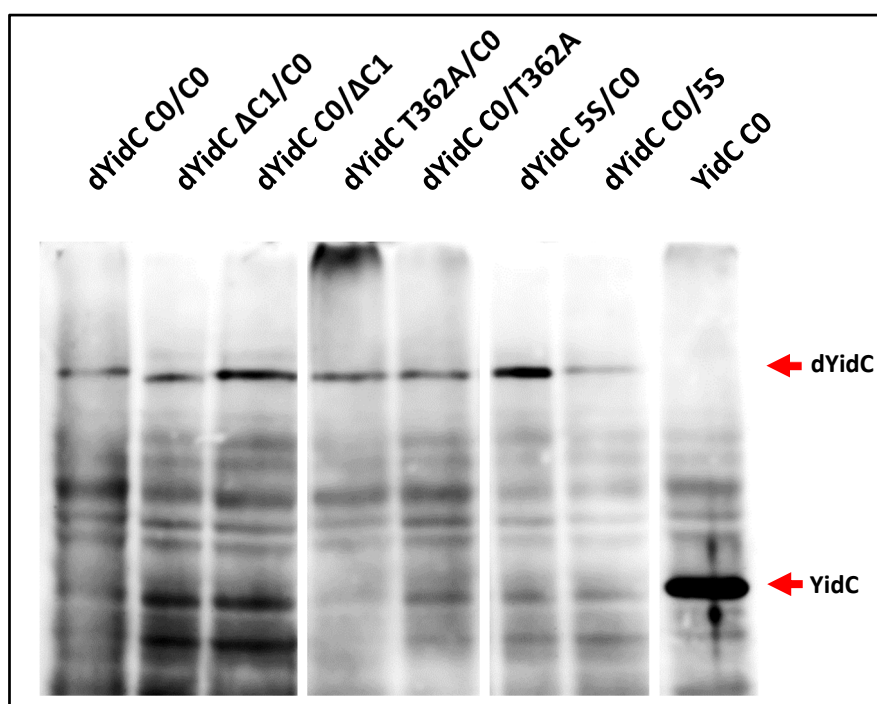
Fig. 72: Expression of the single defective dYidC mutants. All the mutants were expressed including the dYidC 5S/C0 mutant that showed reduced cell growth. Western blot with anti His$_{10}$tag antibody.

dYidC double defective mutants

The next step was to analyze mutants with two defective protomers whether they are still capable to complement for growth of living cells. For this constructs harboring the same, or in some cases different, defective YidC mutants were cloned (see 3.2.1).

None of the dYidC mutants with two defective protomers were capable of fully complementing in *E. coli* Mk6 cells. The positive control shows normal cell growth while the empty pGZ plasmid as negative control was not viable (see Fig. 73).
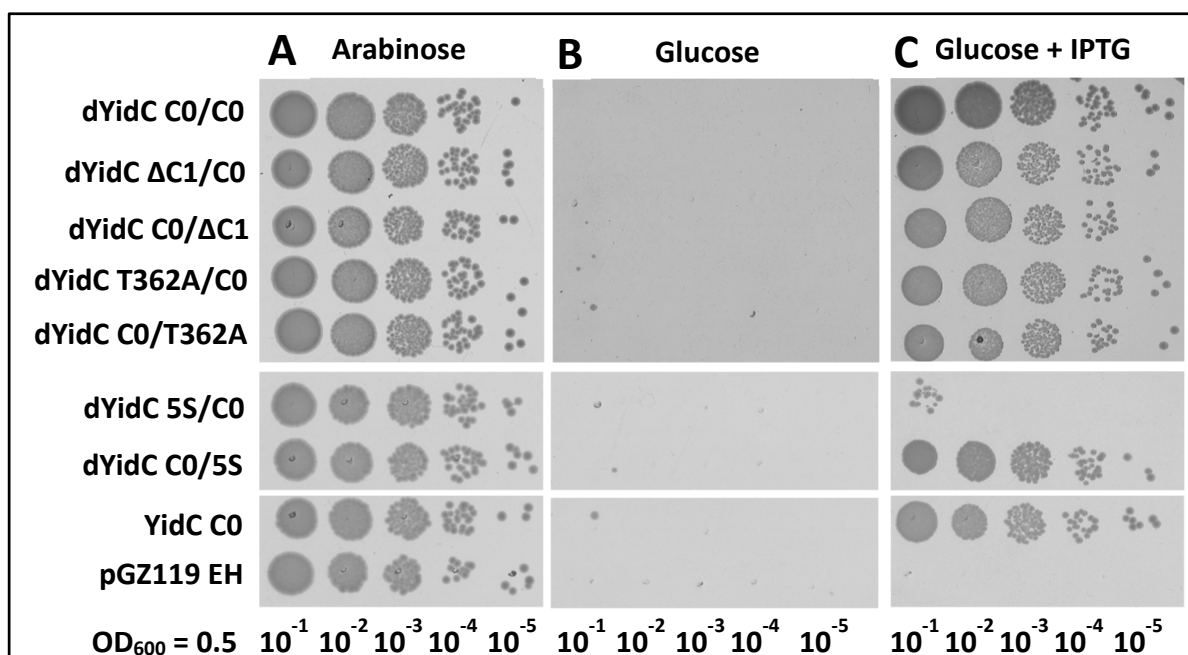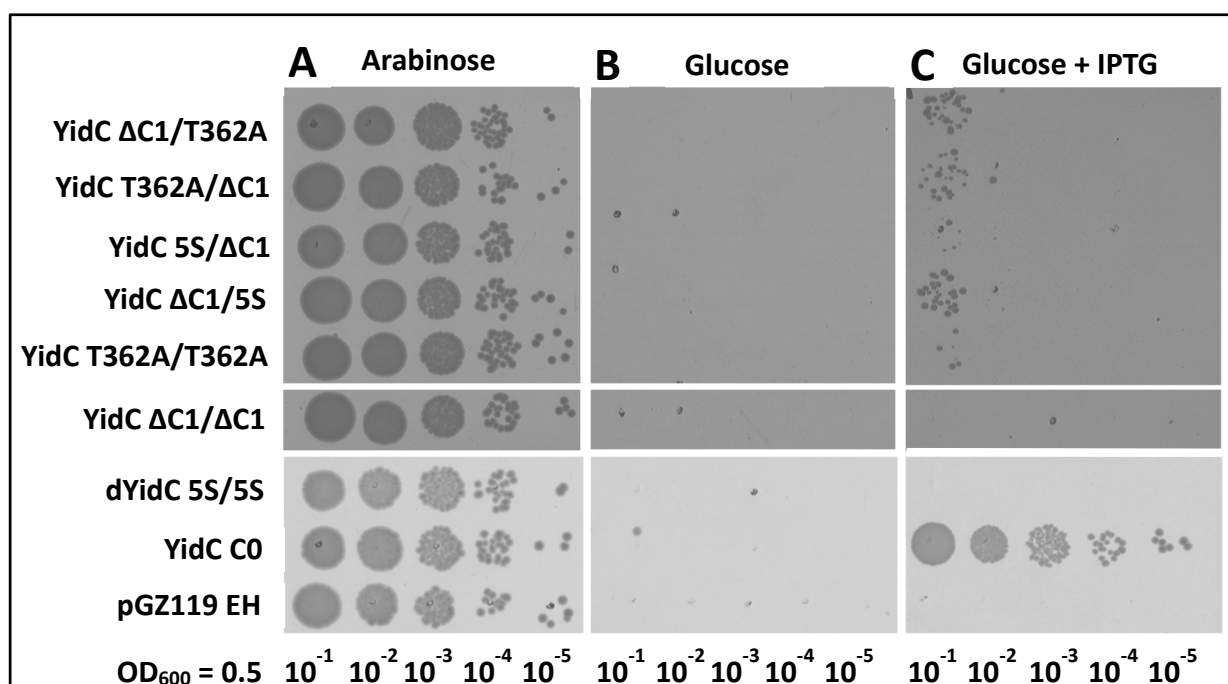

Fig. 73: Complementation assay of the double defective dYidC mutants on LB agar plates in *E. coli* MK6S cells. Cells were transformed with dYidC mutants encoded on the pGZ119 EH plasmid. (A) Control plate containing 0.2% arabinose, allowing the chromosomal YidC to be expressed resulting in normal cell growth. (B) Control plate containing 0.2% glucose, restricting the expression of the chromosomal YidC, leading to no growth without a functional dYidC substitute. (C) Glucose and IPTG plate for testing the different dYidC mutants on their complementation capability. The double defective dYidC mutants show no cell growth indicating no in vivo functionality. The empty vector pGZ119 EH also shows no cell growth.

The Western blots shows that all the tested mutants are expressed in *E. coli* MK6S cells (see Fig. 74). Even though different combinations of defective mutants were tested they were not able to complement each other, indicating that the protomers did not interact with each other or with protomers from other dYidCs to compensate for their respective defects.
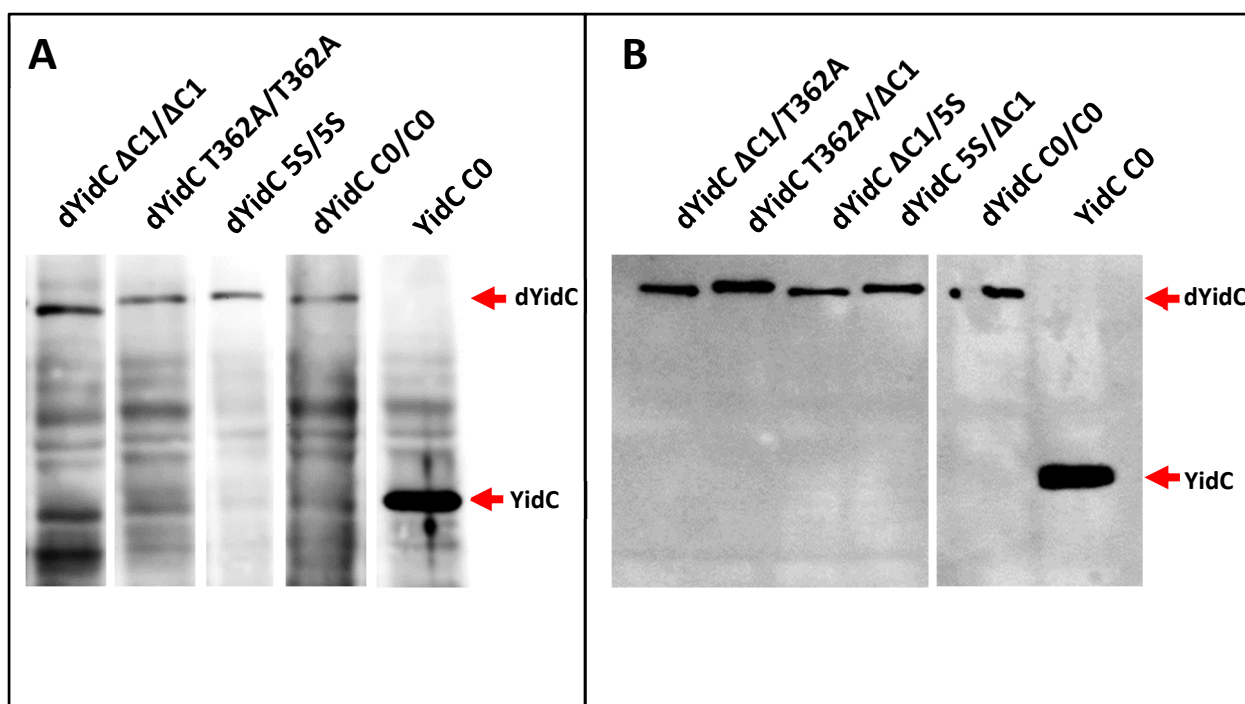
Fig. 74: Expression of the double defective dYidC mutants. (A) Expression of the dYidCs with the same mutation in each protomer. (B) Expression of the dYidC mutants with different mutations per protomer. Western blot with anti His$_{10}$tag antibody.

3.2.4 Substrate binding in YidC ΔC1

Another approach was to test whether a non-functional mutant of YidC is able to interact with one of its substrates. This would give more insight in the functionality of YidC, by checking which parts of the protein still function. For this purpose, the defective mutant ΔC1 (see 3.2.2)
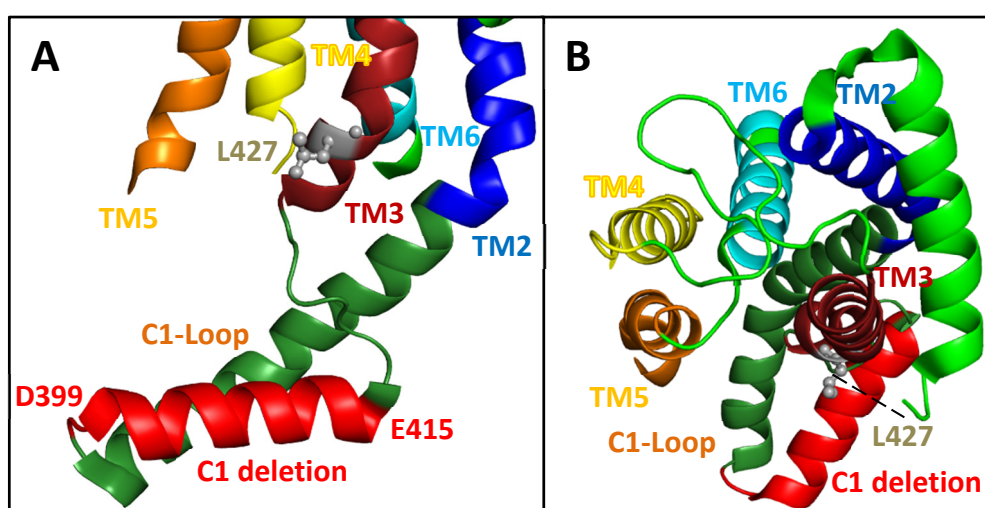
Fig. 75: C1-loop of YidC. (A) Area in YidC with the deletion of the C1-Loop. (B) Top view of the TMs of YidC. Dark green: C1-loop. Red helix: Deleted part of the C1-loop. Deep red: TM3 of YidC. Grey amino acid: Cysteine at position 427 in TM3, inserted for crosslinking purposes. Orange: TM5 Yellow: TM4 Blue: TM2. Figure of YidC visualized with PDB entry 3WVF in PyMol 1.3, the P1 domain has been removed for a better overview (Kumazaki et al. 2014b).

was used for binding studies. In this YidC mutant a part of the big C1-loop was deleted from amino acid 399 to 415 by site directed mutagenesis, resulting in the loss of most of the second half of the C1 loop (see Fig. 75). Additionally, a leucine was mutated into a cysteine at position 427 in the TM3 resulting in the mutant pGZ119EH YidC L427C ΔC1. The M13 H5 procoat V33C mutant was used for this binding study as a substrate for YidC since a strong crosslink had been found for these positions in preceding experiments (see 3.1.2.1). To test the possible interaction with the substrate, pulse experiments with radioactive methionine (^{35}S) were conducted to see if an interaction could be observed between YidC 427C ΔC1 and M13 H5 procoat 33C. Iodine (Sigma) was used for disulfide formation.

In Fig 76, the binding of the M13 procoat 33C substrate to the YidC 427C mutant is clearly visible. Interestingly the ΔC1 variant of this mutant is still able to bind its substrate although weakly (see 3.2.3).
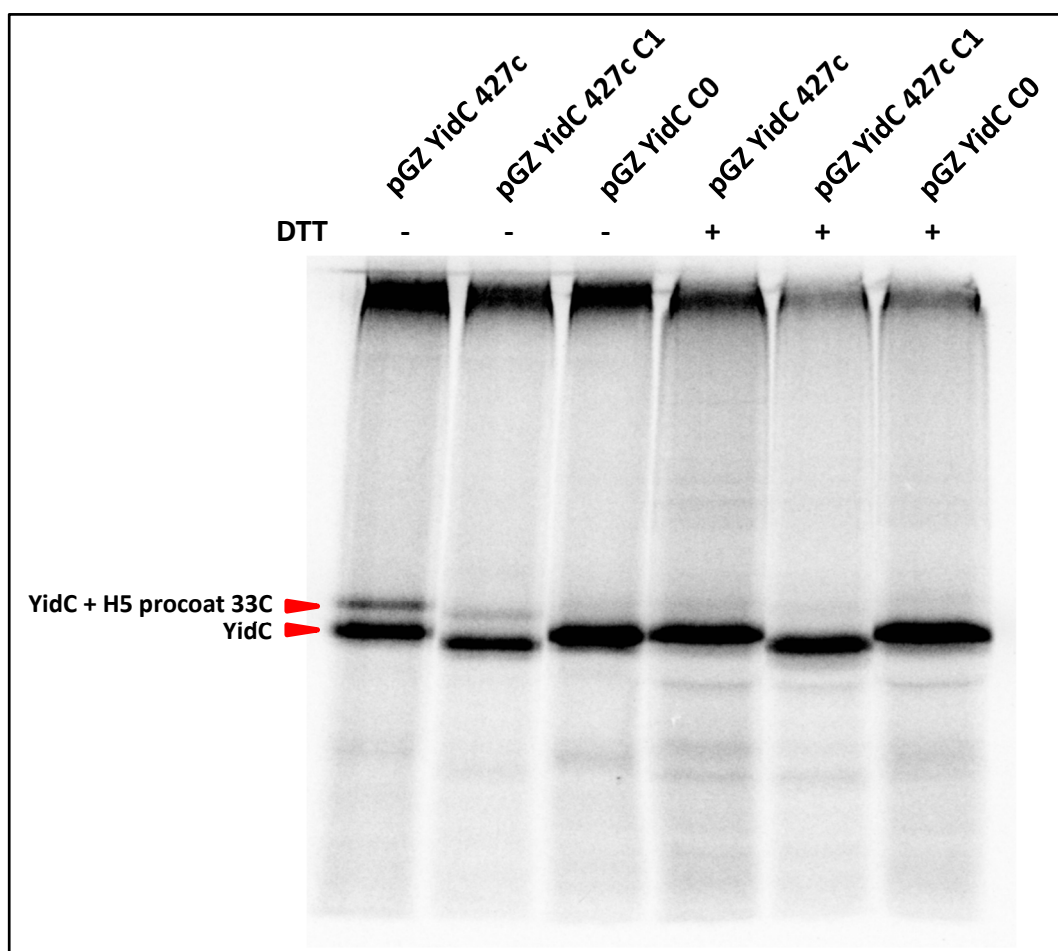
Fig. 76: Crosslinking between H5 procoat 33C and different YidC mutants. 20µl of prepared sample were analyzed on a 10% SDS acrylamide gel. Detection was done by phosphorimaging. Iodine was used as crosslinking agent and the samples were split after the immuno-precipitation. One half was treated with 100mM DTT to dissolve any crosslinks while the other was prepared without DTT.

3.2.5 Purification of the dYidC

The dYidC construct was purified for binding studies with the M13 procoat proteins and for comparison to the purified monomeric YidC. The YidC and dYidC genes were cloned in the pGZ119 EH plasmid for this purpose. Cell growth was performed in LB or TB medium respectively. Purification was done as described before (see 2.8.1 and 2.8.2).

Monomeric and dimeric YidC was purified in parallel from 3 liters TB medium induced with 0.5 mM IPTG for 4 hours. Cells were processed and a sucrose gradient was used as described. For solubilization, 2% of DDM was added to the inner membrane vesicles (IMVs) for 2 hours followed by ultracentrifugation and a 1 hour batch with 150µl bed volume Nickel-Sepharose (IMAC). After the washing step with 40 CV of washing buffer (10% glycerol, 500 mM NaCl, 50 mM Tris, 50 mM imidazole, 0.05% DDM, pH 8) a single elution fraction of 600µl was collected in elution buffer (10% glycerol, 500 mM NaCl, 25 mM MES, 600 mM imidazole, 0.05% DDM, pH 6.5) and 10µl were put on a SDS gel for analysis followed by Coomassie staining (see Fig. 77).
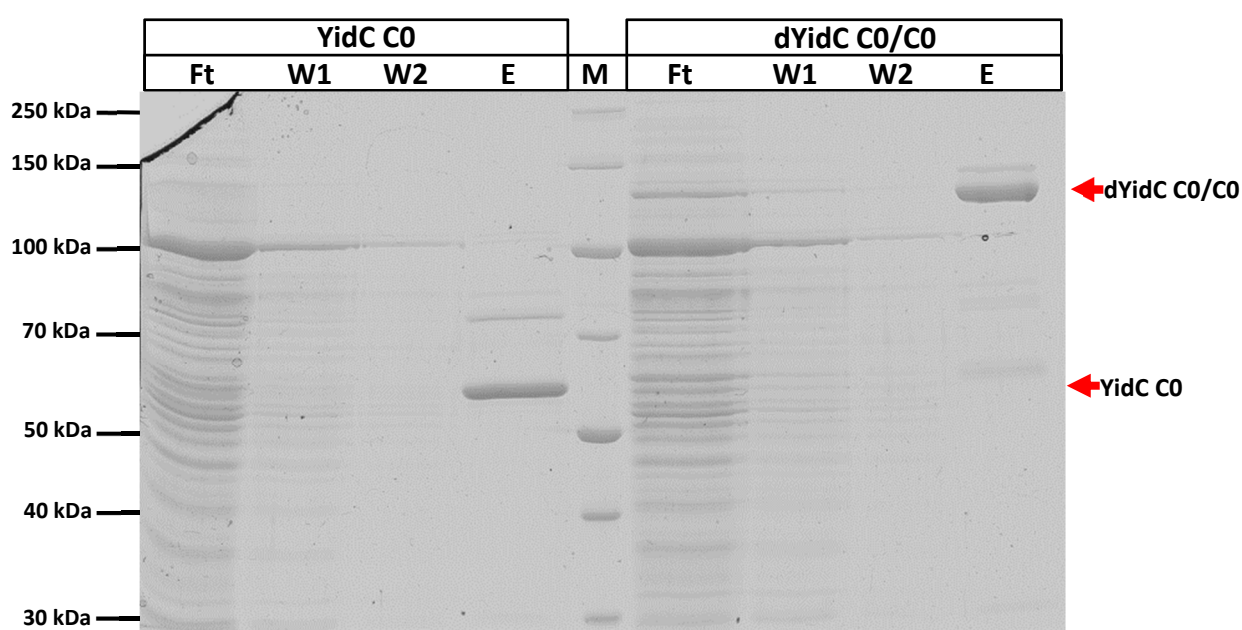
Fig. 77: IMAC of the YidC mono- and dimer. 10µl of each fraction were analyzed. Ft: Flow through of both purifications. W1: Wash fraction after 10CV of washing W2: after 40CV of washing E: Elution fraction of the *E. coli* YidC mono-/dimer respectively. M: Marker PageRuler Broad Range #26630 (Thermo Fisher Scientific). Samples were separated on a 10% SDS acrylamide gel and Coomassie stained. The same gel is already shown in Fig. 1.

Both proteins were further purified by a size exclusion chromatography (SEC) on a Superdex 200 10/300 increase column. Each of the remaining 580 µl of the elution fractions were used for a separate run.

A run with the BIORAD Gel Filtration Standard (#151-1901) was performed as well in buffer G (10% glycerol, 10mM Ada (N-(2-Acetamido)iminodiacetic acid), 300mM NaCl, 0.02%DDM, 0.01% Cymal6 (6-Cyclohexyl-1-Hexyl-β-D-Maltoside), pH6) to determine the size of the purified proteins (see Tab. 31). The

Tab. 31: Obtained values for the utilized standard to determine the size standard curve.

BIO-RAD standard		
kDa	log(kDa)	ml
670	2,82607	7,87606
158	2,19866	10,40385
44	1,64345	13,57023
17	1,23045	15,61907
1,35	0,13033	18,83868
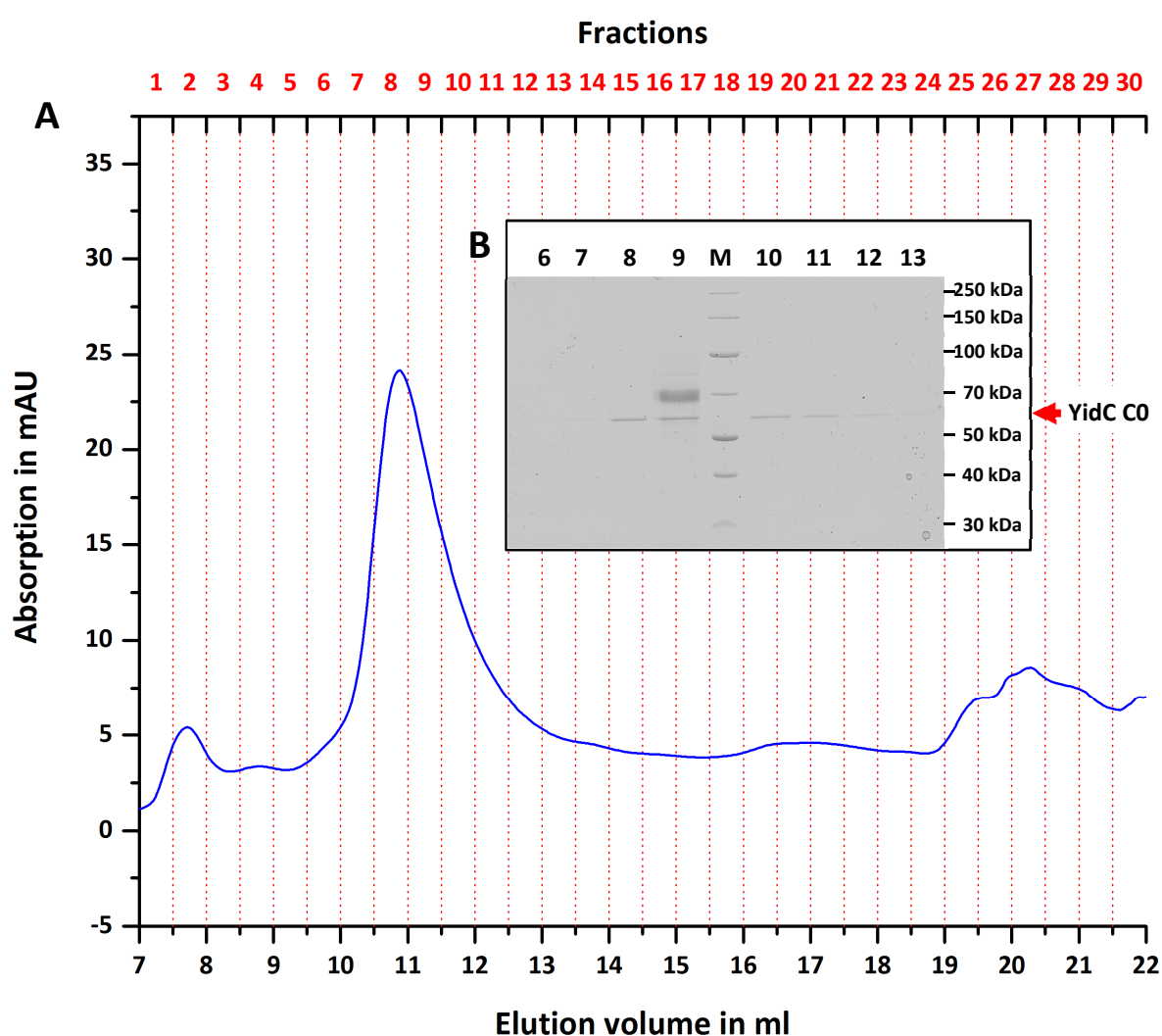
Fig. 78: SEC profile of YidC C0. (A) The elution fraction of 580 µl was loaded on a Superdex 10/300 increase column to gain pure YidC C0 monomer protein. One mayor peak was observed at 10.88 ml elution volume (~146 kDa). Flow rate: 0.4 ml/min System: Äkta purifier Detection: Absorbance at 280 nm Fractionation: 0.5 ml (B) 10% SDS acrylamide gel of the fractions 6 to 12 (major peak), 10µl each, Coomassie stained. Protein bands can be observed at ~60 kDa with the highest amount of protein in fraction 8 showing pure YidC C0 monomer. M: Marker PageRuler Broad Range #26630 (Thermo Fisher Scientific). Fraction 9 was excluded from further experiments due to the contamination with unknown protein. Image created with OriginPro 2015G.

resulting formula y = -0,235x + 4.7214 with a R^2 = 0,97452 was used to calculate the approximate size of the purified proteins in kDa.

The SEC was performed with buffer G at a flowrate of 0.4 ml/min. Protein content was measured at 280nm absorbance. Elution fractions of 0.5 ml were collected and 10 µl of each fraction of interest were analyzed on a 10% SDS gel followed by Coomassie staining. YidC C0 was eluted from approx. 10 ml to 12.5 ml with the peak at 10.88 ml, corresponding to a molecular weight of ~146 kDa. A monomer of YidC C0 (calculated MW: 62.9 kDa per monomer) was most likely eluted inside a DDM/Cymal6 micelle of ~80 kDa (see Fig. 78). The molecular weights were calculated with the standard-curve for the used SEC column.
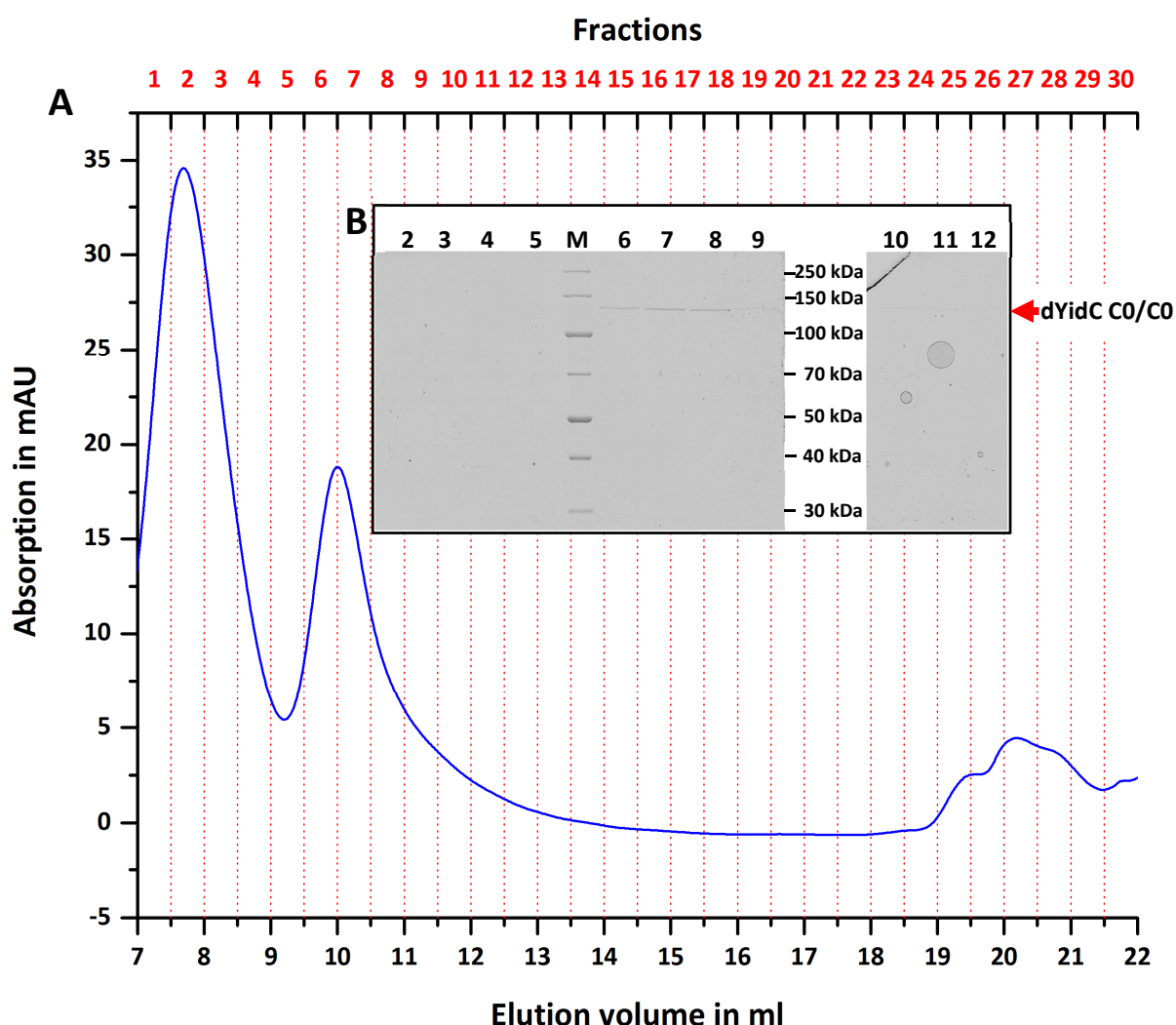
Fig. 79: SEC profile of dYidC C0/C0. (A) The elution fraction of 580µl was loaded on a Superdex 10/300 increase column to gain pure dYidC C0/C0 protein. One major peak was observed at 10.01 ml elution volume (~234 kDa). An additional large peak was observed at 7.69 ml. Flow rate: 0.4 ml/min System: Äkta purifier Detection: Absorbance at 280 nm Fractionation: 0.5 ml (B) 10% SDS gel of the fractions 2 to 12 (void and major peak), 10µl each, Coomassie stained. Protein bands can be observed at 130 kDA with the highest amount of protein in fraction 7 and 8 showing pure dYidC C0/C0 dimer. M: Marker PageRuler Broad Range #26630 (Thermo Fisher Scientific). Image created with OriginPro 2015G.

dYidC C0/C0 was eluted from approx. 9.5 ml to 11 ml with the peak at 10.01 ml, corresponding to a molecular weight of ~234 kDa. This leads to the possibility, that the protomers of the dYidC C0/C0 (calculated MW: 62.5 kDa for the first and 63.4 kDa for the second protomer) were each eluted inside their own DDM/Cymal6 micelle (~50 kDa per micelle) connected by the linker in between them. The large peak at 7.69 ml contained no dYidC and is most likely comprised of aggregates of small proteins (see Fig. 79).

Both purifications were analyzed by normalizing the 280nm absorption data in Origin (OriginPro 2015G) and comparing the results for both proteins. An overlay of both elution profiles, which was obtained by normalizing the overall absorption at 280 nm to values between 0 to 100, with the highest peak being the maximum, to allow the comparison of both profiles. By applying the standard curve for the Superdex 10/300 increase column, sizes of
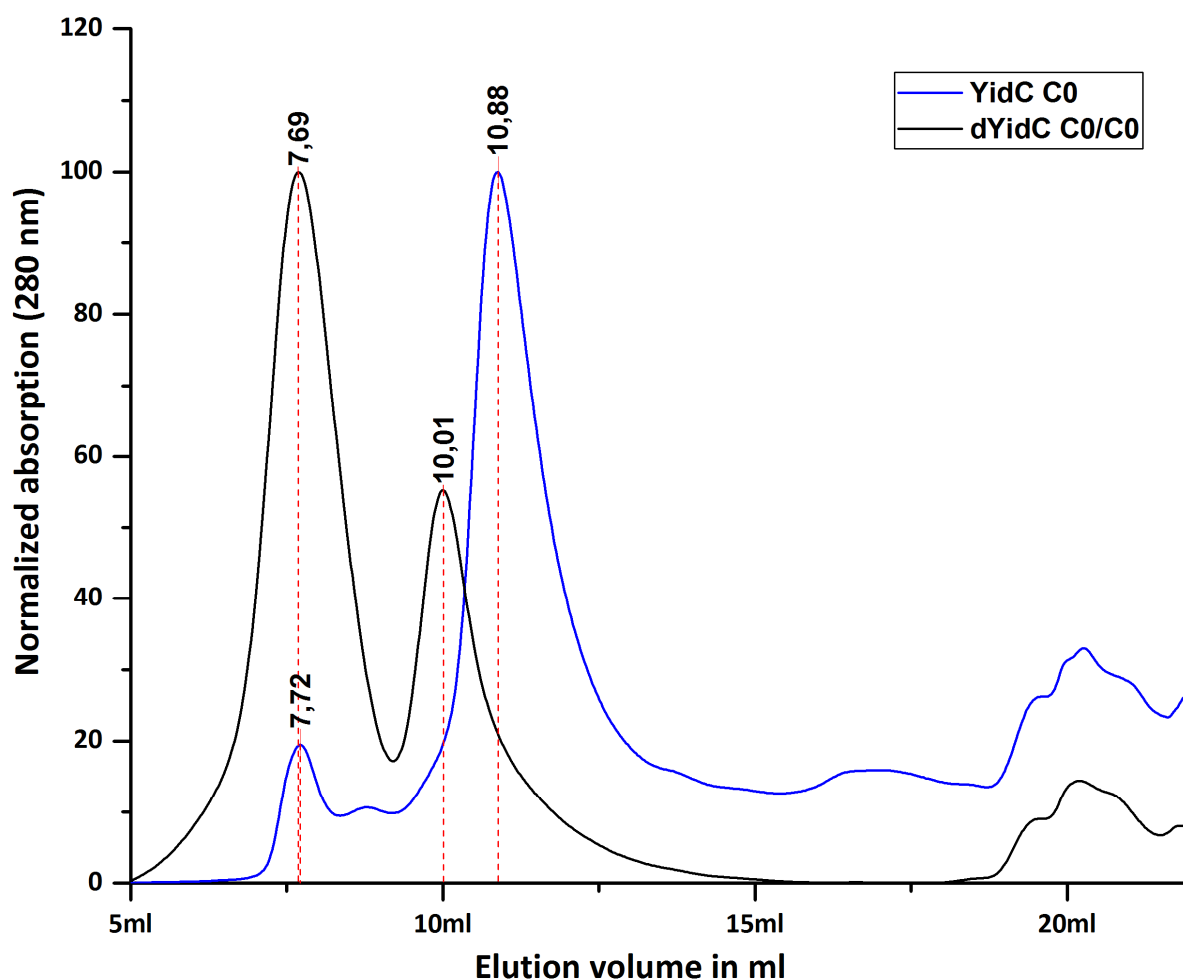
Fig. 80: Overlay of the normalized absorption data of both SECs. Absorption data was normalized to values between 0 and 100 for better comparison. Black: SEC diagram of dYidC C0/C0 Blue: SEC diagram of YidC C0. The distinct peak positions with a difference of 0.87 ml show the size difference of the two purified proteins. The peak at 7.69 ml was most likely formed by aggregates of small unknown proteins. Image created with OriginPro 2015G.

~234 kDa for the dYidC C0/C0 dimer and ~146 kDa for the YidC C0 monomer were obtained. This shows the size difference of the eluted protein that was acquired with the SEC (See Fig. 80).

3.2.6 Substrate binding in the dYidC protomers

The complementation capability of the dYidC raised the question, if each protomer is capable of independently binding a substrate molecule. To perform binding studies between the dYidC and M13 procoat an efficient method was needed to gain sufficient amounts for biochemical analysis of a crosslinked dYidC-M13 procoat complex. To achieve this, DTNB was used as crosslinking agent during cell growth and induction (see 3.1.1).

MK6S cells were transformed with the H5 procoat mutant 33C and the dYidC mutants 427C/427C, 427C/C0 and C0/427C. For control purposes the YidC monomer mutant 427C and C0 were also used. An overnight culture was inoculated 1:100 in LB medium containing ampicillin, chloramphenicol and glucose. The cells were induced at $OD_{600} = 0.5$ with 1mM IPTG. After 10 minutes, 200μM DTNB was added to the cultures and the cells were grown for 3 more hours followed by TCA treatment and subsequent sample preparation without DTT (see 2.9.2). The dYidC is capable of binding its substrate, the H5 procoat protein, separately with each of its protomers (see Fig. 81). The complementation studies (see 3.2.3) showed that the dYidC was functional in cells, even when one of the protomers was defective. The here shown ability to bind substrate in each protomer individually indicated that both protomers are active and function independent from each other. Surprisingly, the bands of the expected crosslinked complexes ran on different heights on the SDS gel, depending to which protomer the substrate was bound. This was an unexpected behavior of the crosslinked products leading to up to four different distinguishable bands. Further investigation will be needed to explain these differences.
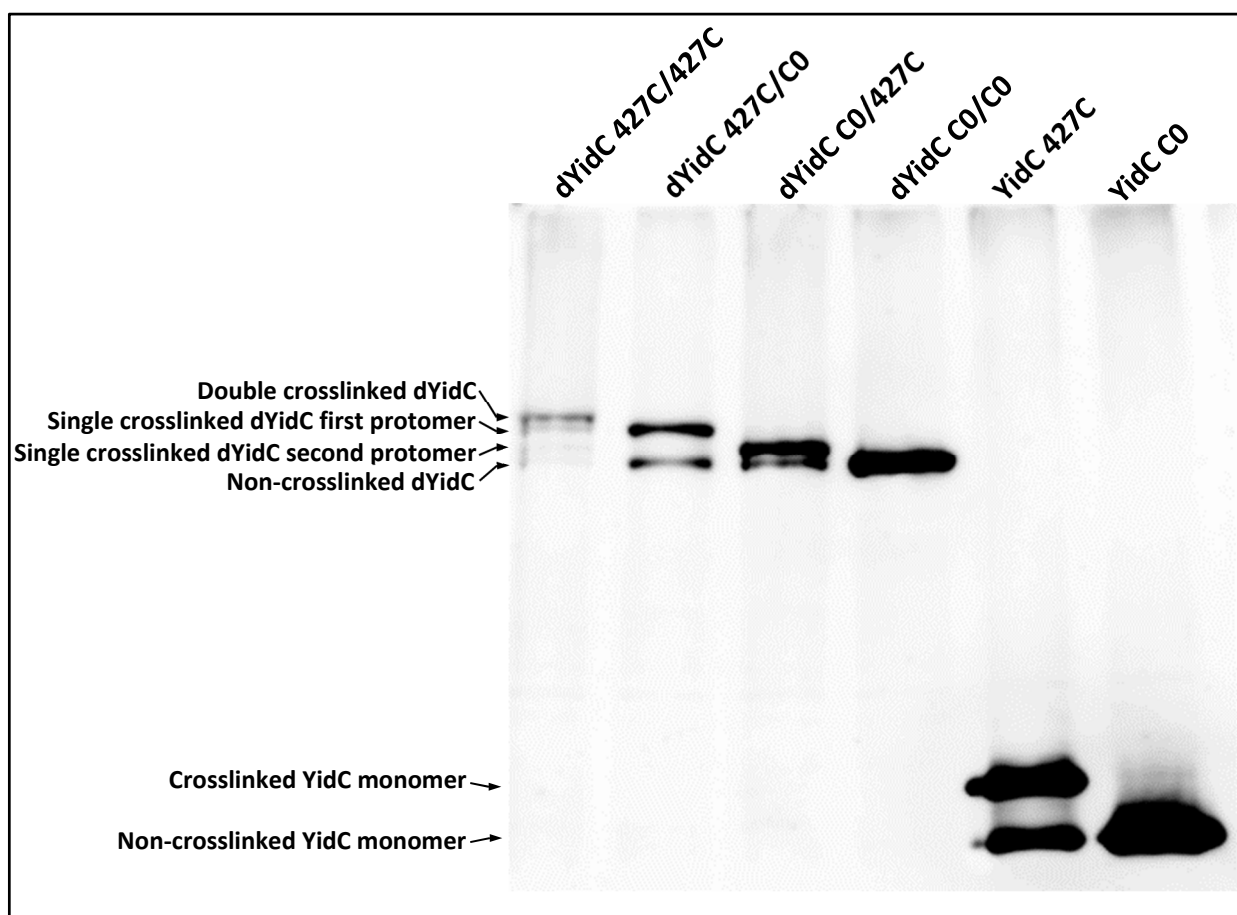
Fig. 81: Crosslinking of the dYidC constructs with H5 procoat 33C. Four bands are observed for the 427C/427C mutant, the topmost being the double crosslinked dYidC followed by the two single crosslinked bands and the lowest non-crosslinked dYidC. In case of the 427C/C0 and C0/427C mutants only two bands can be observed, the crosslinked and non-crosslinked variants of the dYidCs. However, the size of the single crosslinked dYidCs varied significantly depending in which protomer the single cysteine was present. The YidC monomer control shows a clear and strong crosslink with the YidC 427C mutant and none with the cysteine free YidC C0 mutant. Samples were separated on a 10% SDS acrylamide gel. Western blot with anti-His$_{10}$tag antibody.

Prescission protease assay

To adress the issue of the strange running behaviour in the SDS-PAGE, the 3 different dYidC constructs were again crosslinked with H5 M13 procoat 33C and subsequently purified for a prescission protease assay. This would allow to see the individual protomers after separation and to analyze the different shifts in protein size on the SDS gel. For this, a 200 ml LB culture of MK6S cells containing the respective plasmids used for protein expression and crosslinking (see 2.8.2).

The membranes were solubilized in 2% DDM and subsequently purified (see 2.8.2). For the prescission protease assay half of the purified proteins was incubated with the prescission

protease and the other half was used as negative control with water instead of the enzyme (see 2.11).

Fig. 82 shows that the separated protomers of the dYidC differ in size. The calculated size for the first protomer is 62.5 kDa while the second has a molecular weight of 63.4 kDa. This difference is caused by the additional His_{10}tag that the second protomer is carrying at the c-terminus. However, the split crosslinked disconnected protomers do not show the big size difference that the unprocessed crosslinked dYidC proteins did. This led to the assumption
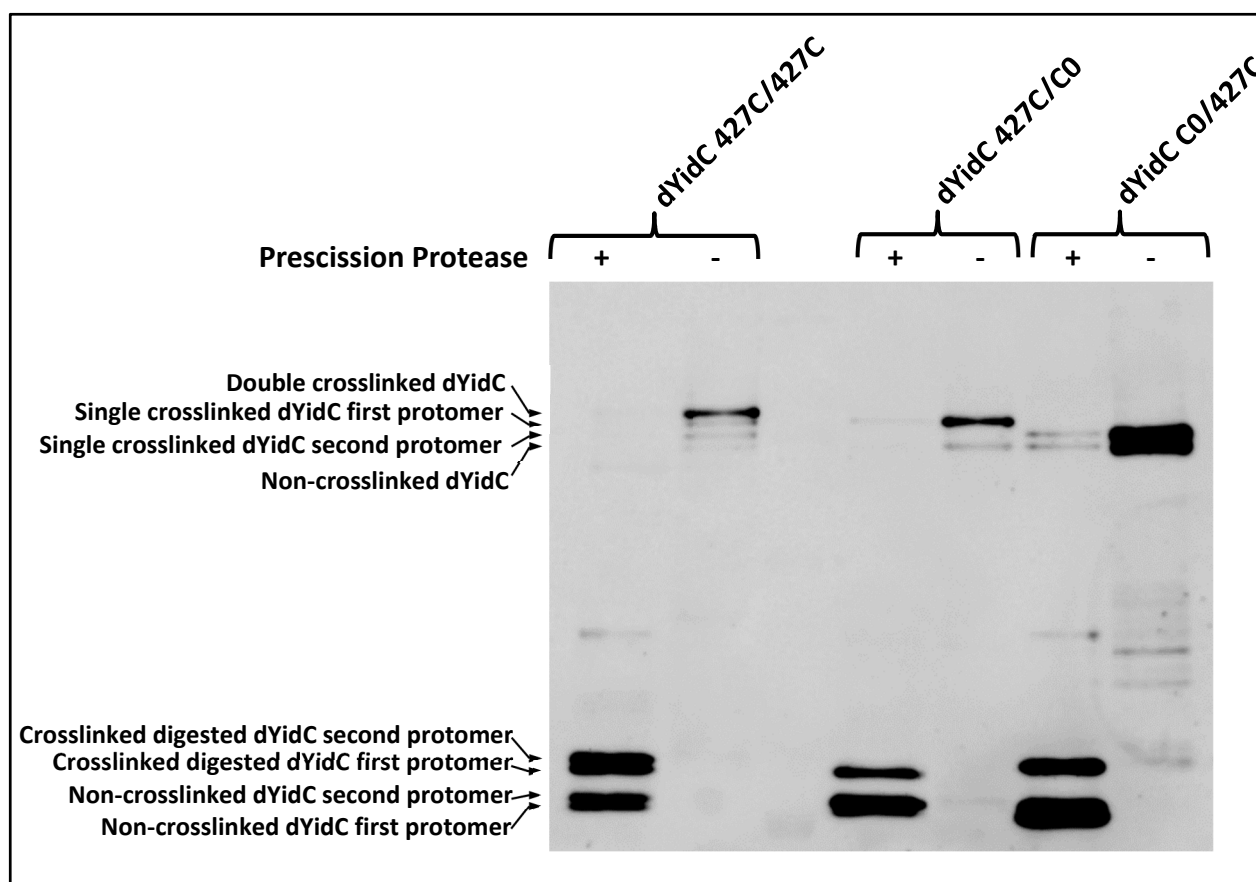
Fig. 82: Prescission processing of crosslinked dYidC constructs. The dYidC mutants 427C/427C, 427C/C0 and C0/427C were crosslinked with H5 procoat 33C and subsequently purified for the prescission protease procession. Samples were separated on a 10% SDS acrylamide gel, detection was performed by western blotting followed by immuno-detection with the YidC100 antibody.

that the different behavior on the gel was caused by a conformational change due to the binding of the substrate in the dYidC and probably the lack of reducing agents to aid in the full unfolding of the protein. However, DTT or β-mercaptoethanol would not be suitable to verify this as these strong reducing agents would destroy the crosslink. Therefore, the prescission protease assay was used to investigate the cause of the unexpected bands.

3.2.7 Translocation assays with different YidC and dYidC mutants

Different YidC and dYidC defective mutants were expressed together with the M13 procoat wild type to test their ability for substrate insertion under depletion conditions in MK6S cells. Only when the M13 procoat protein is inserted correctly by YidC, the leader-peptidase is able to process the precursor protein to the mature coat protein. This can be detected by the reduced molecular weight of M13 coat leading to a shift on a SDS-urea gel. The cells were grown and treated as described (see 2.10). For the monomeric YidC, the construct pGZ119 EH YidC C0 was used as a positive control for insertion and the empty pGZ119 EH vector as a negative control. For the dYidC the cysteine-less mutant pGZ119 EH dYidC C0/C0 was used as positive control and the empty pGZ119 EH vector as a negative control.

Monomeric defective YidC mutants and M13 procoat wild type

The defective monomeric YidC variants (see 3.2.2) were tested for substrate insertion. The experiment was performed as described (see 2.10). Arabinose and glucose were used in the initial experiments to either express or deplete the chromosomal YidC in the cells for control purposes. Arabinose treated cells should always show a high level of insertion of M13 procoat due to the presence of YidC. It was already shown that the here tested defective mutants were not capable of complementing in YidC depleted MK6S cells *in vivo* (see 3.2.3). However, only
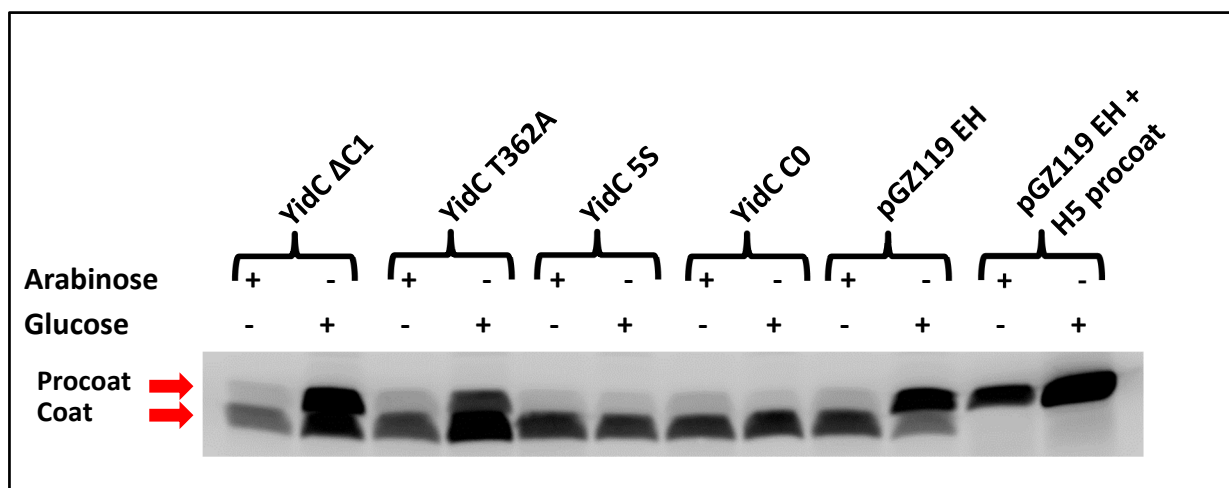
Fig. 83: M13 procoat wild type insertion assay with the defective YidC monomer mutants. MK6S cells were used for the experiment under arabinose and glucose conditions. With arabinose all samples showed the same level of procoat insertion and almost complete processing. Under glucose conditions only YidC ΔC1 shows more procoat then coat and therefore a strong reduction in insertion. The T362A mutant also accumulated procoat though at a lower level, therefore the insertions is less inhibited in comparison. The 5S mutant inserts at the same level as the arabinose treated control and the YidC C0 positive control. Samples analyzed on a 22% urea gel, immunoprecipitation with anti-M13 antibody and detection via phosphorimaging.

the YidC mutant ΔC1 showed an accumulation of procoat and thus a strongly reduced insertion of M13 procoat wild type into the inner cell membrane. In addition, the T362A mutant showed a reduced insertion capability while for the 5S mutant no sign of insertion inhibition was detected. The partial deletion of the C1-loop somehow impedes the insertion process (see Fig. 83).

pGZ119 EH dYidC C0/C0 insertion of M13 procoat wild type

The cysteine-less dYidC C0/C0 was shown to complement growth of MK6S cells (see 3.2.2). To see whether the dYidC is generally capable to catalyze the insertion of the M13 procoat 805wt an experiment was conducted under arabinose and glucose growth conditions. When MK6S cells grow in presence of glucose the chromosomal YidC is depleted and the dYidC has to complement to allow cell growth. The experiment was performed as described (see 2.10).

The dYidC C0/C0 showed the same level of activity as the cysteine-less monomer YidC C0 in terms of substrate insertion (see Fig. 84). This indicates that the dYidC is functionally active and allows cell growth. During the substrate binding studies it was shown that each protomer is capable of binding substrate individually (see 3.2.6). However, in the binding study with the defective mutant YidC ΔC1 it was observed that binding a substrate does not necessarily lead
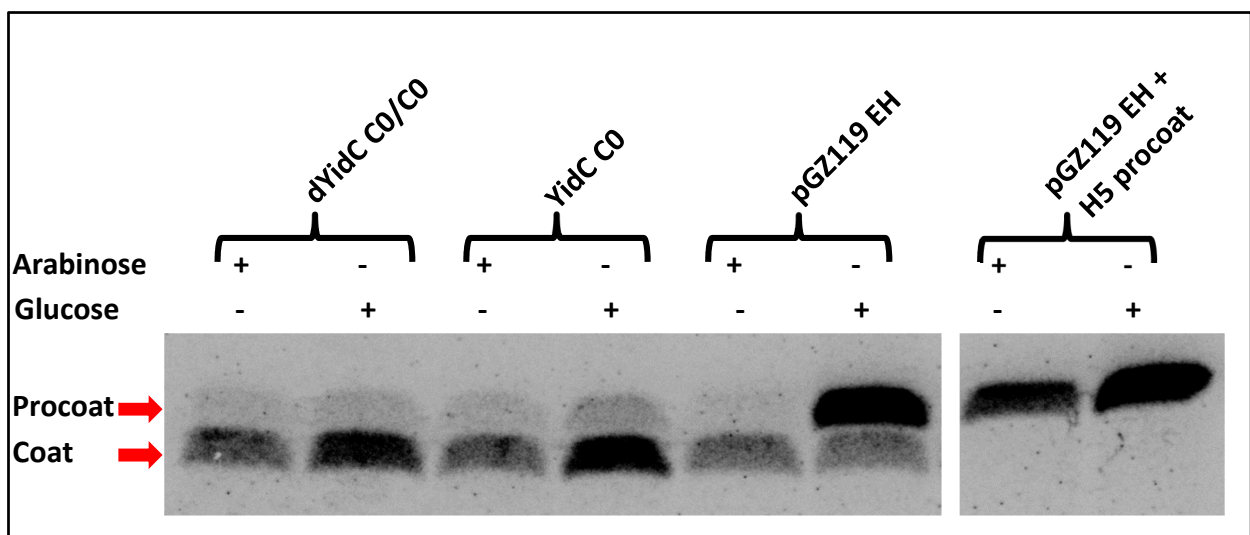
Fig. 84: M13 procoat wildtype insertion assay with the cysteine free dYidC C0/C0 mutant. MK6S cells were used for the experiment. All samples were pulsed under arabinose and glucose conditions. The dYidC is capable of substrate insertion, shown by the processed M13 coat protein. The insertion efficiency is at the same level as for the YidC C0 monomer. The control with the empty pGZ119 EH vector shows strongly reduced insertion and the H5 procoat wild type shows no signs of being processed, even under arabinose conditions. Samples analyzed on a 22% urea gel, immunoprecipitation with anti-M13 antibody and detection via phosphorimaging.

to membrane insertion (see 3.2.4). For the monomeric YidC ΔC1, it was already shown that the M13 procoat wildtype substrate was not efficiently inserted (see 3.2.7).

Next, the different defective mutants in the dYidC protomers were tested to determine if each of the protomers can only bind or actually insert the M13 procoat wild type as its substrate. The cysteine free dYidC C0/C0 was used as a positive control for comparison.

pGZ119 EH dYidC single defective mutant insertion of the M13 procoat wild type

The defective YidC mutants ΔC1, T362A and 5S were cloned in the dYidC protomers leading to mutants with one protomer carrying a defective YidC mutant. These mutants were then tested for the insertion of M13 procoat wild type.

 The dYidC variants with single defective protomers showed clear insertion activity as well as the positive control with the cysteine-less YidC. The negative control showed no processed M13 procoat protein (see Fig. 85). Compared to the experiment in Fig. 84 the amount of remaining unprocessed M13 procoat is higher. The negative control in Fig. 84 also shows small amounts of processed M13 procoat protein. A possibility could be minuscule amounts of residual chromosomal YidC that were present after the three hour depletion phase. On the other hand, the overall expression for the control was much higher as the one in this experiment. Still the results indicate that each protomer is active on its own and can insert M13 procoat independently from the other. If this is also true for other substrates needs to be tested.
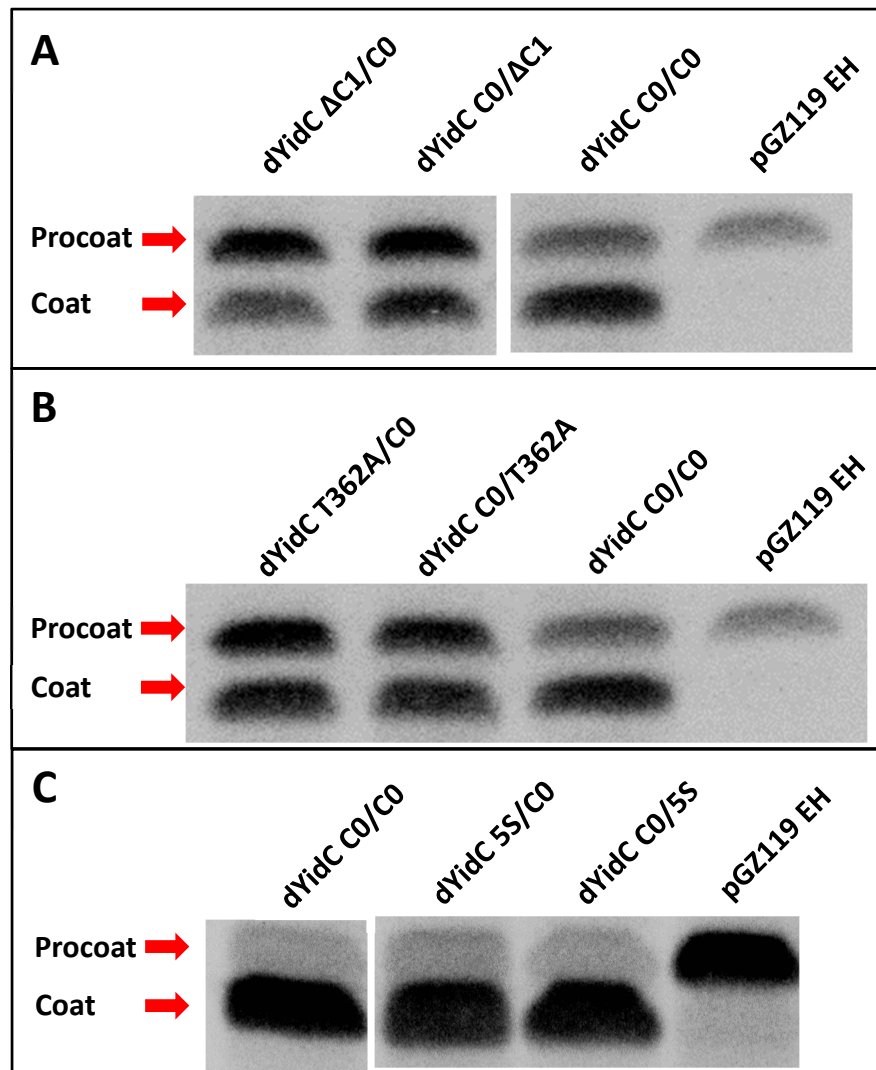
Fig. 85: Insertion of M13 procoat wild type with the single defective dYidC mutants. (A) ΔC1 single defective mutants that show a similar level of insertion as the C0/C0 control. The negative control shows almost no insertion. (B) T362A single defective mutants that show a similar level of insertion as the C0/C0 control. The negative control shows almost no insertion and is the same as in A. (C) 5S single defective mutants that show the same level of insertion as the C0/C0 control. The negative control shows almost no insertion. Samples were separated on a 22% urea gel, immunoprecipitation with anti-M13 antibody and detection via phosphorimaging.

pGZ119 EH dYidC double defective mutant insertion of M13 procoat wild type

The next step was to see how efficient dYidC mutants with two defective protomers would insert the M13 procoat protein. Different combinations were constructed for functional complementation between the defective protomers. Here different defective mutants were also combined in the dYidC to test for possible growth restoring effects, which would also indicate interaction of the protomers with each other.

The ΔC1/ΔC1 and T362A/T362A mutants show strongly reduced insertion and processing indicating impaired insertion functionality (see Fig. 86). While the T362A monomer inserted M13 procoat at a reduced rate (Fig. 83), the dYidC variant harboring this mutant in both protomers shows a much stronger inhibition. The 5S double defective mutant showed high activity, almost at the level of the positive control.

The positive controls in both experiments in Fig. 86 show different levels of procoat processing. The most plausible explanation is residual chromosomal YidC in the MK6S cells in the 5S experiment that caused the higher level of processing. The overall tendency however is still observable.
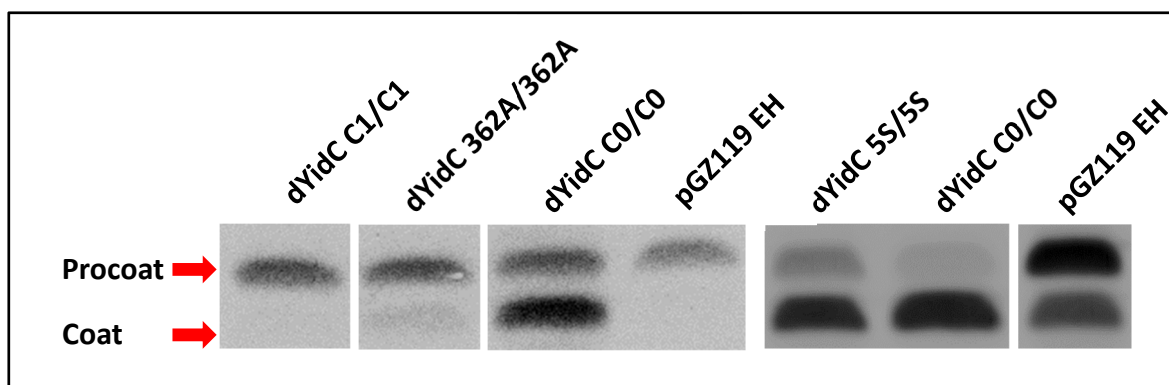
Fig. 86: Insertion of M13 procoat wild type with the ΔC1, T362A and 5S mutants in both protomers of dYidC. The ΔC1/ΔC1 and T362A/T362A dYidC mutants show strongly reduced M13 procoat insertion, similar to the negative control. The 5S/5S mutant shows insertion at an increased level but below of the positive control (C0/C0). Samples were separated on a 22% urea gel, immunoprecipitation with anti-M13 antibody and detection via phosphorimaging.

The dYidC mutants 5S/ΔC1 and ΔC1/5S showed a higher activity than the mutants T362A/ΔC1 and ΔC1/T362A. Even though no tested mutants were able to insert the M13 procoat substrate at the level of the positive control they were still active to a certain extent. This activity is higher than the negative control, where some protein was inserted but at a much lower rate (see Fig. 87).
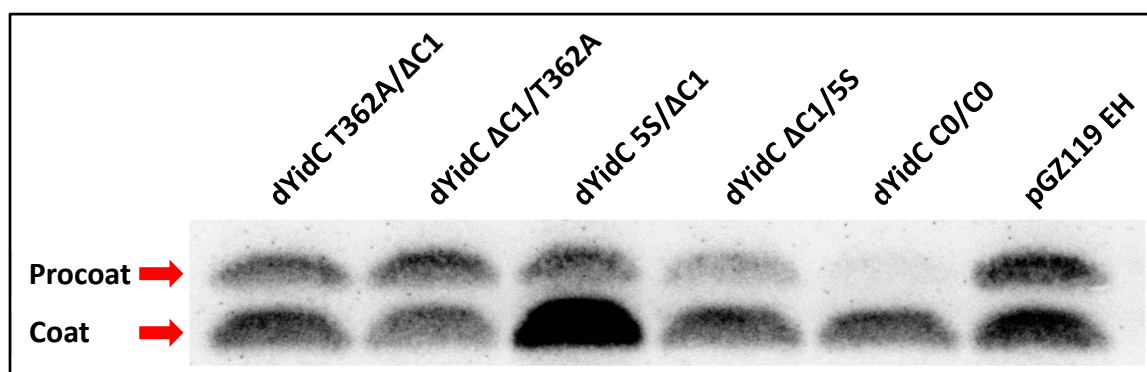
Fig. 87: Insertion of M13 procoat wild type with combinations of ΔC1 with T362A and 5S mutants. The tested mutants showed reduced activity compared to the positive control dYidC C0/C0. The negative control shows higher levels of inhibition than the tested mutants. The coat protein for the 5S/ ΔC1 mutant had a much higher expression than the rest and a lot more processed coat than procoat. Samples were separated on a 22% urea gel, immunoprecipitation with anti-M13 antibody and detection via phosphorimaging.

One possibility that could explain the insertion in the negative control is that residual chromosomally-encoded YidC molecules were still present due to incomplete depletion of the cells. This could be caused by either a leaky promotor or by too short depletion times prior to the experiments. However, the cells were tested for YidC expression under depletion conditions and the depletion time in the experiments was at least 3 hours prior to induction of the plasmid encoded YidC.

4 DISCUSSION

The insertase YidC promotes the insertion of small membrane proteins into the inner bacterial membrane (Samuelson et al. 2000) including the major capsid protein of the M13 bacteriophage (Samuelson et al. 2001). Over the years more data were obtained regarding the structure of YidC and the structural features of the insertase, like the hydrophilic cavity inside the protein (Kumazaki et al. 2014a and 2014b). Data where YidC interacts with its substrates during the insertion process (Klenner and Kuhn 2012, Neugebauer et al. 2012) also became available. An insertion model of YidC (Kumazaki et al. 2014a) proposes an important role of the hydrophilic cavity that was discovered in the structure of YidC. However, many questions still need to be answered regarding the mechanism of the insertion process and the oligomeric state of the active insertase. The latter is still discussed (Lotz et al. 2008, Kohler et al. 2009, Boy and Koch 2009, Kumazaki et al. 2014a/2014b, Shimokawa-Chiba et al. 2015) but not answered up until today though the structure (Kumazaki et al. 2014b) indicates an active monomer. Here we provide data to help elucidating these questions.

In this work an artificial dimer of YidC has been studied to investigate the oligomeric state and thereby elucidate its active configuration. As a measure of activity, the interaction of YidC with one of its substrates, M13 procoat, was taken. In addition, an efficient method to purify protein-protein complexes was established which will also be discussed.

4.1 dYidC as an artificial construct for functionality studies

The oligomeric state of the active YidC insertase has been subject to controversial discussions in the past. Data indicating an active monomer (Kumazaki et al. 2014a/2014b, Shimokawa-Chiba et al. 2015) or dimer (Lotz et al. 2008, Kohler et al. 2009, Boy and Koch 2009) have been published. YidC has also been found to associate with the Sec translocon and is a component of the holotranslocon (Sachelaru et al. 2013, Botte et al. 2016) which makes the insertase a very dynamic and flexible protein with a set of various interactions. To assess in which form YidC is active as an insertase an artificial dimer of two linked YidCs was constructed. This dimer is stably expressed in *E. coli* MK6S cells (see 3.2.3).

The dYidC was used in different experiments to elucidate the active configuration of YidC, which will be discussed here. The first part involves the purification of the stable mono and dimeric YidC followed by binding studies with its substrate M13 procoat. The new method to obtain stable YidC-substrate complexes is also discussed at the end of this chapter.

4.1.1 dYidC can be purified from *E. coli* MK6S cells

Monomeric and dimeric cysteine-free YidC was purified from MK6S cells for biochemical and structural analysis (see 3.2.5). The size exclusion chromatography (SEC) profiles (see 3.2.5) show that both proteins elute at different volumes and therefore are different in size. However, the calculated sizes with the standard curve for the used column differed from the expected molecular weights for the two purified proteins. For the monomer 146 kDa were calculated. Even though a dimer would add up to approx. 125 kDa, it is unlikely that this is the eluted form of YidC. It is more plausible that a single monomer of approx. 62.5 kDa eluted in a large micelle of approx. 84 kDa, which consists of DDM and Cymal6 in a ratio of 2:1. In case of a dimer, the remaining molecular weight difference would be too small for a micelle to form around the complex. The reported size for DDM micelles is around 70 kDa (Strop and Brunger 2005) but the size of the mixture with Cymal6 has not been determined up to date.

For the dimeric YidC protein, the calculated molecular weight is 234 kDa. A dimer of dimers would be too large but a single dimer would result in a micelle size of approx. 110 kDa. This could be possible, if each protomer has its own micelle of approx. 55 kDa with a connection where the linker is located (see Fig. 88).
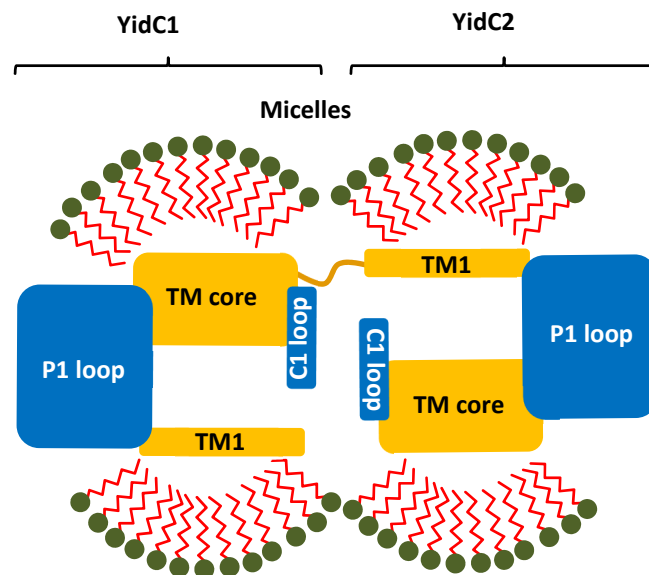
Fig. 88: dYidC with two detergent micelles. A micelle forms around the hydrophobic core of each protomer. Blue: hydrophilic/amphipathic parts of YidC, orange: hydrophobic parts of YidC, green: hydrophilic heads of the detergents DDM and Cymal6, red: hydrophobic tails

The size difference that was observed in the SEC shows the monomeric and dimeric dYidC to elute at different times. This suggests that the monomer does not associate with another YidC to form a dimer. Both proteins were purified extensively and showed only YidC or dYidC after SDS-PAGE and Coomassie staining (see 3.2.5). Small-angle scattering (SAS) could be used to further determine the size and basic structure of the purified proteins (Svergun and Koch 2003) and verify our results. Small amounts of YidC and dYidC with covalent bound substrate have also been purified (see 4.1.2) and applying additional methods, like the SAS, to analyze the structure of these complexes might help understanding the interaction of YidC with M13 procoat.

4.1.2 dYidC separately binds M13 procoat in each of its protomers

M13 procoat is inserted in a YidC-only manner into the inner bacterial membrane (Samuelson et al. 2001). In regards of the here used dYidC for the analysis of the oligomeric state of the active insertase and the interaction with its substrate, a decisive question was, whether each dYidC protomer inserts a substrate protein on its own. In this case, it should be possible to bind one M13 procoat protein to each of the protomers via disulfide crosslinking. This was achieved by treating the cells with DTNB (Bis(3-carboxy-4-nitrophenyl) disulfide) over several

hours and express dYidC with a cysteine at position 427 in one or both protomers and a cysteine mutant at position 33 of the M13 substrate (see 3.2.6). Surprisingly, the dYidC shifted differently during the SDS-PAGE depending on the protomer the substrate was crosslinked to. Substrate binding to the first protomer produced a much larger shift than to the second. This unusual behavior had to be assessed. Purification of the complex and processing it with the prescission protease split the dimer into its protomers. The shifted complexes of the split protomers then ran on the same level again. This was done in a relatively small scale of 200 ml culture and larger amounts of protein could be purified in the future to study the structure of this protein-protein complex.

The unusual running behavior of the crosslinked substrate dYidC-complexes might be caused by a conformational difference depending on which protomer the M13 procoat was bound. This difference is large enough to change the running behavior on the SDS PAGE in the absence of reducing agents, like DTT. The disulfide bonds are maintained in the complex and the conformation of the proteins is kept intact to some extent. Therefore, two things can be concluded. First, the dYidC is capable of independently binding a substrate molecule in each of its protomers, and second, the protomers show differences in their conformations, at least in a substrate-bound state, as long as they are linked to one another.

To achieve binding of the substrate to the dYidC *in vivo* in chemical amounts a protocol was established that allows the constant formation of crosslinked proteins in living cells with DTNB. This was at first necessary because the dYidC was not expressed well enough to be detectable in the pulse experiments. However, this new method also allowed the analysis and purification of protein complexes and was used accordingly in this study.

4.1.3 A YidC-M13 procoat complex can be formed *in vivo*

DTNB has been established as a powerful crosslinking agent that allows expressing and purifying protein complexes from living cells (see 4.1.2). It was shown, that MK6S cells are viable with 200 µM DTNB in culture. Other crosslinkers, like copper phenanthroline or o-PDM were not tolerated by the cells at all in their respective necessary concentrations. Park and Rapoport (2012) used DTNB to successfully crosslink SecY to OmpA-GFP *in vivo*. The conditions were different from the experiments performed in this study, a higher amount of DTNB had been used to mediate the formation of the disulfide bonds (1 mM compared to 200 µM) and the reaction time was significantly shorter (10 min. instead of 3 to 4,5 h). The tolerance limit of DTNB that does not impair cell growth of the *E. coli* cells over longer periods has yet to be determined. In addition, to gain larger amounts of a YidC-M13 procoat complex the reaction must occur during the insertion process. Already inserted M13 procoat can no longer be crosslinked to YidC, which makes the addition of the crosslinking agent at an early stage of the expression necessary. Here data are provided, that show how the oxidation-mediating agent DTNB can be used over longer periods (3 to 4.5 h) *in vivo* to obtain protein complexes in amounts suitable for biochemical analysis.

YidC and its artificial dimer are membrane bound proteins and the tested cysteine residues are deeply buried inside the bilayer of the cell according to the published structure of the protein by Kumazaki et al. (2014b). M13 procoat is also membrane bound even after it is processed into its mature form. Since the uncleavable H5 mutant was used for the experiments and no other parts of the M13 phage were expressed, it is very likely that M13 procoat remains in the membrane after insertion with YidC. When M13 procoat is crosslinked with DTNB to YidC a covalent bound complex with a not yet known conformation is formed. The state of the insertion should depend on the positions that were chosen in both proteins that form the complex. With the right combinations, it should be possible to generate and analyze several insertion states in the future.

4.1.4 Functionality of various defective YidC and dYidC mutants

A variety of potentially defective YidC mutants have been tested for their capability to complement in *E. coli* MK6S cells and to insert M13 procoat into the inner membrane. This was done in scope of a further analysis of dYidC, where these mutations were also tested in the protomers of the protein.

4.1.4.1 YidC T362A, ΔC1 and 5S do not complement in *E. coli* MK6S cells

The conducted complementation assays (see 3.2.3 and Tab. 32) show, that none of tested mutants can complement in depleted MK6S cells albeit being expressed at sufficient levels. The way these mutants are impaired in their functionality is very different.

The YidC ΔC1 deletion mutant shows neither successful insertion of M13 procoat nor complementation

Tab. 32: Overview of the complementation and insertion experiments with YidC defective mutants and the M13 procoat wildtype. Comp.: complementation

Construct	Comp.	Insertion of M13 procoat
YidC C0	Yes	Yes
YidC ΔC1	No	No
YidC T362A	No	Reduced
YidC 5S	No	Yes

capability in *E. coli*. However, this mutant is capable to bind M13 procoat albeit not to insert it (see 3.2.4). The crosslinking signal in the ΔC1 YidC is weaker compared to the non-truncated cysteine mutant but still clearly detectable. The interaction is therefore already impaired to some extent, but binding is still observable. The tested contact site in TM3 of YidC (pos. 427) is located relatively close to the cytoplasmic membrane surface. Other confirmed contacts might not be accessible for the substrate with the deletion in the C1 loop or at least show a much weaker interaction signal. The insertion model published by Kumazaki et al. (2014a) stated an important role of the C1 loop during insertion and Chen et al. (2014) showed that a deletion of the second half of the loop leads to inhibition of insertion for a Procoat-Lep fusion protein. Here, these results were confirmed with the wildtype form of the M13 procoat protein. The C1 deletion might only allow binding to the parts of the hydrophobic slide closer to the cytoplasm but no further interaction with YidC. Crosslinking experiments with cysteines positioned more towards the periplasm in the TM3 or TM5 of YidC could provide further insight into this matter.

YidC T362A has its mutation in the center of the hydrophilic groove. Wickles et al. (2014) published data that show the inability of complementation and he was able to express this

mutant stably. It was concluded, that no conformational issue leads to the lack of functionality. Here, this observation was confirmed. The reason why the T362A mutant impairs YidC is not known yet, though its position indicates an influence in the hydrophilic groove itself. Replacing a hydrophilic threonine with a slightly hydrophobic alanine could influence the groove to a yet unknown extent. The insertion of M13 procoat is reduced but not abolished indicating that the insertion function is influenced by the mutation. Other substrates of YidC were also inserted in a reduced manner or completely abolished, which could explain the inability to complement in *E. coli* cells. Further details are discussed in 4.1.4.2 and 4.1.4.3 with the data obtained from the dYidC insertion and complementation experiments.

The 5S mutant showed insertion of M13 procoat at wild type levels but did not uphold viability. This unusual behavior is quite intriguing and is further discussed in 4.1.4.3 together with the data obtained from the dYidC experiments.

4.1.4.2 Complementation studies with the dYidC and its defective mutants

With the data gained from the monomeric defective YidC mutants (see 4.1.4.1) dYidC constructs were tested where one or both protomers were replaced with inactive variants. The artificial dimer is capable to complement YidC deficient *E. coli* MK6S cells (see 3.2.3). Replacing one protomer with a defective mutant (see Tab. 33) still led to full complementation in most cases. One exception was the 5S/C0 mutant that did not complement even with one functional protomer in the second position. The C0/5S mutant, however, complemented at the same level as the cysteine-free C0/C0 mutant. The other defective mutants, T362A and ΔC1, showed normal growth if paired with a cysteine free YidC in either position (see 3.2.3 and Tab. 33).

Tab. 33: Overview of the complementation capability of the dYidC mutants.

Construct	Comp.
dYidC C0/C0	Yes
dYidC ΔC1/C0	Yes
dYidC C0/ΔC1	Yes
dYidC ΔC1/ΔC1	No
dYidC T362A/C0	Yes
dYidC C0/T362A	Yes
dYidC T362A/T362A	No
dYidC 5S/C0	No
dYidC C0/5S	Yes
dYidC 5S/5S	No
dYidC T362A/ΔC1	No
dYidC ΔC1/T362A	No
dYidC 5S/ΔC1	No
dYidC ΔC1/5S	No

This indicates that the positions of the 5S mutations in the dimer play a role. However, this behavior could not be observed for the other tested defective mutants ΔC1 and T362A in their

respective combinations. In case of the double defective dYidCs, the inability to complement can be explained with the disabled insertion functionality that led to a decline in the insertion of essential substrates like the subunit c of the F_1F_o-ATPase. The 5S/C0 mutant however should still be capable to insert YidC dependent substrates with both protomers since the 5S mutant was found to not interfere with the insertion capability of YidC and a functional protomer is still present as well (see 4.1.4.1). Therefore, a different effect must influence the cells that does not allow growth over night to form colonies. The results of both single defective 5S dYidC mutants show that the position of the 5S protomer plays an essential role for this effect and it most likely influences other functions of YidC than the insertion of YidC-only substrates. This influence manifests over a longer period since expression of the dYidC constructs over three hours is stable (see 3.2.3) but in complementation assays colonies are not formed overnight, indicating a decline in cell growth.

Aside from inserting its substrates, YidC interacts and cooperates with the Sec translocon and is often associated with it (Scotti et al. 2000, Sachelaru et al. 2013). The interaction with the Sec translocon might only be provided by the first protomer and not by the second due to conformational issues that originate in the relatively short linker (see Fig. 89). The second protomer might not be flexible enough due to its very close position to the first, which could
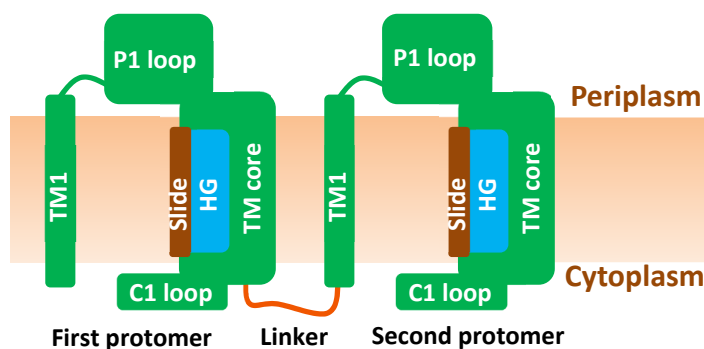
Fig. 89: Diagram of the dYidC construct. The second protomer is linked to the first via a short linker of 12 residues. This results in a very close position of the second protomer to the first in the membrane.

result in a lack of mobility in the membrane. The results from the 5S dYidC constructs strongly indicate such an effect. This would hinder the second YidC in providing full activity in all functional aspects. In addition, the binding studies with a cysteine mutant of H5 M13 procoat and the dYidC show conformational differences depending to which protomer the substrate

is bound, leading to a different running behavior during SDS-Page despite the same molecular weights (see also in 4.1.2).

Li et al. (2014) demonstrated that the TMs of YidC play an essential role for the interaction with the Sec translocon, especially SecDF, and that mutations in the TMs can lead to a loss of viability. Two of the YidC mutations, P431S and M471H, are located near positions where serines were mutated in the 5S YidC (M430S and P468S). A recent study (Sachelaru et al. 2017) proposed a very invasive intercalation of YidC during its interaction with SecY that influences the diameter of the channel. It is possible that the five serines in the 5S mutant disturb this interaction to the point that a successful cooperation of SecYEG with YidC is blocked or at least strongly impaired. The way this potential impairment occurs is not clear. One possibility is a lack of interaction surface between SecY and the 5S mutant of YidC, another could be the blockage of the Sec pore if the conformation of the 5S YidC allows the proposed intercalation (Sachelaru et al. 2017) but the formed complex is non-functional and maybe even unable to dissociate. Either way, essential substrates that require YidC and the Sec translocon for insertion, like the subunit a of the F_1F_o ATPase (Kol et al. 2009) might no longer be inserted, which would result in a stop of cell growth. However, further experiments are needed to confirm these assumptions.

4.1.4.3 The dYidC can insert M13 procoat into the inner membrane

Aside from the complementation capability of the different dYidC mutants, a direct observation of their capability to insert M13 procoat was also of importance. Translocation assays with the M13 procoat wild type construct were performed (see 3.2.7) that display clear insertion and processing for the C0/C0 control and for all single defective mutants of the dYidC (see Tab. 34).

From these results, it can be concluded that one intact YidC in either protomer suffices for proper insertion of the M13 procoat protein *in vivo*. Further experiments with other YidC-only substrates like Pf3 coat or subunit c of the F_1F_o-ATPase might lead to different results. An approach to further investigate the impairing effect of the defective YidC mutants would be the mutation of cysteines into the functional and double defective dYidC mutants and into M13 procoat. Since several contact sites are known, from the crosslinking studies (see 4.2), it should be possible to map to what point the interaction between the defective dYidCs and M13 procoat is still possible. In addition, there could be

Tab. 34: Overview of the insertion assays with different dYidC constructs.

Construct	Insertion of M13 procoat
dYidC C0/C0	Yes
dYidC ΔC1/C0	Yes
dYidC C0/ΔC1	Yes
dYidC ΔC1/ΔC1	Impaired
dYidC T362A/C0	Yes
dYidC C0/T362A	Yes
dYidC T362A/T362A	Strongly Reduced
dYidC 5S/C0	Yes
dYidC C0/5S	Yes
dYidC 5S/5S	Reduced
dYidC T362A/ΔC1	Reduced
dYidC ΔC1/T362A	Reduced
dYidC 5S/ΔC1	Reduced
dYidC ΔC1/5S	Reduced

not yet known varieties in the mapping profiles between the first and the second protomer that would indicate differences in the mechanism of the insertion due to the protomer position inside the dimer. These experiments should be performed with the *in vivo* crosslinking with DTNB because the dYidC is not expressed in sufficient amounts with the radioactive pulse-label approach (data not shown).

Interestingly, Geng et al. (2015) published data that show different C1 deletion mutants that cannot support viability in cells but still insert the c subunit of the F_1F_o ATPase. However, this substrate differs strongly in its conformation compared to the M13 procoat protein. It also has two TMs, but the N and C domains are translocated while the loop stays inside the cell. In addition, the deletions tested were shorter, only 10 amino acids in length, and in different positions than the here used ΔC1 mutant. Five deletion mutants in the C1-loop were tested

(Δ374-383, Δ385-394, Δ392-401, Δ401-410 and Δ410-419) and all showed insertase activity. Chen et al. (2014) showed that PC-Lep is not inserted by the identical ΔC1 deletion as used here but with a different substrate, preCyaA-P2, insertion was possible at a slightly reduced level. These observations indicate that YidC treats its substrates differently during insertion. It also indicates that different mutations in YidC should also have different effects on the interaction with the known substrates. Membrane insertion can therefore be completely abolished, reduced or facilitated at normal levels depending on which YidC defective mutant is coexpressed with a substrate.

The T362A/T362A mutant showed a strongly reduced insertion activity, lower compared to the monomeric T362A YidC. Unlike the 5S/C0 mutant, the T362A/C0 mutant is still capable of upholding cell viability indicating that a different mechanism is impaired in the monomer or the dimeric double defective T362A mutant. Wickles et al. (2014) stated that the threonine at position 362 in YidC is one of the most stabilizing residues according to molecular dynamics (MD) simulations of the protein. Mutating it to alanine lead to the defective variant of YidC that was also used in this work. A structural instability was ruled out since this mutant was stably expressed (Wickles et al. 2014). It is debatable if the T362A substitution interferes enough with the general structure of YidC to destabilize the hydrophilic groove or even disrupt the suggested thinning effect of the membrane which could result in the inhibition of membrane protein insertion. However, if this would be the case the effects must be strong enough for these interferences but weak enough to keep the general structure of YidC intact to avoid degradation of the protein. Further experiments are required to get a clearer picture of the effects of this mutation in the structure and function of YidC.

For the 5S mutants the results of substrate insertion are conflicting with the observed inability of complementation (see 4.1.4.2 and Tab. 33). The ability to insert a certain substrate but lacking the capability to uphold cell viability indicates that the conformation must still be intact to the extent that allows insertion of at least some substrates but affects the functionality essential for subsequent cell generations. The insertion of M13 procoat was monitored over only one minute, where the impact of long-term effects cannot be detected. However, these short-time observations only show a short glimpse of the activity of YidC and dYidC molecules that were inserted into the membrane not too long ago. It is very unlikely that a YidC-only substrate is the cause of the abolished cell growth in the 5S/C0 mutant due to the present

insertion capability in both protomers. This leads to the conclusion that an essential interaction, most likely with another associated insertion/translocation machinery, is the cause of the decline in growth overnight. A possible influence on the cell growth is the aforementioned interaction with the Sec translocon, which might be abolished when the 5S mutant is located in the first protomer (see 4.1.4.2). Essential substrates that require both machineries in cooperation for proper insertion would still be present in the cells over a longer period but would dilute and degrade over several generations until cell growth cannot be supported anymore. This would explain the inability to form colonies with the 5S/C0 mutant despite the functional protomer that is present. It is possible that the growth-inhibiting effect of the 5S/C0 mutant already starts to affect the cells when the 5S mutant is expressed but takes a while to influence the proliferation. To confirm that the cooperation with the Sec translocon is the cause of this effect an insertion assay with a substrate that requires both, YidC and the Sec translocon, for insertion could be performed. This assay could demonstrate that the Sec-YidC cooperation is blocked by the 5S mutant and by testing different expression times for YidC, also show when this effect manifests in the cells. The -5 (AEEEGDD) mutant of PClep (Soman et al. 2014) fulfills the necessary requirements regarding the insertion dependency and could serve as substrate. Another possibility would be to crosslink a cysteine mutant of the Sec translocon to cysteine mutants of the 5S and wild type YidC respectively, to observe differences in their crosslinking profiles.

The ΔC1 mutant in the single defective dYidC constructs indicates that one C1 loop is sufficient for protein insertion. For the T362A mutant, which is located in the hydrophilic groove
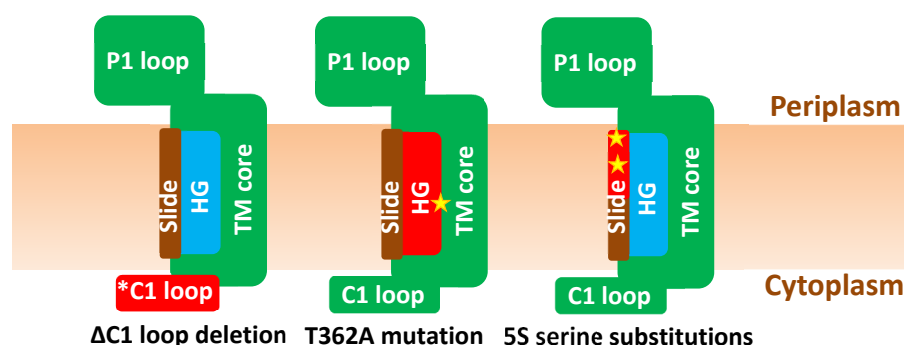
Fig. 90: Location and putative influenced areas of the defective mutations in YidC. The ΔC1 deletion lacks residues 399 to 415 in the C1 loop of YidC whereas the T362A mutant has an alanine in place of a threonine that influences the hydrophilic groove (HG). The serine substitutions of the 5S mutant are located in the center and top of the hydrophobic slide formed by TM3 and TM5 and one single residue in TM4 that is located near the two mutations in TM5. Yellow star/red: influenced/mutated parts of YidC.

(Kumazaki et al. 2014b, see Fig. 90) it can be concluded that one functional groove is also sufficient to facilitate insertion. The results from the complementation and the insertion studies with the dYidC also support these conclusions. One functional protomer is sufficient to allow cell growth and to insert M13 procoat. The 5S mutant and its dYidC constructs were fully functional for M13 procoat insertion. Taken together, the results from the complementation and the binding studies, with the data provided by the ΔC1 and T362A mutants, support the model of YidC as an active monomer.

4.2 Interaction of YidC with its substrate M13 procoat

The insertion mechanism of YidC was analyzed by observing the interaction with M13 procoat using disulfide crosslinking assays. It is proven, that M13 procoat is inserted in a YidC-only manner (Samuelson et al. 2001). However, no interaction sites between M13 procoat and YidC had been previously published. Other substrates, like Pf3 coat, have already been mapped with parts of the insertase (Klenner and Kuhn 2012) but it was also shown, that YidC treats its substrates differently during insertion (Chen et al. 2003).

In the present study, a number of contact sites between M13 procoat and the hydrophobic slide, formed by TM3 and TM5 of YidC, have been found. Different crosslinking methods were used to observe the interaction of the proteins during the insertion process, including the already discussed *in vivo* crosslinking with DTNB. The obtained data and the differences that resulted from the applied methods are discussed here. Furthermore, additional attempts to crosslink M13 procoat to other parts of YidC, like the C1 loop or the hydrophilic groove, are discussed.

4.2.1 Mechanisms of various oxidation mediating agents

Almost all pulse-label crosslinking experiments were performed with copper phenanthroline as a crosslinking agent. However, a few positions were additionally tested with iodine and DTNB.

The chemical mechanisms of the used crosslinking agents are quite different. Iodine acts as an oxidant by forming intermediate products with sulfhydryl groups that, as a result, form a disulfide bond while releasing hydrogen iodide (see Fig. 91) (Fraenkel-Conrat 1955, Danehy et al. 1971). Copper phenanthroline requires the presence of oxygen to be able to constantly catalyze the crosslinking reaction and is not consumed in the process (see Fig. 90) (Kobashi 1968). The general reaction formula for crosslinking with DTNB is also displayed in Fig. 90 and shows the formation of a TNB (2-nitro-5-thiobenzoate) disulfide intermediate that is bound to another thiol group while releasing TNB (Peng et al. 2012, Winther and Thorpe 2014).

Using different crosslinking agents might lead to different interaction profiles of the tested proteins. One problem that can occur is a difference in accessing the cysteines in the target proteins that could result in masking interactions instead of detecting them. Hughson et al. (1997) observed, that treatment of cells with copper phenanthroline or iodine, to map the dimer formation of the Trp chemoreceptor in *E. coli*, generally lead to similar, but not identical, crosslinking profiles. However, this receptor forms a homodimer while the interaction of YidC with M13 procoat is not constant and therefore harder to detect. Checking known contact
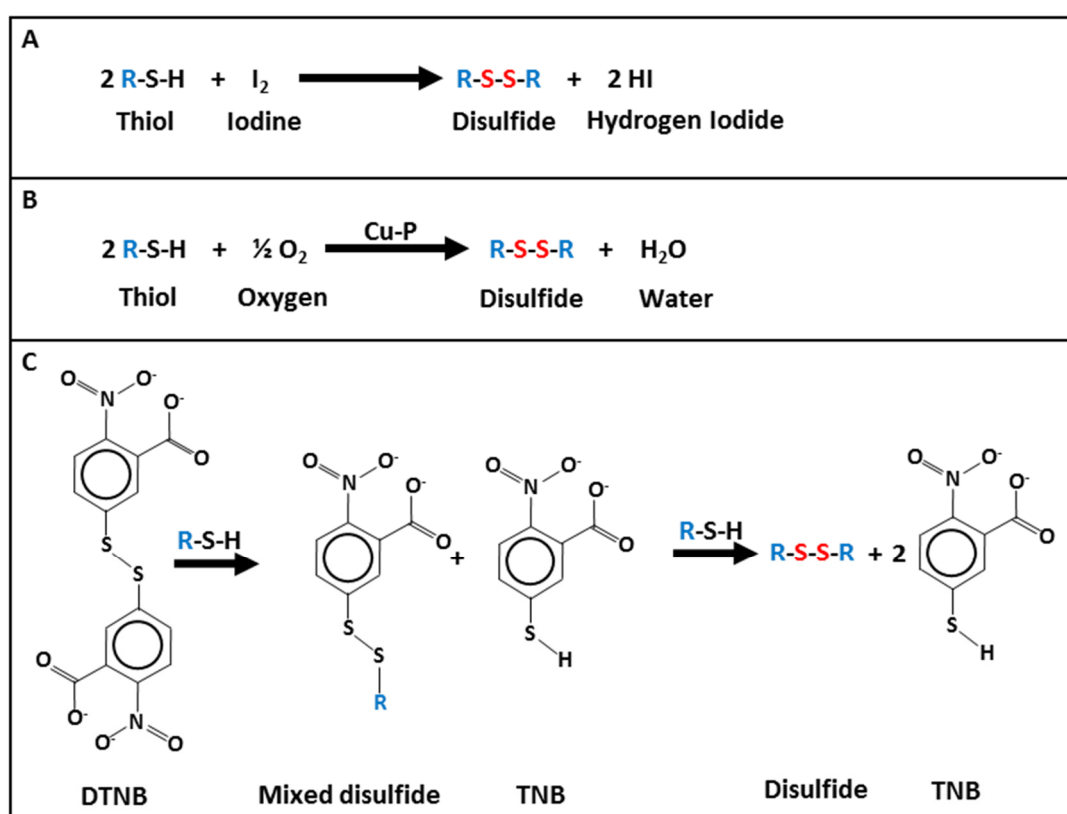
Fig. 91: Reaction formulas of the used crosslinking agents. (A) Crosslinking reaction with iodine. **(B)** Crosslinking with copper phenanthroline as a catalyst for the formation of the disulfide. **(C)** General crosslinking reaction with DTNB. Cu-P: copper phenanthroline, red: formed disulfide, blue: organic group (Fraenkel-Conrat 1955, Danehy et al. 1971, Kobashi 1968, Peng et al. 2012, Winther and Thorpe 2014)

sites with different crosslinking agents and scanning unknown or so far negative sites could provide further data to determine the surrounding conditions for the interactions of YidC with its substrates. Using crosslinking agents with different properties might also allow crosslinking of regions of YidC where copper phenanthroline might not useful due to its oxidizing properties to form disulfide bonds, like the hydrophilic cavity for example.

4.2.2 M13 procoat contacts TM3 and TM5 of YidC extensively during insertion

The discovered contact sites from the radio-active crosslinking experiments with copper phenanthroline are dis-cussed here. The results strongly indicate the important role of TM3 and TM5 for the insertion of M13 procoat. It should be noted, that not all possible combinations have been tested so far (see Tab. 35 and 36).

Tab. 35: Overview of the crosslinking experiments with M13 procoat and TM1/TM3 of YidC. Crosslinking experiments conducted with radioactive pulse-labeling. Columns: YidC cysteine mutants. Rows: H5 procoat cysteine mutants. ++ strong signal, + weak signal, - no signal

	M18C	F424C	P425C	L427C	I428C	Q429C	M430C
H5 A-12C		++		++			+
H5 A-10C		+		+			+
H5 T-9C							
H5 Y24C				+			
H5 V29C		+		++	-	-	-
H5 V30C	++	-	-	++			+
H5 V31C				-			-
H5 I32C		-	-	+	-	-	-
H5 V33C		++		++			+
H5 G34C				++	+		-
H5 A35C				++	++	+	-

The most prominent contact sites in TM3 that were detected via the pulse-labeling method are positions 424 and 427 followed by 430 and 428. The helix projection of TM3 (see Fig. 92) shows, that the strongest signals are located on one side of the TM3 helix. The contact sites are spread over half of one side of the helix with the strongest contacts in the center of the lipid bilayer, which indicates lower affinity to M13 procoat towards residues 428 and 430 but also a flexibility in this region of TM3 during the insertion process. Interestingly, in the published structure (Kumazaki et al. 2014b) the strongest interactions in TM3, position 424 and 427, are facing out toward the cytoplasmic lipid leaflet of the membrane. This indicates that TM3 has to adjust its conformation and rotate itself. This could be promoted by the contact with the M13 procoat protein, which might initiate these changes.

Another interesting observation is the broad range of M13 procoat cysteine mutants that contact residues 424 and 427 in YidC. The L427C mutant is particularly interesting since it

contacts almost all tested M13 procoat cysteine mutants. The positions of the cysteines in M13 procoat range from the center of TM1 (A-12C and A-10C) to a big range in TM2 from the top near the periplasm (Y24C) to the bottom near the cytoplasm (A35C). The only tested

Tab. 36: Overview of the crosslinking experiments with M13 procoat and TM5 of YidC. Crosslinking experiments conducted with radioactive pulse-labeling. Columns: YidC cysteine mutants. Rows: H5 procoat cysteine mutants. ++ strong signal, + weak signal, - no signal

	I501C	F502C	T503C	V504C	F505C	L507C	W508C	F509C
H5 A-12C		+		+	+	+		
H5 A-10C		-		++	+	++		-
H5 T-9C				++	++			
H5 Y24C		-		+	-	-	+	+
H5 V29C								
H5 V30C	++	-	-	++	+	++		
H5 V31C		++	+	++	+	++		
H5 I32C		-		-	+			
H5 V33C		-		-	+			
H5 G34C		-		-				
H5 A35C		-		-				

mutant without a detectable crosslinking signal was H5 M13 procoat V31C in the center of TM2. This broad contact range suggests that the substrate slides along this residue during insertion, allowing interaction with a number of residues within TM3 of YidC. In TM5, the signals were less prominent and a lot more diverse around the helix (see Fig. 92). The strongest signals were found fo r position 502, 504, 505, and 507. According to the structure (Kumazaki

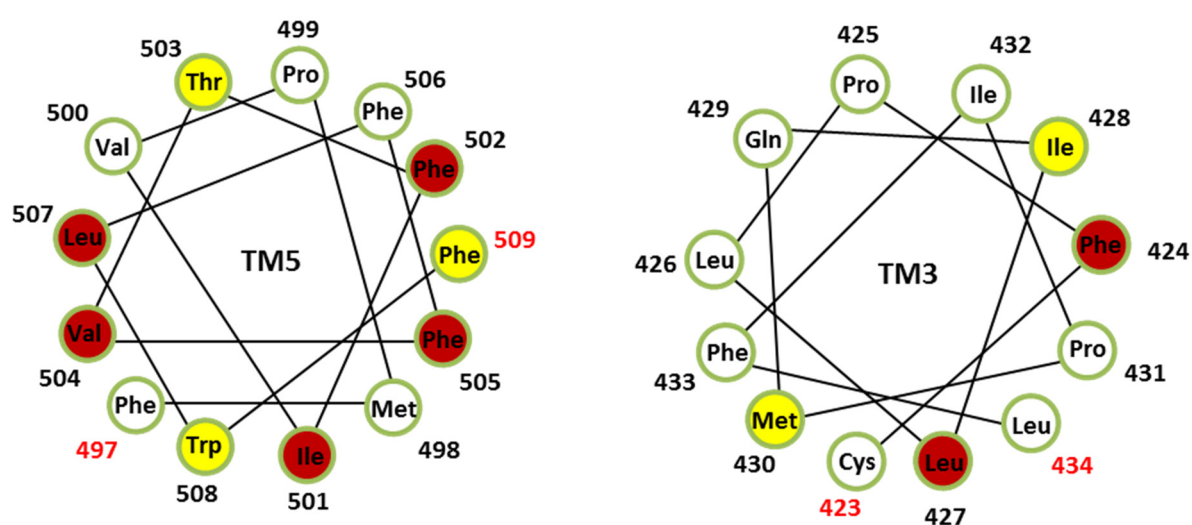**Fig. 92: Helix projections of TM3 and TM5 of YidC.** The projections does not represent an ideal helix and the positions of the residues are taken from the structure of YidC resembling their respective positions. Residues that were contacted by M13 procoat with the pulse labeling approach are marked. Yellow: weak contact, dark red: strong contact, red numbers: start and end residue of the projected helices.

et al. 2014b) the residues 502 and 505 are facing directly into the hydrophobic slide that is formed by TM3 and TM5 (see Fig. 92 and 93) but residue 507 is facing outward into the TM core of YidC. From the weaker contacts, 503 and 508 are also facing out of the gate. Residue 509 is oriented directly into the gate, although at the periplasmic side.

It has been shown that YidC goes through conformational changes in its TM region and P1 domain when a substrate, e.g. Pf3 coat, binds (Winterfeld et al. 2009, Imhof et al. 2011). Kedrov et al. (2016) recently published a model of a bound RNC to YidC based on cryo-EM data. Here, the first TM and the first loop of subunit c

Fig. 93: Top view into the YidC TMs with the marked contact sites in TM3 and TM5. The orientation of the residues in the TMs indicate, that during insertion a degree of flexibility must be present to allow all these contacts. Red: TM3 of YidC, orange: TM5 of YidC, variously colored amino acids: contact sites of M13 procoat. Figure of the gate of YidC created with PDB entry 3WVF in PyMol 1.3. (according to: Kumazaki et al. 2014b)

of the F_1F_o ATPase was exposed as nascent chain. After binding to YidC a conformational change occurred inside the insertase that led to a tilt of TM2 and TM3 and movement of the amphipathic helix EH1, then the nascent chain was found between TM3 and TM5. This model shows the flexibility of TM3 in YidC during insertion and supports the results found here with contact sites spread around the TMs. However, M13 procoat inserts posttranslationally and the mechanism might differ significantly from a cotranslational insertion, where the ribosome directly interacts with YidC. Still, these or similar conformational changes can also be assumed for the insertion of M13 procoat and would explain the contacts with residues that would otherwise not be accessible according to the structure (Kumazaki et al. 2014b, Fig. 93). The contact sites in TM3 can be considered as early interactions with the substrate during insertion compared to those found in TM5 since they are positioned further towards the cytoplasmic side of the membrane. The weaker signals for TM5 could also indicate that due to the insertion being a dynamic and fast process (Winterfeld et al. 2013) the interaction of later stages might not be detectable as efficient as in the beginning.

Interestingly, a very broad range of M13 procoat cysteine mutants also contacts residue 504 of YidC. Unlike the L427C mutant, V504C does not show interaction with residues 33 to 35 of
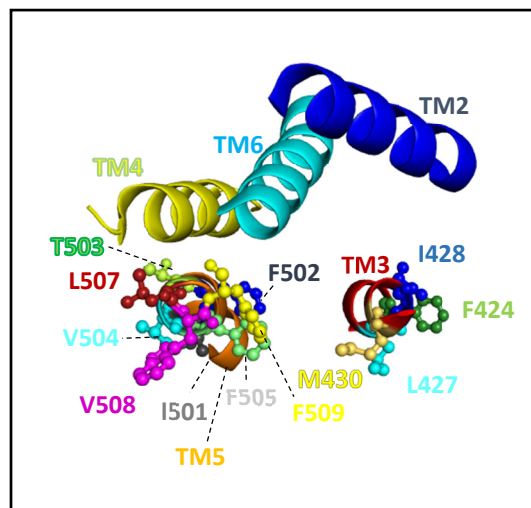
M13 procoat. In the hydrophobic slide formed by TM3 and TM5, residue 504 is positioned closer to the periplasm while 427 is close to the cytoplasm. Both residues are therefore at different "heights" in the hydrophobic slide and the lower positioned L427 near the cytoplasm can contact more residues of M13 procoat during insertion. Residue 502 of YidC shows similar behavior in this regard by also not contacting residues 32 to 35 in the cytoplasmic leaflet region of M13 procoat. This would support the model of "sliding" along the hydrophobic slide of YidC during insertion until the loop of M13 procoat can leave the hydrophilic groove. This would not require the TM regions near the cytoplasm of M13 procoat to contact the periplasmic positioned parts of the gate.

Residue 505 of YidC contacts position 33 in M13 procoat despite being positioned more towards the periplasm than residue 504 in the hydrophobic slide. However, current data for this mutant are not available to the same extend as it is for residue 504 of YidC. Further experiments are needed to fill still existing gaps in order to get a better overall picture.

Contact sites discovered with iodine and DTNB

During the crosslinking studies a variety of crosslinking agents, aside from copper phenanthroline, was tested for their capability to crosslink YidC to M13 procoat (see 4.2.1). Most of them were also used in crosslinking attempts in the hydrophilic groove or to the C1 loop of YidC. In TM3 and TM5 only a small amount of positions was tested however, which led to the detection of five contact sites. An overview is presented and discussed here (see Tab. 37).

Tab. 37:.Overview of the crosslinking experiments with different crosslinking agents. The table shows the contacts that were detectable with different crosslinking agents aside of copper phenanthroline. Columns: YidC cysteine mutants. Rows: H5 procoat cysteine mutants, Cu-P: copper phenanthroline, DTNB: Bis(3-carboxy-4-nitrophenyl) disulfide/Ellman's reagent.

	F424C	L427C	W508C	F509C
Y24C		DTNB	Iodine	Iodine
V33C	Iodine/DNTB	Iodine		

These crosslinking agents were tested with pulse-label experiments and their respective mechanisms have already been reviewed in 4.2.1. Iodine was effective in crosslinking positions 424 and 427 in TM3 and positions 508 and 509 in TM5 of YidC. DTNB crosslinked positions 424 and 427 in YidC with the latter showing a rather weak signal.

The reaction times for the used crosslinking agents was 30 seconds for iodine and 10 minutes for DTNB and copper phenanthroline respectively. The iodine approach creates crosslinking signals during a much shorter time window and does not influence the cell growth too much (see 3.1.1). DTNB does not disturb cell growth as well (see 3.1.1) but the reaction takes a much longer time to form the protein-protein complexes. Copper phenanthroline almost immediately stops cell growth when added to the culture (see 3.1.1) and the long oxidation time together with the disrupted cells could lead to different results if compared to other crosslinking agents. Iodine could be a good candidate for additional testing of YidC-substrate interactions in the future. DTNB was already used in this study for complex purification and analysis (see 4.1.2) and for crosslinking studies via Western blot detection (see 4.2.8) with promising results.

4.2.3 YidC interactions with different substrates

Contact sites for two other YidC substrates have been reported in the past. Pf3 coat (Klenner et al. 2008) and MscL (Neugebauer et al. 2012) have been crosslinked to YidC. Some of the reported contact sites are shared with those discovered in this work.

Klenner & Kuhn (2012) used three different cysteine mutants of Pf3 coat to map YidC for contact sites via *in vivo* crosslinking. These cysteines are positioned near the cytoplasm (V33C), in the center of the TM (V28C) or near the periplasm (G24C) of the inner cell membrane (see Fig. 94). However, Klenner et al. (2008) crosslinked Pf3 coat and YidC only with cysteines placed in similar regions of both proteins. Therefore, no data exists of possible contact sites between residues of YidC and Pf3 coat that are located in different membrane regions in their post-insertion conformations. Therefore, the current insertion model of the substrate "sliding" along the hydrophobic slide during insertion is not conclusive by the available data for Pf3 coat. Testing these different combinations could support the data found for M13 procoat. This would also support the current insertion model (Kumazaki et al. 2014a) for the YidC-only insertion in bacterial cells. The confirmed contact sites in TM3 (424, 427, 430) and TM5 (502, 505, 508) of YidC are consistent with those found for M13 procoat. This indicates similarities in the insertion process of both substrates albeit their differences in size and topology.

Neugebauer et al. (2012) detected contacts with all three used cysteine mutants (I32C, V77C, F85C) of MscL (see Fig. 94). All of them contacted YidC at residue 17, 430 and 505. Consistent with the here reported data the cysteine mutants in the middle of the TMs of MscL were capable to contact YidC near the periplasmic leaflet at position 505. However, further crosslinking experiments are needed for MscL and YidC to get a better overview and to compare it thoroughly to M13 procoat protein. Even though the wild type of MscL is inserted in a strictly YidC dependent manner it was shown that it also contacts SecY to some extent.

However, procoat mutants with additional negative charges in the periplasmic loop became SecYE and YidC dependent for insertion. It has been shown in the past that YidC and SecY are often associated with each other (Scotti et al. 2000) and newer data suggests a very close binding of YidC to the Sec translocon (Sachelaru et al. 2017), where the presence of YidC influences the structure of the pore of the SecY channel. This close proximity could also explain the association of wild type MscL to SecY although its Sec independence.
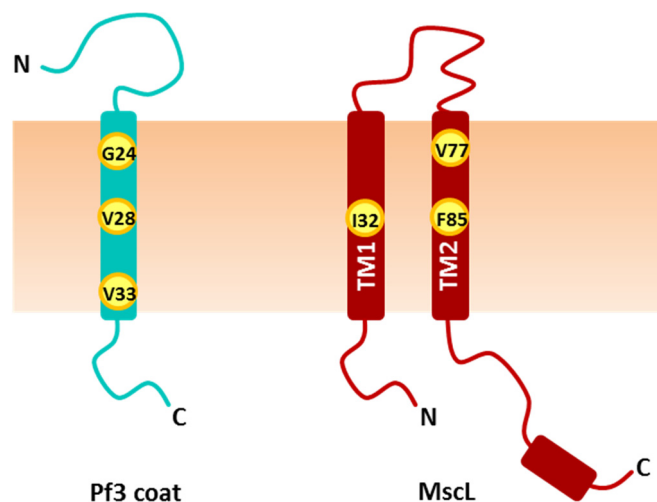
Fig. 94: Utilized cysteine mutants in Pf3 coat and MscL for crosslinking with YidC by Klenner and Kuhn (2012) and Neugebauer et al. (2012) respectively. In Pf3 the picked residues were located near the periplasm in the center of the TM and near the cytoplasm of the cell. For MscL three cysteine mutants were used as well. One in the center of the first TM and two in the second TM, one in the center and one near the periplasm. N: N-terminus, C: C-terminus, teal: Pf3 coat, dark red: MscL

4.2.4 The C1 loop of YidC interacts with M13 procoat

Though only one weak contact was found with residues of the C1 domain, it could well be that M13 procoat contacts the C1 loop of YidC. The chosen residues for cysteine substitution were picked in regards of the published structure (Kumazaki et al. 2014b). These positions all faced towards the surface of the inner membrane (see 3.1.2.2) and seemed to be the best choice for the proposed insertion mechanism where the substrate uses the C1 loop as a platform to "slide" into the YidC (Kumazaki et al. 2014a). However, the C1 region is also very flexible

(Kumazaki et al. 2014b) and the so far tested residues might not be always facing towards the substrate during insertion. The range of flexibility and mobility of different parts of YidC is not completely known yet and the structure shows one of many possible conformations. The structure of a complex with bound substrate has yet to be structurally solved. Utilizing a wider range of cysteine mutants could help stabilizing the contact between YidC and M13 procoat and could then subsequently be used with other substrates for comparison.

Since the insertion is a very fast process (Winterfeld et al. 2013) the time for interacting with the C1 loop could be too short to properly crosslink it to the substrate. A possible attempt could be to use a substrate that contacts YidC but is not inserted, giving it more time near the C1 loop to be crosslinked. Klenner and Kuhn (2012) showed in pulse-experiments, that insertion-deficient Pf3 coat proteins can still contact YidC in the cytoplasmic leaflet in TM3 of YidC. Two arginines were mutated into the N-terminus of Pf3 coat, called Pf3-RR. This mutant was still capable to contact the residues 424 and 427 in TM3 of YidC but not the residues 430 in the membrane core and 435 and 505 in the periplasmic leaflet. For Pf3 coat the additional positive charge in the N-terminus inhibited the insertion and therefore the possibility to contact YidC in the periplasmic leaflet (Kiefer et al. 1997, Klenner and Kuhn 2012). Using this or a similar arrested substrate could help mapping the C1 loop for contact sites.

The C1 loop also played a role in other parts of this study (see 4.1.4). Analyzing its importance for the insertion of M13 procoat is crucial to understand the mechanism. The ΔC1 defective mutant was therefore used for crosslinking experiments with M13 procoat.

4.2.5 Defective ΔC1 YidC can bind M13 procoat in the cytoplasmic leaflet of the membrane

The ΔC1 mutant of YidC, where residues 399 to 415 are deleted, has a truncated C1 loop that prevents proper substrate insertion (see 4.1.4). Interestingly, it was possible to crosslink the V33C mutant of M13 procoat to the ΔC1 defective mutant of YidC at position 427 in the cytoplasmic leaflet of the membrane (see 3.2.4). Complementation and insertion studies (see 4.1.4) showed that the ΔC1 mutant of YidC could neither uphold cell viability nor insert M13 procoat into the inner membrane. This indicates that the C1 loop of YidC is not essential for the initial binding of its substrate but plays an important role during later steps of the insertion. Interestingly, the aforementioned (see 4.2.4) arginine mutants of Pf3 coat show a

similar behavior. The difference is that in this study YidC was mutated/truncated whereas Klenner and Kuhn (2012) substituted residues in the substrate. In both cases, the substrates contact YidC but are not inserted. However, further crosslinking should be performed with cysteine mutants of YidC, which are located in the center of the membrane and towards the periplasm to see how far M13 procoat is reaching into the membrane and the ΔC1 insertase.

4.2.6 Crosslinking attempts inside the hydrophilic groove of YidC

In the performed crosslinking experiments of M13 procoat with the YidC hydrophilic groove the chosen procoat mutants were not crosslinked to the cysteine mutants in the groove of YidC. There are several possibilities why no interaction was observed. The first is that the loop of M13 procoat is not capable of entering the groove deep enough, or that the used crosslinking agent may not enter the groove. The structure of the coat protein could play a role since the loop might not be flexible enough to enter the cavity. Other substrates of YidC that only have one TM, like the Pf3 coat protein, may be more useful in this case. Elongating the loop of M13 procoat could also lead to crosslinking products. A longer more flexible loop might be able to enter the groove more easily. This, however, would generate results with an artificially constructed protein and not with a natural substrate of the insertase.

Another possibility is that substrates do not enter the groove deep enough or at all. Kumazaki et al. (2014a) stated that the hydrophilic groove is constantly filled with approx. 20 water
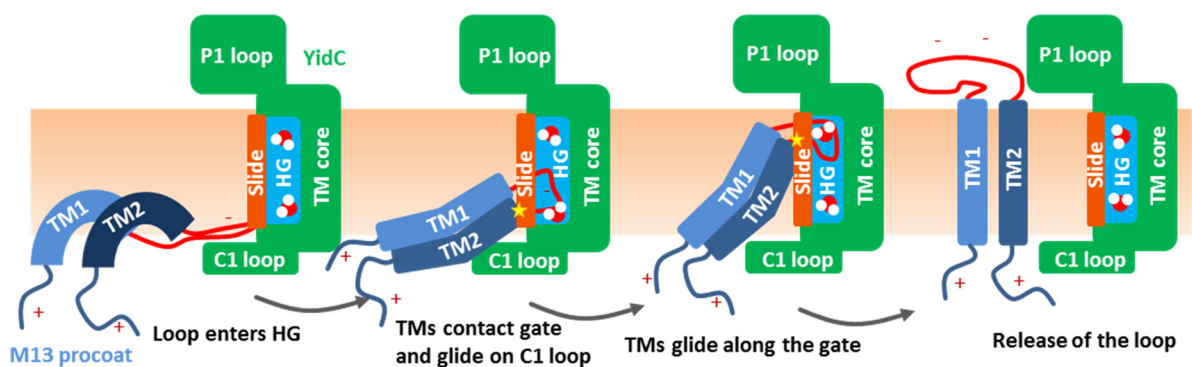
Fig. 95: Model of the insertion of M13 procoat. In this model, the idea of an insertion mechanism without direct contact to the inner side of the hydrophilic groove (HG) is proposed. The water molecules (red dot with two white dots) provide the necessary hydrophilic environment for the passage of the charged loop. When the loop of M13 procoat enters the HG through the hydrophobic slide (formed by TM3 and TM5 of YidC) the TMs glide along the C1 loop before they reach the gate as well. While the loop is in the groove, the TMs contact the gate and glide along it until the loop is released and the insertion is completed. TM core: Core region of YidC formed by the five TMs. + and - : charges of the terminal and loop domains of M13 procoat. Stars: Contacts between YidC and M13 procoat.

molecules. It is debatable if the substrate enters the groove, pushing out the water to interact with YidC directly or if the water itself provides the necessary environment. Either possibility allows the hydrophilic part of M13 procoat to go through the membrane. If the latter would be the case, the substrate would not have the need to contact the inside of YidC rather than make use of the water molecules in the groove. The groove itself would only have the function to hold the water molecules and would not be directly involved in the insertion process (see Fig. 95). This model would only apply to the tested M13 procoat for now, other substrates with different structures might be treated differently by YidC. The N-terminal domain of the single spanning Pf3 coat protein for example could directly interact with YidC since it might be more flexible inside the groove while having approx. the same length as the loop of M13 procoat (Thiaudère et al. 1993, Klenner and Kuhn 2012).

Since the groove is open to the cytoplasm (Shimokawa-Chiba et al. 2015) the inside should be a rather reductive environment similar to the cytosol. This would increase the threshold of oxidant that is needed to successfully crosslink inside YidC. The tested crosslinking agents are, compared to the present water molecules in the groove, relatively large in size. Entering the groove could therefore be difficult since the agent would have to replace several water molecules. If it can enter, the environment inside would change because normally present water would have been replaced. This might influence the insertion process in different ways and impair normally occurring contacts.

Kumazaki et al. (2014a) suspected the conserved arginine (R366 in the *E. coli* YidC) inside the hydrophilic groove to play an important role in the insertion process. Some single-spanning substrates like Pf3 or MifM have acidic residues in their amino-terminal domains that might contact the positively charged arginine during insertion. Removing these charged residues had a negative effect on the insertion efficiency of *B. halodurans* YidC (Kumazaki et al. 2014a) but not of *E. coli* YidC (Chen et al. 2014)

It was shown that MifM directly interacts with the hydrophilic groove of the *B. halodurans* YidC. This was done by substituting several amino acids that are facing into and outside the hydrophilic groove of YidC with the photo-crosslinker p-benzoyl-L-phenylalanine (pBpA). Upon UV-irradiation, a covalent bond is formed with close biomolecules resulting in a site-unspecific binding to potential substrates. It was found that the tested positions that are inside the hydrophilic groove crosslinked to MifM. Therefore, it was concluded that the hydrophilic

groove and the region around the arginine plays an important role during the insertion process in *B. halodurans* YidC (Kumazaki et al. 2014a).

The provided data in this work did not yield any crosslinking signals between residues in the hydrophilic groove of the *E. coli* YidC and its substrate M13 procoat. A number of residues in YidC that are facing inside the groove, including the conserved arginine at position 366, were substituted with cysteines and tested with two different crosslinking agents. Chen et al. (2014) reported that, unlike the arginine in the *B. halodurans* YidC, the arginine in the *E. coli* YidC is not essential for its function and can be substituted with other amino acids, including cysteine. However, the crosslinking method used here is different from the one used by Kumazaki et al. (2014a) which aimed to see interaction without providing the exact position in the substrate that is bound in the crosslinking reaction. The picked positions for the cysteine substitutions might have masked a possible interaction. On the other hand, picking positions near and in the charged loop of M13 procoat was the logic step for the crosslinking experiments. Chen et al. (2014) also demonstrated that the negative charge at the amino-terminus of the substrate Pf3-23Lep does not play a role for the insertion in *E. coli*, which is consistent with the role of 366R in *E. coli* YidC in the hydrophilic groove to function. Putting positive charged residues in the amino-terminus however inhibited insertion of Pf3 coat with the *E. coli* YidC as previously demonstrated (Kiefer et al. 1997, Klenner and Kuhn 2012). Together with our results here, another possibility for the missing interaction between the hydrophilic groove and M13 procoat is that the hydrophilic groove might interact in a different way with the substrates during the insertion process in *E. coli* compared to *B. halodurans*. During insertion, M13 procoat most likely forms a hairpin like structure that allows the simultaneous insertion of both TMs (Engelman and Steitz 1981, Kuhn 1987) with YidC. This would lead to the conclusion, that the insertion of M13 procoat can be facilitated either by the proposed model (see Fig. 95), or by a mechanism where the hydrophilic groove only plays a minor role or is not needed at all and that the hydrophobic slide suffices, at least for the tested substrates. Another possibility is that the loop itself, due to the insertion being a fast process (Winterfeld et al. 2013), might not be present long enough in the hydrophilic groove for a disulfide-bond to form.

4.2.8 Mapping of YidC-substrate interactions with the Western blot approach compared to the pulse-labeling experiments

There are some differences between the results obtained via pulse labeled crosslinking and the Western blot approach with DTNB (see 4.2.2 and Tab. 38), which are worth discussing. In a pulse, the contacts are followed during the synthesis of the proteins whereas the immunochemical Western blot shows long-lived contacts in the hour-range. Unlike in the pulse experiments, it was not possible to crosslink M13 procoat to TM5 of YidC with DTNB. The chosen mutants in TM5 of YidC are closer to the periplasmic surface of the membrane than the ones picked in TM3. It was shown that hydrophilic part of the groove is only accessible from the cytoplasm (Shimokawa-Chiba et al. 2015), which might indicate that DTNB is not able to access the parts of the gate that are close to the periplasm. This can have different reasons although the mechanism of *in vivo* crosslinking in bacterial cells with DTNB is not yet determined. As of now, it can only be speculated, why these contacts cannot be seen with this method.

Tab. 38:.Overview of the crosslinking experiments with M13 procoat and TM3/TM5 of YidC. Crosslinking with DTNB and detection via PAGE and immunodetection with anti-His antibody. Columns: YidC cysteine mutants. Rows: H5 procoat cysteine mutants. ++ strong signal, + weak signal, - no signal

	423C	F424C	P425C	L427C	I428C	Q429C	M430C	F502C	V504C	F505C	L507C
H5 A-12C	++	++	-	++	+	-	++	-	-	-	-
H5 A-10C		-		++			++	-	-	-	-
H5 Y24C		-		-				-	-		
H5 V30C		-		-			++	-	-		
H5 V31C		-	-	-	-	-	+	-	-		
H5 I32C		-	-	++	-	-	+	-	-		
H5 V33C		++		++			+	-	-		
H5 G34C		-		-			+	-	-		
H5 A35C		-		-			+	-	-		

Wickles et al. (2014) attempted *in vitro* crosslinking with DTNB of ribosomal nascent chains (RNCs) of subunit c of the F_1F_o ATPase to YidC but only succeeded with TM3 at position 430 and 431. The tested residues 500 and 503 showed no signal. This is consistent with our *in vivo* data for residues 502, 504, 505 and 507 with M13 procoat, where no crosslinking products were detected. However, position 505 and 507 were only tested with TM1 of M13 procoat, TM2 of M13 procoat might show different behavior, though this is unlikely since residues 505 and 507 in YidC are even closer towards the periplasm of the cell. This strongly indicates that

the contacts between M13 procoat and the periplasmic regions of TM5 of YidC are either too fast for DTNB to facilitate the disulfide formation or that they cannot be formed in this region of YidC with this method.

Hennon and Dalbey (2014) performed crosslinking experiments with double cysteine mutants of YidC to map the flexibility and proximity of the TMs of the protease to each other. Depending on which region inside YidC was crosslinked different crosslinking agents were used. Interestingly, the used polar reagents N,N'-p-Phenylenedimaleimide (p-PDM) and N,N'-o-phenylenedimaleimide (o-PDM) were not able to efficiently crosslink inside the membrane core but facilitated the reaction in the aqueous environment at the membrane border in the cytoplasm (Hennon and Dalbey 2014). DTNB is also a polar reagent and might have similar difficulties to access YidC deep enough from the cytoplasm to reach the periplasmic regions. This indicates that there is a limit on how deep inside YidC DTNB can have an effect, most likely due to a lack of accessibility. The results from Wickles et al. (2014) are consistent with our results regarding the reactivity of DTNB in YidC in substrate crosslinking. Interestingly, copper phenanthroline and iodine had formed crosslinking products in the periplasmic part of the hydrophobic slide during the pulse experiments (see 4.2.2). In the aforementioned study from Wickles et al. (2014) the oxidation time of DTNB was also 10 min long, similar to the experiments performed here with copper phenanthroline. This indicates that the longer oxidation and growth time is not what causes the lack of signals in this region of YidC. DTNB should, however, also be further tested in the *in vivo* pulse experiments for a conclusive comparison.

In the performed experiments, the formation of the desired crosslinking products required a relatively long period of time compared to the established pulse-label crosslinking approach. The possibility of less specific crosslinking due to the longer time could occur in the cells, contacts that might not be obtained with the other method. This, however, was not confirmed and crosslinks discovered by pulse-label crosslinking was not always reproduced with DTNB. On the other hand, the signals obtained via DTNB were always clear and reproducible making this method more precise albeit most likely not as sensitive. The so far established protocols should still be improved to compensate for the lack of sensitivity in the future.

Compared to the observed signals in the pulse-labeling experiments the signals in the *in vivo* approach were generally clearer and easier to evaluate. The strongest signals were detected

for the M430C mutant followed by L427C, F424C and the YidC wild type. Weaker contacts were found for I428C. This shifts the main contact site to a more narrow region of the helix towards the center of the bilayer, compared to the pulse-labeling experiments (see Fig. 96 versus Fig. 92).

The M430C mutant contacts all tested M13 procoat mutants with the strongest signals in the center of TM1 (A-12C and A-10C) and the center of TM2 down to the cytoplasmic side, with the signal strength becoming weaker (see Tab. 38). Residue 427 in YidC contacts the centers of TM1 and TM2 of M13 procoat. These results are quite different from the pulse-labeling experiments with other crosslinking agents, where residue 427 showed the strongest and diverse contacts to M13 procoat while M430C showed less signals. For the 423C mutant only one very strong contact has been determined so far in TM1 (A-12C). Some of these contacts are in accordance with the data published by Klenner and Kuhn (2012) for Pf3 coat and Neugebauer et al. (2012) for MscL (see 4.2.3).

Fig. 96: Helix projection of TM3 of YidC for the DTNB crosslinking approach. The projection does not represent an ideal helix and the positions of the residues are taken from the crystal structure of YidC resembling their respective positions. The residues that crosslinked to M13 procoat with DTNB and detected via immunoblotting are marked. Dark red: strong contact sites, yellow: weak contact site, red numbers: start and end residue of the helix.

Despite the differences in the results of both methods, the residues that are generally contacted by M13 procoat are quite consistent. TM3 plays a central role in the early interaction of YidC with its substrates, which is even contacted in the insertion-deficient ΔC1 YidC mutant (see 4.2.5). As of now, this method is only able to map contacts between YidC and M13 procoat in the membrane core and the cytoplasmic leaflet. This narrows down the possibilities to use DTNB for this purpose. However, the formation of the YidC-substrate complex is reproducible and can be used for other experiments than mapping protein-protein interactions (see 4.1.2 and 4.1.3). This should allow structural analysis of the YidC-M13 procoat complex in the future and the method itself might be applicable to other substrate proteins as well.
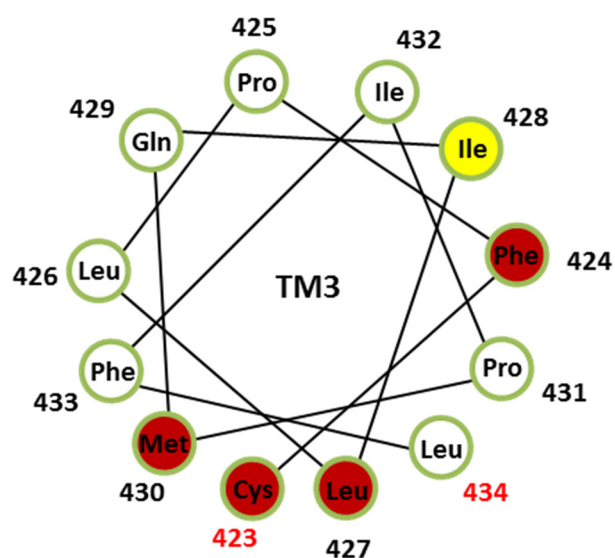
5 SUMMARY

The YidC/Oxa1/Alb3 family consists of insertase homologues that facilitate the insertion and folding of membrane proteins. YidC is located in the inner membrane of bacterial cells. Oxa1 is found in the inner membrane of mitochondria and Alb3 facilitates the insertion of membrane proteins in the thylakoid membranes of chloroplasts (Wang and Dalbey 2011, Hennon et al. 2015). An archaeal homologue was found in *M. jannaschii* showing that this insertase family is present in all domains of life (Dalbey and Kuhn 2015). The insertase family shares a structural feature that is conserved among all discovered members. This is a hydrophilic groove that is open towards the cytoplasm and the membrane core with a hydrophobic slide formed by transmembrane domain (TM) 3 and TM5. YidC functions on its own but also cooperates with the Sec translocon to facilitate the insertion of large membrane proteins. One protein that is membrane-inserted by YidC but is Sec-independent is the major coat protein of the M13 bacteriophage.

The main objectives of this work are the analysis of the insertion mechanism of M13 procoat, the major capsid protein of the M13 bacteriophage, via the YidC-only pathway and the oligomeric state of the active YidC.

The analysis of interactions between YidC and M13 procoat was performed via radioactive disulfide crosslinking mainly using copper phenanthroline as oxidizing agent. M13 procoat contacts YidC extensively in TM3 and TM5. The observed contacts suggest that the M13 procoat substrate "slides" along TM3 and TM5 of the insertase. Additional crosslinking experiments with the hydrophilic groove and the C1 loop of YidC were also performed to test their importance during the insertion process. A contact was found in the C1 loop that indicates a role in the insertion process, which is consistent with the proposed insertion model from Kumazaki et al. (2014a).

Parallel to the radioactive disulfide crosslinking, a protocol using DTNB (Bis(3-carboxy-4-nitrophenyl) disulfide, Ellman's reagent) as the oxidizing reagent and Western blot for detection was established. This method reliably promoted the formation of crosslinking products *in vivo* between YidC and M13 procoat over several hours and many, but not all, mapped at the same sites as in the radioactive approach. In addition, this protocol was used

to purify small amounts of a YidC-substrate complex for biochemical analysis, which could also be applied to other substrates in the future.

The oligomeric state of YidC was investigated by an artificial dimer of the insertase (dYidC) that was constructed by connecting two monomers together with a short linker. This dimer can complement YidC-depleted *E. coli* MK6S cells and facilitates the insertion of M13 procoat *in vivo*. For further analysis of the dYidC three functionally defective YidC mutants, T362A (Wickles et al. 2014), ΔC1 (Chen et al. 2014) and the 5S YidC mutant, were tested for their complementation and insertion capability. All three mutants were not able to complement under YidC depletion conditions. These mutants were then cloned in either one or both protomers of the dYidC. Complementation and insertion assays with these dYidC constructs show that in general one active protomer suffices to uphold cell viability and to facilitate the insertion of M13 procoat. Binding studies using cysteine mutants of the dYidC and M13 procoat for disulfide crosslinking with DTNB demonstrated that each protomer individually binds one substrate molecule. In summary, these experiments strongly support a monomer as the active state of the insertase for YidC-only substrates.

Taken together, this study contributes to the understanding of the insertion of proteins into the inner bacterial cell membrane.

Zusammenfassung

Die YidC/Oxa1/Alb3 Proteinfamilie besteht aus Insertase-Homologen, die die Insertion und Faltung von Membranproteinen vermittelt. YidC ist dabei in der inneren Zellmembran von Bakterien lokalisiert. Oxa1 befindet sich in der inneren Membran von Mitochondrien und Alb3 vermittelt die Insertion von Membranproteinen in der Thylakoidmembran von Chloroplasten (Wang und Dalbey 2011, Hennon et al. 2015). Ein weiteres Homolog wurde im Archaeum *M. jannaschii* gefunden wodurch gezeigt werden konnte, dass diese Insertasefamilie in allen Domänen des Lebens konserviert ist (Dalbey und Kuhn 2015). Alle Homologe besitzen eine hydrophile Kavität als gemeinsames Strukturmerkmal. Diese Kavität ist zum Zytoplasma und zum hydrophoben Membrankern geöffnet und besitzt eine hydrophobe „Rutsche" die von den Transmembrandomänen 3 und 5 gebildet wird. YidC ist in der Lage alleine kleine Proteine zu inserieren kann aber auch mit dem Sec Translokon zusammenarbeiten um die Insertion von großen Membranproteinen zu ermöglichen. Das Haupthüllprotein des M13 Bakteriophagen ist wiederum ein Substrat, das von YidC allein inseriert wird.

Ziele dieser Arbeit sind die Untersuchung des Insertionsmechanismus von M13 Procoat, dem Haupthüllprotein des M13 Bakteriophagen, sowie des oligomeren Zustands des aktiven YidCs.

Um die Interaktion zwischen YidC und M13 Procoat zu untersuchen wurden Disulfid-Crosslinkingexperimente mit radioaktiver Markierung der Proteine durchgeführt. Dabei kam fast ausschließlich Kupferphenanthrolin als Oxidationsmittel zum Einsatz. Es konnte gezeigt werden, dass M13 Procoat dabei sehr häufig mit den Transmembrandomänen 3 und 5 von YidC in Kontakt kommt. Die beobachteten Kontaktprofile deuten dabei auf ein „Gleiten" von M13 Procoat entlang der hydrophoben „Rutsche" in YidC hin. Zusätzlich durchgeführte Crosslinkingexperimente wurden in der hydrophilen Kavität und mit der C1 Schlaufe von YidC durchgeführt. Ein gefundener Kontakt auf der C1 Schlaufe zeigt, dass diese eine Rolle im Insertionsprozess spielt, was wiederum mit einem vorgeschlagenen Insertionsmodell von Kumazaki et al. (2014a) konsistent ist.

Parallel zu den radioaktiven Crosslinkingexperimenten wurde ein neues Protokoll etabliert bei dem DTNB 5,5'-Dithiobis(2-nitrobenzoesäure) als oxidierendes Reagenz zum Einsatz kommt. Die Detektion der Signale erfolgt hierbei über Western Blots und Immundetektion. Mit dieser Methode konnte über mehrere Stunden zuverlässig die Bildung der Protein-Protein Komplexe

aus YidC und M13 Procoat in lebenden *E. coli* Zellen vermittelt werden. Dabei konnten fast alle detektierten Kontaktstellen aus den radioaktiven Versuchen ebenfalls nachgewiesen werden. Zusätzlich kam dieses Protokoll auch bei der Reinigung von kleinen Mengen des YidC-M13 Procoat Komplexes zum Einsatz und kann möglicherweise auch auf andere Substrate angewendet werden.

Der oligomere Zustand von YidC wurde mit einem künstlichen Dimer der Insertase (dYidC) untersucht. Dieses besteht aus zwei YidC Molekülen die über einen kurzen Linker miteinander verbunden sind. Es ist in der Lage YidC-depletierte *E. coli* MK6S Zellen zu komplementieren und zudem M13 procoat in die innere Membran zu inserieren. Für die weitere Untersuchung des dYidCs wurden drei funktionell defekte YidC-Mutanten, T362A (Wickles et al. 2014), ΔC1 (Chen et al. 2014) und die 5S YidC Mutante, auf ihre Fähigkeit zu komplementieren und zu inserieren getestet. Keine der getesteten Mutanten war in der Lage das Zellwachstum unter Depletionsbedingungen zu ermöglichen und wurden nachfolgend in eines oder in beide Protomer des dYidCs kloniert. Über Komplementations- und Insertionsstudien mit diesen dYidC Konstrukten konnte gezeigt werden, dass ein aktives Protomer an sich ausreicht um zu komplementieren und M13 Procoat zu inserieren. Bindungsstudien mit Cysteinmutanten des dYidCs und M13 Procoat, welche mittels DTNB komplexiert wurden, zeigten zudem, dass jedes Protomer für sich ein Substratprotein bindet. Die in dieser Studie durchgeführten Experimente zeigen, dass ein Monomer die aktive Konfiguration der Insertase darstellt, welche die Insertion von YidC-abhängigen Substraten vermittelt.

Die Ergebnisse dieser Arbeit tragen zu einem besseren Verständnis der Insertion von Proteinen in die innere Bakterienzellmembran bei.

REFERENCES

Allen, W.J., Corey, R.A., Oatley, P., Sessions, R.B., Baldwin, S.A., Radford, S.E., Tuma, R., Collinson, I., 2016. Two-way communication between SecY and SecA suggests a brownian ratchet mechanism for protein translocation. *Elife* 5, 1–23.

Armstrong, J., Hewitt, J.A., Perham, R.N., 1983. Chemical modification of the coat protein in bacteriophage fd and orientation of the virion during assembly and disassembly. *EMBO J.* 2, 1641–1646.

Armstrong, J., N. Perham, R., Walker, J.E., 1981. Domain structure of bacteriophage fd adsorption protein. *FEBS Lett.* 135, 167–172.

Ataide, S.F., Schmitz, N., Shen, K., Ke, A., Shan, S. -o., Doudna, J.A., Ban, N., 2011. The Crystal Structure of the Signal Recognition Particle in Complex with Its Receptor. *Science* 331, 881–886.

Banner, D.W., Nave, C., Marvin, D.A., 1981. Structure of the protein and DNA in fd filamentous bacterial virus. *Nature* 289, 814–816.

Berks, B.C., 1996. A common export pathway for proteins binding complex redox cofactors? *Mol. Microbiol.* 22, 393–404.

Berks, B.C., Sargent, F., Palmer, T., 2000. The Tat protein export pathway. *Mol Microbiol.* 35, 260–274.

Blount, P., Sukharev, S.I., Moe, P.C., Schroeder, M.J., Guy, H.R., Kung, C., 1996. Membrane topology and multimeric structure of a mechanosensitive channel protein of Escherichia coli. *EMBO J.* 15, 4798–4805.

Bogsch, E.G., Sargent, F., Stanley, N.R., Berks, B.C., Robinson, C., Palmer, T., 1998. An Essential Component of a System with Homologues in Plastids and Mitochondria. *J. Biol. Chem.* 106, 18003–18006.

Bonnefoy, N., Chalvet, F., Hamel, P., Slonimski, P.P., Dujardin, G., 1994. OXA1, a Saccharomyces cerevisiae nuclear gene whose sequence is conserved from prokaryotes to eukaryotes controls cytochrome oxidase biogenesis. *J. Mol. Biol.* 239, 201-212

Borowska, M.T., Dominik, P.K., Anghel, S.A., Kossiakoff, A.A., Keenan, R.J., 2015. A YidC-like Protein in the Archaeal Plasma Membrane. *Structure* 23, 1715–1724.

Botte, M., Zaccai, N.R., Nijeholt, J.L. à., Martin, R., Knoops, K., Papai, G., Zou, J., Deniaud, A., Karuppasamy, M., Jiang, Q., Roy, A.S., Schulten, K., Schultz, P., Rappsilber, J., Zaccai, G., Berger, I., Collinson, I., Schaffitzel, C., 2016. A central cavity within the holo-translocon suggests a mechanism for membrane protein insertion. *Sci. Rep.* 6, 38399.

Boy, D., Koch, H.-G., 2009. Visualization of Distinct Entities of the SecYEG Translocon during Translocation and Integration of Bacterial Proteins. *Mol. Biol. Cell* 20, 1804–1815.

Brown, S., Fournier, M.J., 1984. The 4.5 S RNA gene of Escherichia coli is essential for cell growth. *J. Mol. Biol.* 178, 533–50.

Brundage, L., Hendrick, J.P., Schiebel, E., Driessen, A.J.M., Wickner, W., 1990. The purified E. coli integral membrane protein SecY/E is sufficient for reconstitution of SecA-dependent precursor protein translocation. *Cell* 62, 649–657.

Bulaj, G., 2005. Formation of disulfide bonds in proteins and peptides. *Biotechnol. Adv.* 23, 87–92.

Carson, M.J., Barondess, J.I.M., Beckwith, J.O.N., 1991. The FtsQ Protein of Escherichia coli : Membrane Topology , Abundance , and Cell Division Phenotypes Due to Overproduction and Insertion Mutations. *J. Bacteriol.* 173, 2187–2195.

Chen, J.C., Weiss, D.S., Ghigo, J., Beckwith, J.O.N., Al, C.E.T., Acteriol, J.B., 1999. Septal Localization of FtsQ , an Essential Cell Division Protein in Escherichia coli. *J. Bacteriol.* 181, 521–530.

Chen, M., Samuelson, J.C., Jiang, F., Müller, M., Kuhn, A., Dalbey, R.E., 2002. Direct interaction of YidC with the Sec-independent Pf3 coat protein during its membrane protein insertion. *J. Biol. Chem.* 277, 7670–7675.

Chen, M., Xie, K., Nouwen, N., Driessen, A.J.M., Dalbey, R.E., 2003. Conditional lethal mutations separate the M13 procoat and Pf3 coat functions of YidC. Different YidC structural requirements for membrane protein insertion. *J. Biol. Chem.* 278, 23295–23300.

Chen, Y., Soman, R., Shanmugam, S.K., Kuhn, A., Dalbey, R.E., 2014. The role of the strictly conserved positively charged residue differs among the gram-positive, gram-negative, and chloroplast YidC homologs. *J. Biol. Chem.* 289, 35656–35667.

Chiba, S., Lamsa, A., Pogliano, K., 2009. A ribosome-nascent chain sensor of membrane protein biogenesis in Bacillus subtilis. *EMBO J.* 28, 1–15.

Click, E.M., Webster, R.E., 1998. The TolQRA proteins are required for membrane insertion of the major capsid protein of the filamentous phage f1 during infection. *J. Bacteriol.* 180, 1723–1728.

Creighton, T.E., Zapun, A., Darby, N.J., 1995. Mechanisms and catalysts of disulphide bond formation in proteins. *Trends Biotechnol.* 13, 18–23.

Cross, B.C.S., Sinning, I., Luirink, J., High, S., 2009. Delivering proteins for export from the cytosol. *Nat. Rev. Mol. Cell Biol.* 10, 255–64.

Dalbey, R.E., Kuhn, A., 2015. Membrane Insertases Are Present in All Three Domains of Life. *Structure* 23, 1559–1560.

Dalbey, R.E., Kuhn, A., Zhu, L., Kiefer, D., 2014. The membrane insertase YidC. *Biochim. Biophys. Acta - Mol. Cell Res.* 1843, 1489–1496.

Danehy, J.P., Egan, C.P., Switalski, J., 1971. Oxidation of organic divalent sulfur by iodine. III. Further evidence for sulfenyl iodides as intermediates and for the influence of structure on the occurrence of cyclic intermediates in the oxidation of thiols. *J. Org. Chem.* 36, 2530–2534.

Day, L.A., Marzec, C.J., Reisberg, S.A., Casadevall, A., 1988. DNA packing in filamentous bacteriophages. *Annu. Rev. Biophys. Biophys. Chem.* 17, 509–539.

de Gier, J.-W., Scotti, P.A., Sääf, A., Valent, Q.A., Kuhn, A., Luirink, J., von Heijne, G., 1998. Differential use of the signal recognition particle translocase targeting pathway for inner membrane protein assembly in Escherichia coli. *Proc. Natl. Acad. Sci. U. S. A.* 95, 14646–14651.

Deng, L., Malik, P., Perham, R.N., 1999. Interaction of the globular domains of pIII protein of filamentous bacteriophgae fd with the F-pilus of Escherichia coli. *Virology* 277, 271–277.

du Plessis, D.J.F., Berrelkamp, G., Nouwen, N., Driessen, A.J.M., 2009. The lateral gate of SecYEG opens during protein translocation. *J. Biol. Chem.* 284, 15805–15814.

Du Plessis, D.J.F., Nouwen, N., Driessen, A.J.M., 2006. Subunit a of cytochrome o oxidase requires both YidC and SecYEG for membrane insertion. *J. Biol. Chem.* 281, 12248–12252.

Duong, F., Wickner, W., 1997. Distinct catalytic roles of the SecYE, SecG and SecDFyajC subunits of preprotein translocase holoenzyme. *EMBO J.* 16, 2756–2768.

Ellman, G.L., 1959. Tissue sulfhydryl groups. *Arch. Biochem. Biophys*. 82, 70–77.

Endemann, H., Model, P., 1995. Location of filamentous phage minor coat proteins in phage and in infected cells. *J. Mol. Biol.* 250, 496–506.

Engelman, D.M., Steitz, T.A., 1981. The spontaneous insertion of proteins into and across membranes: The helical hairpin hypothesis. *Cell* 23, 411–422.

Erlandson, K.J., Miller, S.B.M., Nam, Y., Osborne, A.R., Zimmer, J., Rapoport, T.A., 2008. A role for the two-helix finger of the SecA ATPase in protein translocation. *Nature* 455, 984–987.

Facey, S.J., Neugebauer, S.A., Krauss, S., Kuhn, A., 2007. The Mechanosensitive Channel Protein MscL Is Targeted by the SRP to The Novel YidC Membrane Insertion Pathway of Escherichia coli. *J. Mol. Biol.* 365, 995–1004.

Falk, S., Ravaud, S., Koch, J., Sinning, I., 2010. The C terminus of the Alb3 membrane insertase recruits cpSRP43 to the thylakoid membrane. *J. Biol. Chem.* 285, 5954–5962.

Falke, J., Koshland, D., 1987. Global flexibility in a sensory receptor: a site-directed cross-linking approach. *Science* 237, 1596–1600.

Feng, J.N., Russel, M., Model, P., 1997. A permeabilized cell system that assembles filamentous bacteriophage. *Proc. Natl. Acad. Sci. U. S. A.* 94, 4068–73.

Fraenkel-Conrat, H., 1955. The reaction of tobacco mosaic virus with iodine. *J. Biol. Chem.* 217, 373–81.

Fulford, W., Model, P., 1988. Regulation of bacteriophage f1 DNA replication. I. New functions for genes II and X. *J. Mol. Biol.* 203, 49–62.

Gallusser, A., Kuhn, A., 1990. Initial steps in protein membrane insertion. Bacteriophage M13 procoat protein binds to the membrane surface by electrostatic interaction. *EMBO J.* 9, 2723–9.

Geng, Y., Kedrov, A., Caumanns, J.J., Crevenna, A.H., Lamb, D.C., Beckmann, R., Driessen, A.J.M., 2015. Role of the cytosolic loop C2 and the C terminus of YidC in ribosome binding and insertion activity. *J. Biol. Chem.* 290, 17250–17261.

Giron-Monzon, L., Manelyte, L., Ahrends, R., Kirsch, D., Spengler, B., Friedhoff, P., 2004. Mapping Protein-Protein Interactions between MutL and MutH by Cross-linking. *J. Biol. Chem.* 279, 49338–49345.

Girvin, M.E., Rastogi, V.K., Abildgaard, F., Markley, J.L., Fillingame, R.H., 1998. Solution structure of the transmembrane H+-transporting subunit c of the F1F0 ATP synthase. *Biochemistry* 37, 8817–8824.

Gray, C.W., Brown, R.S., Marvin, D.A., 1981. Adsorption complex of filamentous fd virus. *J. Mol. Biol.* 146, 621–627.

Green, R., Rogers, E.J., 2013. Transformation of Chemically Competent E. coli. In: *Methods in Enzymology*. pp. 329–336.

Greene, N.P., Porcelli, I., Buchanan, G., Hicks, M.G., Schermann, S.M., Palmer, T., Berks, B.C., 2007. Cysteine scanning mutagenesis and disulfide mapping studies of the TatA component of the bacterial twin arginine translocase. *J. Biol. Chem.* 282, 23937–23945.

Haigh, N.G., Webster, R.E., 1999. The pI and pXI assembly proteins serve separate and essential roles in filamentous phage assembly. *J. Mol. Biol.* 293, 1017–1027.

Hanahan, D., 1983. Studies on transformation of Escherichia coli with plasmids. *J. Mol. Biol.* 166, 557–580.

Haniu, M., Narhi, L.O., Arakawa, T., Elliott, S., Rohde, M.F., 1993. Recombinant human erythropoietin (rHuEPO): cross-linking with disuccinimidyl esters and identification of the interfacing domains in EPO. *Protein Sci.* 2, 1441–1451.

Hartl, F.U., Bracher, A., Hayer-Hartl, M., 2011. Molecular chaperones in protein folding and proteostasis. *Nature* 475, 324–332.

Hell, K., Herrmann, J.M., Pratje, E., Neupert, W., Stuart, R.A., 1997. Oxa1p mediates the export of the N- and C-termini of pCoxII from the mitochondrial matrix to the intermembrane space. *FEBS Lett.* 418, 367–370.

Hell, K., Herrmann, J.M., Pratje, E., Neupert, W., Stuart, R.A., 1998. Oxa1p, an essential component of the N-tail protein export machinery in mitochondria. *Proc. Natl. Acad. Sci.* 95, 2250–2255.

Hennon, S.W., Dalbey, R.E., 2014. Cross-linking-based flexibility and proximity relationships between the TM segments of the Escherichia coli YidC. *Biochemistry* 53, 3278–3286.

Hennon, S.W., Soman, R., Zhu, L., Dalbey, R.E., 2015. YidC/Alb3/Oxa1 family of insertases. *J. Biol. Chem.* 290, 14866–14874.

Hensel, M., Deckers-Hebestreit, G., Schmid, R., Altendorf, K., 1990. Orientation of subunit c of the ATP synthase of Escherichia coli--a study with peptide-specific antibodies. *Biochim. Biophys. Acta* 1016, 63–70.

Herrmann, J.M., 2013. The bacterial membrane insertase YidC is a functional monomer and binds ribosomes in a nascent chain-dependent manner. *J. Mol. Biol.* 425, 4071–4073.

Herrmann, J.M., Neupert, W., Stuart, R.A., 1997. Insertion into the mitochondrial inner membrane of a polytopic protein, the nuclear-encoded Oxa1p. *EMBO J.* 16, 2217–2226.

Herskovits, A.A., Bochkareva, E.S., Bibi, E., 2000. New prospects in studying the bacterial signal recognition particle pathway. *Mol. Microbiol.* 38, 927–939.

Hino, N., Hayashi, A., Sakamoto, K., Yokoyama, S., 2007. Site-specific incorporation of non-natural amino acids into proteins in mammalian cells with an expanded genetic code. *Nat. Protoc.* 1, 2957–2962.

Hino, N., Okazaki, Y., Kobayashi, T., Hayashi, A., Sakamoto, K., Yokoyama, S., 2005. Protein photo-cross-linking in mammalian cells by site-specific incorporation of a photoreactive amino acid. *Nat. Methods* 2, 201–206.

Hofschneider, P.H., 1963. Untersuchungen über „kleine" E. coli K 12 Bakteriophagen. Z. *Naturforschg.* 203–210.

Huber, D., Jamshad, M., Hanmer, R., Schibich, D., Döring, K., Marcomini, I., Kramer, G., Bukau, B., 2017. SecA Cotranslationally Interacts with Nascent Substrate Proteins In Vivo. *J. Bacteriol.* 199, e00622-16.

Hughson, a G., Lee, G.F., Hazelbauer, G.L., 1997. Analysis of protein structure in intact cells: crosslinking in vivo between introduced cysteines in the transmembrane domain of a bacterial chemoreceptor. *Protein Sci.* 6, 315–22.

Hunter, G.J., Rowitch, D.H., Perham, R.N., 1987. Interactions between DNA and coat protein in the structure and assembly of filamentous bacteriophage fd. *Nature* 327, 252–254.

Imhof, N., Kuhn, A., Gerken, U., 2011. Substrate-dependent conformational dynamics of the escherichia coli membrane insertase YidC. *Biochemistry* 50, 3229–3239.

Jack, R.L., Sargent, F., Berks, B.C., Sawers, G., Palmer, T., 2001. Constitutive Expression of Escherichia coli tat Genes Indicates an Important Role for the Twin-Arginine Translocase during Aerobic and Anaerobic Growth. *J. Bacteriol.* 183, 1801–1804.

Jiang, F., Yi, L., Moore, M., Chen, M., Rohl, T., Van Wijk, K.J., de Gier, J.-W., Henry, R., Dalbey, R.E., 2002. Chloroplast YidC homolog Albino3 can functionally complement the bacterial YidC depletion strain and promote membrane insertion of both bacterial and chloroplast thylakoid proteins. *J. Biol. Chem.* 277, 19281–19288.

Jiang, W., Hermolin, J., Fillingame, R.H., 2001. The preferred stoichiometry of c subunits in the rotary motor sector of Escherichia coli ATP synthase is 10. *Proc. Natl. Acad. Sci. U. S. A.* 98, 4966–71.

Kedrov, A., Sustarsic, M., De Keyzer, J., Caumanns, J.J., Wu, Z.C., Driessen, A.J.M., 2013. Elucidating the native architecture of the YidC: Ribosome complex. *J. Mol. Biol.* 425, 4112–4124.

Kedrov, A., Wickles, S., Crevenna, A.H., van der Sluis, E.O., Buschauer, R., Berninghausen, O., Lamb, D.C., Beckmann, R., 2016. Structural Dynamics of the YidC:Ribosome Complex during Membrane Protein Biogenesis. *Cell Rep.* 17, 2943–2954.

Kiefer, D., Hu, X., Dalbey, R.E., Kuhn, A., 1997. Negatively charged amino acid residues play an active role in orienting the Sec-independent Pf3 coat protein in the Escherichia coli inner membrane. *EMBO J.* 16, 2197–2204.

Kiefer, D., Kuhn, A., 1999. Hydrophobic forces drive spontaneous membrane insertion of the bacteriophage Pf3 coat protein without topological control. *EMBO J.* 18, 6299–6306.

Klenner, C.D., Kuhn, A., 2012. Dynamic disulfide scanning of the membrane-inserting Pf3 coat protein reveals multiple YidC substrate contacts. *J. Biol. Chem.* 287, 3769–3776.

Klenner, C.D., Yuan, J., Dalbey, R.E., Kuhn, A., 2008. The Pf3 coat protein contacts TM1 and TM3 of YidC during membrane biogenesis. *FEBS Lett.* 582, 3967–3972.

Klostermann, E., Droste Gen Helling, I., Carde, J.-P., Schünemann, D., 2002. The thylakoid membrane protein ALB3 associates with the cpSecY-translocase in Arabidopsis thaliana. *Biochem. J.* 368, 777–781.

Kobashi, K., 1968. Catalytic oxidation of sulfhydryl groups by o-phenanthroline copper complex. *Biochim. Biophys. Acta - Gen. Subj.* 158, 239–245.

Koch, H.-G., Moser, M., Schimz, K.L., Müller, M., 2002. The integration of YidC into the cytoplasmic membrane of Escherichia coli requires the signal recognition particle, SecA and SecYEG. *J. Biol. Chem.* 277, 5715–5718.

Kogata, N., Nishio, K., Hirohashi, T., Kikuchi, S., Nakai, M., 1999. Involvement of a chloroplast homologue of the signal recognition particle receptor protein, FtsY, in protein targeting to thylakoids. *FEBS Lett.* 447, 329–333.

Kohler, R., Boehringer, D., Greber, B., Bingel-Erlenmeyer, R., Collinson, I., Schaffitzel, C., Ban, N., 2009. YidC and Oxa1 Form Dimeric Insertion Pores on the Translating Ribosome. *Mol. Cell* 34, 344–353.

Kol, S., Majczak, W., Heerlien, R., van der Berg, J.P., Nouwen, N., Driessen, A.J.M., 2009. Subunit a of the F1F0 ATP Synthase Requires YidC and SecYEG for Membrane Insertion. *J. Mol. Biol.* 390, 893–901.

Kuhn, A., 1987. Bacteriophage M13 procoat protein inserts into the plasma membrane as a loop structure. *Science* 238, 1413–1415.

Kuhn, A., Kreil, G., Wickner, W., 1986. Both hydrophobic domains of M13 procoat are required to initiate membrane insertion. *EMBO J.* 5, 3681–3685.

Kuhn, A., Wickner, W., 1985a. Conserved residues of the leader peptide are essential for cleavage by leader peptidase. *J. Biol. Chem.* 260, 15914–15918.

Kuhn, A., Wickner, W., 1985b. Isolation of mutants in M13 coat protein that affect its synthesis, processing, and assembly into phage. *J. Biol. Chem.* 260, 15907–15913.

Kumazaki, K., Chiba, S., Takemoto, M., Furukawa, A., Nishiyama, K., Sugano, Y., Mori, T., Dohmae, N., Hirata, K., Nakada-Nakura, Y., Maturana, A.D., Tanaka, Y., Mori, H., Sugita, Y., Arisaka, F., Ito, K., Ishitani, R., Tsukazaki, T., Nureki, O., 2014a. Structural basis of Sec-independent membrane protein insertion by YidC. *Nature* 509, 516–20.

Kumazaki, K., Kishimoto, T., Furukawa, A., Mori, H., Tanaka, Y., Dohmae, N., Ishitani, R., Tsukazaki, T., Nureki, O., 2014b. Crystal structure of Escherichia coli YidC, a membrane protein chaperone and insertase. *Sci. Rep.* 4, 7299.

Kusters, R., Lentzen, G., Eppens, E., van Geel, A., van der Weijden, C.C., Wintermeyer, W., Luirink, J., 1995. The functioning of the SRP receptor FtsY in protein-targeting in E. coli is correlated with its ability to bind and hydrolyse GTP. *FEBS Lett.* 372, 253–258.

Lee, G.F., Lebert, M.R., Lilly, a a, Hazelbauer, G.L., 1995. Transmembrane signaling characterized in bacterial chemoreceptors by using sulfhydryl cross-linking in vivo. *Proc. Natl. Acad. Sci. U. S. A.* 92, 3391–3395.

Lee, H.C., Bernstein, H.D., 2001. The targeting pathway of Escherichia coli presecretory and integral membrane proteins is specified by the hydrophobicity of the targeting signal. *Proc. Natl. Acad. Sci. U. S. A.* 98, 3471–3476.

Li, Z., Boyd, D., Reindl, M., Goldberg, M.B., 2014. Identification of YidC residues that define interactions with the Sec apparatus. *J. Bacteriol.* 196, 367–377.

Linderoth, N.A., 1997. The Filamentous Phage pIV Multimer Visualized by Scanning Transmission Electron Microscopy. *Science* 278, 1635–1638.

Long, D., Martin, M., Sundberg, E., Swinburne, J., Puangsomlee, P., Coupland, G., 1993. The maize transposable element system Ac/Ds as a mutagen in Arabidopsis: identification of an albino mutation induced by Ds insertion. *Proc. Natl. Acad. Sci. U. S. A.* 90, 10370–10374.

Lotz, M., Haase, W., Kühlbrandt, W., Collinson, I., 2008. Projection Structure of yidC: A Conserved Mediator of Membrane Protein Assembly. *J. Mol. Biol.* 375, 901–907.

Lycklama a Nijeholt, J. a., Driessen, a. J.M., 2012. The bacterial Sec-translocase: structure and mechanism. *Philos. Trans. R. Soc. B Biol. Sci.* 367, 1016–1028.

Mandel, G., Wickner, W., 1979. Translational and post-translational cleavage of M13 procoat protein: extracts of both the cytoplasmic and outer membranes of Escherichia coli contain leader peptidase activity. *Proc. Natl. Acad. Sci.* 76, 236–240.

Mansfeld, J., Vriend, G., Bauke, W., Veltman, O.R., Den, B. van, Venema, G., Eijsink, V.G.H., Dijkstra, B.W., Burg, B. Van Den, Ulbrich-Hofmann, R., 1997. Extreme Stabilization of a Thermolysin-like Protease by an Engineered Disulfide Bond. *J. Biol. Chem.* 272, 11152–11156.

Marvin, D.A., Symmons, M.F., Straus, S.K., 2014. Structure and assembly of filamentous bacteriophages. *Prog. Biophys. Mol. Biol.* 114, 80–122.

Miller, J.D., Bernstein, H.D., Walter, P., 1994. Interaction of E. coli Ffh/4.5S ribonucleoprotein and FtsY mimics that of mammalian signal recognition particle and its receptor. *Nature* 367, 657–659.

Montoya, G., Svensson, C., Luirink, J., Sinning, I., 1997. Crystal structure of the NG domain from the signal-recognition particle receptor FtsY. *Nature* 385, 365–368.

Moore, M., Harrison, M.S., Peterson, E.C., Henry, R., 2000. Chloroplast Oxa1p homolog albino3 is required for post-translational integration of the light harvesting chlorophyll-binding protein into thylakoid membranes. *J. Biol. Chem.* 275, 1529–1532.

Morag, O., Sgourakis, N.G., Baker, D., Goldbourt, A., 2015. The NMR–Rosetta capsid model of M13 bacteriophage reveals a quadrupled hydrophobic packing epitope. *Proc. Natl. Acad. Sci.* 112, 971–976.

Müller, M., 2005. Twin-arginine-specific protein export in Escherichia coli. *Res. Microbiol.* 156, 131–136.

Nagler, C., Nagler, G., Kuhn, A., 2007. Cysteine residues in the transmembrane regions of M13 procoat protein suggest that oligomeric coat proteins assemble onto phage progeny. *J. Bacteriol.* 189, 2897–2905.

Natale, P., Brüser, T., Driessen, A.J.M., 2008. Sec- and Tat-mediated protein secretion across the bacterial cytoplasmic membrane-Distinct translocases and mechanisms. *Biochim. Biophys. Acta - Biomembr.* 1778, 1735–1756.

Neugebauer, S.A., Baulig, A., Kuhn, A., Facey, S.J., 2012. Membrane protein insertion of variant MscL proteins occurs at YidC and SecYEG of Escherichia coli. *J. Mol. Biol.* 417, 375–386.

Or, E., Navon, A., Rapoport, T.A., 2002. Dissociation of the dimeric SecA ATPase during protein translocation across the bacterial membrane. *EMBO J.* 21, 4470–4479.

Parang, K., Kohn, J.A., Saldanha, S.A., Ã, P.A.C., 2002. Development of photo-crosslinking reagents for protein kinase ^ substrate interactions. *FEBS Lett.* 520, 156–160.

Park, E., Rapoport, T.A., 2012. Bacterial protein translocation requires only one copy of the SecY complex in vivo. *J. Cell Biol.* 198, 881–893.

Parlitz, R., Eitan, A., Stjepanovic, G., Bahari, L., Bange, G., Bibi, E., Sinning, I., 2007. Escherichia coli Signal Recognition Particle Receptor FtsY Contains an Essential and Autonomous Membrane-binding Amphipathic Helix. *J. Biol. Chem.* 282, 32176–32184.

Pasch, J.C., Nickelsen, J., Schünemann, D., 2005. The yeast split-ubiquitin system to study chloroplast membrane protein interactions. *Appl. Microbiol. Biotechnol.* 69, 440–447.

Peluso, P., Shan, S.O., Nock, S., Herschlag, D., Walter, P., 2001. Role of SRP RNA in the GTPase cycles of Ffh and FtsY. *Biochemistry* 40, 15224–15233.

Peng, H., Chen, W., Cheng, Y., Hakuna, L., Strongin, R., Wang, B., 2012. Thiol reactive probes and chemosensors. *Sensors (Switzerland)* 12, 15907–15946.

Phillips, G.J., Silhavy, T.J., 1992. The E. coli ffh gene is necessary for viability and efficient protein export. *Nature* 359, 744–746.

Pop, O.I., Soprova, Z., Koningstein, G., Scheffers, D.J., Van Ulsen, P., Wickström, D., de Gier, J.-W., Luirink, J., 2009. YidC is required for the assembly of the MscL homopentameric pore. *FEBS J.* 276, 4891–4899.

Powers, E.T., Morimoto, R.I., Dillin, A., Kelly, J.W., Balch, W.E., 2009. Biological and chemical approaches to diseases of proteostasis deficiency. *Annu. Rev. Biochem.* 78, 959–991.

Rakonjac, J., 2012. Filamentous bacteriophages: Biology and Applications. *eLS.* DOI: 10.1002/9780470015902.a0000777

Rakonjac, J., Feng, J.N., Model, P., 1999. Filamentous phage are released from the bacterial membrane by a two-step mechanism involving a short C-terminal fragment of pIII. *J. Mol. Biol.* 289, 1253–65.

Rakonjac, J., Model, P., 1998. Roles of pIII in filamentous phage assembly. *J. Mol. Biol.* 282, 25–41.

Rapoza, M.P., Webster, R.E., 1995. The Products of Gene I and the Overlapping in-Frame Gene XI are Required for Filamentous Phage Assembly. *J. Mol. Biol.* 248, 627–638.

Rasched, I., Oberer, E., 1986. Ff coliphages: structural and functional relationships. *Microbiol. Mol. Biol. Rev.* 50, 401–427.

Russel, M., Linderoth, N.A., Šali, A., 1997. Filamentous phage assembly: Variation on a protein export theme. *Gene* 192, 23–32.

Russel, M., Model, P., 1989. Genetic analysis of the filamentous bacteriophage packaging signal and of the proteins that interact with it. *J. Virol.* 63, 3284–95.

Russel, M. and Model, P. 2006. Filamentous Phage. In: R. Calendar, *The Bacteriophages*, 2nd Ed. Oxford: *Oxford University Press*, pp.146 - 160.

Sachelaru, I., Petriman, N.A., Kudva, R., Kuhn, P., Welte, T., Knapp, B., Drepper, F., Warscheid, B., Koch, H.-G., 2013. YidC occupies the lateral gate of the SecYEG translocon and is sequentially displaced by a nascent membrane protein. *J. Biol. Chem.* 288, 16295–16307.

Sachelaru, I., Winter, L., Knyazev, D.G., Zimmermann, M., Vogt, A., Kuttner, R., Ollinger, N., Siligan, C., Pohl, P., Koch, H.-G., 2017. YidC and SecYEG form a heterotetrameric protein translocation channel. *Sci. Rep.* 7, 101.

Samuelson, J.C., Chen, M., Jiang, F., Möller, I., Wiedmann, M., Kuhn, A., Phillips, G.J., Dalbey, R.E., 2000. YidC mediates membrane protein insertion in bacteria. *Nature* 406, 637–641.

Samuelson, J.C., Jiang, F., Yi, L., Chen, M., de Gier, J.-W., Kuhn, A., Dalbey, R.E., 2001. Function of YidC for the insertion of M13 procoat protein in Escherichia coli: Translocation of mutants that show differences in their membrane potential dependence and Sec requirement. *J. Biol. Chem.* 276, 34847–34852.

Samuelsson, T., Olsson, M., Wikström, P.M., Johansson, B.R., 1995. The GTPase activity of the Escherichia coli Ffh protein is important for normal growth. *Biochim. Biophys. Acta - Mol. Cell Res.* 1267, 83–91.

Sanger, F., Nicklen, S., Coulson, A.R., 1977. DNA sequencing with chain-terminating inhibitors. *Proc. Natl. Acad. Sci.* 74, 5463–5467.

Sargent, F., Stanley, N.R., Berks, B.C., Palmer, T., 1999. Sec-independent Protein Translocation in Escherichia coli. *J. Biol. Chem.* 274, 36073–36082.

Scheffers, D.J., Robichon, C., Haan, G.J., Den Blaauwen, T., Koningstein, G., Van Bloois, E., Beckwith, J., Luirink, J., 2007. Contribution of the FtsQ transmembrane segment to localization to the cell division site. *J. Bacteriol.* 189, 7273–7280.

Schuenemann, D., Gupta, S., Persello-Cartieaux, F., Klimyuk, V.I., Jones, J.D., Nussaume, L., Hoffman, N.E., 1998. A novel signal recognition particle targets light-harvesting proteins to the thylakoid membranes. *Proc. Natl. Acad.* Sci. 95, 10312–1316.

Scotti, P.A., Urbanus, M.L., Brunner, J., de Gier, J.-W., von Heijne, G., van der Does, C., Driessen, A.J.M., Oudega, B., Luirink, J., 2000. YidC, the Escherichia coli homologue of mitochondrial Oxa1p, is a component of the Sec translocase. *EMBO J.* 19, 542–9.

Settles, A.M., Martienssen, R., 1998. Old and new pathways of protein export in chloroplasts and bacteria. *Trends Cell Biol.* 8, 494–501.

Shimokawa-Chiba, N., Kumazaki, K., Tsukazaki, T., Nureki, O., Ito, K., Chiba, S., 2015. Hydrophilic microenvironment required for the channel-independent insertase function of YidC protein. *Proc. Natl. Acad. Sci.* 112, 5063–5068.

Simons, G.F., Konings, R.N., Schoenmakers, J.G., 1981. Genes VI, VII, and IX of phage M13 code for minor capsid proteins of the virion. *Proc. Natl. Acad. Sci. U. S. A.* 78, 4194–8.

Siu, F.Y., Spanggord, R.J., Doudna, J. a, 2007. SRP RNA provides the physiologically essential GTPase activation function in cotranslational protein targeting. *RNA* 13, 240–250.

Slonczewski, J., Foster, J. 2010. *Microbiology*. Second Ed. New York: *W.W. Norton*.

Soman, R., Yuan, J., Kuhn, A., Dalbey, R.E., 2014. Polarity and charge of the periplasmic loop determine the YidC and sec translocase requirement for the M13 procoat lep protein. *J. Biol. Chem.* 289, 1023–1032.

Steinbacher, S., Bass, R., Strop, P., Rees, D.C., 2007. Structures of the Prokaryotic Mechanosensitive Channels MscL and MscS. *Curr. Top. Membr.* 58, 1–24.

Stiegler, N., Dalbey, R.E., Kuhn, A., 2011. M13 procoat protein insertion into YidC and SecYEG proteoliposomes and liposomes. *J. Mol. Biol.* 406, 362–370.

Strop, P., Brunger, A.T., 2005. Refractive index-based determination of detergent concentration and its application to the study of membrane proteins. *Protein Sci.* 14, 2207–2211.

Sundberg, E., 1997. ALBIN03, an Arabidopsis Nuclear Gene Essential for Chloroplast Differentiation, Encodes a Chloroplast Protein That Shows Homology to Proteins Present in Bacterial Membranes and Yeast Mitochondria. *Plant Cell Online* 9, 717–730.

Svergun, D.I., Koch, H.J., 2003. Small-angle scattering studies of biological macromolecules in solution. *Reports Prog. Phys.* 66, 1735–1782.

Szegedi, S.S., Garrow, T.A., 2004. Oligomerization is required for betaine-homocysteine S - methyltransferase function. *Arch. Biochem. Biophys.* 426, 32–42.

Szyrach, G., Ott, M., Bonnefoy, N., Neupert, W., Herrmann, J.M., 2003. Ribosome binding to the Oxa1 complex facilitates co-translational protein insertion in mitochondria. *EMBO J.* 22, 6448–6457.

Thiaudière, E., Soekarjo, M., Kuchinka, E., Kuhn, A., Vogel, H., 1993. Structural characterization of membrane insertion of M13 procoat, M13 coat, and Pf3 coat proteins. *Biochemistry* 32, 12186–96.

Tomishige, M., Vale, R.D., 2000. Controlling kinesin by reversible disulfide cross-linking: Identifying the motility-producing conformational change. *J. Cell Biol.* 151, 1081–1092.

Trakselis, M.A., Alley, S.C., Ishmael, F.T., Unit, C.C., Road, H., Kingdom, U., Genetics, S., 2005. Identification and Mapping of Protein - Protein Interactions by a Combination of Cross-Linking , Cleavage , and Proteomics. *Bioconjug. Chem.* 16, 741–750.

Tu, C.J., Schuenemann, D., Hoffman, N.E., 1999. Chloroplast FtsY, chloroplast signal recognition particle, and GTP are required to reconstitute the soluble phase of light-harvesting chlorophyll protein transport into thylakoid membranes. *J. Biol. Chem.* 274, 27219–27224.

Van Bloois, E., Haan, G.J., de Gier, J.-W., Oudega, B., Luirink, J., 2006. Distinct requirements for translocation of the N-tail and C-tail of the Escherichia coli inner membrane protein CyoA. *J. Biol. Chem.* 281, 10002–10009.

Van Bloois, E., Jan Haan, G., de Gier, J.-W., Oudega, B., Luirink, J., 2004. F1F0 ATP synthase subunit c is targeted by the SRP to YidC in the E. coli inner membrane. *FEBS Lett.* 576, 97–100.

Van Der Laan, M., Bechduft, P., Kol, S., Nouwen, N., Driessen, A.J.M., 2004. F1F0 ATP synthase subunit c is a substrate of the novel YidC pathway for membrane protein biogenesis. *J. Cell Biol.* 165, 213–222.

Van Der Laan, M., Houben, E.N., Nouwen, N., Luirink, J., Driessen, a J., 2001. Reconstitution of Sec-dependent membrane protein insertion: nascent FtsQ interacts with YidC in a SecYEG-dependent manner. *EMBO Rep.* 2, 519–523.

van Wezenbeek, P.M.G.F., Hulsebos, T.J.M., Schoenmakers, J.G.G., 1980. Nucleotide sequence of the filamentous bacteriophage M13 DNA genome: comparison with phage fd. *Gene* 11, 129–148.

von Heijne, G., 1985. Signal sequences. The limits of variation. *J. Mol. Biol.* 184, 99–105.

von Heijne, G., 2005. Signal Peptides. *Encycl. Life Sci.* 1–3.

Wallin, E., von Heijne, G., 1998. Genome-wide analysis of integral membrane proteins from eubacterial, archaean, and eukaryotic organisms. *Protein Sci.* 7, 1029–38.

Wang, P., Dalbey, R.E., 2011. Inserting membrane proteins: The YidC/Oxa1/Alb3 machinery in bacteria, mitochondria, and chloroplasts. *Biochim. Biophys. Acta - Biomembr.* 1808, 866–875.

Welsh, L.C., Symmons, M.F., Sturtevant, J.M., Marvin, D.A., Perham, R.N., 1998. Structure of the capsid of Pf3 filamentous phage determined from X-ray fibre diffraction data at 3.1 A resolution. *J. Mol. Biol.* 283, 155–177.

Wickles, S., Singharoy, A., Andreani, J., Seemayer, S., Bischoff, L., Berninghausen, O., Soeding, J., Schulten, K., van der Sluis, E.O., Beckmann, R., 2014. A structural model of the active ribosome-bound membrane protein insertase YidC. *Elife* 3, e03035.

Winterfeld, S., Ernst, S., Börsch, M., Gerken, U., Kuhn, A., 2013. Real Time Observation of Single Membrane Protein Insertion Events by the Escherichia coli Insertase YidC. *PLoS One* 8, e59023.

Winterfeld, S., Imhof, N., Roos, T., Bär, G., Kuhn, A., Gerken, U., 2009. Substrate-induced conformational change of the Escherichia coli membrane insertase YidC. *Biochemistry* 48, 6684–6691.

Winther, J.R., Thorpe, C., 2014. Quantification of thiols and disulfides. *Biochim. Biophys. Acta* 1840, 838–846.

Wolfe, P.B., Rice, M., Wickner, W., 1985. Effects of two sec genes on protein assembly into the plasma membrane of Escherichia coli. *J. Biol. Chem.* 260, 1836–1841.

Yi, L., Celebi, N., Chen, M., Dalbey, R.E., 2004. Sec/SRP requirements and energetics of membrane insertion of subunits a, b, and c of the Escherichia coli F1F0 ATP synthase. *J. Biol. Chem.* 279, 39260–39267.

Zimmer, J., Nam, Y., Rapoport, T.A., 2008. Structure of a complex of the ATPase SecA and the protein-translocation channel. *Nature* 455, 936–43.

Zybailov, B.L., 2013. Large Scale Chemical Cross-linking Mass Spectrometry Perspectives. *J. Proteomics Bioinform.* 1, 1–25.

ABBREVIATIONS

A. aeolicus	*Aquifex aeolicus*
ADA	N-(2-Acetamido)iminodiacetic acid
Alb3	Albino-3, chloroplast insertase homolog
amp	ampicillin
ara	arabinose
ATP	adenosine triphosphate
B. halodurans	*Bacillus halodurans*
bp	base pairs
C1 loop	cytoplasmic domain of YidC between TM2 and TM3
cap	chloramphenicol
cpSRP	chloroplast signal recognition particle
cryo-EM	cryo-electron microscopy
Cu-P	copper phenanthroline
CV	column volume
Cymal6	6-Cyclohexyl-1-Hexyl-β-D-Maltoside
c-region	C-terminal region of a signal sequence
C-terminal	carboxyl-terminal
Da	dalton
DDM	n-dodecyl-β-d-maltoside
DMSO	dimethylsulfoxide
DNA	deoxyribonucleic acid

dNTP	deoxynucleoside triphosphate
DTNB	Bis(3-carboxy-4-nitrophenyl) disulfide
DTT	dithiothreitol
DUF	domain of unknown function
E. coli	*Escherichia coli*
EDTA	ethylenediaminotetraacetic acid
et al.	*et alii*; and others
EtOH	ethanol
Ffh	fifty-four-homolog, SRP54-homolog
FtsQ	filamentous temperature sensitive Q, cell division protein
FtsY	filamentous temperature sensitive Y, prokaryotic SRP-receptor
GFP	green fluorescent protein
glc	glucose
GTP	guanosine triphosphate
h	hour
$_{dd}H_2O$	double-deionized water
HCl	hydrochloric acid
HEPES	4-(2-hydroxyethyl)-1-piperazineethanesulfonic acid
His-tag	histidine-tag
h-region	hydrophobic core region of a signal sequence
I	iodine
IEC	ion exchange chromatography

IMAC	immobilized metal ion affinity chromatography
IMV	inner membrane vesicle
IPTG	isopropyl-β-D-thiogalactoside
kDa	kilodalton
LB	Luria-Bertani
MD	molecular dynamics (simulation)
MES	2-(N-morpholino)ethanesulfonic acid
min	minute
mM	millimolar
mRNA	messenger ribonucleic acid
MscL	mechanosensitive channel of large conductance
MW	molecular weight
M. jannaschii	*Methanocaldococcus jannaschii*
NaCl	sodium chloride
Ni^{2+}	nickel
nm	nanometer
nM	nanomolar
n-region	amino-terminal region of a signal sequence
N-terminal	amino-terminal
OD	optical density
OMV	outer membrane vesicle
o-PDM	N,N'-(o-Phenylene)dimaleimide

Oxa1 oxidase assembly protein 1, mitochondrial insertase homolog

P1 loop large periplasmic domain of YidC between TM1 and TM2

PAGE polyacrylamide gel electrophoresis

PBS phosphate buffered saline

PClep Procoat-Leaderpeptidase, fusion protein

PCR polymerase chain reaction

PDB protein data bank

pH potential hydrogen

PMF proton motive force

PMSF phenylmethylsulfonyl fluoride

RbCl rubidium chloride

RNA ribonucleic acid

RNC ribosome nascent chain

rpm revolutions per minute

RT room temperature

S. cerevisiae *Saccharomyces cerevisiae*

SDS sodium dodecyl sulfate

SEC size exclusion chromatography

SRP signal recognition particle

Zysorbin *Staphylococcus aureus* protein A for immunoprecipitation

T. maritima *Thermotoga maritima*

TAE tris-acetate-EDTA buffer

TAT	twin arginine translocation
TCA	trichloroacetic acid
TF	trigger factor
TM	transmembrane (segment)
Tris	trishydroxymethylaminomethane
tRNA	transfer ribonucleic acid
UV	ultraviolet
wt	wild type
YidC	bacterial membrane insertase
α	anti, alpha
µM	micromolar

ACKNOWLEDGEMENTS

Eidesstattliche Versicherung gemäß § 7 Absatz 7 der Promotionsordnung der Universität Hohenheim zum Dr. rer. nat.

1. Bei der eingereichten Dissertation zum Thema

   The function of *E. coli* YidC for the membrane insertion of the M13 procoat protein

   handelt es sich um meine eigenständig erbrachte Leistung.

2. Ich habe nur die angegebenen Quellen und Hilfsmittel benutzt und mich keiner unzulässigen Hilfe Dritter bedient. Insbesondere habe ich wörtlich oder sinngemäß aus anderen Werken übernommene Inhalte als solche kenntlich gemacht.

3. Ich habe nicht die Hilfe einer kommerziellen Promotionsvermittlung oder -beratung in Anspruch genommen.

4. Die Bedeutung der eidesstattlichen Versicherung und der strafrechtlichen Folgen einer unrichtigen oder unvollständigen eidesstattlichen Versicherung sind mir bekannt.

Die Richtigkeit der vorstehenden Erklärung bestätige ich: Ich versichere an Eides Statt, dass ich nach bestem Wissen die reine Wahrheit erklärt und nichts verschwiegen habe.

_____   _____

Ort und Datum   Unterschrift

CURRICULUM VITAE

Personal data

Name	Dirk Spann
Date of birth	18.11.1985
Place of birth	Stuttgart, Germany
Nationality	German

Education

2017 / 12 – 2011 / 09	PhD student at the University of Hohenheim, Institut für Mikrobiologie, Prof. Dr. rer. nat. Andreas Kuhn
2010 / 04 – 2009 / 06	Diploma thesis "Sequenzierung zweier Gene mehrerer Iridoviren und Entwicklung einer Realtime-PCR für deren Nachweis", University of Hohenheim, Institut für Umwelt- und Tierhygiene, Prof. Dr. med. vet. Reinhard Böhm
2011 / 09 – 2005 / 09	Studies of agricultural biology, Dipl. agr. biol., University of Hohenheim
2005 / 06 – 1996 / 09	Abitur at the Wirtemberg-Gymnasium, Stuttgart